

Sympatry of genetic lineages of *Parisotoma notabilis* s. l. (Collembola, Isotomidae) in the East European Plain

Anastasia Striuchkova¹, Irina Malykh¹, Mikhail Potapov¹, Nataliya Kuznetsova¹

¹ Department of Zoology and Ecology, Institute of Biology and Chemistry, Moscow State Pedagogical University, Moscow, Russia

Corresponding author: Anastasia Striuchkova (astr2502@yandex.ru)

Academic editor: Louis Deharveng | Received 28 September 2022 | Accepted 29 November 2022 | Published 21 December 2022

<https://zoobank.org/A3E44AFD-7AAG-483F-B358-11EA8C39648B>

Citation: Striuchkova A, Malykh I, Potapov M, Kuznetsova N (2022) Sympatry of genetic lineages of *Parisotoma notabilis* s. l. (Collembola, Isotomidae) in the East European Plain. ZooKeys 1137: 1–15. <https://doi.org/10.3897/zookeys.1137.95769>

Abstract

Parisotoma notabilis (Schaeffer, 1896) is one of the most abundant eurytopic species of springtails in temperate regions of the northern hemisphere, and is often used as a model species for studies on the genetics of soil microarthropod populations. Six genetic lineages (L0, L1, L2, L3, L4-Saltzwedel, L4-Hebert) are known which are distributed mainly parapatrically in Western and Central Europe. Individuals of *P. notabilis* from 21 locations on the East European Plain were analyzed. Three genetic lineages were found: L1, L2, L4-Hebert. In contrast to Western and Central Europe, the coexistence of two or three lineages was revealed in about half of the locations on the East European Plain. The most diverse genetic composition of *P. notabilis* populations was noted in natural forests and slightly disturbed habitats, while the least diverse was in places with a high anthropogenic influence.

Keywords

28S rDNA, cryptic diversity, genetic lineages, microarthropods, soil fauna, springtails

Introduction

Parisotoma notabilis Schaeffer, 1896 (Collembola: Isotomidae) is a cosmopolitan species which occurs in almost every biotope in temperate regions of the Western Palearctic, and predominates in most communities of Collembola (Potapov 2001). This species is eurytopic and is moderately tolerant to disturbed habitats (Kuznetsova 2002),

showing resistance to pesticides (Petersen and Krogh 1987), heavy metals (Eitminaviciute 2006; Winkler et al. 2018), application of various fertilizers (Buchholz et al. 2017) and moderate trampling (Nadezhdina and Kuznetsova 2010). One of the reasons for its success is parthenogenesis, which allows *P. notabilis* to be one of the first colonizers of disturbed habitats (Alvarez et al. 1997). Although males sometimes occur, the parthenogenetic form is found across the entire distribution range of this species (Chernova et al. 2009).

Parisotoma notabilis is morphologically uniform in spite of its occurrence in wide range of habitats (Potapov 1991, 2001). Genetic studies reveal heterogeneity of the species in the COI gene (Chahartaghi 2007). As such, four lineages of *P. notabilis* (L0–L3) have previously been proposed based on genetic analysis of both the COI and the D2 region of the 28S genes (Porco et al. 2012a). These results were confirmed (Saltzwedel et al. 2017) also by D3–D5 region of 28S and histone H3, and supplemented by two new genetic lineages of L4 (Hebert et al. unpub. data; Anslan and Tedersoo 2015; Saltzwedel et al. 2017). Unfortunately, the two different new lineages (see Results) were named the same “L4”. To distinguish them, we refer to the lineages as “L4-Hebert” and “L4-Saltzwedel” in the paper. The average genetic *p*-distances between lineages were very high: from 15% to 18% for the COI gene, from 5% to 11% for histone H3, and from 0.5% to 1.9% for D3–D5 region 28S (Saltzwedel et al. 2017). For comparison, the interspecies COI divergence for closely related species of Collembola ranges from 16.35% to 24.55% (Sun et al. 2018). This suggests that *P. notabilis* may have as yet undetected morphological differences that would warrant subspecies and possibly species status, if detected.

Genetic variation of *P. notabilis* suggests lineages may be parapatric as distributional data show some geographical specificity of lineages. Specifically, L1 and L2 are the most widely distributed lineages in Europe; the lineage L1 is widespread in the south and east of Europe, while L2 is found in western and northern Europe and in the Pyrenees. The L0 shows a fairly continuous range from the English Channel and along the coasts of the North and Baltic Seas. The lineage L3 has been found only in Paris and Greece (Porco et al. 2012a; Saltzwedel et al. 2017), the L4-Hebert lineage in Canada and Estonia (Hebert et al. unpub. data; Anslan and Tedersoo 2015), and the L4-Saltzwedel in Croatia (Saltzwedel et al. 2017). Coexistence of the lineages was recorded once in eastern Canada, where three lineages were mixed together (Porco et al. 2012a; Saltzwedel et al. 2017). Eastern Europe was poorly studied: only two localities have previously been examined in the territory of the European part of Russia: Karelia (L2 – 5 ind.) and the Moscow region (L1 – 5 ind.) (Saltzwedel et al. 2017). Also, the coexistence and ecological segregation of the lineages of *P. notabilis* has not been investigated. The reaction to habitat disturbance is also unknown. Cases of such segregation of genetic lineages are known, for example, in another widespread springtail species - *Lepidocyrtus lanuginosus* (L.), which differs in distribution along a disturbance gradient (Zhang et al. 2018), as well as in the *Isotomurus palustris* group (Carapelli et al. 1995). However, it remains

unclear how common the phenomenon of genetic segregation of genetic lineages is in Collembola.

In this paper we provide new data on the three lineages of *P. notabilis* in the eastern regions of Europe and we test two hypotheses: 1) whether the genetic lineages of *P. notabilis* in the Eastern Europe are distributed parapatrically, as in Western Europe; and 2) whether different genetic lineages of *P. notabilis* react differently to habitat disturbance.

Material and methods

Sample collection

The study was conducted in the central region of the East European Plain, mainly around Moscow, which includes a wide range of habitats from natural forests to urban lawns. The territory is located in a belt of mixed and broad-leaved forests. The climate is temperate continental, the average annual amplitude of temperature variation is 28 °C, and 600–800 mm of precipitation falls per year (Kulbachevskii 2021). Three types of habitats representing different disturbance were selected: natural forests (10 locations), forest parks (six locations), urban lawns (five locations). One 2-litre sample of the litter and / or topsoil was taken from 1 × 1 m area in each location. Samples were taken from 21 locations from October 2020 to February 2021 (Appendix 1). Springtails were extracted into 96% alcohol using Tullgren funnels, without heating, until the samples were completely dry (7–10 days).

The extracted material was sorted under a stereomicroscope. The possible mixing with coexisting congeners of *P. notabilis* was considered. Apart from *P. notabilis*, four species of the genus *Parisotoma* have been recorded in the East European Plain: *P. agrelli* Delamare Deboutteville, 1950, *P. ekmani* Fjellberg, 1977, *P. reducta* Rusek, 1984, and *P. trichaetosa* Martynova, 1977; all four species are rare and only the latter species was recorded in the Moscow region previously. In appearance all four species are easy to separate from *P. notabilis* by having an almost white corpus and smaller eye spots. The first three congeners occur only in northern areas and are rarely recorded in the central region of the East European Plain. The littoral *P. agrelli* lives only on the Arctic Ocean shore, while the Asiatic *P. reducta* is distributed in the very north-east corner the East European Plain. The boreal *P. ekmani* can probably occur towards the central part of the East European Plain via peat-bogs although it was never recorded there in spite of intensive study of the region (its distribution is given in more detail in Potapov 1991, 2001). *Parisotoma trichaetosa* was formally recorded in the Moscow region (Potapov et al. 2021). It is an invasive Asiatic species (Potapov and Janion-Scheepers 2019) with two known single records in the area under study. *Parisotoma trichaetosa* is distinct by its overall appearance, quadridentate mucro, and many other characters. The differentiating characters of *P. notabilis* and its congeners mentioned above are given in Table 1. Apart from *P. notabilis*, other species of *Parisotoma* were not recorded in our samples.

Table 1. Key differentiating morphological characters of species of *Parisotoma* recorded in the East European Plain. Abbreviations: Omma: number of ommatidia, Postlab: number of postlabial setae, VT: number of laterodistal setae on ventral tube, Subcx: presence of outer seta on 2-nd subcoxa of first pair of legs, Mucro: number of teeth on mucro, s: number of s-setae on tergites.

Species	Omma	Postlab	VT	Subcx	Mucro	s
<i>P. notabilis</i>	3–4	4+4	3+3	-	3	complete
<i>P. agrelli</i>	1	3+3	3+3	+	3	complete
<i>P. ekmani</i>	1	4+4	4+4	-	3	reduced
<i>P. reducta</i>	1	3+3	3+3	+	3	complete
<i>P. trichaetosa</i>	1	4+4	3+3	-	4	reduced

Our preliminary sorting of specimens of *P. notabilis* was confirmed by the identification by the ribosomal 28S gene region. Besides, the specimens from several samples of each lineage were mounted on slides and identified using existing identification keys (Potapov 2001; Fjellberg 2007).

Molecular analyses

The lineages of this species can be identified by both the mitochondrial COI gene and the ribosomal 28S gene (D2 region, Porco et al. 2012a; D3–D5 region, Saltzwedel et al. 2017). We used only the D3–D5 region of 28S which showed higher positive PCR products. Ninety-seven individuals from 21 locations were selected for analysis. DNA extraction was performed using the Thermo Scientific Phire Tissue Direct PCR Master Mix. DNA was extracted from single individuals in 20 µl DNA Dilution Buffer and 0.5 µl DNA Release Additive and incubated at 98 °C for 2 min. This technique allows DNA extraction with relatively little damage to the original material, enabling vouchers to be deposited. A 573 bp D3–D5 fragment of the nuclear 28S rDNA was amplified using the primers 28Sa 5'-GAC CCG TCT TGA AGC ACG-3' and 28Sbout 5'-CCC ACA GCG CCA GTT CTG CTT ACC-3' (Whiting 2002; Prendini et al. 2005). COI was amplified using the primers ColFol-for 5'-TTT CAA CAA ATC ATA ARG AYA TYG G-3' and ColFol-rev 5'-TAA ACT TCN GGR TGN CCA AAA AAT CA-3' (Ramirez-Gonzalez et al. 2013). This data was used to correlate the results with L4-Hebert, for which there are no data on D3–D5 fragment of 28S. To a master mix consisting of 7 µl of nuclease-free Water, 10 µl of Phire Tissue Direct PCR Master Mix, 1 µl of forward and reverse primers were added 1 µl of individual DNA. PCR conditions included one initial activation step at 98 °C for 5 min, followed by 30 amplification cycles of denaturation at 98 °C for 5 s, annealing at 57 °C (28S) or 55 °C (COI) for 5 s, elongation at 72 °C for 20 s and a final elongation step at 72 °C for 1 min. The result of the PCR was evaluated by electrophoresis in agarose gel with ethidium bromide. PCR products were purified using an enzyme mix of 0.5 µl of exonuclease I (Exo I) and 1 µl of recombinant alkaline phosphatase (rSAP) per 5 µl of PCR product, according to the protocol: 37 °C for 15 min and 80 °C for 15 min. The purified prod-

uct was dried with the addition of the forward primer. Sequencing was performed in the Synthol laboratory. The sequences obtained were edited in Chromas Lite (v. 2.6.6) (<http://technelysium.com.au/wp/chromas/>). Sequences were then aligned using BioEdit (v. 7.2) (Hall et al. 2011). Tree construction and calculation of genetic distances between lineages (K2P-pairwise distances) were performed using the MEGA-X program (v.11) (Tamura et al. 2021). Tree calculation was performed with the Maximum Likelihood method with the Jukes-Cantor + Gamma Distributed parametric model proposed by MEGA-X (lowest BIC = 4531.333, AICc = 2599.369) for the 28S gene, and the Neighbor-Joining method with Tamura 3-parameter + Gamma Distributed parametric model for the COI gene. Sequences were obtained for 87 individuals for a D3–D5 fragment of the 28S gene 573 bp and 12 individuals for a COI gene 619–657 bp, which are additional confirmation of the results. The tree for the 28S gene is based on our data and those of Saltzwedel et al. (2017). GenBank (www.ncbi.nlm.nih.gov/GenBank) accession numbers are listed in the Appendix 1. Detail data on genetic lineages records were placed in the international Global Biodiversity Information Facility (GBIF) in the ‘sampling event dataset’ format (Striuchkova et al. 2022).

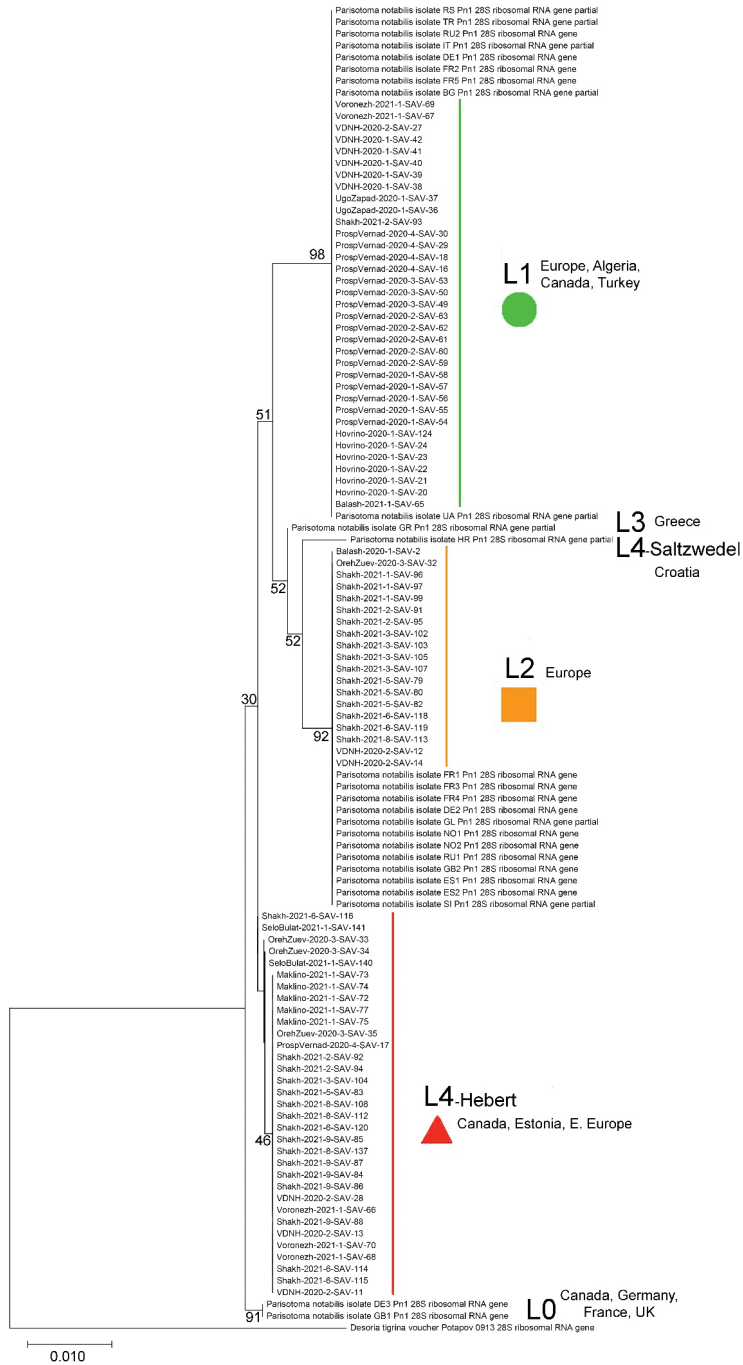
Results

Genetic lineages

The constructed tree revealed three genetic lineages of *P. notabilis*: L1, L2, and L4-Hebert (Fig. 1). The last one is not represented for D3–D5 region of 28S in GenBank. It was identified by COI according to blast results in the BOLD database (Hebert et al. unpub. data, Anslan and Tedersoo 2015). Genetic distances (observed K2P-distances in %) between the lineage L4-Hebert (this study) and L4-Saltzwedel for COI gene = 17.6%. The genetic distances between the L1, L2 and L4-Hebert lineages for the D3–D5 region of 28S ranged from 0.9% to 1.4% in our material. Mean genetic distances between all known lineages and intralines distances are given in Table 2. Neighbor-Joining genetic tree and intralines and interlines K2P-pairwise distances for the COI gene are presented in Appendices 2 and 3, respectively.

Table 2. Intralines and interlines K2P-pairwise distances (%) of the lineages *Parisotoma notabilis* in the East European Plain for D3–D5 region of 28S gene.

Lineage	Intralines	Interlines				
		L0	L1	L2	L3	L4-Saltzwedel
L1	0	1.23	0			
L2	0	1.23	1.41	0		
L3	0	0.70	0.89	0.53	0	
L4-Saltzwedel	0	1.59	1.77	1.06	0.88	0
L4-Hebert	0	0.50	0.90	1.03	0.50	1.06



Including data from Saltzwedel et al. 2017.
Our data is highlighted with colored vertical lines.

Figure 1. Maximum Likelihood genetic tree of six lineages of *P. notabilis* based on the D3-D5 region of 28S gene fragment (Bootstrap support values shown on the branches, scale bar shows genetic distance) including data from Saltzwedel et al. (2017) availed in GenBank. Our data is highlighted with colored vertical lines.

Coexistence of genetic lineages

Numerous cases of sympatry of the lineages were revealed (Fig. 2). Two lineages were found in one third of the locations (41%), with three lineages in 12% of the locations. Almost half (47%) of the locations contained only one lineage. Table 3 shows the ratios of the number of sites with lineage sympatry / number of total sites sampled based on the literature (Porco et al. 2012a; Saltzwedel et al. 2017) and our data.

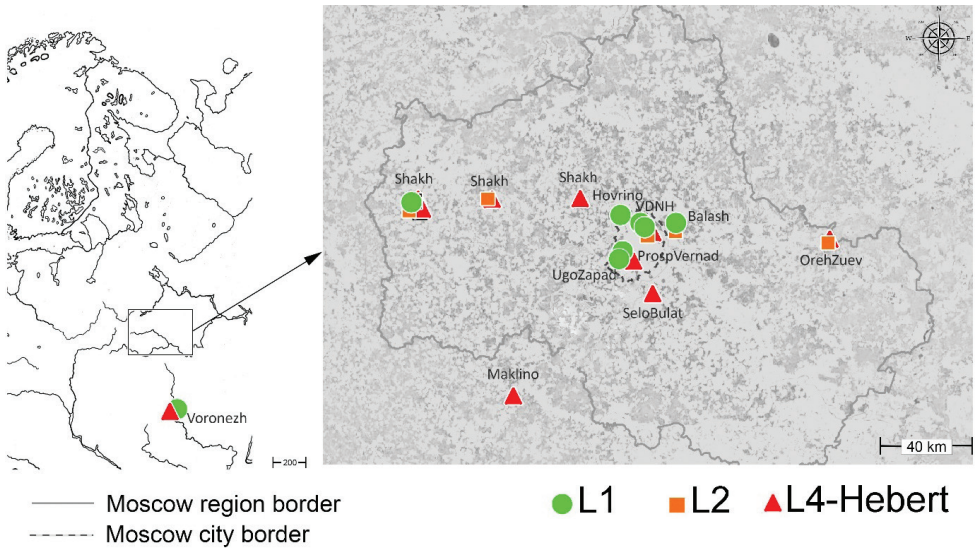


Figure 2. Records of the genetic lineages of *Parisotoma notabilis* (green circle - L1, orange square - L2, red triangle - L4-Hebert). See Appendix 1 for location data for each lineage.

Table 3. Local diversity of genetic lineages in different regions of Europe.

Region	Total number of individuals	Total number of locations	Ratio	Reference
Western and Central Europe	191	27	0.18*	Porco et al. 2012a**
	110	24	0.08	Saltzwedel et al. 2017***
East European Plain	87	21	0.5*	This study

* excluding locations with 1 or 2 individuals. ** excluding data from Canada and Algeria. *** excluding data from Russia

Ecological specificity of the lineages L1, L2 and L4-Hebert

L1 and L4-Hebert lineages were recorded in the urban areas, and all three lineages - in the partly disturbed (forest parks) and undisturbed (forests) habitats. In the forests, the occurrence of L2 and L4-Hebert lineages was about the same, while L1 was sporadic. In forest parks, L1 was the most common, the L4-Hebert was less common, while L2 was rare. In the city (urban areas), L1 absolutely dominated (Fig. 3).

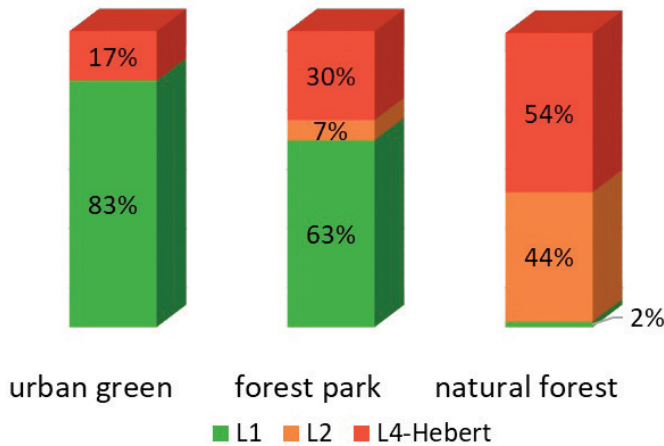


Figure 3. Records of genetic lineages of *P. notabilis* (L1, L2 and L4-Hebert) in different groups of habitats, % of the number of samples in the habitats of the group.

Discussion

Genetic lineages

The L1 and L2 lineages of *P. notabilis* were already cited in the East European Plain (Saltzwedel et al. 2017). The lineage L4-Hebert has been identified based on the sequences COI available in GenBank (Hebert et al. unpub. data; Anslan and Tedersoo 2015). The L4-Hebert for D4–D5 region of 28S is most similar with the L0 and L3 lineages (0.50%) which have not yet found in the East European Plain. The L4-Hebert lineage showed the greatest differences with the L1, L2, and L4-Saltzwedel lineages (0.90–1.05%). Updated data in the present study agree with the previously estimated average genetic distance between the most common lineages of *P. notabilis* L1 and L2 in Europe and Canada (1.4% vs. 1.39% according to Saltzwedel et al. 2017). The L4-Hebert lineage is probably widespread in the East European Plain, because we recorded it also in Voronezh, which is about 500 km south of Moscow.

Coexistence of genetic lineages

Previously, studies on the genetic structure of *P. notabilis* populations showed mainly parapatric distribution of lineages. The simultaneous presence of two or three lineages was noted only in 13% of the total number of locations studied (Porco et al. 2012a; Saltzwedel et al. 2017). Consequently, the sympatry of the lineages in Canada was thought to be possible independent introductions of the species, that is, they consider the case likely to be accidental (Porco et al. 2012a). In our data, the sympatry of the lineages showed markedly more frequency than in the west - almost in half of the locations studied (Table 3). The ratio number of sites with lineages sympatry / number of total sites sampled is greater in our findings. In Western and Central Europe this value is 0.8–0.18, while in the East European Plain it is 0.5. The joint occurrence of lineages was noted not only in different

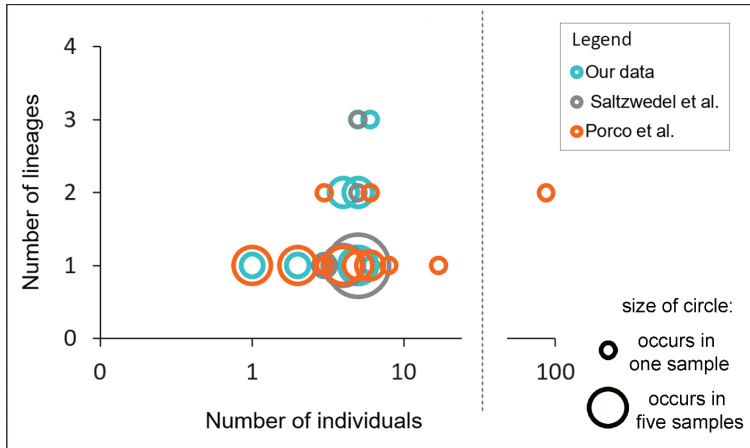


Figure 4. Dependence of the number of detected *P. notabilis* lineages on the number of individuals analyzed in a sample in Europe. The larger the circle, the more samples contain a certain combination of the number of lineages and the number of individuals.

areas of the Moscow region, but also in Voronezh. In Eastern Europe, sympatry of the lineages L2 and L4-Hebert was also found in Estonia (Anslan and Tedersoo 2015).

Presumably, the number of detected lineages in one location may depend on the number of individuals analyzed from a core. Our data shows, however, that even small samples of 4 or 5 individuals sometimes revealed up to three genetic lineages (Fig. 4), while a sample of 17 individuals in Hamburg (Germany) was represented by only one lineage (Porco et al. 2012a). Our material is collected over a relatively small area compared to extensive data from Western Europe. It is possible that the urban condition contributes to the conservation of invasive species (Rebele 1994) and also should concern genetic lineages. Nevertheless, it is hard to ignore that several lineages are found in true natural forests (Shakh-2021-2) located more than 100 km away Moscow city. It is likely that the relatively separated lineages of *P. notabilis* in Western and Central Europe do co-occur in the east. One of the reasons for this phenomenon may be the geologically young postglacial landscape of the region we studied. This flat area had no refugia and broke free from ice only a few tens of thousands of years ago (Velichko et al. 2004) and so it is still an arena of active migratory flows and evolutionarily young communities, which is especially evident in the sedentary groups of organisms (Markova et al. 2008). The species introduced into such young communities are more successful than those introduced into ancient communities. A similar explanation can supplement the discussion of the reasons for the sympatry of *P. notabilis* lineages in Canada as a result of their introduction to North America (Porco et al. 2012a; Saltzwedel et al. 2017). Our hypothesis on parapatry of the lineages in the East European Plain has not been confirmed.

At present, it is difficult to conclude how widespread sympatry of genetic lineages is. For example, sympatry of genetic lineages was found in *Deutonura monticola* (Cassagnau) and *Heteromurus major* (Moniez) among 16 genetically studied Collembola species (Porco et al. 2012b).

Ecological specialization of lineages

Genetic studies of springtails often do not consider the habitats where the material was collected from, or, at least, do not specify them. Saltzwedel et al. (2017) preliminarily supposed that environmental conditions may select for different lineages of *P. notabilis*. We investigated the genetic composition of *P. notabilis* populations not only in natural but also in disturbed habitats. The results showed an association of the L1 lineage with disturbed habitats but L2 and L4-Hebert with natural habitats. This indicates possible differences in tolerance to disturbance among genetic lineages.

The different habitat preferences of genetic lineages reflect the process of ecological diversification within one species, and can lead to the emergence of new species resulting from ecological speciation. For many taxa, such cases were noted based on the action of different selection vectors according to the gradient speciation model (Doebeli and Dieckmann 2003; Endler 2020). This phenomenon was found, for example, in the “*palustris*” group of the genus *Isotomurus*, the genetic analysis of which made it possible to distinguish six species within *I. palustris* (Mueller) *sensu lato* distributed in different sections of the river floodplain profile (Carapelli et al. 1995). Subsequently, broad genetic variability was discovered in many Collembola species, but the cryptic diversity of this taxon was mostly described in terms of genetic lineages rather than independent species (Porco et al. 2012a). Obviously, more genetic, morphological, and ecological information must be accumulated to standardize the criteria for distinguishing Collembola species.

Information on the ecological preferences of genetic lineages is sporadic. Thus, in the widespread springtail species *Lepidocyrtus lanuginosus* the genetic lineage L1 was abundant and occurred in each of the three habitats studied (forests, grassland, arable fields), L2 only in forests, and L3 only in pastures and arable fields (Zhang et al. 2018). A similar diversification is found in *P. notabilis*: one lineage is unspecialized to habitats (L4-Hebert), while two are more specialized, one to natural forests (L2), the other to disturbed habitats (L1). In both species the environmental factors leading to lineage specialization remain unclear. The adaptations of the lineage may be of ecophysiological, nutritional, demographic or migrational nature.

Our results are preliminary and call for more data. However, the assumption that different genetic lineages of *P. notabilis* prefer different degrees of habitat disturbance seems convincing at this point. Samples along the disturbance gradient can reveal the diversity of lineages for one location. The cosmopolitan species *P. notabilis*, abundant in natural and disturbed habitats, is a promising model object for studying the phylogeography of Collembola populations.

Conclusions

Sequencing of the 28S gene is practical and convenient to identify already known genetic lineages while data on the COI gene are needed to describe new lineages. Three genetic lineages of *Parisotoma notabilis* have been detected in the East European Plain: L1, L2, and L4-Hebert. Mean genetic distances between the lineages in the studied

D3–D5 region of ribosomal 28S gene region ranged from 0.9% to 1.4%. About half of the samples in central part of East European Plain included more than one lineage of *P. notabilis*. The samples from different habitats may include different genetic lineages of the species, which is important to take into account in phylogeographic reconstructions. The most diverse genetic composition of *P. notabilis* populations was observed in natural forests and forest parks; only two lineages were found in urban environments. Genetic lineages of *P. notabilis* show ecological specialization: L1 likely prefers disturbed habitats, although L2 and L4-Hebert predominate in natural forests, which requires further research. It is also necessary to focus on the search for characters that could allow the morphological differentiation of the lineages.

Acknowledgements

The authors are grateful to SE Spiridonov, NV Petrova and MD Antipova for advice on molecular genetic analysis and anonymous reviewers for important comments. This work was supported by Grant No. 22-24-00984 of the Russian Science Foundation.

References

- Alvarez T, Frampton GK, Goulson D (1997) Population dynamics of epigeic Collembola in arable fields: the importance of hedgerow proximity and crop type. *Pedobiologia* 41: 110–114. <http://sro.sussex.ac.uk/id/eprint/51314/> [November 10, 2022]
- Anslan S, Tedersoo L (2015) Performance of cytochrome c oxidase subunit I (COI), ribosomal DNA Large Subunit (LSU) and Internal Transcribed Spacer 2 (ITS2) in DNA barcoding of Collembola. *European Journal of Soil Biology* 69: 1–7. <https://doi.org/10.1016/j.ejsobi.2015.04.001>
- Buchholz J, Querner P, Paredes D, Bauer T, Strauss P, Guernion M, Scimia J, Cluzeau D, Burel F, Kratschmer S, Winter S, Pothhoff M, Zaller JG (2017) Soil biota in vineyards are more influenced by plants and soil quality than by tillage intensity or the surrounding landscape. *Scientific Reports* 7(1): e17445. <https://doi.org/10.1038/s41598-017-17601-w>
- Carapelli A, Frati F, Fanciulli PP, Dallai R (1995) Genetic differentiation of six sympatric species of *Isotomurus* (Collembola, Isotomidae); is there any difference in their microhabitat preference? *European Journal of Soil Biology (France)*. <https://agris.fao.org/agris-search/search.do?recordID=FR9606618> [September 26, 2021]
- Chahartaghi M (2007) Trophic niche differentiation, sex ratio and phylogeography of European Collembola. phd. Technische Universität. <http://elib.tu-darmstadt.de/diss/000850> [June 10, 2021]
- Chernova NN, Potapov MB, Savenkova Y, Bokova A (2009) Ekologicheskaya Rol' Partenogeneza u Kollembol. *Zoologicheskii Jurnal* 88: 1455–1470. <https://naukarus.com/ekologicheskaya-rol-partenogeneza-u-kollembol> [November 10, 2022]
- Doebeli M, Dieckmann U (2003) Speciation along environmental gradients. *Nature* 421(6920): 259–264. <https://doi.org/10.1038/nature01274>

- Eitminavičiute I (2006) Microarthropod communities in anthropogenic urban soils. 1. Structure of microarthropod complexes in soils of roadside lawns. *Entomological Review* 86(S2): S128–S135. <https://doi.org/10.1134/S0013873806110029>
- Endler JA (2020) Geographic variation, speciation and clines. (MPB-10), Volume 10. Princeton University Press. <https://doi.org/10.12987/9780691209456>
- Fjellberg A (2007) 42 The Collembola of Fennoscandia and Denmark, Part II: Entomobryomorpha and Symphypleona. Brill, Leiden. <https://doi.org/10.1163/ej.9789004157705.i-265> [November 10, 2022]
- Hall T, Biosciences I, Carlsbad C (2011) BioEdit: An important software for molecular biology. *GERF Bulletin of Biosciences* 2: 60–61.
- Kulbachevskii AO (2021) Doklad o sostoyanii okrujayuschei sredi v gorode Moskve v 2020 godu. Moscow, 330 pp. <https://www.mos.ru/eco/documents/doklady/view/259642220/> [February 28, 2022]
- Kuznetsova N (2002) Biotopic groups of Collembolans in the mixed forest subzone of Eastern Europe. *Entomological Review* 82: 1047–1057. <https://istina.msu.ru/publications/article/128149331/> [November 10, 2022]
- Markova A, Kolfshoten T, Bohnke S, Kosinsev PA, Mol J, Puzachenko A, Simakova AN, Smirnov N, Verpoorte A Golovachev IV (2008) Evolution of European Ecosystems during Pleistocene–Holocene Transition (24–8 Kyr BP). KMK Scientific Press, Moscow. [November 10, 2022]
- Nadezhdina TS, Kuznetsova NA (2010) The influence of recreational load on soil-dwelling collembolans in different forest associations. *Entomological Review* 90(4): 415–422. <https://doi.org/10.1134/S0013873810040020>
- Petersen H, Krogh PH (1987) Effects of perturbing microarthropod communities of a permanent pasture and a ryefield by an insecticide and a fungicide. In: *Soil fauna and soil fertility*. Moscow, 217–229.
- Porco D, Potapov M, Bedos A, Busmachiu G, Weiner WM, Hamra-Kroua S, Deharveng L (2012a) Cryptic Diversity in the Ubiquist Species *Parisotoma notabilis* (Collembola, Isotomidae): A Long-Used Chimeric Species? *PLoS ONE* 7(9): e46056. <https://doi.org/10.1371/journal.pone.0046056>
- Porco D, Bedos A, Greenslade P, Janion C, Skarżyński D, Stevens MI, van Vuuren BJ, Deharveng L, Porco D, Bedos A, Greenslade P, Janion C, Skarżyński D, Stevens MI, van Vuuren BJ, Deharveng L (2012b) Challenging species delimitation in Collembola: Cryptic diversity among common springtails unveiled by DNA barcoding. *Invertebrate Systematics* 26(6): 470–477. <https://doi.org/10.1071/IS12026>
- Potapov M (1991) Species of the genus *Isotoma* subgenus *Parisotoma* Bagnall, 1940 and *Sericeotoma* subgen. nov. (Collembola, Isotomidae) of USSR fauna. *Acta Zoologica Cracoviensia* 34: 267–301. [http://www.isez.pan.krakow.pl/journals/azc/pdf/azc_i/34\(1\)/34\(1\)_06.pdf](http://www.isez.pan.krakow.pl/journals/azc/pdf/azc_i/34(1)/34(1)_06.pdf) [November 10, 2022]
- Potapov M (2001) Synopses on Palaearctic Collembola: Isotomidae. *Abhandlungen und Berichte des Naturkundemuseums Gorlitz* 73: 1–603. <https://www.nhbs.com/synopses-on-palaearctic-collembola-volume-3-isotomidae-book> [November 10, 2022]

- Potapov M, Janion-Scheepers Ch (2019) Longitudinal invasions of Collembola within the Palearctic: new data on non-indigenous species. In: Abstracts of 10th International Seminar on Apterygota. Paris, France, 46–46. https://isa10.sciencesconf.org/data/pages/ISA10_2019_Programme_Final.pdf [November 10, 2022]
- Potapov M, Kuznetsova NA, Janion-Scheepers C, Bokova AI, Panina KS (2021) Alien species of Collembola in agroecosystems in the European part of Russia. In: Invasion of alien species in Holarctic. Borok-VI., 184.
- Prendini L, Weygoldt P, Wheeler WC (2005) Systematics of the *Damon variegatus* group of African whip spiders (Chelicerata: Amblypygi): Evidence from behaviour, morphology and DNA. *Organisms, Diversity & Evolution* 5(3): 203–236. <https://doi.org/10.1016/j.ode.2004.12.004>
- Ramirez-Gonzalez R, Yu DW, Bruce C, Heavens D, Caccamo M, Emerson BC (2013) PyroClean: Denoising pyrosequences from protein-coding amplicons for the recovery of interspecific and intraspecific genetic variation. *PLoS ONE* 8(3): e57615. <https://doi.org/10.1371/journal.pone.0057615>
- Rebele F (1994) Urban ecology and special features of urban ecosystems. *Global Ecology and Biogeography Letters* 4(6): 173–187. <https://doi.org/10.2307/2997649>
- Saltzwedel H, Scheu S, Schaefer I (2017) Genetic structure and distribution of *Parisotoma notabilis* (Collembola) in Europe: Cryptic diversity, split of lineages and colonization patterns. *PLoS ONE* 12(2): e0170909. <https://doi.org/10.1371/journal.pone.0170909>
- Striuchkova A, Potapov M, Kuznetsova N, Malykh I (2022) Genetic lineages of *Parisotoma notabilis* s. l. (Collembola, Isotomidae) in the East European Plain. Version 1.3. Moscow Pedagogical State University (MPSU). Sampling event dataset. <https://doi.org/10.15468/5rm9kz> [accessed via GBIF.org on 2022-12-07]
- Sun X, Bedos A, Deharveng L (2018) Unusually low genetic divergence at COI barcode locus between two species of intertidal *Thalassaphorura* (Collembola: Onychiuridae). *PeerJ* 6: e5021. <https://doi.org/10.7717/peerj.5021>
- Tamura K, Stecher G, Kumar S (2021) MEGA11: Molecular Evolutionary Genetics Analysis Version 11. *Molecular Biology and Evolution* 38(7): 3022–3027. <https://doi.org/10.1093/molbev/msab120>
- Velichko AA, Faustova MA, Gribchenko YN, Pisareva VV, Sudakova NG (2004) Glaciations of the East European Plain—distribution and chronology. *Developments in Quaternary Science* 2: 337–354. [https://doi.org/10.1016/S1571-0866\(04\)80083-6](https://doi.org/10.1016/S1571-0866(04)80083-6)
- Whiting MF (2002) Mecoptera is paraphyletic: Multiple genes and phylogeny of Mecoptera and Siphonaptera. *Zoologica Scripta* 31(1): 93–104. <https://doi.org/10.1046/j.0300-3256.2001.00095.x>
- Winkler D, Bidló A, Bolodár-Varga B, Erdő Á, Horváth A (2018) Long-term ecological effects of the red mud disaster in Hungary: Regeneration of red mud flooded areas in a contaminated industrial region. *The Science of the Total Environment* 644: 1292–1303. <https://doi.org/10.1016/j.scitotenv.2018.07.059>
- Zhang B, Chen T-W, Mateos E, Scheu S, Schaefer I (2018) Cryptic species in *Lepidocyrtus lanuginosus* (Collembola: Entomobryidae) are sorted by habitat type. *Pedobiologia* 68: 12–19. <https://doi.org/10.1016/j.pedobi.2018.03.001>

Appendix I

Table A1. Sample locations and GenBank Accession numbers of genetic lineages of *Parisotoma notabilis*.

Habitat	Label	GPS Coordinates	N	Lineage	GenBank Accession number						
					28S	COI					
Urban green	Balash-2021-1*	55°49'54.1069'N, 37°58'2.7689'W	1	L1	OM714597						
	ProspVernad-2020-1	55°40'54.2149'N, 37°30'22.6072'W	5	L1	OM746101–OM746105						
	UgoZapad-2020-1*	55°39'34.8097'N, 37°28'46.7176'W	2	L1	OM778178, OM778179						
	VDNH-2020-1	55°48'58.5949'N, 37°39'0.3845'W	5	L1	OM778173–OM778177						
	Voronezh-2021-1	51°39'33.9962'N, 39°12'7.1375'W	2	L1	OM778153, OM778154,						
Forest Park	Hovrino-2020-1	55°52'24.7849'N, 37°28'42.3077'W	6	L1	OM728286–OM728291	OP861639– OP861643 (L1)					
							ProspVernad-2020-2	55°41'8.5393'N, 37°30'4.5928'W	5	L1	OM746085–OM746089
							ProspVernad-2020-3	55°41'9.5113'N, 37°29'46.7008'W	3	L1	OM746096–OM746098
	ProspVernad-2020-4	55°40'53.4301'N, 37°29'59.8372'W	4	L1	OM746081–OM746084,	OP866972 (L1)					
							1	L4-Hebert	OM746095		
	VDNH-2020-2	55°48'48.6229'N, 37°39'55.4105'W	1	L1	OM778143, OM778144,	OP861659 (L2)					
							2	L2	OM778150–OM778152,		
							3	L4-Hebert	OM778181		
	Maklino-2021-1	54°59'43.8770'N, 36°27'25.7931'W	5	L4-Hebert	OM746090–OM746094						
	Nature forest	Balash-2020-1*	55°49'52.4545'N, 37°54'22.9853'W	1	L2	OM714532					
OrehZuev-2020-3		55°46'43.2060'N, 39°16'13.9757'W	1	L2	OM745895, OM746106–						
							3	L4-Hebert	OM746108		
SeloBulat-2021-1*		55°31'1.9789'N, 37°40'38.7112'W	2	L4-Hebert	OM746099, OM746100						
Shakh-2021-1		55°56'33.8150'N, 35°31'45.7780'W	3	L2	OM778155–OM778157						
Shakh-2021-2		55°55'55.7450'N, 35°37'9.4468'W	1	L1	OM778148, OM778149,	OP861657 (L2)					
							2	L2	OM778169–OM778171		
Shakh-2021-3		55°56'0.2990'N, 35°37'20.9560'W	4	L2	OM778164–OM778168	OP861658 (L2)					
							1	L4-Hebert			
Shakh-2021-5		55°59'1.6022'N, 35°35'41.5816'W	3	L2	OM778145–OM778147,						
							1	L4-Hebert	OM778180		
Shakh-2021-6		55°59'2.4266'N, 35°35'50.4664'W	2	L2	OM757828–OM757831,	OP861662– OP861664					
							4	L4-Hebert	OM778140, OM778141		
Shakh-2021-8	55°59'30.6829'N, 36°14'57.8500'W	1	L2	OM778142, OM778161–							
						3	L4-Hebert	OM778163			
Shakh-2021-9	55°59'14.9005'N, 37°2'57.3605'W	5	L4-Hebert	OM778135–OM778139							

*Not used in calculating the number of lineages per location. N: number of specimens

**GenBank Accession number of Saltzwedel et al. (2017) used in building the tree (Fig. 1.): KJ792225, KJ792230, KJ792235, KJ792240, KJ792244, KJ792249, KJ792254, KJ792263, KJ792268, KJ792272, KJ792277, KJ792282, KJ792287, KJ792291, KJ792295, KJ792299, KJ792304, KJ792309, KJ792314, KJ792319, KJ792324, KJ792327, KJ792332, KJ792335, KJ792340.

Appendix 2

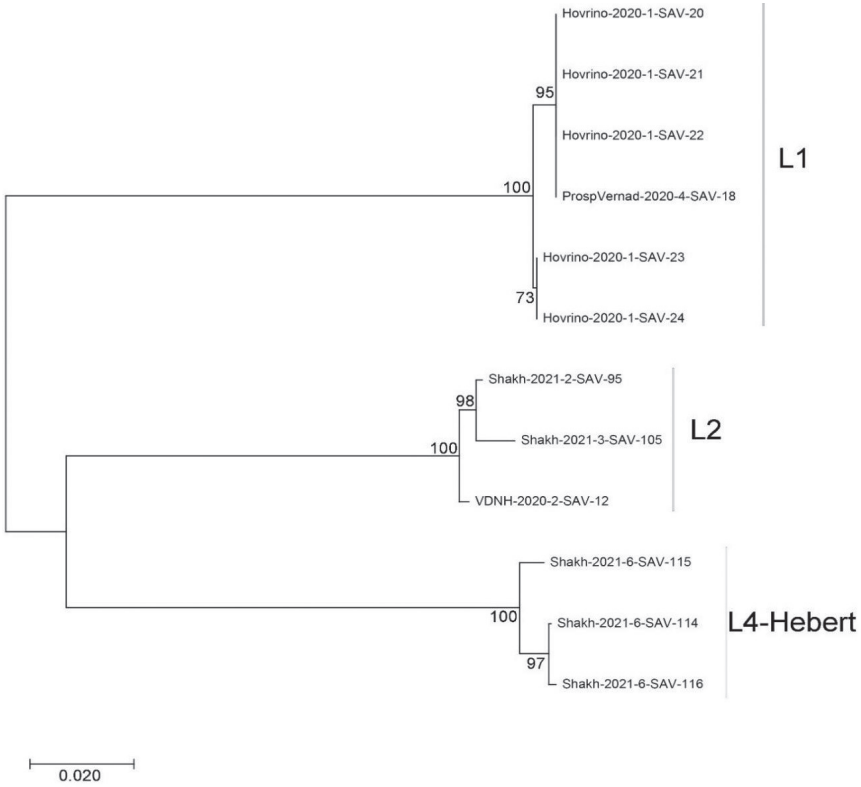


Figure A1. Neighbor-Joining genetic tree of three lineages of *P. notabilis* based of COI gene fragment (Bootstrap support values showed on the branches, bar is genetic distance).

Appendix 3

Table A2. Intralinesage and interlinesage K2P-pairwise distances (%) of tree lineages *Parisotoma notabilis* in the East European Plain for COI gene.

Lineage	Intralinesage	Interlinesage	
		L1	L2
L1	0.20	0	
L2	0.76	19.84	0
L4-Hebert	0.59	20.74	17.33

Molecular data from the holotype of the enigmatic Bornean Black Shrew, *Suncus ater* Medway, 1965 (Soricidae, Crocidurinae), place it in the genus *Palawanosorex*

Jonathan A. Nations^{1,2,3,4}, Thomas C. Giarla⁵, Muhd Amsyari Morni⁶, Julius William Dee⁶, Mark T. Swanson^{1,2}, Anna E. Hiller^{1,2}, Faisal Ali Anwarali Khan⁶, Jacob A. Esselstyn^{1,2}

1 Museum of Natural Science, Louisiana State University, Baton Rouge, LA 70803, USA **2** Department of Biological Sciences, Louisiana State University, Baton Rouge, LA 70803, USA **3** Current Address: Department of the Geophysical Sciences, University of Chicago, Chicago, IL 60637, USA **4** Current Address: Field Museum of Natural History, Chicago, IL 60605, USA **5** Department of Biology, Siena College, 515 Loudon Rd., Loudonville, NY 12211, USA **6** Faculty of Resource Science and Technology, Universiti Malaysia Sarawak, 94300 Kota Samarahan, Sarawak, Malaysia

Corresponding author: Jonathan A. Nations (jonnations@gmail.com)

Academic editor: Nedko Nedyalkov | Received 29 August 2022 | Accepted 3 November 2022 | Published 21 December 2022

<https://zoobank.org/2D39D3D7-01B2-47D1-90C4-6102B909C5D9>

Citation: Nations JA, Giarla TC, Morni MA, William Dee J, Swanson MT, Hiller AE, Khan FAA, Esselstyn JA (2022) Molecular data from the holotype of the enigmatic Bornean Black Shrew, *Suncus ater* Medway, 1965 (Soricidae, Crocidurinae), place it in the genus *Palawanosorex*. ZooKeys 1137: 17–31. <https://doi.org/10.3897/zookeys.1137.94217>

Abstract

Although Borneo has received more attention from biologists than most other islands in the Malay Archipelago, many questions regarding the systematic relationships of Bornean mammals remain. Using next-generation sequencing technology, we obtained mitochondrial DNA sequences from the holotype of *Suncus ater*, the only known specimen of this shrew. Several shrews collected recently in Sarawak are closely aligned, both morphologically and mitochondrially, with the holotype of *S. ater*. Phylogenetic analyses of mitochondrial sequences indicate that the *S. ater* holotype and new Sarawak specimens do not belong to the genus *Suncus*, but instead are most closely related to *Palawanosorex muscorum*. Until now *Palawanosorex* has been known only from the neighboring Philippine island of Palawan. Additional sequences from nuclear ultra-conserved elements from the new Sarawak specimens strongly support a sister relationship to *P. muscorum*. We therefore transfer *ater* to *Palawanosorex*. The new specimens demonstrate that *P. ater* is more widespread in northern Borneo than previously recorded. Continued sampling of Bornean mammal diversity and reexamination of type material are critical in understanding the evolutionary history of the biologically rich Malay Archipelago.

Keywords

Borneo, *Palawanosorex*, Southeast Asia, Sunda Shelf, ultraconserved elements

Introduction

The biological richness of Borneo inspired the fields of evolutionary biology and biogeography (Wallace 1869). Nevertheless, Borneo's flora and fauna remain woefully understudied. One mammalian group that exemplifies this problem is the white-toothed shrews (Soricidae, Crocidurinae). Currently, five species are recognized from the island, three in the genus *Crocidura* Wagler, 1832 (*C. foetida* Peters, 1870, *C. neglecta* Jenkins, 1888, and *C. baluensis* Thomas, 1898) and two in the genus *Suncus* Ehrenberg, 1832 (*S. ater* Medway, 1965, and *S. hosei* Thomas, 1893). However, uncertainty remains regarding the number of species, particularly due to the presence of three named subspecies of *C. foetida* and the possible presence of *C. nigripes* Miller & Hollister, 1921 (Hinckley et al. 2022). The lack of clarity regarding the diversity of shrews from Borneo is primarily due to the paucity of specimens from the island and, secondarily, a lack of genetic data from type material.

Arguably the most enigmatic shrew from Borneo is the Black Shrew, *Suncus ater*, which, to our knowledge, is known only from the holotype. The holotype (MCZ 36547; Museum of Comparative Zoology, Harvard University, Cambridge, MA, USA) was collected in 1937 around 1675 m (5,500 ft) elevation on Mount Kinabalu, Sabah, Malaysia (Griswold 1939). It was originally identified as *C. foetida*. However, Medway (1965) revisited the shrews of Borneo and determined that this specimen represented an undescribed species of the widespread genus *Suncus*. The generic identification was largely attributed to the presence of a fifth unicuspid that is characteristic of *Suncus* but is lacking in *Crocidura*. Additionally, the dark black pelage, dark hands and feet, and short tail relative to head-body length clearly distinguished the specimen from *C. foetida*. Medway (1965) suggested that this shrew is vastly different from any other Southeast Asian shrew but closely aligned with *Suncus dayi* Dobson, 1888 from southern India.

No other specimens of *S. ater* have been reported in the literature. However, a single specimen labeled as *S. ater* is cataloged in the Field Museum of Natural History, Chicago, USA (FMNH 159012). We inspected this specimen and quickly determined it to be much smaller than the type of *S. ater* (length of skull = 14 mm vs 21 mm in the *S. ater* holotype), and instead it likely represents *S. hosei*, a putative member of the *Suncus etruscus* Savi, 1822 species complex (Corbet and Hill 1992; Hutterer 2005; Omar et al. 2013). We recently sampled small mammals from two locations in northern Sarawak, Malaysia (Fig. 1) and recovered several medium-sized, dark-colored shrews with relatively short tails and a fifth unicuspid that match the physical description of *S. ater* (Medway 1965). We sequenced mitochondrial DNA from the holotype of *S. ater* and mitochondrial and nuclear DNA from the new Sarawak specimens to determine the phylogenetic placement of the holotype and our new specimens.

Methods

Fieldwork

We surveyed small mammals in two locations in Sarawak, Malaysia (Fig. 1): Mount Mulu (in 2017) and Mount Murud (in 2019). Both surveys used pitfall lines, which typically consisted of 5–10 large, 20–30 L buckets with a tarp drift fence, though occasionally we added smaller 1–3 L buckets. On Mount Mulu we set two pitfall lines of large buckets at 1650 m and one pitfall line of large buckets at 1800 m for a total of ca. 300 pitfall-nights. On Mount Murud we set pitfall lines (mixed large and small buckets) at 1480 m, 1660 m, 1770 m, 2000 m, 2250 m, and 2400 m for a total of ca. 440 pitfall-nights. Specimens were deposited at the Louisiana State University Museum of Natural Science, Baton Rouge, USA (LSUMZ). Specimens were measured, weighed, and then preserved in formalin (often with the skull removed and cleaned) or prepared as dried museum skins with dried and cleaned skeletons. Tissues were preserved in 95% ethanol. All collecting methods followed the recommended guidelines of the American Society of Mammalogists (Sikes et al. 2016).

Specimen sampling, DNA extraction, and sequencing

Using a phenol-chloroform extraction protocol (Tsai et al. 2020), we extracted DNA from skin clips of the holotype of *S. ater* and a species from an outgroup genus (*Solisorex pearsoni* Thomas, 1924), as well as fresh tissues from three recently collected specimens from Sarawak that are morphologically aligned with *S. ater* (LSUMZ 40511, 40514, 40522). We modified the phenol-chloroform extraction of Tsai et al. (2020) by using a refrigerated centrifuge set at 3 °C during the ethanol precipitation steps. In addition to the phenol-chloroform extraction, we extracted genomic DNA from tissue samples (liver) from six Sarawak shrew specimens morphologically similar to *S. ater* (LSUMZ 40511, 40514, 40522, 40695, 40696, 40697) using Qiagen DNEasy Blood & Tissue kits (Qiagen, Germantown, Maryland) following the manufacturer's instructions.

Phenol-chloroform extractions from skin clip samples (*S. ater* holotype and *S. pearsoni*) were treated with a New England BioLabs (Ipswich, MA) PreCR Repair Kit following the manufacturer's instructions to repair preservation-related damage. For the phenol-chloroform extractions from the three fresh samples, we mechanically sheared the DNA to a 400–600 bp size range using an Epigentek Episonic sonicator. We prepared genomic libraries for all five phenol-chloroform extractions with a KAPA Hyper Prep kit and dual indexed iTru adapters (Glenn et al. 2019) following Esselstyn et al. (2017). Because the *S. ater* holotype extraction had a very small amount of DNA, we used diluted index primers at 1.25 μM (a quarter of the standard molarity) for this specimen. We then pooled the libraries and enriched them for the standard Tetrapods 5k loci (Faircloth et al. 2012) and 27 exons using the probe set introduced by Esselstyn et al. (2021) and manufactured by Arbor Biosciences (Ann Arbor, MI). We removed short fragments less than 150 base pairs from the enriched pools with a QIAGEN GeneRead Size Selection kit and

confirmed the absence of adapter dimers with an Agilent Bioanalyzer using a DNA-High Sensitivity Kit. We then combined the enriched libraries into an equimolar pool with an unenriched library from the *S. ater* holotype specimen in order to enhance the likelihood of sequencing mitochondrial fragments from this specimen. Novogene (Beijing, China) sequenced these libraries on an Illumina HiSeq 4000 PE 150 lane (Illumina Inc., San Diego, CA, USA). For the six fresh tissue Qiagen DNEasy extractions, we amplified the mitochondrial protein coding gene cytochrome *b* [CYTB] using Polymerase Chain Reaction (PCR) following the protocol described in Esselstyn et al. (2009).

Bioinformatics

We processed the UCEs in PHYLUCE v. 1.7.1 (Faircloth 2016), following Tutorial III guidelines. We processed raw Illumina reads with illumiprocessor (Faircloth 2013) and assembled trimmed reads into contigs using both Trinity v. r2013.08.14 (Grabherr et al. 2011) and SPAdes v. 3.14.1 (Prjibelski et al. 2020); we chose the assembler run that resulted in the largest number of UCE loci for final analyses. Contigs matching the UCE probes were aligned in MAFFT v. 7.475 (Katoh and Standley 2013) and edge-trimmed in PHYLUCE using trimmomatic (Bolger et al. 2014). Unfortunately, we did not obtain UCEs from the *S. ater* holotype. To obtain mitochondrial bycatch from the UCE data for three samples (the *S. ater* holotype, LSUMZ 40514, 40522) we also assembled reads into contigs using both metaSPAdes v. 3.14.1 (Nurk et al. 2017) and MEGAHIT (Li et al. 2016) as part of the MitoFinder pipeline (Allio et al. 2020). We then searched through the assembled contigs using several different mitochondrial genomes as references to improve our recovery of the mitochondrial data: *Suncus murinus* Linnaeus, 1766, *Crocidura attenuate* Milne-Edwards, 1872, *C. dongyangjiangensis* Liu Yang et al., 2020, *C. lasiura* Dobson, 1890, *C. russula* Hermann, 1780, *C. grayi* (Dobson, 1890), *C. fuliginosa* Blyth, 1855, and *C. beata* Miller, 1910 (GenBank: NC_024604.1, KP120863.2, NC_056167.1, KR007669.1, NC_056768.1, KR537885.1, C_042762.1, KR537889.1). The resulting contigs were combined with the original Trinity or SPAdes contigs from the UCE assemblies and then aligned and annotated for 15 mitochondrial genes using the *Crocidura shantungensis* Miller, 1901 mitochondrial genome (GenBank: OM038325) as a reference in Geneious. Finally, we downloaded previously published mitochondrial and UCE sequences from other outgroups, mostly matching the taxon sampling in Hutterer et al. (2018).

We assembled an alignment of ten mitochondrial genes using a combination of newly generated sequences and sequences from GenBank (Suppl. material 1). For several outgroup species (*Crocidura palawanensis* Taylor, 1934, *C. russula*, *C. sibirica* Dukelski, 1930, and *Suncus murinus*), gene sequences were pulled from whole mitochondrial genomes that were available via GenBank. We included CYTB sequences from the recently collected Bornean material, as well as CYTB and 16s rRNA sequences from *Suncus dayi* to test the relationship proposed by Medway (1965). We partitioned the dataset by gene and, for all but 16s rRNA, by codon position (28 data subsets). We tested for the best partitioning scheme and best fitting model using ModelFinder (Kalyaanamoorthy et

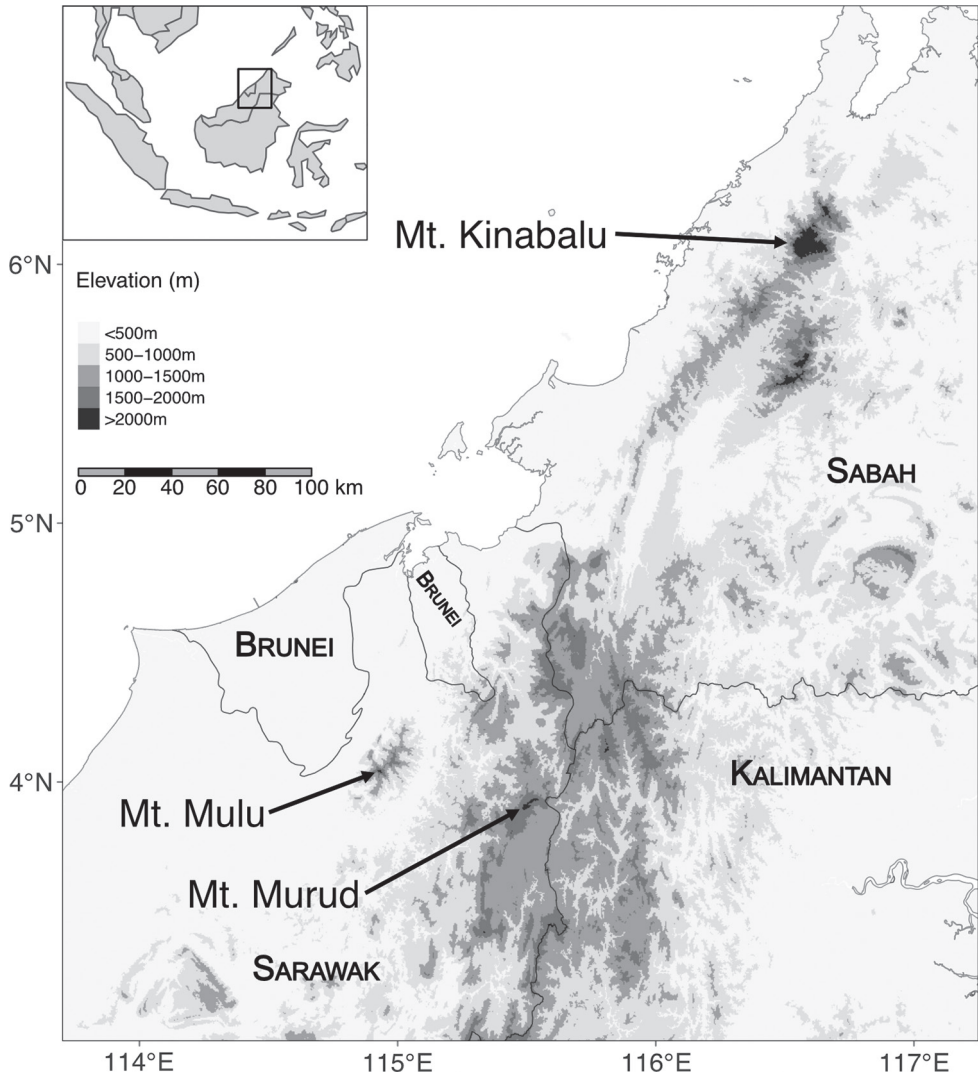


Figure 1. Map of northern Borneo showing the type locality of *Suncus ater* (Mount Kinabalu) and recently surveyed sites in Sarawak (Mounts Mulu and Murud).

al. 2017) in IQ-TREE (Minh et al. 2020). We then conducted a maximum-likelihood (ML) phylogenetic analysis in IQ-TREE, assessing nodal support with 1000 ultrafast bootstrap replicates. In order to verify our results with a lower percentage of missing data, we constructed a second alignment of nine mitochondrial genes by removing eight samples that were only represented with CYTB. We repeated the same IQ-TREE analysis on this second mitochondrial DNA alignment of 20 samples. We generated CYTB p -distances for each sample in the first 28 specimen alignment, and the p -distances of nine mitochondrial genes from the second 20 specimen alignment.

We analyzed the 19-specimen UCE dataset using two different approaches: (1) a concatenated ML analysis, and (2) a two-step species tree analysis. For the concatenated analysis, we first identified a set of alignments that met two requirements: each had to comprise at least 14 sequences (i.e., 75% complete) and be at least 300 bp long. We concatenated the alignments in PHYLUCE and analyzed the dataset in IQ-TREE following the same protocol as for the mitochondrial dataset (except we did not partition the dataset). For the two-step species-tree analysis, we first inferred a gene tree in IQ-TREE for each UCE alignment with at least four sequences and at least 300 bp. For each alignment, we tested substitution models but did not estimate nodal support. We then subjected the resulting gene trees to TreeShrink (Mai and Mirarab 2018) to remove any outlier long branches. This final set of gene trees was then used as input for a species tree analysis in ASTRAL v. 5.7.7 (Zhang et al. 2018). Nodal support was measured using local posterior probabilities, a quartet-based support metric.

Results

Fieldwork

The 2017 and 2019 fieldwork in Sarawak recovered three species of shrews: *Crocidura foetida*, *C. neglecta*, and several specimens of a medium-sized, dark-colored shrew with relatively short tails. Nearly all shrews were captured in pitfall traps. *Crocidura foetida* and *C. neglecta* were captured in the same traplines as the dark-colored shrews, suggesting all syntopy among all three species.

Phylogenetics

The 10-gene mitochondrial dataset comprised 10,399 bp of sequence data; 48.0% of the data matrix was missing. Newly generated mitochondrial sequence data are available on GenBank (Suppl. material 1). ModelFinder partitioned the dataset into seven subsets and identified the best-fitting nucleotide substitution model for each (Suppl. material 2). The mitochondrial phylogeny shows that the holotype of *Suncus ater* is sister to the six recently collected, dark-colored shrews from northern Sarawak (Fig. 2). Furthermore, the *S. ater* clade is sister to a clade of the Palawan endemic, *Palawanosorex muscorum* Hutterer et al., 2018, a recently described crocidurine genus (Hutterer et al. 2018). The second nine-gene mitochondrial dataset had 29% missing data. The resulting estimated phylogeny is similar to the 10-gene topology, with the only changes occurring in the branching pattern of distantly related *Crocidura* taxa (Suppl. material 3). We found that the average CYTB *p*-distance between the five *P. muscorum* samples and the six newly collected, dark colored shrews is 11.77% (SD = 0.50%). These two species are distant relatives of species currently placed in the genus *Suncus*. The average mtDNA *p*-distance of *P. muscorum* and the two newly collected, dark-colored shrews in the nine-gene alignment, without CYTB, is 17.75%. The average nine-gene mtDNA *p*-distance of the *S. ater* holotype and the two newly collected, dark-colored shrews is 3.6%.

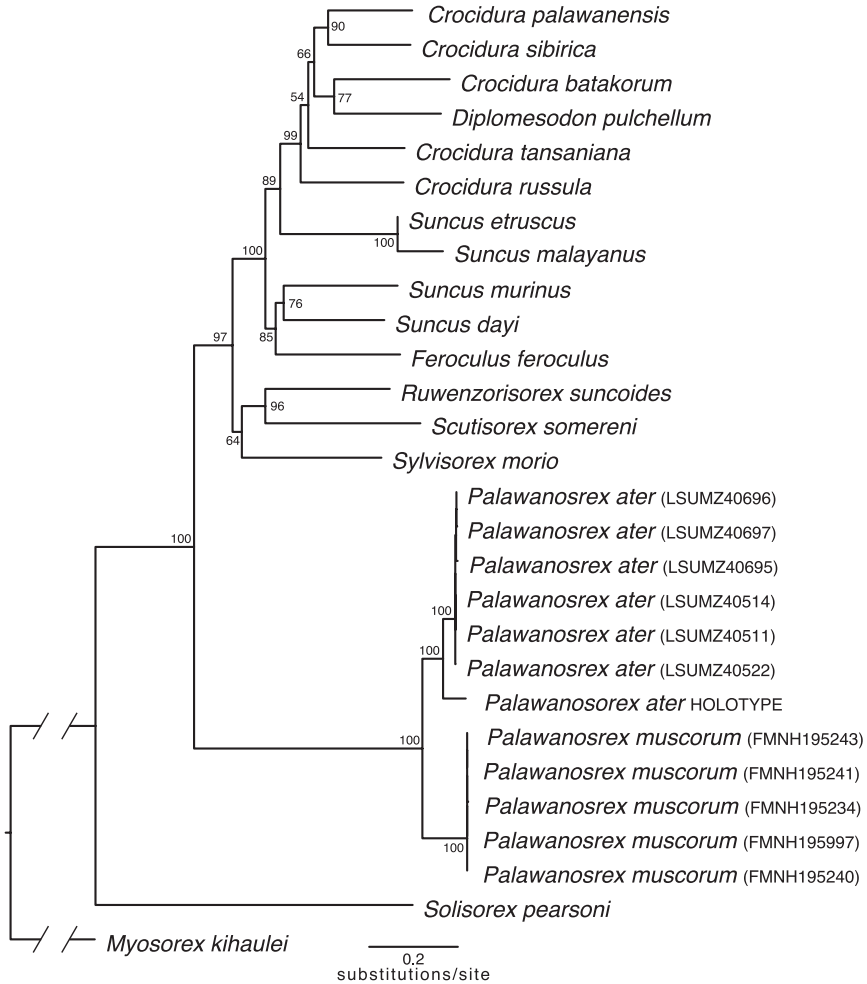


Figure 2. Maximum-likelihood crocidurine mitochondrial gene tree inferred in IQTree. Bootstrap values are given at the nodes. The holotype of *ater* (MCZ36574) forms a clade with the specimens recently collected in Sarawak. The outgroup branch to *Myosorex kahaulei* has been truncated.

The complete UCE dataset (which included only those alignments with more than four sequences and that were at least 300 bp long) included 3,757 loci and 2,175,243 bp of sequence data; 12.9% of the alignments overall were represented by missing data. The mean locus length was 579 bp (range: 300–1,864). All Illumina reads and UCE sequences are available as NCBI BioProject PRJNA901984 (Suppl. material 1). UCE data were not recovered from the *S. ater* holotype. However, the concatenated ML phylogeny places the Sarawak specimens as sister to *P. muscorum*. The *S. ater* + *P. muscorum* clade is not aligned with any species in the genus *Suncus* (Fig. 3A). The two-step species tree recovered nearly the same topology as the concatenated ML phylogeny with no changes to the relationship between *S. ater*, *P. muscorum*, and other members of the genus *Suncus* (Fig. 3B).

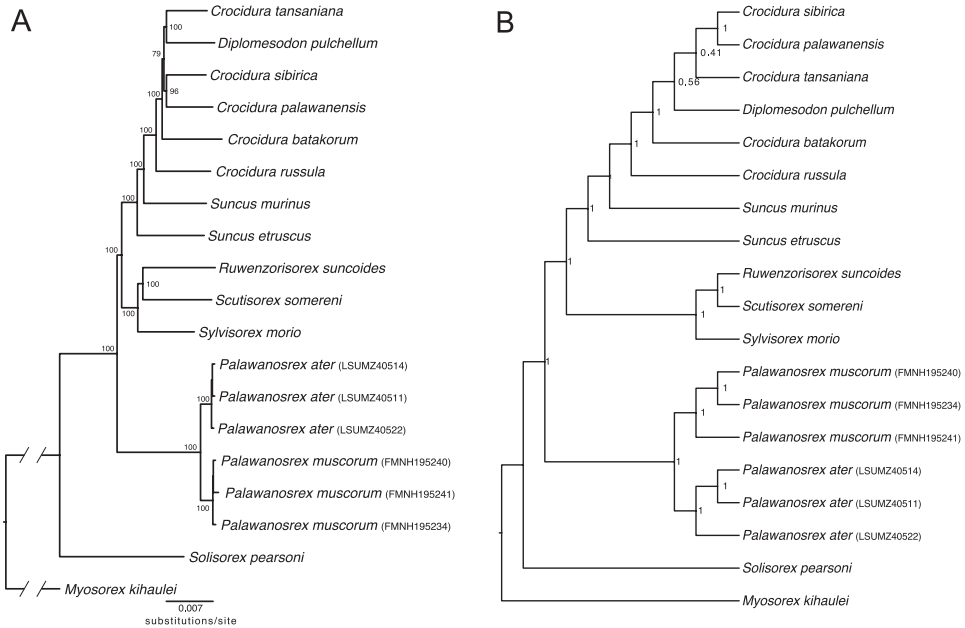


Figure 3. Phylogenetic hypotheses from UCE data. The tree topologies are very similar between the two methods. **A** phylogenetic tree inferred using 3,757 concatenated UCE loci (2,175,243 base pairs) in IQTree. Bootstrap supports are provided at the nodes. The branch leading to outgroup *Myosorex kibaulei* has been truncated for display **B** species tree inferred using ASTRAL. Nodal supports are given in local posterior probabilities. ASTRAL tree is presented as ultrametric with uninformative branch lengths.

Nomenclature

Mitochondrial DNA from the holotype of *Suncus ater* revealed that it is closely aligned with the six newly collected, dark-colored shrews from Borneo, and that this clade is sister to the species *Palawanosorex muscorum*, a recently described genus and species known only from the Philippine island of Palawan, north of Borneo (Hutterer et al. 2018). Phylogenetic estimates from UCE data support the mitochondrial results, showing that the newly collected Bornean shrews, which are mitochondrially aligned to the *S. ater* holotype, are sister to *P. muscorum*. However, *P. muscorum* is much larger, has a much longer tail that lacks any bristles, and has several cranial characters that clearly distinguish it from *S. ater* (Fig. 4; see detailed comparison by Hutterer et al. 2018: 526), and the average CYTB distance between these two species is 11.77%, indicating a long history of reproductive isolation. Therefore, molecular evidence strongly demonstrates that *S. ater* has a sister relationship with *P. muscorum*. For this reason, we transfer *S. ater* to *Palawanosorex*. Furthermore, based on mitochondrial DNA and morphological data, we also assign the specimens collected in two localities in Sarawak to *P. ater*, substantially increasing the known geographic range of this species and demonstrating that it is not confined to the slopes of Mount Kinabalu in Sabah, Malaysia.

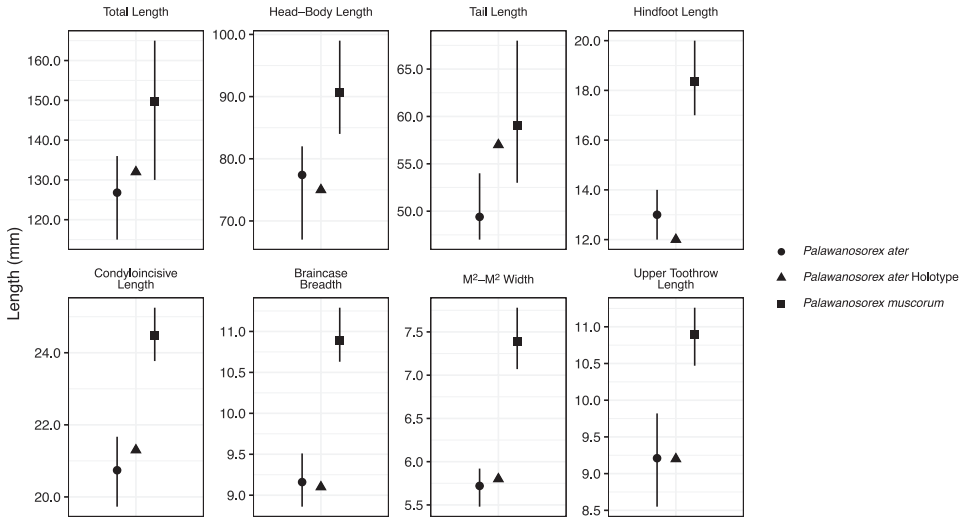


Figure 4. The holotype of *Palawanosorex ater* largely matches the external and cranial measurements of *P. ater* specimens captured in Sarawak, not *P. muscorum*. Each panel represents a measurement, and the *y*-axis represents the measurement length in mm. Each species is represented by a different shape. The upper and lower bounds of the point intervals represent the maximum and minimum values for each measurement for each species. Measurements are limited to those reported in the description of *Suncus ater* (Medway 1965). *Palawanosorex ater* measurements are taken from six specimens collected in Sarawak, Malaysia. *Palawanosorex muscorum* measurements are taken from Hutterer et al. (2018: tables 1, 2). LSUMZ 40695 has a cropped tail and was removed from the total length and tail length measurements.

We note that many of the proposed synapomorphies of the genus *Palawanosorex* no longer apply. The body size and appendage lengths of *P. ater* are all much smaller than *P. muscorum*. Additionally, as noted by Hutterer et al. (2018), *P. ater* does not have the long claws, bare interdigital surfaces, bristle-free tail, wide antorbital bridge, nor the reduced-size P4 and molars of *P. muscorum*. We do note that, although lacking in the *P. ater* holotype, the Sarawak specimens do have dorsal foramina in various stages of fusion (Fig. 5), similar to *P. muscorum* (Hutterer et al. 2018).

Discussion

Our investigation of the phylogenetic placement of the enigmatic Bornean Black Shrew revealed that it represents the second member of the newly described crocidurine genus *Palawanosorex* (Hutterer et al. 2018). As such, five species from three crocidurine genera (*Crocidura*, *Palawanosorex*, and *Suncus*) are considered endemic to Borneo, although recent phylogeographic studies have shown that this number may be an underestimate (Hinckley et al. 2022). All of the native, non-volant mammals endemic to Palawan have their closest relatives in Borneo (Heaney 1986; Esselstyn et al. 2004; Piper et al. 2011).

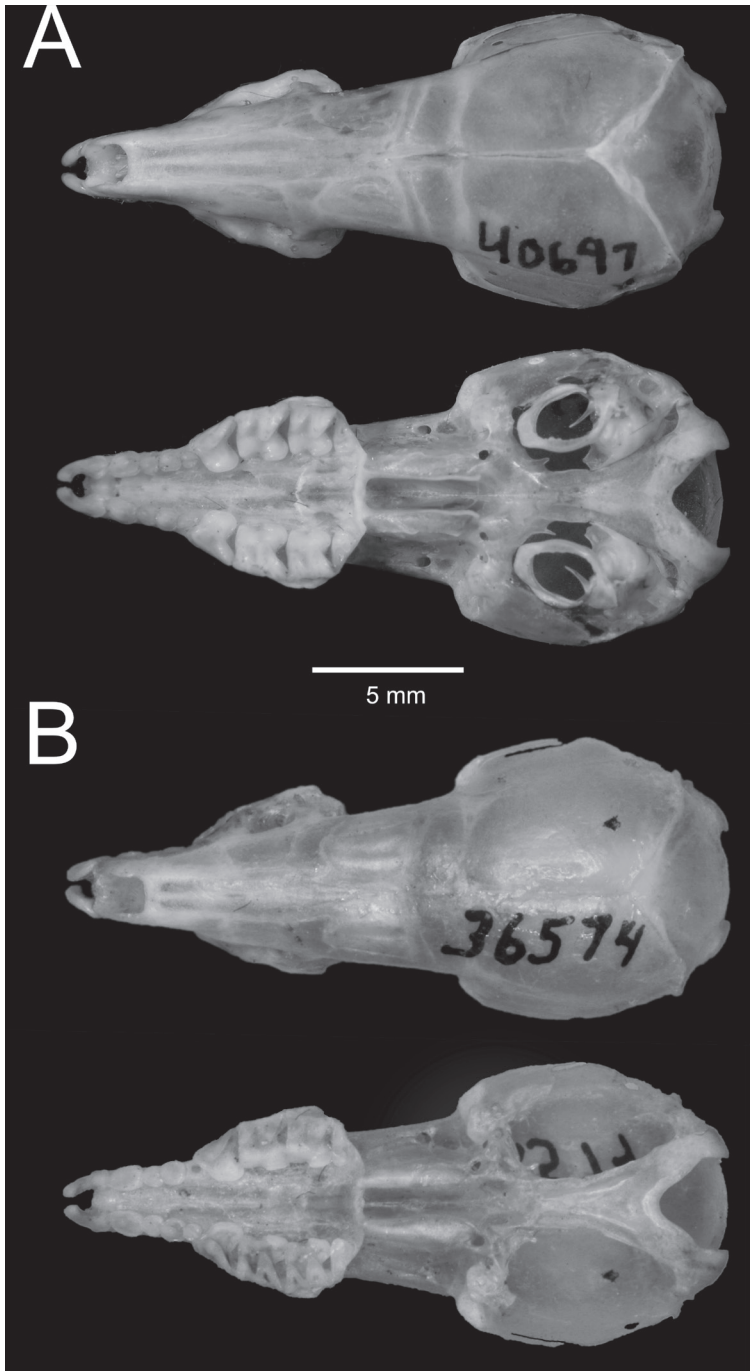


Figure 5. **A** dorsal and ventral views of the cranium of LSUMZ 40697, *Palawanosorex ater*, collected on Mount Murud, Sarawak, Malaysia. Photo by Heru Handika **B** dorsal and ventral views of the holotype of *P. ater*, MCZ 36574, collected on Mt. Kinabalu, Sabah, Malaysia. Photo by Museum of Comparative Zoology, Harvard University, President and Fellows of Harvard College.

Hutterer et al. (2018) hypothesized, correctly, that, given additional sampling, a close relative of *P. muscorum* would be found on Borneo. These authors anticipated that any newly discovered relatives would share more morphological characters with the type species, which caused the relationship between *P. ater* and *P. muscorum* to go unrecognized (Fig. 4; Hutterer et al. 2018). Generating DNA sequence data from the holotype of *P. ater* was critical in resolving this taxonomic enigma, an approach increasingly used to resolve species limits for poorly known lineages (Kirchman et al. 2010; Kirwan et al. 2015; McGuire et al. 2018; Krabbe et al. 2020; Esselstyn et al. 2021) and groups with convoluted taxonomic histories (Chomicki and Renner 2015; Hedin et al. 2018; Contreras-Ortiz et al. 2019; Giarla and Voss 2020; Cong et al. 2021; Vences et al. 2022). We also verified the identity of the first modern specimens of *P. ater* following a sampling gap of 80 years since the collection of, and 55 years since the description of, the type of this species.

Palawanosorex ater was first placed in the genus *Suncus* largely by the presence of the fifth unicuspid. However, Medway (1965) also noted that this species does not resemble any other Southeast Asian crocidurine and suggested that it may be closely aligned with *Suncus dayi* from southern India, which our results refute (Fig. 2). If, prior to the availability of molecular data, simply possessing a fifth unicuspid and therefore not being a *Crocidura* was sufficient evidence to place a species in the genus *Suncus*, then a thorough systematic evaluation of South and Southeast Asian *Suncus* species is warranted. Several *Suncus* species remain poorly studied. The Bornean Pygmy Shrew, *Suncus hosei*, has often been aligned with the widespread *Suncus etruscus* complex, though authors have shown some hesitancy in this placement (e.g., Hutterer 2005) and this hypothesis lacks genetic evidence. Similarly, the scantily studied Flores Shrew, *Suncus mertensi* Kock, 1974, was hypothesized to be a relic of an earlier insular fauna (van der Hoek Ostende et al. 2006), the precise pattern that the genus *Palawanosorex* appears to represent (Hutterer et al. 2018). Only through comprehensive surveys of Southeast Asian fauna and targeted sampling of genetic material from historical specimens can we continue to piece together the complex biogeographic history of this dynamic region.

Acknowledgements

We thank the Sarawak Department of Forestry for providing permits for this work. The citizens of Ba'kalalan and the employees of Mount Mulu National Park provided logistical assistance critical to this project. Wan Nur Syafinaz Wan Azman, Syamzuraini Zolkapley, Quentin Martinez, and Heru Handika assisted in the fieldwork. The Museum of Comparative Zoology kindly loaned us a small sample from the type specimen. We thank Heru Handika and Mark Omura (MCZ) for providing photographs. This work was funded by NSF DEB-1441634 and DEB-1754393 to JAE, an NSF Postdoctoral Fellowship (DBI 2010756), an American Society of Mammalogists Fellowship and Jim Patton Award to JAN, and the Alfred L. Gardner and Mark S. Hafner Mammalogy Fund. Rainer Hutterer and one anonymous reviewer provided feedback that improved this manuscript.

References

- Allio R, Schomaker-Bastos A, Romiguier J, Prosdocimi F, Nabholz B, Delsuc F (2020) MitoFinder: Efficient automated large-scale extraction of mitogenomic data in target enrichment phylogenomics. *Molecular Ecology Resources* 20(4): 892–905. <https://doi.org/10.1111/1755-0998.13160>
- Bolger AM, Lohse M, Usadel B (2014) Trimmomatic: A flexible trimmer for Illumina sequence data. *Bioinformatics* 30(15): 2114–2120. <https://doi.org/10.1093/bioinformatics/btu170>
- Chomicki G, Renner SS (2015) Watermelon origin solved with molecular phylogenetics including Linnaean material: Another example of museomics. *The New Phytologist* 205(2): 526–532. <https://doi.org/10.1111/nph.13163>
- Cong Q, Shen J, Zhang J, Li W, Kinch LN, Calhoun JV, Warren AD, Grishin NV (2021) Genomics reveals the origins of historical specimens. *Molecular Biology and Evolution* 38(5): 2166–2176. <https://doi.org/10.1093/molbev/msab013>
- Contreras-Ortiz N, Rodríguez-García T, Quintanilla S, Bernal-Villegas J, Madriñán S, Gómez-Gutiérrez A (2019) The origin of Humboldt and Bonpland's holotype of *Oncidium ornithorhynchum*, clarified using +200-year-old DNA. *Taxon* 68(3): 471–480. <https://doi.org/10.1002/tax.12067>
- Corbet GB, Hill JE (1992) *The Mammals of the Indomalayan Region: a Systematic Review*. Oxford University Press, Oxford, [viii +] 488 pp.
- Esselstyn JA, Widmann P, Heaney LR (2004) The mammals of Palawan Island, Philippines. *Proceedings of the Biological Society of Washington* 117: 271–302.
- Esselstyn JA, Timm RM, Brown RM (2009) Do geological or climatic processes drive speciation in dynamic archipelagos? The tempo and mode of diversification in Southeast Asian shrews. *Evolution* 63(10): 2595–2610. <https://doi.org/10.1111/j.1558-5646.2009.00743.x>
- Esselstyn JA, Oliveros CH, Swanson MT, Faircloth BC (2017) Investigating difficult nodes in the placental mammal tree with expanded taxon sampling and thousands of ultraconserved elements. *Genome Biology and Evolution* 9(9): 2308–2321. <https://doi.org/10.1093/gbe/evx168>
- Esselstyn JA, Achmadi AS, Handika H, Swanson MT, Giarla TC, Rowe KC (2021) Fourteen new, endemic species of shrew (genus *Crocidura*) from Sulawesi reveal a spectacular island radiation. *Bulletin of the American Museum of Natural History* 454(1): 1–108. <https://doi.org/10.1206/0003-0090.454.1.1>
- Faircloth BC, McCormack JE, Crawford NG, Harvey MG, Brumfield RT, Glenn TC (2012) Ultraconserved elements anchor thousands of genetic markers spanning multiple evolutionary timescales. *Systematic Biology* 61(5): 717–726. <https://doi.org/10.1093/sysbio/sys004>
- Faircloth BC (2013) Illumiprocessor: a trimmomatic wrapper for parallel adapter and quality trimming. <https://doi.org/10.6079/J9ILL>
- Faircloth BC (2016) PHYLUCE is a software package for the analysis of conserved genomic loci. *Bioinformatics* 32(5): 786–788. <https://doi.org/10.1093/bioinformatics/btv646>
- Giarla TC, Voss RS (2020) DNA sequence data from the holotype of *Marmosa elegans coquimbensis* Tate, 1931 (Mammalia: Didelphidae) resolve its disputed relationships. *American Museum Novitates* 3946(3946): 1–8. <https://doi.org/10.1206/3946.1>
- Glenn TC, Nilsen RA, Kieran TJ, Sanders JG, Bayona-Vásquez NJ, Finger JW, Pierson TW, Bentley KE, Hoffberg SL, Louha S, Garcia-De Leon FJ, del Rio Portilla MA, Reed KD,

- Anderson JL, Meece JK, Aggrey SE, Rekaya R, Alabady M, Belanger M, Winker K, Faircloth BC (2019) Adapterama I: Universal stubs and primers for 384 unique dual-indexed or 147,456 combinatorially-indexed Illumina libraries (iTru & iNext). PeerJ 7: e7755. <https://doi.org/10.7717/peerj.7755>
- Grabherr MG, Haas BJ, Yassour M, Levin JZ, Thompson DA, Amit I, Adiconis X, Fan L, Raychowdhury R, Zeng Q, Chen Z, Mauceli E, Hacohen N, Gnirke A, Rhind N, di Palma F, Birren BW, Nusbaum C, Lindblad-Toh K, Friedman N, Regev A (2011) Full-length transcriptome assembly from RNA-Seq data without a reference genome. Nature Biotechnology 29(7): 644–652. <https://doi.org/10.1038/nbt.1883>
- Griswold JA (1939) Up Mount Kinabalu II. The Scientific Monthly 48: 504–518.
- Heaney LR (1986) Biogeography of mammals in SE Asia: Estimates of rates of colonization, extinction and speciation. Biological Journal of the Linnean Society. Linnean Society of London 28(1–2): 127–165. <https://doi.org/10.1111/j.1095-8312.1986.tb01752.x>
- Hedin M, Derkarabetian S, Blair J, Paquin P (2018) Sequence capture phylogenomics of eyeless *Cicurina* spiders from Texas caves, with emphasis on US federally-endangered species from Bexar County (Araneae, Hahniidae). ZooKeys 769: 49–76. <https://doi.org/10.3897/zookeys.769.25814>
- Hinckley A, Camacho-Sanchez M, Ruedi M, Hawkins MT, Mullan M, Cornellas A, Tuh Yit Yuh F, Leonard JA (2022) Evolutionary history of Sundaland shrews (Eulipotyphla: Soricidae: *Crociodura*) with a focus on Borneo. Zoological Journal of the Linnean Society 194(2): 478–501. <https://doi.org/10.1093/zoolinnean/zlab045>
- Hutterer R (2005) Order Soricomorpha. In: Wilson DE, Reeder DM (Eds) Mammal Species of the World. 3rd Edn. The Johns Hopkins University Press, Baltimore, 220–311.
- Hutterer R, Balete DS, Giarla TC, Heaney LR, Esselstyn JA (2018) A new genus and species of shrew (Mammalia: Soricidae) from Palawan Island, Philippines. Journal of Mammalogy 99(3): 518–536. <https://doi.org/10.1093/jmammal/gyy041>
- Kalyaanamoorthy S, Minh BQ, Wong TK, Von Haeseler A, Jermini LS (2017) ModelFinder: Fast model selection for accurate phylogenetic estimates. Nature Methods 14(6): 587–589. <https://doi.org/10.1038/nmeth.4285>
- Katoh K, Standley DM (2013) MAFFT multiple sequence alignment software version 7: Improvements in performance and usability. Molecular Biology and Evolution 30(4): 772–780. <https://doi.org/10.1093/molbev/mst010>
- Kirchman JJ, Witt CC, McGuire JA, Graves GR (2010) DNA from a 100-year-old holotype confirms the validity of a potentially extinct hummingbird species. Biology Letters 6(1): 112–115. <https://doi.org/10.1098/rsbl.2009.0545>
- Kirwan GM, Schweizer M, Copete JL (2015) Multiple lines of evidence confirm that Hume's Owl *Strix butleri* (Hume, 1878) is two species, with description of an unnamed species (Aves: Non-Passeriformes: Strigidae). Zootaxa 3904(1): 28–50. <https://doi.org/10.11646/zootaxa.3904.1.2>
- Krabbe NK, Schulenberg TS, Hosner PA, Rosenberg KV, Davis TJ, Rosenberg GH, Lane DF, Andersen MJ, Robbins MB, Cadena DC (2020) Untangling cryptic diversity in the High Andes: revision of the *Scytalopus [magellanicus]* complex (Rhinocryptidae) in Peru reveals three new species. The Auk 137(2): ukaa003. <https://doi.org/10.1093/auk/ukaa003>
- Li D, Luo R, Liu CM, Leung CM, Ting HF, Sadakane K, Yamashita H, Lam TW (2016) MEGAHIT v1.0: A fast and scalable metagenome assembler driven by advanced

- methodologies and community practices. *Methods* (San Diego, Calif.) 102: 3–11. <https://doi.org/10.1016/j.ymeth.2016.02.020>
- Mai U, Mirarab S (2018) TreeShrink: Fast and accurate detection of outlier long branches in collections of phylogenetic trees. *BMC Genomics* 19(5): 23–40. <https://doi.org/10.1186/s12864-018-4620-2>
- McGuire JA, Cotoras DD, O’Connell B, Lawalata SZ, Wang-Claypool CY, Stubbs A, Huang X, Wogan GO, Hykin SM, Reilly SB, Bi K, Riyanto A, Arida E, Smith LL, Milne H, Streicher JW, Iskandar DT (2018) Squeezing water from a stone: High-throughput sequencing from a 145-year old holotype resolves (barely) a cryptic species problem in flying lizards. *PeerJ* 6: e4470. <https://doi.org/10.7717/peerj.4470>
- Medway L (1965) Mammals of Borneo: Field keys and an annotated checklist. *Journal of the Malaysian Branch of the Royal Asiatic Society* 36: 1–193.
- Minh BQ, Schmidt HA, Chernomor O, Schrempf D, Woodhams MD, Von Haeseler A, Lanfear R (2020) IQ-TREE 2: New models and efficient methods for phylogenetic inference in the genomic era. *Molecular Biology and Evolution* 37(5): 1530–1534. <https://doi.org/10.1093/molbev/msaa015>
- Nurk S, Meleshko D, Korobeynikov A, Pevzner PA (2017) metaSPAdes: A new versatile metagenomic assembler. *Genome Research* 27(5): 824–834. <https://doi.org/10.1101/gr.213959.116>
- Omar H, Hashim R, Bhassu S, Ruedi M (2013) Morphological and genetic relationships of the *Crocidura monticola* species complex (Soricidae: Crocidurinae) in Sundaland. *Mammalian Biology* 78(6): 446–454. <https://doi.org/10.1016/j.mambio.2013.04.004>
- Piper PJ, Ochoa J, Robles EC, Lewis H, Paz V (2011) Palaeozoology of Palawan Island, Philippines. *Quaternary International* 233(2): 142–158. <https://doi.org/10.1016/j.quaint.2010.07.009>
- Prjibelski A, Antipov D, Meleshko D, Lapidus A, Korobeynikov A (2020) Using SPAdes de novo assembler. *Current Protocols in Bioinformatics* 70(1): e102. <https://doi.org/10.1002/cpbi.102>
- Sikes RS, Animal Care and Use Committee of the American Society of Mammalogists (2016) 2016 Guidelines of the American Society of Mammalogists for the use of wild mammals in research and education. *Journal of Mammalogy* 97(3): 663–688. <https://doi.org/10.1093/jmammal/gyw078>
- Tsai WL, Schedl ME, Maley JM, McCormack JE (2020) More than skin and bones: Comparing extraction methods and alternative sources of DNA from avian museum specimens. *Molecular Ecology Resources* 20(5): 1220–1227. <https://doi.org/10.1111/1755-0998.13077>
- Van den Hoek Ostende L, Van Der Berch G, Awe Due R (2006) First fossil insectivores from Flores. *Hellenic Journal of Geosciences* 41: 67–72.
- Vences M, Köhler J, Crottini A, Hofreiter M, Hutter CR, du Preez L, Preick M, Rakotoarison A, Rancilhac L, Raselimanana AP, Rosa GM, Scherz MD, Glaw F (2022) An integrative taxonomic revision and redefinition of *Gephyromantis* (*Laurentomantis*) *malagasius* based on archival DNA analysis reveals four new mantellid frog species from Madagascar. *Vertebrate Zoology* 72: 271–309. <https://doi.org/10.3897/vz.72.e78830>
- Wallace AR (1869) *The Malay Archipelago: the land of the orang-utan and the bird of paradise: a narrative of travel, with studies of man and nature*. MacMillan and Co., London, 548 pp. <https://doi.org/10.5962/bhl.title.131886>

Zhang C, Rabiee M, Sayyari E, Mirarab S (2018) ASTRAL-III: Polynomial time species tree reconstruction from partially resolved gene trees. BMC Bioinformatics 19(S6, Supplement 6): 15–30. <https://doi.org/10.1186/s12859-018-2129-y>

Supplementary material 1

GenBank Accession numbers for genetic sequences used in this study

Authors: Nations JA

Data type: genetic

Copyright notice: This dataset is made available under the Open Database License (<http://opendatacommons.org/licenses/odbl/1.0/>). The Open Database License (ODbL) is a license agreement intended to allow users to freely share, modify, and use this Dataset while maintaining this same freedom for others, provided that the original source and author(s) are credited.

Link: <https://doi.org/10.3897/zookeys.1137.94217.suppl1>

Supplementary material 2

Best-fitting nucleotide substitution model for each gene in the mitochondrial DNA analysis

Authors: Nations JA

Data type: genetic

Copyright notice: This dataset is made available under the Open Database License (<http://opendatacommons.org/licenses/odbl/1.0/>). The Open Database License (ODbL) is a license agreement intended to allow users to freely share, modify, and use this Dataset while maintaining this same freedom for others, provided that the original source and author(s) are credited.

Link: <https://doi.org/10.3897/zookeys.1137.94217.suppl2>

Supplementary material 3

Maximum-likelihood crocidurine mitochondrial gene tree, without CYTB, inferred in IQTree

Authors: Nations JA

Data type: image (eps file)

Copyright notice: This dataset is made available under the Open Database License (<http://opendatacommons.org/licenses/odbl/1.0/>). The Open Database License (ODbL) is a license agreement intended to allow users to freely share, modify, and use this Dataset while maintaining this same freedom for others, provided that the original source and author(s) are credited.

Link: <https://doi.org/10.3897/zookeys.1137.94217.suppl3>

Abyssal fauna of polymetallic nodule exploration areas, eastern Clarion-Clipperton Zone, central Pacific Ocean: Amphinomidae and Euprosinidae (Annelida, Amphinomida)

Lenka Neal¹, Helena Wiklund^{1,2,3}, Laetitia M. Gunton⁴, Muriel Rabone¹,
Guadalupe Bribiesca-Contreras¹, Thomas G. Dahlgren^{2,3,5}, Adrian G. Glover¹

1 Life Sciences Department, Natural History Museum, London SW7 5BD, UK **2** Department of Marine Sciences, University of Gothenburg, Box 463, 40530 Gothenburg, Sweden **3** Gothenburg Global Biodiversity Centre, Box 463, 40530 Gothenburg, Sweden **4** Australian Museum Research Institute, 1 William Street, Sydney NSW 2010, Australia **5** NORCE Norwegian Research Centre, Bergen, Norway

Corresponding author: Adrian G. Glover (a.glover@nhm.ac.uk)

Academic editor: Andrew Davinack | Received 4 May 2022 | Accepted 1 August 2022 | Published 22 December 2022

<https://zoobank.org/9407DC6E-B6B0-46AF-A9C7-F8DDCF542457>

Citation: Neal L, Wiklund H, Gunton LM, Rabone M, Bribiesca-Contreras G, Dahlgren TG, Glover AG (2022) Abyssal fauna of polymetallic nodule exploration areas, eastern Clarion-Clipperton Zone, central Pacific Ocean: Amphinomidae and Euprosinidae (Annelida, Amphinomida). ZooKeys 1137: 33–74. <https://doi.org/10.3897/zookeys.1137.86150>

Abstract

This is a contribution in a series of taxonomic publications on benthic fauna of polymetallic nodule fields in the eastern abyssal Clarion-Clipperton Zone (CCZ). The material was collected during environmental surveys targeting exploration contract areas ‘UK-1’, ‘OMS’ and ‘NORI-D’, as well as an Area of Particular Environmental Interest, ‘APEI-6’. The annelid families Amphinomidae and Euprosinidae are investigated here. Taxonomic data are presented for six species from 41 CCZ-collected specimens as identified by a combination of morphological and genetic approaches; of the six species, three are here described as new, one species is likely to be new but in too poor condition to be formalised and the two others likely belong to known species. Description of three new species *Euprosinella georgievae* **sp. nov.**, *Euprosinopsis ahearni* **sp. nov.**, and *Euprosinopsis halli* **sp. nov.** increases the number of formally described new annelid species from the targeted areas to 21 and CCZ-wide to 52. Molecular data suggest that four of the species reported here are known from CCZ only, but within CCZ they have a wide distribution. In contrast, the species identified as *Bathychloeia* cf. *sibogae* Horst, 1910 was found to have a wide distribution within the Pacific based on both morphological and molecular data, using comparative material from the abyssal South Pacific. *Bathychloeia* cf. *balloniformis* Böggemann, 2009 was found to be restricted to APEI-6 based

on DNA data available from CCZ specimens only, but morphological data from other locations suggest potentially a wide abyssal distribution. The genus *Euphrosinopsis* was previously known only from Antarctic waters, and *Euphrosinella georgievae* **sp. nov.** was recovered as a sister taxon to the Antarctic specimens of *Euphrosinella* cf. *cirratiformis* in our molecular phylogenetic analysis, strengthening the hypothesised link between the deep-sea and Antarctic benthic fauna.

Keywords

Amphinomida, CCZ, COI, deep-sea mining, molecular phylogeny, species distribution, taxonomic novelty, 18S, 16S

Introduction

The Clarion-Clipperton Zone (CCZ) polymetallic nodule region, a vast area (ca. 6 million km²) of the central abyssal Pacific, has been explored in recent decades for its deep-sea mineral resources and their potential for commercial mining (e.g., Gollner et al. 2017; Glover et al. 2018; Smith et al. 2021). Such exploration is managed through exploration licenses, regulated by the International Seabed Authority (ISA), which stipulates the need for biodiversity baseline studies, environmental impact assessments and the establishment of preservation areas (Lodge et al. 2014; Washburn et al. 2021). This paper is based on material collected within areas of the eastern CCZ prospected by 1) the UK Seabed Resources Ltd (UKSRL), exploration contract area ‘UK-1’, 2) the Ocean Mineral Singapore exploration contract area ‘OMS’, and 3) Nauru Ocean Resources Inc (NORI), exploration contract area ‘NORI-D’. Additional material studied was collected from the Area of Particular Environmental Interest ‘APEI-6’.

The knowledge of the biodiversity and distribution of benthic taxa found within areas of potential mining operations is paramount to informed environmental impact assessments and conservation efforts (Smith et al. 2011, 2021). Both biodiversity and species ranges remain poorly understood within this area mainly due to under-sampling and the lack of comparable datasets produced by different research groups and contractors. The latter factor is greatly confounded by the lack of formal descriptions of the fauna given that most represent species new to science (Glover et al. 2018). This lack of knowledge is particularly acute for sediment infauna, a benthic component of fauna that cannot be captured by video or camera surveys. In general, annelids dominate the abyssal sediment macrofauna, constituting 50–75% of macrofaunal abundance and species richness, and are therefore considered a key component of benthic biodiversity (e.g., Glover et al. 2002; Smith et al. 2008). Annelids also exhibit a broad range of feeding types and life-history strategies and are frequently used to evaluate anthropogenic disturbance in shallow-water habitats (Dean 2008). Thus, evaluation of the diversity and species ranges of annelids is critical to predicting and managing the impacts of proposed nodule mining in the CCZ.

Our main objective has been to provide taxonomic hypotheses on macrofaunal annelids collected from the targeted areas within the CCZ based on morphology and molecular data. These data build up on previous taxonomic work on annelids from the target areas (Wiklund et al. 2019; Drennan et al. 2021; Neal et al. 2022) as well as wider CCZ area (Janssen et al. 2015; Blake 2019; Bonifácio and Menot 2019) and ultimately provide further insights into annelid species distribution in the deep-sea realm. Up to this date, 52 annelid species have been formally described from CCZ, with the focus on families Spionidae (Paterson et al. 2016; Neal et al. 2022), Orbiniidae (Blake 2017, 2020), Polynoidae (Bonifácio and Menot 2019), Cirratulidae (Blake 2016, 2019), Opheliidae, Scalibregmatidae, and Traviisiidae (Wiklund et al. 2019), Syllidae (Maciolek 2020) and Nereididae (Drennan et al. 2021).

Annelids of order Amphinomida are commonly known as fire worms due to the skin burning sensation upon contact with their chaetae caused by a complex mixture of defensive toxins (Verdes et al. 2018), although the exact nature of the toxin delivery is still a matter of debate (Righi et al. 2021a, b; Tilic and Bartolomaeus 2021). Most Amphinomida species are carnivores or scavengers, but some may also ingest detritus and algae (Fauchald and Jumars 1979; Jumars et al. 2015). Amphinomida has a widespread distribution, occurring from the intertidal to deep waters, with good representation in extreme environments such as the Antarctic shelf (Kudenov 1993), chemosynthetic habitats (e.g., Fiege and Bock 2009; Borda et al. 2013; Barroso et al. 2018, 2021), hypoxic environments (Jeffreys et al. 2012) and polluted sites such as fish farms (LN pers. obs.). One species even inhabits the lumen of the digestive tract of a deep-sea spatangoid (Emson et al. 1993).

In terms of their systematics, Amphinomida were regarded as part of the Errantia (e.g., Rouse and Fauchald 1997) until molecular studies revealed their phylogenetic position basally within Annelida and as a sister group to sipunculids (e.g., Weigert et al. 2014). Such relationship with the unsegmented and sessile worms is hard to explain based only on morphology as no synapomorphies have been found to date (Beckers and Tilic 2021). Currently, the order Amphinomida contains two accepted families, Amphinomidae Lamarck, 1818 and Euphrosinidae Williams, 1852 (Read and Fauchald 2021). As a result of recent molecular phylogenetic analyses (Wiklund et al. 2008; Borda et al. 2015) Amphinomidae have been further divided into two subfamilies Amphinominae Lamarck, 1818 and Archinominae Kudenov, 1991. Amphinomidae has 180 species belonging to 22 genera, with the bulk of Amphinominae living in shallow warm and temperate waters, while members of Archinominae tend to inhabit deep-sea extreme habitats. The less diverse Euphrosinidae contains approximately 60 accepted species belonging to only four genera (Read and Fauchald 2021). Most of euphrosinid diversity lies within the geographically widespread genus *Euphrosine* Lamarck, 1818 with 54 species, while the small and rarely encountered genera *Palmyreuphrosyne* Fauvel, 1913; *Euphrosinella* Detinova, 1985 and *Euphrosinopsis* Kudenov, 1993 tend to be confined to the deep-sea and the Antarctic shelf (Kudenov 1993).

Materials and methods

Fieldwork

The first UKSR ABYSSLINE cruise (AB01) took place in October 2013 onboard the RV ‘Melville’ and targeted the UK-1 exploration contract area (Fig. 1). The second cruise (AB02) took place in February–March 2015 onboard RV ‘Thomas G. Thompson’ and sampled a wider area (Fig. 1), including: UK-1 (depth ca. 4200 m) and OMS (depth ca. 4200 m) exploration contract areas and APEI-6 (depth ca. 4050 m), an area exempted from mining activities (Wedding et al. 2013). The Resource Cruise 01 (RC01) took place aboard the marine vessel M/V ‘Pacific Constructor’ between February and March 2020 and targeted exploration contract areas UK-1 and OMS (Fig. 1). Nauru Ocean Resources Inc (**NORI**) Campaign 05a (DG05a) cruise took place between October and November 2020 and the 05d (DG05d) cruise took place between April and June 2021, both expeditions were onboard ‘Maersk Launcher’ to the NORI-D exploration contract area (depth ca. 4300 m) (Fig. 1).

For a comprehensive description of the methodological pipeline, see Glover et al. (2016b). Briefly, specimens were collected using box corer and Brenke epibenthic sledge (EBS) (Brenke 2005). Geographic data from sampling activities were recorded on a central GIS database (Fig. 1). Live-sorting of specimen samples was carried out onboard all four vessels in a ‘cold-chain’ pipeline, with material maintained in chilled (2–4 °C), filtered seawater. Specimens were assigned preliminarily identification and imaged live using stereo microscopes with attached digital cameras (Glover et al. 2016b). Specimens were then stored in individual microtube vials filled with aqueous solution of 80% non-denatured ethanol labelled appropriately and entered into a local database. Samples were kept chilled throughout their transportation to the Natural History Museum, London, UK (**NHMUK**).

Morphological laboratory work

In the laboratory, preserved specimens were re-examined using stereo and compound microscopes. They were identified to morphospecies, and the best-preserved examples (voucher specimens) were then used to provide informal descriptions with key morphological features photographed with digital camera. Shirlastain A was used during the morphological examination on some specimens, in order to better observe certain characters. Scanning electron microscopy (**SEM**) using a SEM FEI Quanta 650 was conducted on selected specimens, following graded ethanol dehydration, critical point drying, and gold coating. Figures were assembled using Adobe Photoshop CS6 software. In some instances, a fine line was used to outline and highlight particular morphological features where such features were unclear from images alone. Line drawings were made using camera lucida system.

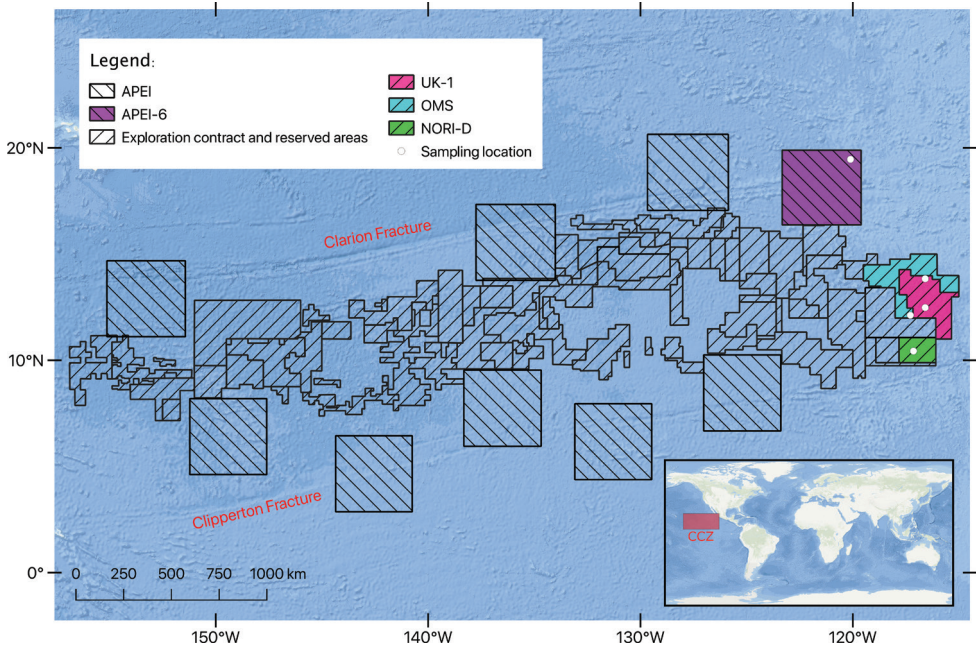


Figure 1. Map of CCZ of exploration areas and areas of particular interest, with targeted areas where samples of this study were collected highlighted in colours (see legend for explanation).

Additionally, Amphinomidae specimens recently collected from the abyssal South Pacific (ca. 4000 m) as part of the RV ‘Investigator’ voyage ‘Sampling the Abyss’ were made available for examination (see also Gunton et al. 2021). These specimens were examined as described above. Material registered and lodged at the Australian Museum is prefixed (AM W.).

Molecular laboratory work

Extraction of DNA was done with DNeasy Blood and Tissue Kit (Qiagen) using a Hamilton Microlab STAR Robotic Workstation. Approximately 1800 bp of 18S were amplified using the primers 18SA 5'-AYCTGGTTGATCCTGCCAGT-3' (Medlin et al. 1988) and 18SB 5'-ACCTTGTTACGACTTTTACTTCCTC-3' (Nygren and Sundberg 2003), ca. 450 bp of 16S were amplified with the primers ann16Sf 5'-GCGGTATCCTGACCGTRCWAAGGTA-3' (Sjölin et al. 2005) and 16SbrH 5'-CCGGTCTGAACTCAGATCACGT-3' (Palumbi 1996), and ca. 650 bp of cytochrome *c* oxidase were amplified using LCO1490 5'-GGTCAACAAATCATAAAGATATTGG-3' (Folmer et al. 1994) and COI-E 5'-TATACTTCTGGGTGTCCGAAGAATCA-3' (Bely and Wray 2004). PCR mixtures contained 1 µl of each primer (10 µM), 2 µl template DNA and 21 µl of Red Taq DNA Polymerase 1.1X MasterMix (VWR) in a mixture of total 25 µl. The PCR amplification profile for all gene fragments consisted of initial denaturation at 95 °C for 5 min, 35 cycles of denaturation at 94 °C for 45 s, annealing at 55 °C for 45 s, extension at

72 °C for 2 min, and a final extension at 72 °C for 10 min. PCR products were purified using Millipore Multiscreen 96-well PCR Purification System, and sequencing was performed on an ABI 3730XL DNA Analyser (Applied Biosystems) at The Natural History Museum Sequencing Facility, using the same primers as in the PCR reactions plus two internal primers for 18S, 620F 5'-TAAAGYTGYTGCAGTTAAA-3' (Nygren and Sundberg 2003) and 1324R 5'-CGGCCATGCACCACC-3' (Cohen et al. 1998). Overlapping sequence fragments were merged into consensus sequences using Geneious (Kearse et al. 2012) and aligned using MAFFT (Katoh et al. 2002) for 18S and 16S, and MUSCLE (Edgar 2004) for COI, both programs used as plugins in Geneious, with default settings.

Molecular data were used to place species covered in this study within the Amphinomida phylogenetic relationships. The phylogenetic analyses were done in two parts, producing one tree for Euphrosinidae with a taxon from Amphinomidae as root, and one for Amphinomidae with a taxon from Euphrosinidae as root. Sequences added from GenBank are listed in Supplementary data with taxon names and sequence accession numbers. The program jModelTest (Posada 2008) was used to assess the best model for each partition with BIC, which suggested the for MrBayes possible GTR+I+G as the best model for all genes. The data was partitioned into two genes (18S and 16S) for Euphrosinidae and three genes (18S, 16S and COI) for Amphinomidae, and the evolutionary model mentioned above was applied to each partition. The parameters used for the partitions were unlinked. Bayesian phylogenetic analyses (BAs) were conducted with MrBayes v. 3.2.6 (Ronquist et al. 2012). Analyses were run three times for 10,000,000 generations. Of these, the first 2,500,000 generations were discarded as burn-in. The tree files were interpreted with FigTree ver. 1.4.4 (available from <http://tree.bio.ed.ac.uk/software/figtree/>). Uncorrected 'p' for one of the species, *Bathychloeia* cf. *sibogae* was calculated from a COI alignment of 534 characters using Mesquite (Maddison and Maddison 2021).

Taxonomic assignments

Here we use a phylogenetic species concept *sensu* Donoghue (1985) with species determined by DNA-based phylogenetic analysis. The poor morphological preservation and the subsequent lack of morphological data did not always allow for formal description of a new species. Instead, we provide the lowest-level taxonomic name possible aided by phylogenetic information. In these cases, we use an informal naming system where the voucher specimen number is used as the informal species name. Therefore, *Paramphinome* sp. NHM_6022E is the informal species name for all specimens that belong to the same species as the specimen number NHM_6022E. This avoids confusion with the use of sp. A, sp. B, sp. C etc. where informal and confusing synonyms can easily arise. Newly formalised species were named in honour of the scientists, technicians, and crew of the vessels used during the CCZ cruises reported here, with the names being selected from a randomised list from all on board. Type material, DNA specimen vouchers and DNA extractions are deposited at the Natural History Museum, London. A full list of all taxa including Natural History Museum Accession Numbers (NHMUK), NHM Molecular Collection Facility (NHM-MCf), and NCBI GenBank accession numbers are provided in Table 1.

Table 1. List of taxa presented in this paper – family, DNA taxonomy ID (a species-level identification based on combined DNA and morphological evidence), cruise record number, GUID (Global Unique Identifier link to data record at <http://data.nhm.ac.uk>), NHMUK registration number (NHMUK), Molecular Collection facility (MCF) sample ID number (MCF no.) and NCBI GenBank accession numbers (COI/16S/18S AK no.) for successfully sequenced genetic markers. GenBank numbers for phylogenetic analysis data downloaded from GenBank are presented in Suppl. material 1.

DNA taxonomy ID	NHM no.	GUID	Reg no. NHMUK	MCF no.	COI AK no.	16S AK no.	18S AK no.
Family Amphinomidae							
<i>Bathychloeia</i> cf. <i>balloniiformis</i>	NHM_2107	c79b4600-e8e9-4484-b06a-e18330a1421d	ANEA 2022.630	0118302190	ON903198	ON900088	ON905671
<i>Bathychloeia</i> cf. <i>balloniiformis</i>	NHM_2109	ac3dd714-64ac-44ea-9168-22437dc3fba	ANEA 2022.631	0118302189		ON900113	
<i>Bathychloeia</i> cf. <i>sibogae</i> juvenile	NHM_6880_HW01	06f82805-e608-4715-af62-ab1d44df2a79	ANEA 2022.632	0118302159	ON903200	ON900089	
<i>Bathychloeia</i> cf. <i>sibogae</i>	NHM_0821	73a7200a-ac19-4c0c-8381-8d4509a318cf	ANEA 2022.633	0118302202	ON903197	ON900100	ON905670
<i>Bathychloeia</i> cf. <i>sibogae</i>	NHM_2906	d3848fcf-4cb2-49fd-b49c-e09422419a70	ANEA 2022.634	0118302177		ON900116	
<i>Bathychloeia</i> cf. <i>sibogae</i> juvenile	NHM_2115	2cbc0d92-247c-4197-bd7a-4715adfb5e8f4	ANEA 2022.635	0118302188		ON900114	
<i>Bathychloeia</i> cf. <i>sibogae</i>	NHM_3539	083df63d-60c7-48ae-95c4-6a11a61b01e8	ANEA 2022.636	0118302158	ON903199	ON900118	
<i>Bathychloeia</i> cf. <i>sibogae</i>	NHM_8922	805f34aa-ec4f-4318-b18b-46447350aa1e	ANEA 2022.637	0118302156	ON903201		
<i>Paramphinoe</i> sp. NHM_6022E	NHM_1167D	fd4902df-ae2d-44cf-991f-31905434c2a1	ANEA 2022.638				
<i>Paramphinoe</i> sp. NHM_6022E	NHM_4044	56235559-3f2c-426e-b4cd-37462593a4ba	ANEA 2022.639	0118302160			
<i>Paramphinoe</i> sp. NHM_6022E	NHM_6022E	bd4b405d-3e56-4671-909e-fd9c3e7fbcf	ANEA 2022.640	0118302162		ON900125	ON905673
Family Euphosinidae							
<i>Euphosinopsis halli</i> sp. nov.	NHM_0779	1a683870-d904-4c2c-bf1a-a34ead0a42fc	ANEA 2022.641	0118302182		ON900099	
<i>Euphosinopsis halli</i> sp. nov. (holotype)	NHM_4339	670dfd34-338d-4edc-8856-b0a9a728efc9	ANEA 2022.642	0118302157		ON900119	ON905672
<i>Euphosinopsis halli</i> sp. nov. (paratype)	NHM_6018	ab26e2ea-ab87-4013-8106-e817c0485cc9	ANEA 2022.643	0118302167		ON900124	
<i>Euphosinopsis abearni</i> sp. nov.	NHM_0095	a351cb41-736c-4390-8ad8-02c0358b73e0	ANEA 2022.644	0118302201		ON900092	ON905668
<i>Euphosinopsis abearni</i> sp. nov.	NHM_0888	4d76b4e2-569d-4a17-9276-3cc721cbdf72	ANEA 2022.645	0118302187		ON900101	
<i>Euphosinopsis abearni</i> sp. nov. (paratype, SEM)	NHM_0551	241b828d-a574-47f2-995d-0bdef239c427	ANEA 2022.646	0118302186		ON900094	
<i>Euphosinopsis abearni</i> sp. nov.	NHM_5042	1662fd8b-54a5-4f97-9083-02dbb2df7e39	ANEA 2022.647	0118302178		ON900121	
<i>Euphosinopsis abearni</i> sp. nov.	NHM_1737A	4f372c07-c466-4b6c-91a9-229cd7c7a17d	ANEA 2022.648	0118302171		ON900107	
<i>Euphosinopsis abearni</i> sp. nov.	NHM_1876	6ad5c2b3-ccc8-4195-a19f-3913de511e71	ANEA 2022.649	0118302175		ON900112	
<i>Euphosinopsis abearni</i> sp. nov.	NHM_0550	92791783-35c2-4fbf-80b0-2b074ef70828	ANEA 2022.650	0118302203		ON900093	
<i>Euphosinopsis abearni</i> sp. nov.	NHM_1302	7aabc644-2cc6-4671-8c1a-f826eeeb0b46	ANEA 2022.651	0118302168		ON900105	

DNA taxonomy ID	NHM no.	GUID	Reg no. NHMUK	MCF no.	COI AK no.	16S AK no.	18S AK no.
<i>Euphrosinopsis abearni</i> sp. nov.	NHM_1302A (holotype)	479933d3-9943-4d87- a1b8-ea120bd8f4ee	ANEA 2022.652	0118302169		ON900104	
<i>Euphrosinopsis abearni</i> sp. nov.	NHM_1737	2ca3e584-a68d-4ea5- 98d2-75ce10515386	ANEA 2022.653	0118302173		ON900110	
<i>Euphrosinopsis abearni</i> sp. nov.	NHM_1737C (paratype)	efe95a8c-fc88-4849- ad26-1df3d292ef20	ANEA 2022.654	0118302172		ON900109	
<i>Euphrosinopsis abearni</i> sp. nov.	NHM_0616	4758bf19-c6d0-42e0- b5ba-e83e203d2e18	ANEA 2022.655	0118302185		ON900096	
<i>Euphrosinopsis abearni</i> sp. nov.	NHM_0759	b0f9162f-a861-4eb2- 89a1-ce25c2bd09c4	ANEA 2022.656	0118302184		ON900097	
<i>Euphrosinopsis abearni</i> sp. nov.	NHM_1839	02a5acc7-841e-4f50- bf03-57ba21f02f7c	ANEA 2022.657	0118302174		ON900111	
<i>Euphrosinella georgievae</i> sp. nov.	NHM_0587	b7a0bf33-0dc4-4f61- 90de-35865647a99f	ANEA 2022.658	0118302191		ON900095	ON905669
<i>Euphrosinella georgievae</i> sp. nov.	NHM_0777	a8f0e776-d7b6-4ec6- a549-78f40f17d89b	ANEA 2022.659	0118302183		ON900098	
<i>Euphrosinella georgievae</i> sp. nov.	NHM_1737B	2784df45-ec0-4151- b12d-11d955985faa	ANEA 2022.660			ON900108	
<i>Euphrosinella georgievae</i> sp. nov.	NHM_0910	05dfb32c-fc3a-4028- bf09-3eb840175661	ANEA 2022.661	0118302181		ON900102	
<i>Euphrosinella georgievae</i> sp. nov.	NHM_1134 (paratype)	00590d2b-f952-4c69- 8bc2-ac2a408da17a	ANEA 2022.662	0118302180		ON900103	
<i>Euphrosinella georgievae</i> sp. nov.	NHM_1514	96cb7b69-c0ea-4559- 9b57-3abe6af4a4c7	ANEA 2022.663	0118302170		ON900106	
<i>Euphrosinella georgievae</i> sp. nov.	NHM_2391 (holotype)	1ce8325f-74de-47de- a776-2dc50b8d69ae	ANEA 2022.664	0118302176		ON900115	
<i>Euphrosinella georgievae</i> sp. nov.	NHM_4975	677b7d67-d9cc-4ebd- 8d79-cf5da5dc40da	ANEA 2022.665	0118302165		ON900120	
<i>Euphrosinella georgievae</i> sp. nov.	NHM_6087	ecbfaccd-5ee2-49d6- be73-51eb91678487	ANEA 2022.666	0118302166		ON900126	
<i>Euphrosinella georgievae</i> sp. nov.	NHM_5802	c0e408c3-91e7-408f- aaef-3be86507105a	ANEA 2022.667	0118302164		ON900123	
<i>Euphrosinella georgievae</i> sp. nov.	NHM_5057	d92b1574-eccb-443c- a15d-b79357360b59	ANEA 2022.668	0118302179		ON900122	
<i>Euphrosinella georgievae</i> sp. nov.	NHM_7235	55637dc0-f9b9-4586- 9bfb-7a821c785279	ANEA 2022.669	0118302163		ON900127	
<i>Euphrosinella georgievae</i> sp. nov.	NHM_2908	fba3fab7-ac4b-4415- a73c-a2ba6cd44601	ANEA 2022.670	0118302161		ON900117	

Data handling

The field and laboratory work led to a series of databases and sample sets that were integrated into a ‘data-management pipeline’. This included the transfer and management of data and samples between a central collections database, a molecular collections database and external repositories (GenBank, WoRMS, OBIS, GBIF, GGBN, ZooBank) through DarwinCore archives (Suppl. material 1). This provides a robust data framework to support DNA taxonomy, in which openly available data and voucher material are key to quality data standards. A further elaboration of the data pipeline is published in Glover et al. (2016b).

Systematics section

Amphinomidae Lamarck, 1818

Archinominae Kudenov, 1991

***Bathychloeia* Horst, 1910**

Type species. *Bathychloeia sibogae* Horst, 1910.

Diagnosis (modified from Böggemann (2009)). Body small, fusiform. Prostomium divided into an anterior and posterior lobe, with a median antenna on posterior lobe; paired lateral antennae and palps on anterior lobe. Eyes present or absent. Caruncle with well-developed folds and crenulations. Branchiae bipinnate from chaetiger 5 or 6, where enlarged. Dorsal, lateral and ventral cirri cirriform. Chaetae bifurcate. Pygidial cirri paired, cirriform to digitiform.

Remarks. As the name *Bathychloeia* suggests, this genus was established for deep-water representatives similar to forms in predominantly shallow water genus *Chloeia* Lamarck, 1818. *Chloeia* was established by Lamarck (1818) to accommodate *Chloeia flava* described from the Indian Ocean by Pallas in 1766 and currently contains 20 species occurring in the Indian, Pacific, and Atlantic oceans (Hartman 1959; Barroso and Paiva 2011). This genus is morphologically characterised by fusiform body shape and bipinnate branchiae. However, such characteristics are also shared with the rare, uniquely deep-sea genera *Bathychloeia* Horst, 1910 and *Chloenopsis* Fauchald, 1977. *Bathychloeia* has been distinguished from *Chloeia* by Horst (1910, 1912) mainly due to the presence of enlarged branchiae on chaetiger 5 (the first branchial chaetiger). This genus currently contains two deep-sea species, type species *B. sibogae* Horst, 1910 described from Malay Archipelago, depth of 1100 m and *B. balloniformis* Böggemann, 2009 described from the abyssal Atlantic. Similarly, *Chloenopsis* Fauchald, 1977 has been established to accommodate species originally described by McIntosh (885) as *Chloenea atlantica* from the Canary Islands, depth ca. 2800 m. The validity of these genera and their separation from *Chloeia* has never been phylogenetically tested, but has been previously questioned (Böggemann 2009).

***Bathychloeia* cf. *balloniformis* Böggemann, 2009**

Figs 2A–G, 3A–F, 4A

Material examined. NHM_2107, NHMUK ANEA 2022.630, coll. 20/03/2015, EBS, 19.46457, -120.02542, 4026 m, APEI-6, <http://data.nhm.ac.uk/object/c79b4600-e8e9-4484-b06a-e18330a1421d>; NHM_2109, NHMUK ANEA 2022.631, coll. 20/03/2015, EBS, 19.46457, -120.02542, 4026 m, APEI-6, <http://data.nhm.ac.uk/object/ac3dd714-64ac-44ea-9168-22437dc3cfba>.

Comparative material. Amphinomidae spp.; AM. W.52607; 3 specimens; IN2017; sta. V03_110; 4005 m; South Pacific, Australia, off Fraser Island (-25.220, 154.160); col. 11/06/2017; EBS.

Diagnosis. This very small species is represented by two specimens, up to 2.9 mm long and 0.75 mm wide for ten chaetigers. Body compact, spindle-shaped, of bloated appearance (Figs 2A–C, F, 3A, 4A). Preserved specimens pale yellow (Figs 2A, 3A), live specimens translucent to slightly tanned.

Prostomium rounded, longer than wide; anterior lobe broadly rounded, bearing a pair of cirriform lateral antennae (Figs 2C, 3C), a pair of slightly shorter ventrolateral palps and posteriorly prostomium with longer median antenna (Figs 2C, 3C). Prostomium with pair of very small reddish eyes (Fig. 2A, D); posteriorly extended into a conspicuous caruncle reaching the anterior margin of 3rd chaetiger; caruncle large, ramified, and with deeply folded margins (Fig. 2B, C).

Parapodia biramous. Parapodial appendages often broken off, where attached dorsal, lateral and ventral cirri observed, including on chaetiger 1 (Fig. 3C, D). In anterior chaetigers cirri slightly more robust with thickened bases. Bipinnate branchiae observed only on chaetiger 6, with a large primary stalk and up to seven short lateral branches (Figs 2B, C, G, 3E). Branchiae on preceding segments likely absent (no scars or stalks observed), but those on subsequent segments likely present, but damaged (scars or stalks observed). Chaetae mostly broken off, only few long bifurcate noto- and

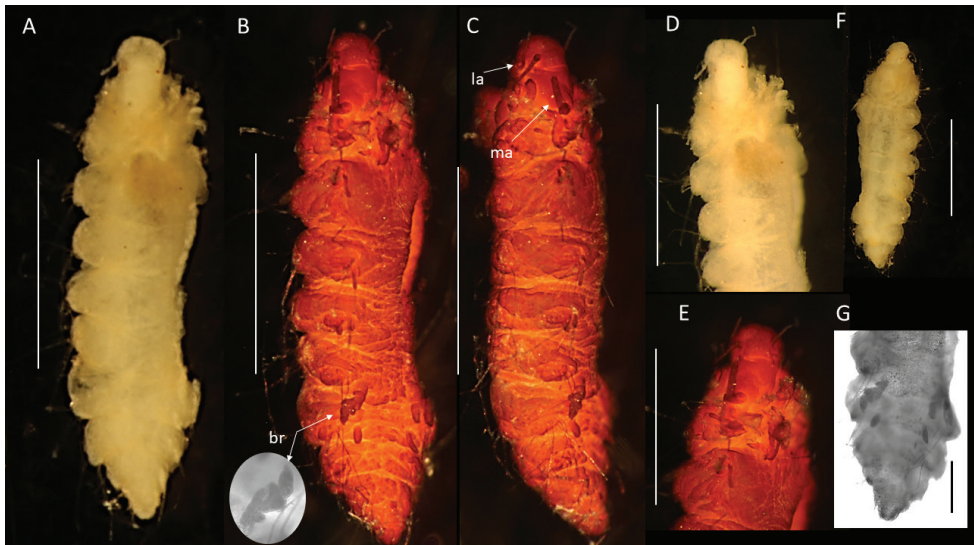


Figure 2. *Bathychloeia* cf. *balloniformis* (specimen, NHMUK ANEA.2022.630) **A** preserved specimen in dorsal view **B** specimen stained with Shirlastain in dorsal view, branchia (br) on chaetiger 6 marked by arrow, insert – detail of the same **C** specimen stained with Shirlastain in lateral view, median antenna (ma) and lateral antenna (la) marked by arrow **D** anterior end in dorsal view **E** anterior end in dorsal view stained with Shirlastain **F** preserved specimen in ventral view **G** posterior end in dorsal view stained with Shirlastain. Scale bars: 1 mm (**A–F**); 250 μ m (**G**).

neurochaetae arising directly from body wall observed, where observed prongs smooth. Pygidium as a conical lobe (Fig. 2G), with dorsal anus and with a pair of short terminal cirri (Fig. 3F).

Molecular information. Specimen, NHMUK ANEA.2022.630, was successfully sequenced for 16S, 18S and COI while for specimen, NHMUK ANEA.2022.631, only 16S was obtained (Table 1). There were no identical sequences for either 16S or COI found on the GenBank. In the phylogenetic tree this species falls out as sister taxon to *Bathychloeia* cf. *sibogae* and the *Bathychloeia* clade is in an unresolved trichotomy with clades consisting of species from the genera *Chloeia* and *Notopygos*, although this trichotomy has low support (Fig. 5A).

Remarks. The CCZ-collected specimens correspond morphologically to another abyssal species *Bathychloeia balloniformis* Böggemann, 2009 described from Cape and Guinea Basins in SE Atlantic, 5048–5144 m depth. The specimens agree in small, spindle-shaped body, having ca. 10 chaetigers, the form of greatly folded and crenulated caruncle and the form and distribution of branchiae (see comparative Fig. 4A, C). Additionally, specimens recently collected from the abyssal South Pacific (ca. 4000 m) as part of the RV ‘Investigator’ voyage ‘Sampling the Abyss’ were made available for examination (see also Gunton et al. 2021). Originally identified as Amphinomidae sp. (Fig. 4B), morphologically these specimens also agree well with the description of *Bathychloeia balloniformis* from the NE Atlantic (Fig. 4C) and with CCZ-collected specimens

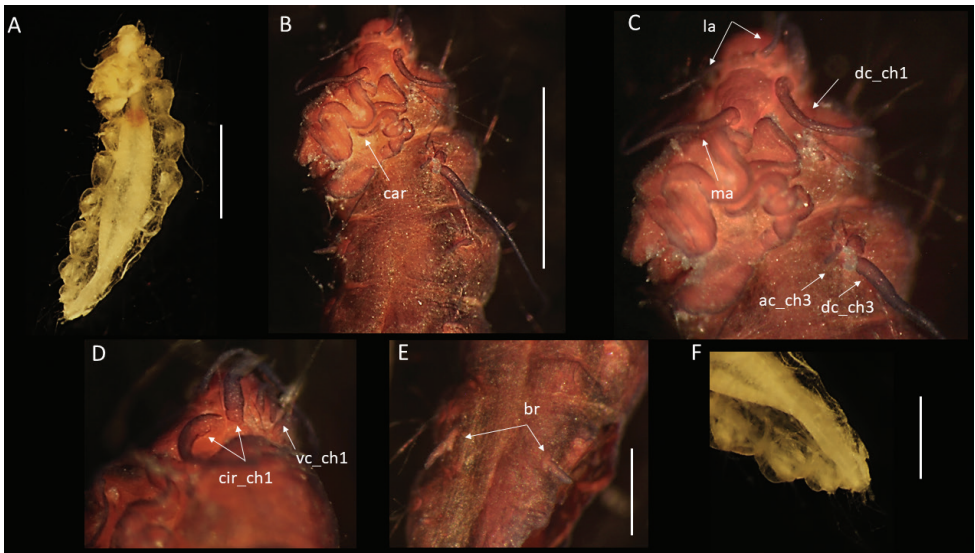


Figure 3. *Bathychloeia* cf. *balloniformis* (specimen NHMUK ANEA.2022.631) **A** preserved specimen in dorsal view **B** anterior end in dorsal view with caruncle (car) marked by arrow, specimen stained with Shirlastain **C** anterior end in dorsal view with median antenna (ma), lateral antennae (la), cirri (dc) on chaetiger 1 and on chaetiger 3 (ac, dc) marked by arrows, specimen stained with Shirlastain **D** anterior end in lateral view, cirri of chaetiger 1 marked by arrows, ventral cirrus (vc) **E** branchiae on chaetiger 6 (arrows) **F** posterior end in dorsal view with two anal cirri. Scale bars: 1 mm (**A, B**); 500 µm (**E, F**).

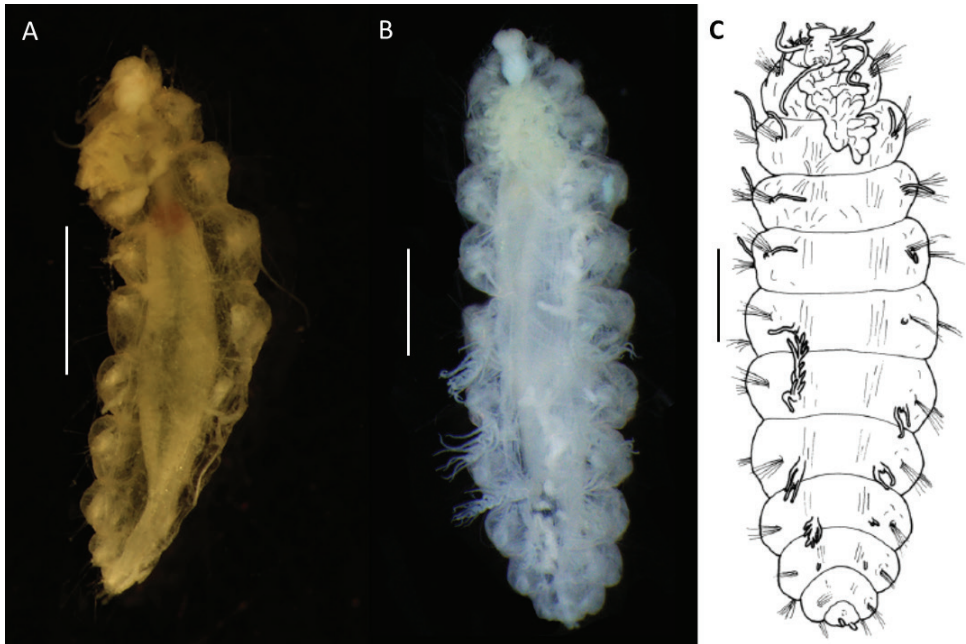


Figure 4. Comparative figure of **A** *Bathychloeia* cf. *balloniformis* (CCZ specimen NHMUK ANEA.2022.631) in dorsal view **B** Amphinomidae sp. (AM W.52607) specimen in dorsal view **C** drawing of *Bathychloeia balloniformis* in dorsal view (after Böggemann 2009). All scale bars: 1 mm.

(Figs 2, 3, 4A). However, molecular work on specimens from South Pacific was not successful and no molecular work was carried out on specimens from the abyssal Atlantic (Böggemann pers. comm.). Due to lack of molecular data from the other locations, we cautiously ascribe CCZ-collected specimens to *Bathychloeia* cf. *balloniformis*.

Distribution. Central Pacific Ocean, Eastern CCZ, in the Area of Particular Environmental Interest, ‘APEI-6’ only (Fig. 1).

Bathychloeia cf. *sibogae* Horst, 1910

Figs 6A–F, 7A–G, 8A–E, 9A–H, 10A, B

Material examined. NHM_6880HW, NHMUK ANEA 2022.632, coll. 12/05/2021, box core, 10.3244, -117.1875, 4280 m, NORI-D, <http://data.nhm.ac.uk/object/06f82805-e608-4715-af62-ab1d44df2a79>; NHM_0821, NHMUK ANEA 2022.633, coll. 20/02/2015, EBS, 12.53717, -116.60417, 4425 m, UK-1, <http://data.nhm.ac.uk/object/73a7200a-ae19-4c0c-8381-8d4509a318cf>; NHM_2906, NHMUK ANEA 2022.634, coll. 20/02/2015, EBS, 12.53717, -116.60417, 4425 m, UK-1, <http://data.nhm.ac.uk/object/d3848fcf-4cb2-49fd-b49c-e09422419a70>; NHM_2115, NHMUK ANEA 2022.635, coll. 20/03/2015, EBS, 19.46457, -120.02542, 4026 m, UK-1, <http://data.nhm.ac.uk/object/2cbc0d92-247c-4197-bd7a-4715adb5e8f4>; NHM_3539, NHMUK

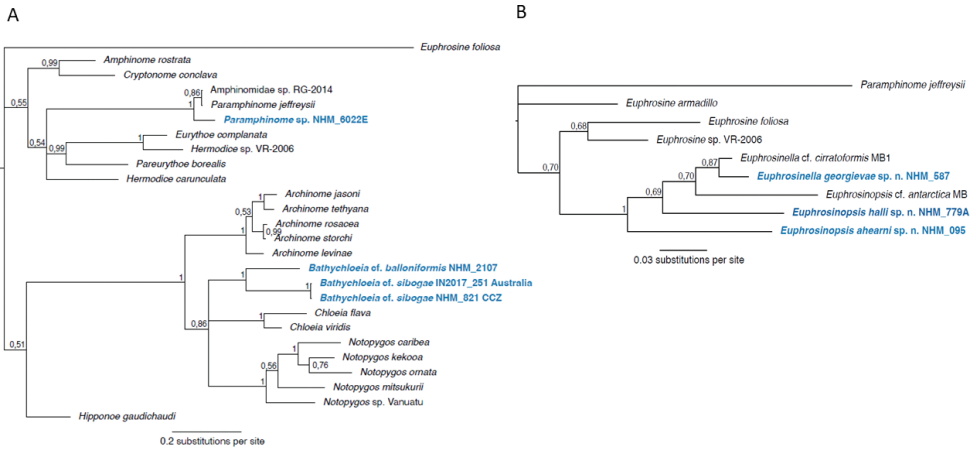


Figure 5. Majority-rule consensus trees from the Bayesian analyses with posterior probability values on nodes. Taxon names highlighted in blue are news species or new sequences for already known species. **A** Amphinomidae phylogenetic tree using a combined datasets for COI, 16S, and 18S with 26 terminal taxa of which *Euphosine foliosa* (Euphosinidae) was used as a root **B** Euphosinidae phylogenetic tree using a combined datasets for 16S and 18S with nine terminal taxa of which *Paramphinoe jeffreysii* (Amphinomidae) was used as a root.

ANEA 2022.636, coll. 02/03/2020, box core, 14.11729, -116.46109, 4148 m, OMS, <http://data.nhm.ac.uk/object/083df63d-60e7-48ae-95c4-6a11a61b01e8>; NHM_8922, NHMUK ANEA 2022.637, coll. 14/05/2018, box core, 10.39247, -117.46752, 4350 m, NORID-D, <http://data.nhm.ac.uk/object/805f34aa-ec4f-4318-b18b-46447350aa1e>.

Comparative material. *Bathychloeia* cf. *sibogae*; NHMUK ANEA.2022.455-456; 2 specimens; IN_251; IN2017_V03_110; 4010 m; South Pacific, Australia, off Fraser Island (-25.220, 154.160); col. 11/06/2017; EBS. *Bathychloeia* cf. *sibogae*; AM W.52608 (1 specimen); IN2017_V03_103; South Pacific, Australia, off Moreton Bay (-27.008, 154.223); 4260 to 4280 m; coll. 10/06/2017; EBS. *Bathychloeia* cf. *sibogae*; AM W.52609 (2 specimens); IN2017_V03_096; South Pacific, Australia, off Byron Bay (-28.678, 154.204); 2591 to 2566 m; coll. 07/06/2017; EBS. *Bathychloeia* cf. *sibogae*; AM W.52610 (1 specimen); IN2017_V03_102; South Pacific, off Moreton Bay (-27.009, 154.223); 4274 to 4264 m; coll. 10/06/2017; beam trawl.

Diagnosis. Body size variable, up to 18 mm long and 6 mm wide for larger specimens with 15 or 16 chaetigers (Figs 6A, 7A, 8A); smaller specimens up to 2 mm long and 0.7 mm wide (Fig. 8C, D). Body oval and compact; tapering anteriorly and posteriorly with mid-body chaetiger widest. Body pale yellow in alcohol, with rusty brown pigmentation in the mid furrow on anterior part of prostomium (Fig. 6C). Live large specimens pink in colour (Fig. 8A).

Prostomium indistinctly divided into an anterior and a posterior lobe; tightly surrounded by reduced first chaetigerous segment. Anterior lobe rounded, bearing a pair of lateral cirriform antennae plus a pair of slightly shorter ventrolateral palps. Posterior lobe bell-shaped, ca. as long as wide. One pair of tiny red eyes present (Fig. 7B) Pros-

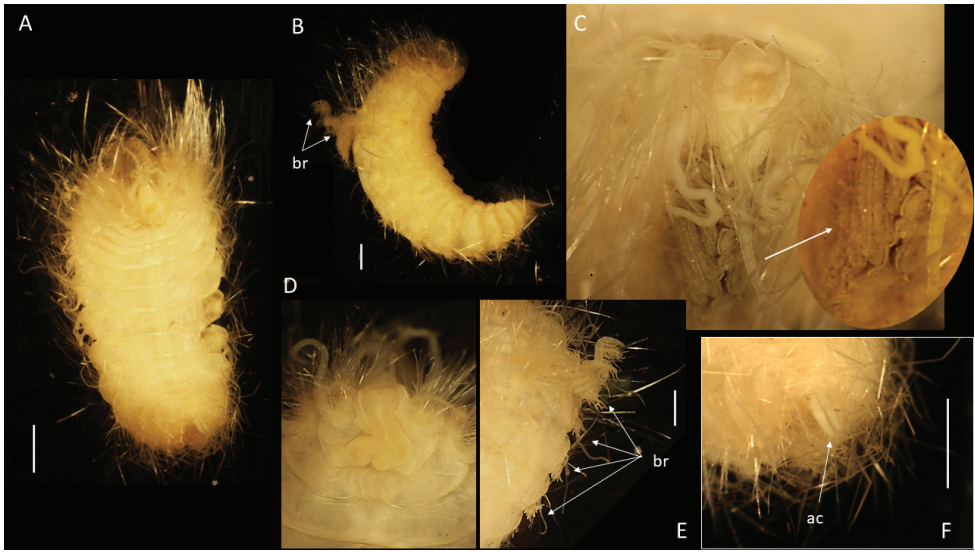


Figure 6. *Bathychloeia* cf. *sibogae* (specimen NHMUK ANEA.2022.633) **A** preserved specimen in ventral view **B** specimen in lateral view with large pair of branchiae on chaetiger 5 marked by arrows **C** anterior end in dorsal view with prostomium and caruncle (insert) **D** detail of mouth and anterior end in ventral view **E** branchiae on chaetiger 5-8 marked by arrows **F** detail of anterior end with anal cirri marked by arrow. Scale bars: 1 mm. Abbreviations: br – branchiae, ac – anal cirri.

tomium posteriorly extended into a conspicuous caruncle, reaching anterior margin of chaetiger 4, mostly free from the body wall, wedge-shaped with greatly undulated lateral margins with ca. 10 folds in larger specimens (Figs 6C, 7A, C) and simple “tongue-like” structure in smaller specimens (Fig. 8C). Slender cirriform style of median antenna ca. $\frac{1}{2}$ the length of caruncle.

Parapodia biramous with distinctly separated rami, bearing cirri that are easily detached. Dorsal and lateral cirri slender, filiform, and long, present in notopodia; dorsal cirrus inserted dorsolaterally to notochaetae, lateral cirrus, inserted medially behind notopodial chaetae. Ventral cirri also filiform and elongated (particularly in chaetiger 1, Fig. 7E), but on subsequent chaetigers shorter than dorsal or lateral cirri. First pair of branchiae always on chaetiger 5 where greatly enlarged (Figs 6B, E, 7F, 10A, B). In large specimens branchiae with a large primary stalk with up to six smaller branches, each with many long slender lateral filaments (Figs 7F, 10A, B); subsequent branchiae (if detected) much reduced in size (Fig. 6E), bipinnate with up to seven branches (Fig. 8B). In smaller specimens branchiae of chaetiger 5 also enlarged, but simpler, bipinnate, with a slender main stalk and up to seven pairs of lateral filaments (Fig. 8E).

Notopodia with chaetae much larger and usually thicker than those of neuropodia, almost forming a “cage” over dorsum, obscuring the branchiae in some specimens, but very fragile and easily lost in most specimens, best preserved in juvenile specimens (Fig. 9A). Both noto- and neurochaetae bifurcate of various lengths, and thickness of shafts and prongs (Fig. 9B–H). Long prongs mainly with smooth margin (Fig. 9B,

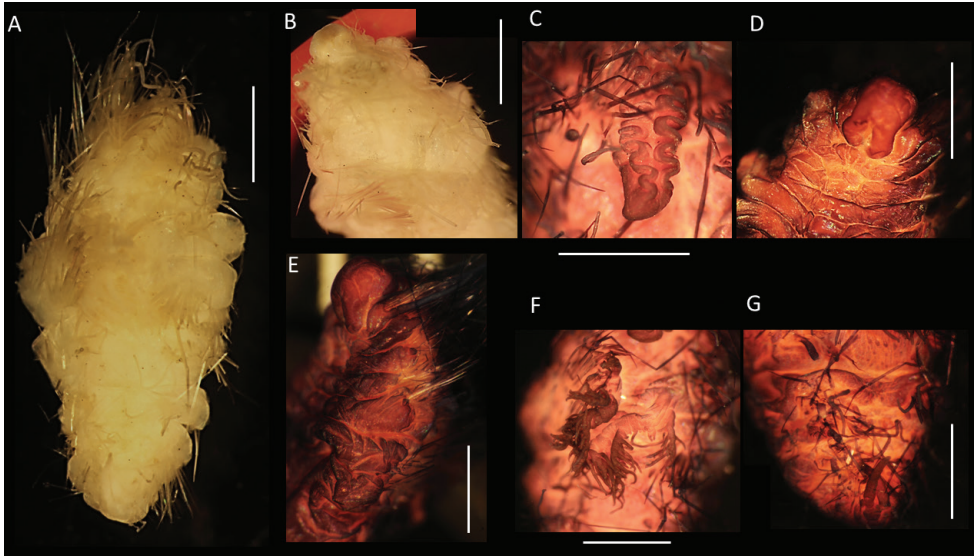


Figure 7. *Bathychloeia* cf. *sibogae* (specimen NHMUK ANEA.2022.634) **A** preserved specimen in dorsal view **B** anterior end in dorsal view **C** detail of the posterior end of caruncle **D** anterior end and mouth in ventral view **E** anterior end in lateral view with long ventral cirri on chaetiger 1 **F** large pair of branchiae on chaetiger 5 **G** posterior end in dorsal view with pair of anal cirri. Scale bars: 1 mm.

D, E, F, H) or variably developed serrated margin on inner (Fig. 9C) or outer margin (Fig. 9G). Pygidium with dorsal anus and a pair of digitiform elongated cirri (Fig. 7G).

Variation. Molecular analysis suggests that smaller and larger specimens that differ predominantly in the form of caruncle and form of branchiae as described above, represent the same species. Therefore, the size difference likely represents different developmental changes.

Molecular information. Only one CCZ specimen of *B. cf. sibogae*, specimen NHMUK ANEA.2022.633, was sequenced for all three genes, 16S, 18S and COI (Table 1). Three other specimens were successfully sequenced for COI and five for 16S only (Table 1). In addition, 16S (GenBank accession numbers ON900090 and ON900091) and COI (GenBank accession numbers ON903195 and ON903196) sequences were obtained from two specimens in the comparative material (NHMUK ANEA.2022. 455-456) that were collected from the abyssal South Pacific (off Australia). The COI sequences from this species matched four sequences on GenBank with accession numbers KJ736482-KJ736485, all four from other areas within CCZ (Janssen et al. 2015). In the phylogenetic tree, the specimens from CCZ and Australia fall as a sister taxon to *Bathychloeia* cf. *balloniformis* (Fig. 5B). The *Bathychloeia* clade is in an unresolved trichotomy with clades consisting of species from the genera *Chloeia* and *Notopygos*, although the trichotomy has low support (Fig. 5A). Uncorrected 'p' from a COI alignment of 534 characters shows values among the nine *B. cf. sibogae* specimens ranging from 0.0 to 0.015, while the lowest value between *B. cf. sibogae* and its closest relative in our phylogenetic analysis, *B. cf. balloniformis*, is 0.18.

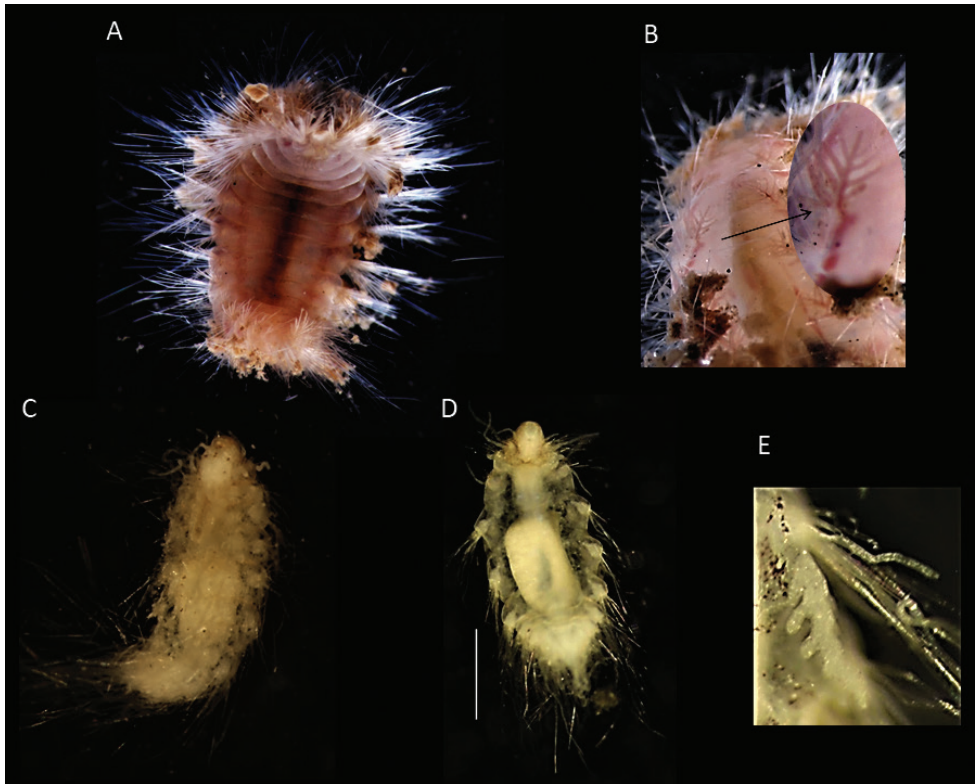


Figure 8. *Bathychloeia* cf. *sibogae* CCZ-collected specimens **A** large live specimen (NHMUK ANEA.2022.633) in ventral view **B** live specimen (NHMUK ANEA.2022.633) with midbody segments and associated branchiae in dorsal view, insert – the detail of branchiae from chaetiger 9 **C** small (juvenile) preserved specimen (NHMUK ANEA.2022.635) in dorsolateral view **D** small (juvenile) preserved specimen (NHMUK ANEA.2022.632) in dorsal view **E** detail of enlarged branchiae on chaetiger from specimen (NHMUK ANEA.2022.632). Scale bar: 1 mm.

Remarks. The enlarged branchiae of chaetiger 5 suggest close affiliation of CCZ specimens to *Bathychloeia sibogae* Horst, 1910 described from the Banda Sea, depth of 1100 m. Since its original description and subsequent re-description (Horst 1912), specimens assigned to *B. sibogae* or *B. cf. sibogae* have been reported from vastly different geographic and more importantly bathymetric areas such as the Tasman Sea and off Kenya (Kirkegaard 1995), Guinea Basin in SE Atlantic in depths of 5048–5144 m (Böggemann 2009) and South Pacific in depths of 2566 m and 4260 m (Gunton et al. 2021). Further, Böggemann (2009) suggested that syntypes (BMNH1885.12.1.11) of *Chloenopsis atlantica* (McIntosh) from the NE Atlantic (Canary Islands, ca. 2800 m depth) may in fact belong to *B. sibogae* due to presence of similar branchiae and two notopodial cirri.

Although the original definition of *B. sibogae* given by Horst (1910) was limited, a more detailed re-description was provided by Horst later (Horst 1912). The type specimen ZMA.V.POL.124 was on loan and therefore not available for examination at

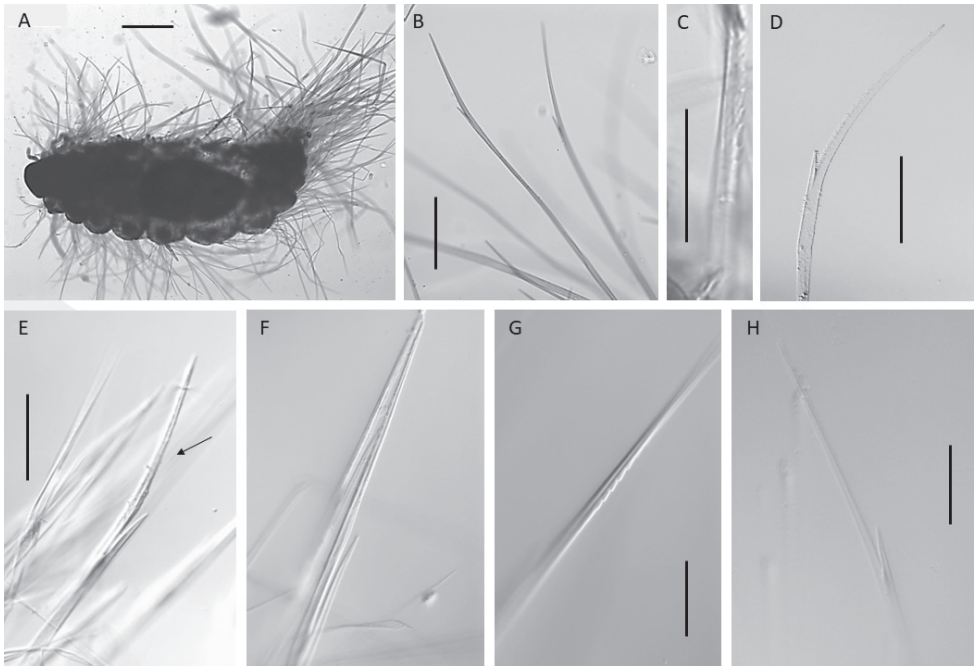


Figure 9. *Bathychloeia* cf. *sibogae* (specimen NHMUK ANEA.2022.635) **A** overview of specimen in dorsal view **B** slender furcate notochaetae **C** prong with distinct serration on inner margin **D** slender short furcate chaeta **E** long stout furcate chaeta (marked by arrow) **F** smooth prongs **G** faintly serrated prong, outer margin **H** slender furcate chaeta. Scale bars: 250 μm (**A**); 100 μm (**B**), 50 μm (**C**, **D**, **G**, **H**); 100 μm (**E**).

the time of writing (J Bleeker, pers. comm.). Based on re-description of Horst (1912) CCZ specimens differ mainly in the presence of red eyes and form of branchiae that are bi-pinnate but with many slender filaments developed on lateral branches (Fig. 10A, B), a character not reported by Horst (Fig. 10D). CCZ specimens also correspond well with those reported by Böggemann (2009) from the abyssal SE Atlantic in having similar body shape and body size, presence of tiny eyes, form and distribution of parapodial cirri, well developed highly crenulated and folded caruncle (in larger specimens), enlarged branchiae on chaetiger 5 and form of pygidial cirri. However, Böggemann (2009) did not report the presence of long filaments of branchial lateral branches (Fig. 10E). Additionally, specimens identified as *B. cf. sibogae* collected from the abyssal South Pacific were also available for morphological and molecular comparison (see also Gunton et al. 2021). Morphologically the South Pacific specimens agreed with those collected from CCZ, with long filaments on lateral branchial branches either present or absent (Fig. 10C). Significantly, the molecular data (CO1, 16S and 18S markers) suggested that CCZ and South Pacific specimens belong to the same species, therefore the presence/absence of filaments on lateral branchial branches may be a matter of preservation or developmental character. Currently, no molecular data

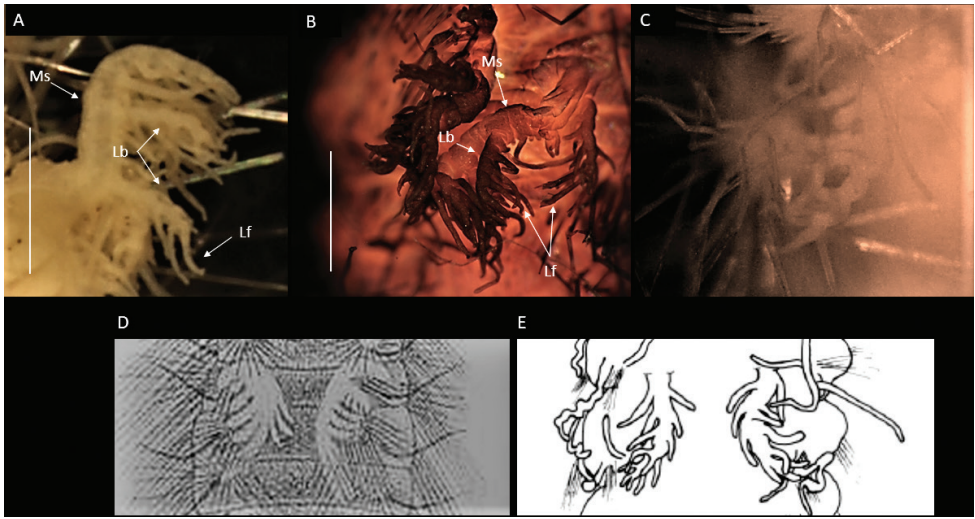


Figure 10. Comparative figure of form of enlarged branchiae from chaetiger 5 showing variation in development of long branchial filaments, Ms – Main stalk, Lb – lateral branches, Lf – long filaments **A** *Bathychloeia* cf. *sibogae* CCZ specimen, NHMUK ANEA.2022.633, in lateral view **B** *Bathychloeia* cf. *sibogae* CCZ specimen, NHMUK ANEA.2022.634, specimen stained with Shirlastain, in dorsal view **C** *Bathychloeia* cf. *sibogae* South Pacific specimen NHM_215 in dorsal view **D** *Bathychloeia* *sibogae* after Horst (1912) **E** *Bathychloeia* *sibogae* after Böggemann (2009). Scale bars: 1 mm.

are available from the SE Atlantic specimens or from the type locality. Although it is unlikely that abyssal specimens belong to the same species as that described by Horst (1910) from 1100 m, due to lack of molecular data from type locality we cautiously ascribe CCZ-collected specimens to *Bathychloeia* cf. *sibogae*.

Distribution. Central Pacific Ocean, Eastern CCZ, in the exploration areas UK-1, OMS, NORI-D (Fig. 1) and based on previous study in GBR (German) and IFREMER (French) exploration areas (Janssen et al. 2015). Abyssal South Pacific, off Australia, ca. 4000 m.

Ecology. It is of interest that a closely related form to the CCZ species known as *Cholenopsis atlantica* (McIntosh, 1885) has been described in association with a sponge growing on a dead coral coated with manganese of peroxide (McIntosh 1885), while the CCZ species has been collected from the sediment associated with manganese nodules.

Paramphinome M. Sars in G. Sars, 1872

Type species. *Paramphinome pulchella* M. Sars in G. Sars, 1872.

Diagnosis. Small but long long-bodied forms. Prostomium posteriorly with Y-shaped or elongated caruncle. Branchiae comb-shaped, limited to the anterior chaetigers. First chaetiger with curved hooks in notopodia.

***Paramphinome* sp. NHM_6022E**

Figs 11A–C, 12A–I

Material examined. NHM_1167D, NHMUK ANEA 2022.638, coll. 26/02/2015, EBS, 12.11550, -117.16450, 4100 m, OMS, <http://data.nhm.ac.uk/object/fd4902df-aef2-44cf-991f-31905434c2a1>; NHM_4044, NHMUK ANEA 2022.639, coll. 06/03/2020, box core, 13.27406, -116.69997, 4185 m, UK-1, <http://data.nhm.ac.uk/object/56235559-3f2c-426e-b4cd-37462593a4ba>; NHM_6022E, NHMUK ANEA 2022.640, coll. 13/11/2020, box core, 10.35780, -117.15931, 4284 m, NORI-D, <http://data.nhm.ac.uk/object/bd4b405d-3e56-4671-909e-fd9c3e7fbcf>.

Diagnosis (after Fauchald (1977)). All very small, poorly preserved and posteriorly incomplete specimens (Fig. 11A–C). Specimen NHMUK ANEA.2022.638, 1.65 mm long and 0.35 mm wide for ca. 7 discernible chaetigers. Prostomium broad, rounded, slightly longer than wide; with a pair of palps and lateral antennae and posteriorly with median antenna; all prostomial appendages tiny and globular to ovoid (Fig. 12A, B). Two pairs of tiny reddish eyes (Fig. 12A) in trapezoidal arrangement, plus a pair of tiny, pigmented spots present posteroventrally on prostomium (Fig. 12B). Caruncle as a low-lying lobe, reduced, difficult to observe.

Parapodia biramous. Dorsal cirri small and ovoid (Fig. 12F), ventral cirri not observed. Two pairs of branchiae present on chaetiger 4 and 5, comb-shaped with two main stalks branching into 4 terminal lobes (Figs 11A, B, 12C, D). Stout, distally strongly curved hook present in each notopodium of chaetiger 1 (Fig. 12E). Other observable chaetae include stout spines, slightly subdistally swollen (Fig. 12G); slender bifurcate chaetae, their prongs significantly differing in length, the long prong marginally serrated (Fig. 12H) and slender, long, smooth chaetae (Fig. 12I). Posterior segments and pygidium not observed.

Molecular information. Only one specimen, NHMUK ANEA.2022.640, was successfully sequenced for 16S and 18S (Table 1). There were no identical sequences for 16S on GenBank. In the phylogenetic tree this species falls as a sister taxon to *Paramphinome jeffreysii* and an unidentified specimen, Amphinomidae sp. RG-2014 (Fig. 5A).

Remarks. Three very small posteriorly incomplete specimens were collected in CCZ samples. They differ from known species by its very small size and low number of branchial pairs (only two pairs) and undeveloped prostomial appendages, which are tiny and globular. While body size, number of segments and number of branchial pairs were previously linked to developmental stages (e.g., Kudenov 1993; Barroso and Paiva 2008), we believe that the three specimens presented here, collected during three different cruises up to eight years apart, represent a small-bodied species rather than juveniles.

Of the known deep-sea *Paramphinome* species, none were described from the abyssal depths. *Paramphinome pacifica* Fauchald & Hancock, 1981 has been described from NE Pacific Ocean: off central Oregon (USA), 1800–2900 m; (type locality: Cascadia Abyssal Plain, 2860 m). *Paramphinome australis* Monro, 1930 has type locality off Signy Island, South Orkney Islands, Southern Ocean in depths between 244–344 m,

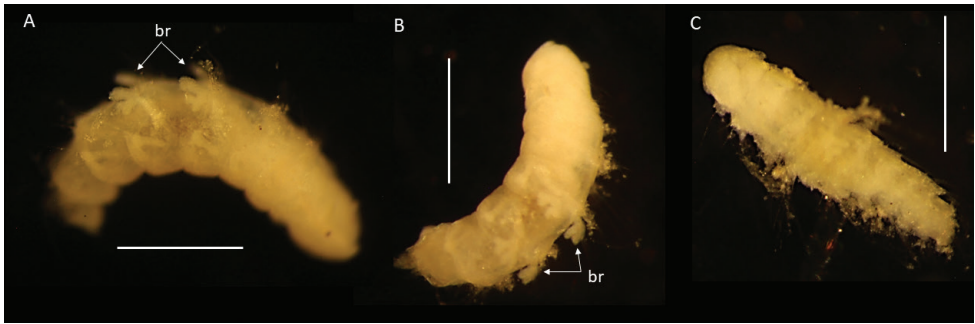


Figure 11. *Paramphinome* sp. NHM_6022E **A, B** preserved specimen NHMUK ANEA.2022.638 in dorsolateral view, branchiae (br) of chaetigers 4 and 5 marked by arrows **C** preserved specimen, NHMUK ANEA.2022.639, in dorsal view. Scale bars: 500 μ m.

although it has been widely reported from the Southern Ocean (Kudenov 1993) and also the abyssal Atlantic (Böggemann 2009). *Paramphinome posterobranchiata* Barroso & Paiva, 2008 has type locality in South Atlantic, off Brazil at 1600 m depth. Finally, *P. jeffreysii* has type locality in St. Lawrence estuary (shallow depths), but has been widely reported, even from great depths (e.g., Gunton et al. 2015) and specimens ascribed to this taxon likely represents different species (see Fig. 5A).

It is likely that the CCZ-collected specimens represent a new species; however, their tiny size and poor morphological preservation prevent its formal description, therefore the specimens are assigned to morphospecies only.

Distribution. Central Pacific Ocean, Eastern CCZ, the exploration contract areas UK-1, OMS, and NORI-D (Fig. 1).

Euphrosinidae Williams, 1852

Euphrosinella Detinova, 1985

Type species. *Euphrosine cirratiformis* Averincev, 1972.

Diagnosis (modified from Kudenov (1993)). Prostomium with five appendages, including median antenna, two lateral antennae and two palps. Eyes present or absent. Caruncle free from the body wall for most of its length. Ringent chaetae absent.

Remarks. Genus *Euphrosinella* was established by Detinova (1985) to accommodate species originally described by Averincev (1972) as *Euphrosine cirratiformis*. She distinguished *Euphrosinella* from *Euphrosine* mainly on the bases of the presence of five (instead of three) prostomial appendages. Characters such as the extent of fusion of caruncle to body wall and the absence of ringent chaetae were also suggested by Detinova (1985) but questioned by Kudenov (1993). The genus currently contains only two valid species, both from the deep waters and/or Antarctic habitats. *Euphrosinella cirratiformis* is widely distributed in the Antarctic waters and was considered circumpolar (Kudenov 1993), although recent molecular data suggest

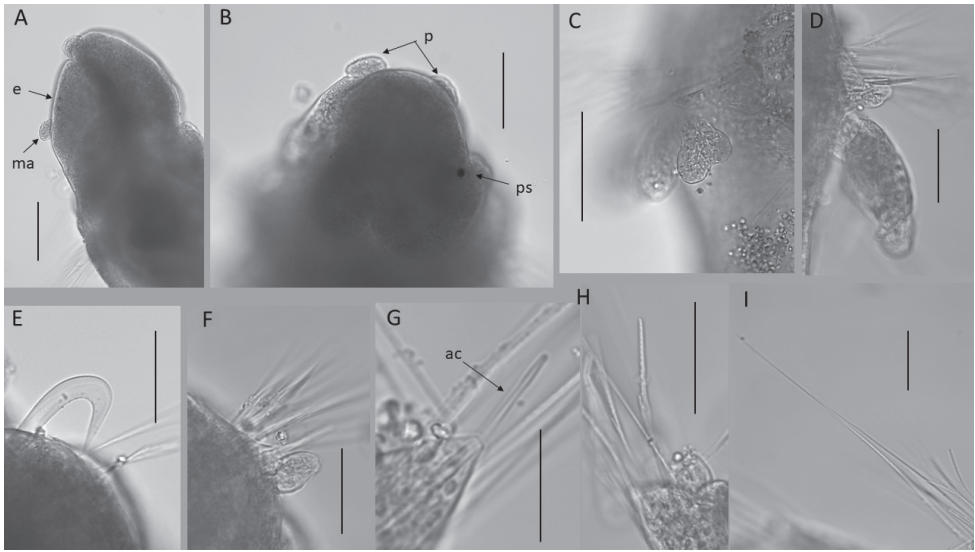


Figure 12. *Paramphinome* sp. NHM_6022E (specimen, NHMUK ANEA.2022.638) **A** anterior end in lateral view, with eyes and median antenna **B** prostomium in ventral view with palps and pigmented spots **C** detail of branchiae from chaetiger 4 in dorsolateral view **D** branchiae and dorsal lobe from chaetiger 4 in lateral view **E** notopodial hook from chaetiger 1 **F** dorsal lobe from chaetiger 2 **G** protruding acicular spine (ac) **H** spinose bifurcate chaeta **I** long spinose neurochaeta. Scale bars: 100 µm (**A–C**); 50 µm (**D–I**). Abbreviations: e – eyes, ma – median antenna, p – palps, ps – pigmented spots, ac – acicular spines.

the presence of at least two distinct species (Brasier et al. 2016). The second species, *Euphrosinella paucibranchiata* (Hartman 1960) has been described from deep waters off California (Santa Cruz Basin, 1737 m depth) and has not been widely reported since.

***Euphrosinella georgievae* sp. nov.**

<https://zoobank.org/EE13C699-0E67-4060-893C-0AB0BB5E0045>

Figs 13A–G, 14A–F, 15A, 16A–G

Material examined. NHM_0587, NHMUK ANEA 2022.658, coll. 17/02/2015, EBS, 12.38624, -116.54867, 4202 m, UK-1, <http://data.nhm.ac.uk/object/b7a0bf33-0dc4-4f61-90de-35865647a99f>; NHM_0777, NHMUK ANEA 2022.659, coll. 20/02/2015, EBS, 12.38624, -116.54867, 4202 m, UK-1, <http://data.nhm.ac.uk/object/a8f0e776-d7b6-4ec6-a549-78f40f17d89b>; NHM_1737B, NHMUK ANEA 2022.660, coll. 11/03/2015, EBS, 12.17383, -117.19283, 4045 m, OMS, <http://data.nhm.ac.uk/object/2784df45-ee0-4151-b12d-11d955985faa>; NHM_0910, NHMUK ANEA 2022.661, coll. 23/02/2015, EBS, 12.57133, -116.6105, 4198 m, UK-1, <http://data.nhm.ac.uk/object/05dfb32c-fc3a-4028-bf09-3eb840175661>; NHM_1134 (paratype), NHMUK ANEA 2022.662, coll. 26/02/2015, EBS, 12.1155, -117.1645, 4100 m, OMS, <http://data.nhm.ac.uk/object/00590d2b-f952-4c69-8bc2->

ac2a408da17a; NHM_1514, NHMUK ANEA 2022.663, coll. 05/03/2015, EBS, 12.51316667, -116.491333, 4252 m, UK-1, <http://data.nhm.ac.uk/object/96cb7b69-c0ea-4559-9b57-3abe6af4a4c7>; NHM_2391 (holotype), NHMUK ANEA 2022.664, coll. 20/02/2015, EBS, 12.53717, -116.60417, 4425 m, UK-1, <http://data.nhm.ac.uk/object/1ce8325f-74de-47de-a776-2dc50b8d69ae>; NHM_4975, NHMUK ANEA 2022.665, coll. 28/10/2020, box core, 11.013923, -116.258737, 4234 m, NORI-D, <http://data.nhm.ac.uk/object/677b7d67-d9cc-4ebd-8d79-cf5da5dc40da>; NHM_6087, NHMUK ANEA 2022.666, coll. 14/11/2020, box core, 10.647709, -117.226887, 4183 m, NORI-D, <http://data.nhm.ac.uk/object/eebfaecd-5ee2-49d6-be73-51eb91678487>; NHM_5802, NHMUK ANEA 2022.667, coll. 11/10/2020, box core, 10.475094, -117.384872, 4306 m, NORI-D, <http://data.nhm.ac.uk/object/c0e408e3-91e7-408f-aaef-3be86507105a>; NHM_5057, NHMUK ANEA 2022.668, coll. 30/10/2020, box core, 10.929036, -116.26351, 4262 m, NORI-D, <http://data.nhm.ac.uk/object/d92b1574-eccb-443c-a15d-b79357360b59>; NHM_7235, NHMUK ANEA 2022.669, coll. 14/05/2021, box core, 10.3773, -117.1558, 4302 m, NORI-D, <http://data.nhm.ac.uk/object/55637dc0-f9b9-4586-9bfb-7a821c785279>; NHM_2908, NHMUK ANEA 2022.670, coll. 20/02/2015, EBS, 12.53717, -116.60417, 4425 m, UK-1, <http://data.nhm.ac.uk/object/fba3fab7-ae4b-4415-a73c-a2ba6cd44601>.

Diagnosis. *Holotype* (NHMUK ANEA.2022.664) complete (except for tissue sampled for DNA), 4.2 mm long and 1.1 mm wide without chaetae for 15 chaetigers (Fig. 13A). *Paratype* (NHMUK ANEA.2022.662) complete (except for tissue sampled for DNA), with 13 chaetigers (Fig. 14A). Body short, oval, flattened, pale yellow in alcohol (Figs 13A, 14A). Prostomium longer than wide, with five prostomial appendages (Fig. 15A). Pair of short slender palps (Figs 13C, 14C, D); pair of slender lateral antenna (Figs 13C, 14C, D); median antenna of caruncle with long thick ceratophore and slender cirrus only slightly longer than caruncle (Fig. 13C). Caruncle as oval lobe reaching to anterior margin of chaetiger 4, mostly free of body wall, with median keel and two pairs of lateral ridges, with median keel slightly thicker than the lateral ones (Fig. 13C, D). Eyes not observed.

Parapodia biramous, two rami well separated. Parapodia of chaetiger 1 well developed, not reduced, with dorsal, lateral, and ventral cirri (Fig. 13C). Parapodial appendages of subsequent chaetigers in the following dorsoventral order: dorsal cirrus, branchia, lateral cirrus, ventral cirrus (Fig. 15C). All cirri as single filaments of various length and thickness with dorsal cirrus longest (extending over three chaetigers in mid-body) (Figs 13E, 14E); lateral cirrus shorter and more stout inserted in the middle of notochaetal bundle (Fig. 13E, F); ventral cirrus slightly shorter than lateral cirrus, slender. Branchia one per chaetiger, simple (unbranched) cirrus, inserted laterally to dorsal cirrus, very short (ca. $\frac{1}{2}$ the length of mid body chaetiger) (Figs 13E, F, 14E, 15C).

All chaetae well developed, but prone to breakage, all bifurcate (Fig. 16A). Notochaetae in approximately three tiers; differing mainly in their length and thickness with notochaetae of mid tier longest and thickest (Fig. 16B–E); prongs mostly smooth (Fig. 16B, C, E) or few with very faint serration (Fig. 16D); ratio of short to long prong in the short chaetae of anterior tier ranges from 1:3.5–4 (where possible to establish);

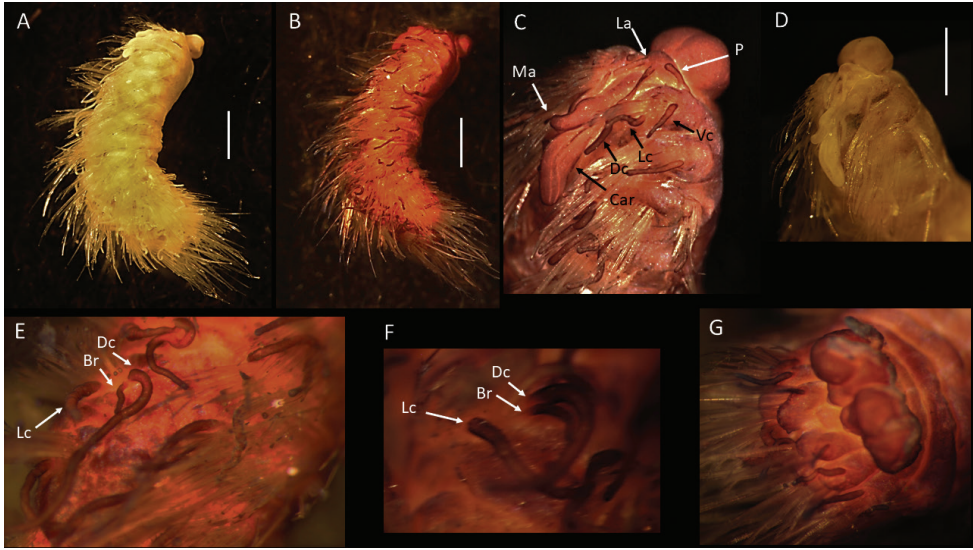


Figure 13. *Euphrosinella georgievae* sp. nov. (holotype, NHMUK ANEA 2022.664) **A** preserved specimen in lateral views **B** specimen stained with Shirlastain in lateral view **C, D** detail of anterior end and prostomium with palps (P), lateral antennae (La), median antenna (Ma), caruncle (Car) and first chaetiger – dorsal cirrus (Dc), lateral cirrus (Lc) and ventral cirrus (Vc) marked by arrows **E, F** midbody chaetigers in dorsal view with branchiae (Br), dorsal (Dc) and lateral cirri (Lc) marked by arrows **G** pygidium in distal view. Scale bars: 1 mm. Abbreviations: Ma – median antenna, La – lateral antennae, P – palps, Vc – ventral cirrus, Lc – lateral cirrus, Dc – dorsal cirrus, Car – caruncle, Br – branchiae.

in long chaetae of mid-tier ratio ranges from 1:4 to 1:5 (where possible to establish). Ringent notochaetae absent. Neurochaetae less numerous and thinner than notochaetae; all bifurcate, of varying lengths, prongs with noticeable serration (Fig. 16F, G), few prongs appearing smooth. Pygidium with paired anal cirri, resembling cylindrical tube feet (Figs 13G, 14B, F).

Molecular information. One specimen, NHMUK ANEA.2022.658, was sequenced for 16S and 18S genes, while the 13 additional specimens were sequenced for 16S only (Table 1). There were no identical sequences for 16S on GenBank. In the phylogenetic tree this species falls as a sister taxon to *Euphrosinella* cf. *cirratiformis* from Antarctica (Fig. 5B).

Remarks. *Euphrosinella georgievae* sp. nov. is consistent with the genus *Euphrosinella* in having five prostomial appendages, caruncle mostly free from body wall and absence of ringent chaetae. Only two valid species in *Euphrosinella* are currently known as mentioned earlier. A known Pacific species *Euphrosinella paucibranchiata* can be distinguished by having some branchiae branched, as well as much shallower depth distribution of 1737 m in Santa Cruz Basin. *Euphrosinella georgievae* sp. nov. is more similar to the Antarctic species *E. cirratiformis* in having simple unbranched branchiae. The species also share a similar form and length of caruncle and median antenna. However, the two species differ in the following characters: 1. The presence of two pairs of eyes in the Antarctic species, while CCZ

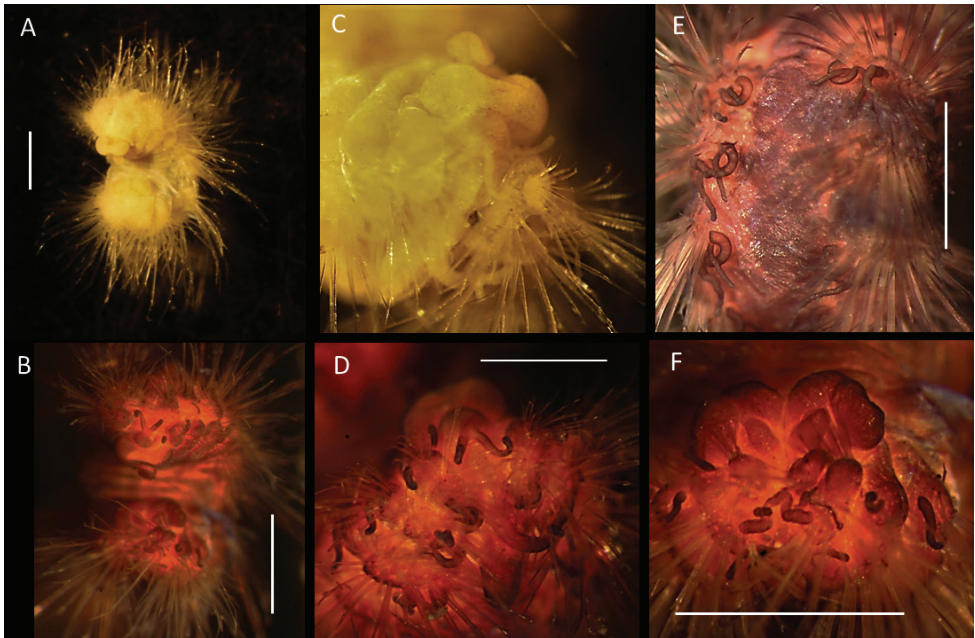


Figure 14. *Euphrosinella georgievae* sp. nov. (paratype NHMUK ANEA.2022.662) **A** preserved specimen in dorsolateral view **B** specimen stained with Shirlastain, in dorsolateral view **C** detail of anterior end in dorsolateral view **D** detail of prostomium, with palps and lateral antennae **E** dorsal view of midbody chaetigers, showing branchiae and dorsal cirri **F** detail of pygidium in distal view. Scale bars: 1 mm.

specimens are eyeless; 2. Notochaetae arranged in 3 tiers in new species, rather than 2 tiers in the known species and 3. Branchiae are not developed on first chaetiger in *E. georgievae* sp. nov., whilst they are present in *E. cirratiformis*. As further evidence, the molecular data suggest that Antarctic specimens identified in a previous study as *Euphrosinella* cf. *cirratiformis* (see Brasier et al. 2016) are different to the specimens of *E. georgievae* sp. nov. (Fig. 5B).

Distribution. Central Pacific Ocean, Eastern CCZ, the exploration areas UK-1, OMS, and NORI-D (Fig. 1).

Etymology. This species is named for Dr. Magdalena Georgieva, who took part in ABYSSLINE expeditions to CCZ. She also collected *Bathychloeia* cf. *sibogae* specimens from CCZ used in this study as well as samples from the South Pacific during the RV Investigator cruise used here as a comparative material.

Euphrosinopsis Kudenov, 1993

Type species. *Euphrosinopsis antipoda* Kudenov, 1993.

Diagnosis (after Kudenov (1993)). Prostomium with five appendages, including median antenna, two lateral antennae, and two palps. No prostomial eyes, with one

pair of eyes deeply embedded lateral to median antenna. Caruncle free from the body wall for most of its length.

Remarks. The genus *Euphrosinopsis* is currently endemic to Antarctica and has been established to accommodate three known Antarctic species (Kudenov 1993): *E. antarctica* (Hartmann-Schröder & Rosenfeldt, 1992), *E. crassiseta* Kudenov, 1993, and *E. horsti* Kudenov, 1993. It is similar to *Euphrosinella* in having five prostomial appendages and reduced fusion of caruncle to the body wall. The main difference from both *Euphrosine* and *Euphrosinella* considered by Kudenov (1993) was the lack of prostomial eyes and presence of large, deeply embedded eyes positioned laterally to median antenna.

***Euphrosinopsis abearni* sp. nov.**

<https://zoobank.org/CF28C891-3176-4233-9FA4-34DB9451B395>

Figs 15B, 17A–F, 18A–F, 19A–I

Material examined. NHM_0095, NHMUK ANEA 2022.644, coll. 11/10/2013, box core, 13.79335, -116.70308, 4081 m, UK-1, <http://data.nhm.ac.uk/object/a351cb41-736c-4390-8ad8-02c0358b73e0>; NHM_0888, NHMUK ANEA 2022.645, coll. 23/02/2015, EBS, 12.571333, -116.6105, 4198 m, UK-1, <http://data.nhm.ac.uk/object/4d76b4e2-569d-4a17-9276-3ce721cbdf72>; NHM_0551 (paratype, SEM), NHMUK ANEA 2022.646, coll. 17/02/2015, EBS, 12.386243, -116.54867, 4202 m, UK-1, <http://data.nhm.ac.uk/object/241b828d-a574-47f2-995d-0bdef239c427>; NHM_5042, NHMUK ANEA 2022.647, coll. 30/10/2020, box core, 10.92936, -116.26351, 4262 m, NORI-D, <http://data.nhm.ac.uk/object/1662fd8b-54a5-4f97-9083-02dbb2df7e39>; NHM_1737A, NHMUK ANEA 2022.648, coll. 11/03/2015, EBS, 12.17383, -117.19283, 4045 m, OMS, <http://data.nhm.ac.uk/object/4f372c07-c466-4b6c-91a9-229cd7c7a17d>; NHM_1876, NHMUK ANEA 2022.649, coll. 13/03/2015, EBS, 12.0415, -117.21717, 4094 m, OMS, <http://data.nhm.ac.uk/object/6ad5c2b3-ece8-4195-a19f-3913de511e71>; NHM_0550, NHMUK ANEA 2022.650, 17/02/2015, EBS, 12.386243, -116.54867, 4202 m, UK-1, <http://data.nhm.ac.uk/object/92791783-35c2-4fbf-80b0-2b074ef70828>; NHM_1302, NHMUK ANEA 2022.651, coll. 01/03/2015, EBS, 12.257333, -117.3021667, 4302 m, OMS, <http://data.nhm.ac.uk/object/7aabe644-2ec6-4671-8c1a-f826eeeb0b46>; NHM_1302A (holotype), NHMUK ANEA 2022.652, coll. 01/03/2015, EBS, 12.257333, -117.3021667, 4302 m, OMS, <http://data.nhm.ac.uk/object/479933d3-9943-4d87-a1b8-ea120bd8f4ee>; NHM_1737, NHMUK ANEA 2022.653, coll. 11/03/2015, EBS, 12.17383, -117.19283, 4045 m, OMS, <http://data.nhm.ac.uk/object/2ca3e584-a68d-4ea5-98d2-75ce10515386>;

NHM_1737C (paratype), NHMUK ANEA 2022.654, coll. 11/03/2015, EBS, 12.17383, -117.19283, 4045 m, OMS, <http://data.nhm.ac.uk/object/efe95a8c-fc88-4849-ad26-1df3d292ef20>; NHM_0616, NHMUK ANEA 2022.655, coll. 17/02/2015, EBS, 12.386243, -116.54867, 4202 m, UK-1, <http://data.nhm.ac.uk/object/4758bf19-c6d0-42e0-b5ba-e83e203d2e18>; NHM_0759, NHMUK ANEA

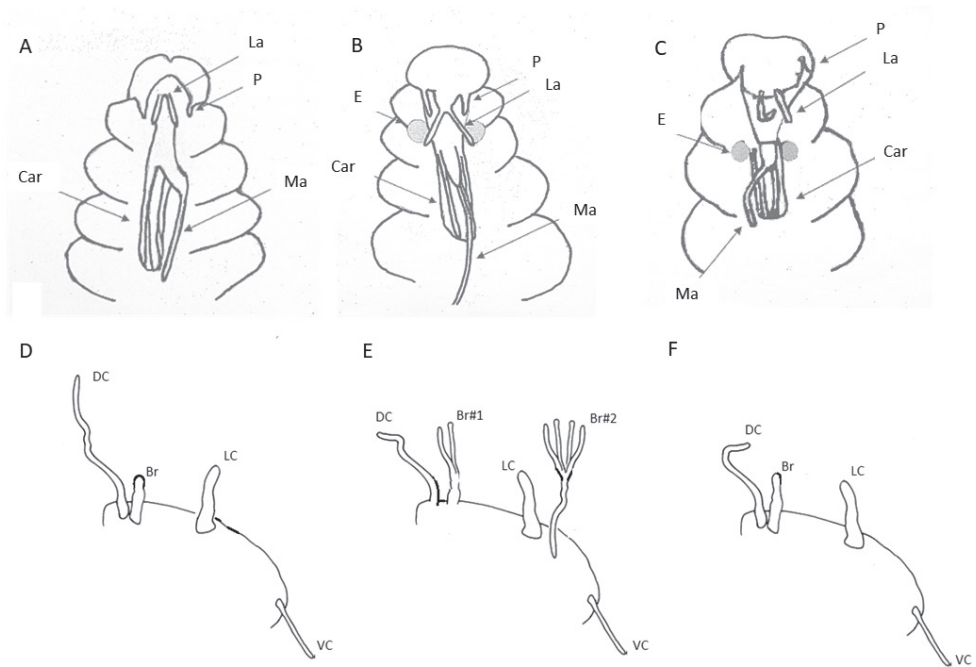


Figure 15. Diagrammatic representation of prostomial (**A–C**) and parapodial appendages from mid-body chaetigers (**D, E**) of CCZ-collected Euphosinidae species (relative lengths preserved, but not drawn to scale) **A** *Euphosinella georgievae* sp. nov. **B** *Euphosinopsis ahearni* sp. nov. **C** *Euphosinopsis halli* sp. nov. **D** *Euphosinella georgievae* sp. nov. **E** *Euphosinopsis ahearni* sp. nov. **F** *Euphosinopsis halli* sp. nov. Abbreviations: P – palps, La – lateral antennae, Ma – median antenna, Car – caruncle, E – eyes, DC – dorsal cirrus, LC – lateral cirrus, VC – ventral cirrus, Br – branchiae.

2022.656, coll. 20/02/2015, EBS, 12.53717, -116.60417, 4425 m, UK-1, <http://data.nhm.ac.uk/object/b0f9162f-a861-4eb2-89a1-ce25c2bd09c4>; NHM_1839, NHMUK ANEA 2022.657, coll. 12/03/2015, box core, 12.0999, -117.1966, 4051 m, OMS, <http://data.nhm.ac.uk/object/02a5ace7-841e-4f50-bf03-57ba21f02f7c>.

Diagnosis. Holotype (NHMUK ANEA.2022.652) complete (except for tissue sampled for DNA), 2.2 mm long and 0.8 mm wide without chaetae for 12 chaetigers (Fig. 17A–F). **Paratype** (NHMUK ANEA.2022.654) complete (except for tissue sampled for DNA), 2.8 mm long and 1 mm wide for 12 chaetigers (Fig. 18A–F). **Paratype** (NHMUK ANEA.2022.646, SEM specimen) anterior fragment only (Fig. 19A–I). Body short, oval, flattened, pale yellow in alcohol (Figs 17A, 18B), with a patch of light brown pigmentation on prostomium (Fig. 18C). Live specimen pale with blueish hues (Fig. 18A). Prostomium longer than wide, with 5 prostomial appendages (Fig. 15B). Pair of short slender palps (Figs 17C, 18D); pair of slender lateral antenna (at least twice the length of palps) (Figs 17C, 18D) and median antenna of caruncle with long thick ceratophore and very long slender cirrus reaching dorsally to chaetiger 7 (Fig. 17F). Caruncle as oval lobe reaching to anterior margin of chaetiger 4, mostly

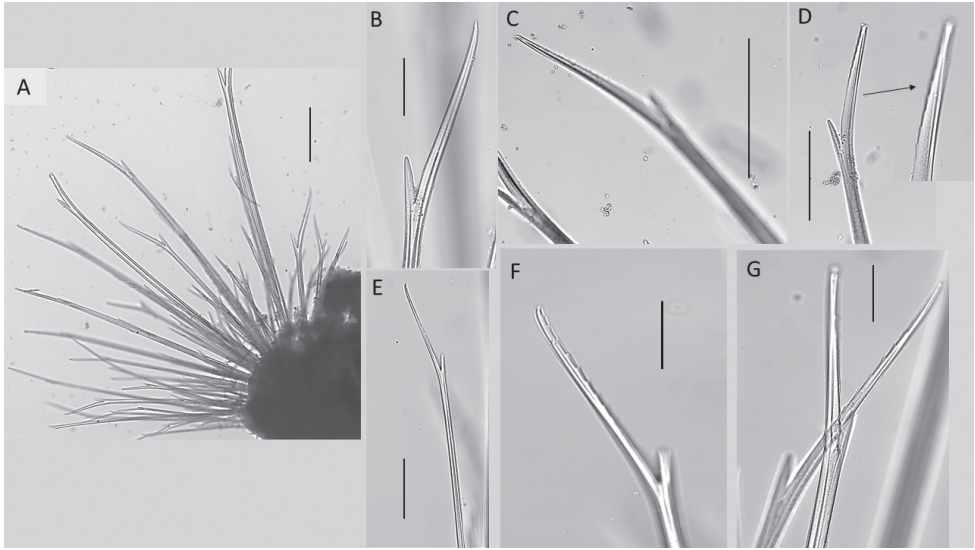


Figure 16. *Euphrosinella georgievae* sp. nov. (specimen NHMUK ANEA.2022.658) **A** mid body parapodium **B** notochaeta from anterior tier **C** notochaeta from mid-tier **D** notochaeta from posterior tier, detail of serration (insert) **E–G** examples of neurochaetae. Scale bars: 100 μm (**A, B, E**); 200 μm (**C**); 250 μm (**D**); 50 μm (**F, G**).

free of body wall, with median keel and two pairs of lateral ridges, median keel slightly thicker than the lateral ones. Single pair of large, spherical eyes, deeply embedded, lateral to median antenna and caruncle (Figs 15B, 18A).

Parapodia biramous, two rami well separated. Parapodia of chaetiger 1 well developed, not reduced, parapodial cirri, branchiae or ringent chaetae not observed. In subsequent parapodia, parapodial appendages in the following dorsoventral order: dorsal cirrus, 1st branchia, lateral cirrus, 2nd branchia, ventral cirrus (Fig. 15E). Dorsal cirrus as a single very long filament (extending over two chaetigers in mid-body segments) (Fig. 18F); the lateral cirrus as a shorter, stouter filament (Fig. 17D, E); ventral cirri often missing, when observed, very slender (Fig. 18E). Branchiae up to two pairs present per segment in mid-body, first branchia attached laterally to dorsal cirrus (Figs 15E, 18F), second branchia attached laterally to lateral cirrus (Figs 15E, 17D), both branchiae branched with 2–4 very long and slender branches (Figs 15E, 17D, E, 18E, F).

Chaetae fragile, prone to breakage, of two main types: 1. Numerous, bifurcate chaetae arranged in three rows in notopodia; their shafts of various length and thickness (Fig. 19A); their prongs variable in length with short furcate chaetae in anterior tier having the ratio of short to long prong ca. 1:3.5 (where possible to establish), the prong ratio of longest chaetae in the mid tier 1:4–5 (where possible to establish); prongs mainly smooth or with faint serration (Fig. 19C–E); 2. Ringent chaetae (sensu Kudenov 1993) present in notopodia only, numerous (ca. 20 per notopodium) (Fig. 19A, B), composed of two curved prongs of unequal length and thickness, both

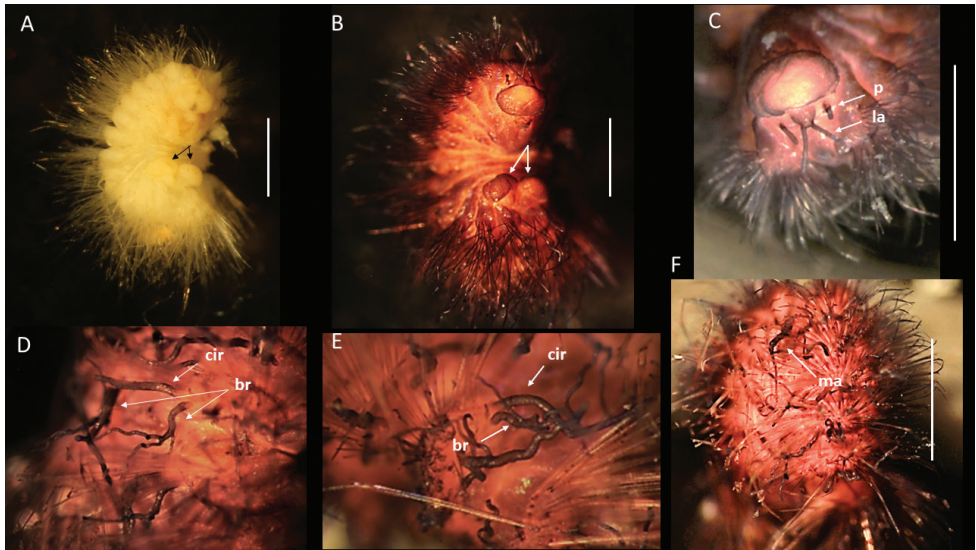


Figure 17. *Euphrosinopsis ahearni* sp. nov. (holotype NHMUK ANEA.2022.652) **A** preserved specimen in dorsolateral view, pygidial cirri marked by arrows **B** specimen Shirlastained in dorsolateral view, pygidial cirri marked by arrows **C** detail of prostomium in dorsal view with palps (p) and lateral antennae (la) marked by arrows **D, E** branched branchiae (br) and lateral cirrus (cir) of midbody chaetigers **F** detail of midbody chaetigers, median antenna (ma) marked by arrow. Scale bars: 1 mm. Abbreviations: P – palps, la – lateral antennae, cir – cirrus, br – branchiae, ma – median antenna.

with distinct serration, the long prong distally with slender tip, short prong broad and distally rounded (Fig. 19F–I). Neurochaetae numerous, but thinner than notochaetae, all bifurcate, of varying lengths prongs appearing smooth. Pygidium with paired anal cirri, resembling cylindrical tube feet (Fig. 17A, B).

Molecular Information. Specimen (NHMUK ANEA.2022.644) was sequenced for 16S and 18S while 14 other specimens were sequenced for 16S only. There were no identical sequences for 16S on GenBank (Table 1). The relationships between *Euphrosinella* and *Euphrosinopsis* in the phylogenetic tree is unresolved (Fig. 5B). As COI sequencing was not successful in this study, all euphrosinid species are represented by only 16S and 18S.

Remarks. The CCZ species agrees well with the genus *Euphrosinopsis* in having five prostomial appendages, caruncle partially free from the body wall and the presence of large, deeply embedded eyes lateral to median antenna and caruncle. However, this species shows differences from all known species in this genus, suggesting it belongs to a new species. *Euphrosinopsis crassiseta* (type locality: Weddell Sea, 3697 m) can be easily distinguished by having only small, cirriform branchia per segment rather than two pairs of branched branchiae, by the absence of ringent chaetae and presence of coarsely serrated neurochaetae. *Euphrosinopsis horsti* (type locality: Pacific Antarctic Ridge, 3219–3255 m) also has only one very small, cirriform branchia per segment. Ringent chaetae are present in the known species, but

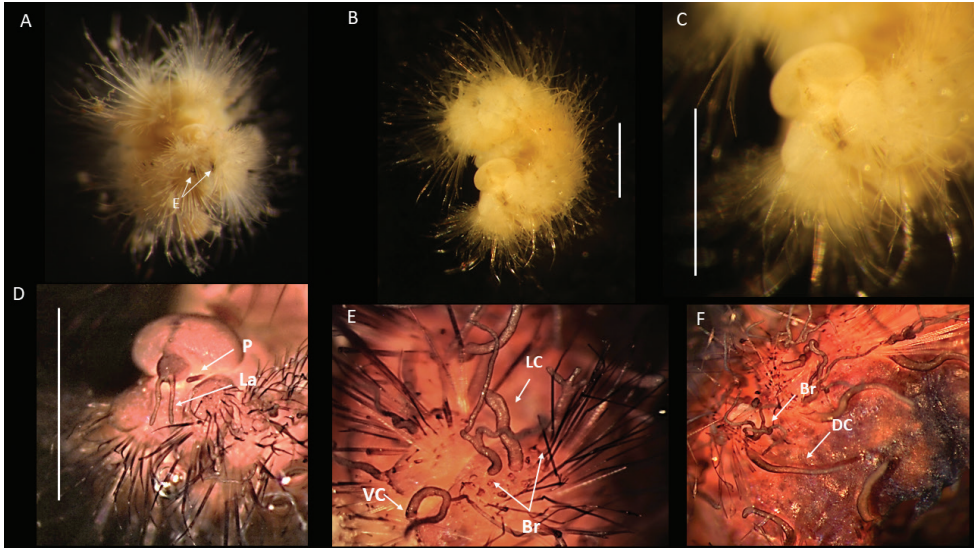


Figure 18. *Euphrosinopsis abearni* sp. nov. (paratype NHMUK ANEA.2022.654, unless stated otherwise) **A** live image of paratype (NHMUK ANEA.2022.646), with eyespots (E) marked by arrows **B** preserved specimen in dorsolateral view **C** anterior end in dorsolateral view **D** detail of prostomium (specimen stained with Shirlastain) with palp (P) and lateral antennae (La) marked by arrows **E** two pairs of branched branchiae (Br), lateral cirrus (LC) and ventral cirrus (VC) of midbody chaetigers **F** dorsal cirrus (DC) and branchia (Br) of midbody chaetigers. Scale bars: 1 mm. Abbreviations: E – eyes, P – palps, La – lateral antennae, Br – branchiae, LC – lateral cirrus, VC – ventral cirrus, DC dorsal cirrus.

they possess a distal tooth in the gap, which is absent in the new species. Finally, the most similar species, *Euphrosinopsis antarctica* can be distinguished by having up to three branchiae per segment, the first branched, but the others cirriform and style of median antenna of similar length to caruncle, rather than much longer as in the new species.

Thus, *Euphrosinopsis abearni* sp. nov. can be distinguished mainly by having two pairs of branched branchiae in midbody chaetigers, both with very long thin branches. That is also the main distinguishing character from its congener from the CCZ, *E. halli* sp. nov. also described in this study, which possess only single cirriform branchia in each parapodium. Both new species possess ringent notochaetae, that can be distinguished as follow: 1. They are numerous (ca. 20 per notopodium) and easily observed in *E. abearni* sp. nov., whilst only few (ca. 5 per notopodium) can be found in *E. halli* sp. nov.; 2. The serration of inner margin is more pronounced in *E. abearni* sp. nov. and 3. The distal tip is shorter and stubbier in *E. abearni* sp. nov. Further, the caruncle is more developed in *E. abearni* sp. nov. reaching to chaetiger four, not two as in *E. halli* sp. nov., and style of median antenna is much longer than caruncle in the former species, whilst they are ca. the same length in the latter.

Distribution. Central Pacific Ocean, Eastern CCZ, the exploration areas UK-1, OMS, and NORI-D (Fig. 1).

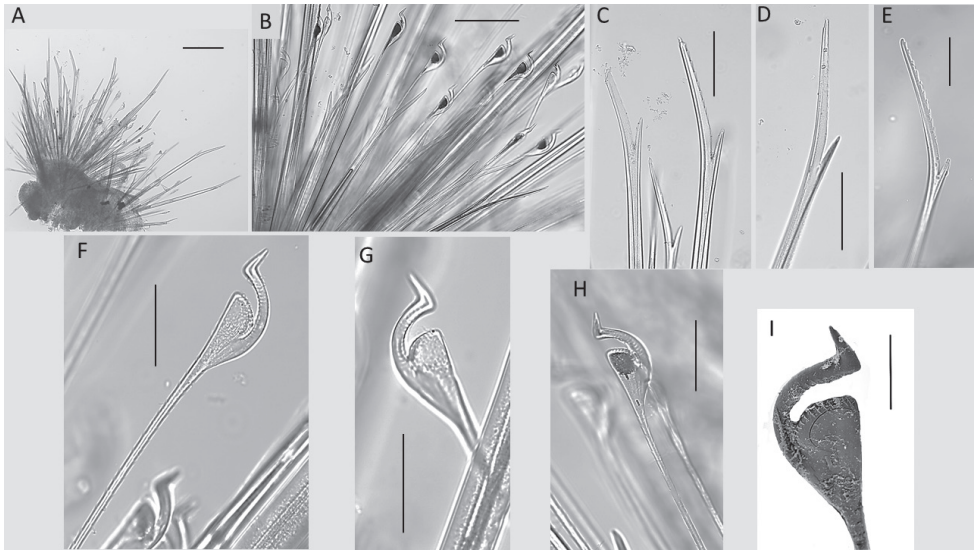


Figure 19. *Euphrosinopsis abearni* sp. nov. (paratype NHMUK ANEA.2022.646) **A** mid-body parapodium **B** notochaetae – anterior tier bifurcate and mid-tier ringent chaetae **C** bifurcate notochaetae posterior tier **D, E** details of variously serrated bifurcate notochaetae **F, G** examples of non-pigmented ringent notochaetae **H** details of pigmented ringent chaeta **I** SEM micrograph of ringent chaeta. Scale bars: 250 μ m (**A**); 100 μ m (**B–D**); 50 μ m (**E–H**); 20 μ m (**I**).

Etymology. This species is named for Patrick A’Hearn, technician from the University of Washington onboard the RV Thomas G Thompson.

***Euphrosinopsis halli* sp. nov.**

<https://zoobank.org/83A9C528-4FBE-4836-82DC-C31BDA5C2B09>

Figs 15C, 20A–E, 21 A–E

Material examined. NHM_0779, NHMUK ANEA 2022.641, coll. 20/02/2015, EBS, 12.53717, -116.60417, 4425 m, UK-1, <http://data.nhm.ac.uk/object/1a683870-d904-4c2c-bf1a-a34ead0a42fc>; NHM_4339 (holotype), NHMUK ANEA 2022.642, coll. 11/03/2020, box core, 12.17997, -117.065277, 4117 m, UK-1, <http://data.nhm.ac.uk/object/670dfd34-338d-4edc-8856-b0a9a728efc9>; NHM_6018 (paratype), NHMUK ANEA 2022.643; coll. 13/11/2020, box core, 10.35780, -117.15931, 4284 m, NORID, <http://data.nhm.ac.uk/object/ab26e2ea-ab87-4013-8106-e817c0485cc9>.

Diagnosis. **Holotype** (NHMUK ANEA.2022.642) complete (except for tissue sampled for DNA), 1.3 mm long and 0.75 mm wide without chaetae for 11 chaetigers. **Paratype** (NHMUK ANEA.2022.643) complete (except for tissue sampled for DNA), 1.5 mm long and 0.75 mm wide for 12 chaetigers. Body short, oval, flattened, pale yellow in alcohol (Fig. 20A). Prostomium longer than wide, with 5 prostomial

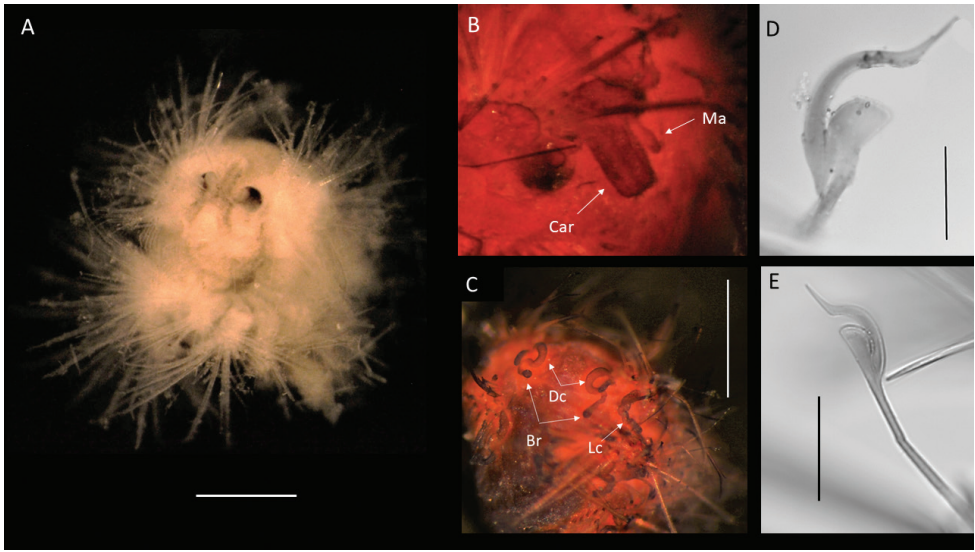


Figure 20. *Euphrosinopsis halli* sp. nov. **A** preserved holotype NHMUK ANEA.2022.642, eye spots visible **B** holotype NHMUK ANEA.2022.642 stained with Shirlastain, showing caruncle (car) and median antenna (Ma) **C** specimen NHMUK ANEA.2022.641 stained with Shirlastain, showing branchiae (Br) and dorsal cirri (Dc) and lateral cirrus (Lc) **D, E** ringent chaetae from specimen NHMUK ANEA.2022.641. Scale bars: 500 µm (**A, C**); 25 µm (**D**); 50 µm (**E**). Abbreviations: Ma – median antenna, Car – caruncle, Br – branchiae, Dc – dorsal cirrus, Lc – lateral cirrus.

appendages (Fig. 15C). Pair of short slender palps; pair of slender lateral antenna; median antenna of caruncle with long thick ceratophore and slender cirrus of similar length to caruncle (Figs 15C, 20B). Caruncle as oval lobe reaching to chaetiger 2, mostly free of body wall, with median keel and two pairs of lateral ridges, median keel slightly thicker than the lateral ones (Fig. 20B). Single pair of large, spherical eyes, deeply embedded, lateral to median antenna and caruncle (Figs 15C, 20A).

Parapodia biramous, two rami well separated. With parapodial appendages observed dorso-ventrally as follow (Figs 15F, 20C): long slender dorsal cirrus, often curved into S-shape in middle chaetigers; single cirriform branchia attached laterally to dorsal cirrus; lateral cirrus similar to branchia in form, but more robust; slender cirriform ventral cirrus.

Chaetae fragile, prone to breakage, of two main types: 1. Numerous, bifurcate chaetae arranged in approximately three rows in notopodia; their shafts of various length and thickness (Fig. 21A); development of filelike teeth on shafts ranging from smooth (Fig. 21C) to well developed (Fig. 21D, E); their prongs variable in length with short furcate chaetae in anterior tier having the ratio of short to long prong ranging from 1:2-2.5 (where possible to establish), the prong ratio of longest chaetae in the mid tier ranging from 1:3.5-4 (where possible to establish); prongs mainly smooth or with extremely faint serration only visible under high magnification (Fig. 21B).

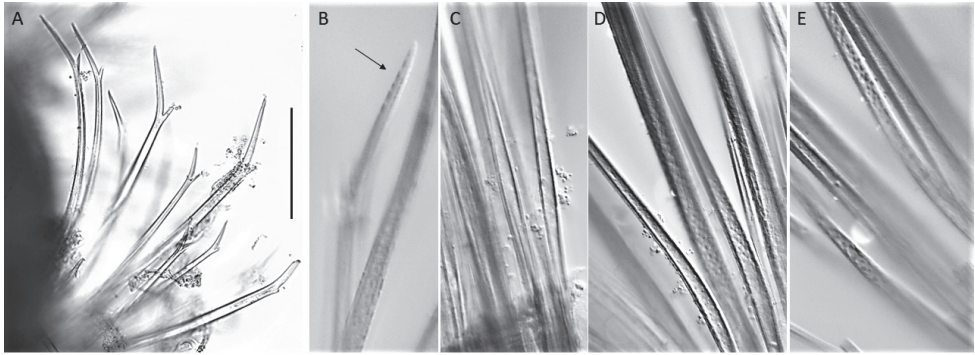


Figure 21. *Euphrosinopsis halli* sp. nov. (holotype NHMUK ANEA.2022.642) **A** long and short furcate notochaetae **B** faint serration of long prong (marked by arrow) **C** smooth shafts of dorsalmost notochaetae **D** shafts with file-like teeth of middle chaetae **E** shafts with file-like teeth of ventralmost chaetae. Scale bar: 250 μ m.

2. Ringent chaetae (sensu Kudenov 1993) present in notopodia only, few in numbers (ca. 5 per notopodium), composed of two curved prongs of unequal length and thickness, both with indistinct serration, the long prong distally with slender elongated tip, short prong broad and distally rounded (Fig. 20D, E). Neurochaetae similar less numerous, thinner, and shorter than notochaetae, all bifurcate, prongs appearing smooth, often broken off. Pygidium with pair of cirri resembling cylindrical tube feet.

Molecular information. Specimen NHMUK ANEA.2022.641, was sequenced for 16S and 18S while paratype NHMUK ANEA.2022.643 and holotype NHMUK ANEA.2022.642 were sequenced for 16S only (Table 1). There were no identical sequences for 16S on GenBank. The relationships between *Euphrosinella* and *Euphrosinopsis* in the phylogenetic tree is unresolved (Fig. 5B). As COI sequencing was not successful in this study, all euphrosinid species are represented by only 16S and 18S, and in the case of the species from GenBank, only 16S.

Remarks. CCZ species agrees well with the genus *Euphrosinopsis* in having five prostomial appendages, caruncle partially free from the body wall and the presence of large, deeply embedded eyes lateral to median antenna and caruncle. However, this species shows differences from all known species in this genus, suggesting it belongs to a new species. The presence of single, small, unbranched cirriform branchia per parapodium suggest affiliation with *E. crassiseta* and *E. horsti*, which share the same character. However, the new species differs from *E. crassiseta* in possessing the ringent chaetae and lacking the coarse serration on neurochaetae. The most similar species, *E. horsti* can be easily separated by having anal cirri fused instead of typical cylindrical tube feet as in the new species. For comparison with another new *Euphrosinopsis* species also described in this study see the remarks section for *E. ahearni* sp. nov.

Distribution. Central Pacific Ocean, Eastern CCZ, the exploration areas UK-1 and NORI-D (Fig. 1).

Etymology. This species is named for Preben Hall, the captain onboard the ship Maersk Launcher that was used in NORI-D expeditions in 2020 and 2021.

Discussion

This study has added six annelid species, three of those formally described and one likely new, and 41 records to the knowledge of the benthic annelid macrofauna of the CCZ, bringing a published record from the targeted areas (Fig. 1) to 54 annelid species, with 19 of them formalised (see also Wiklund et al. 2019; Drennan et al. 2021).

Unlike other annelid taxa, each Amphinomida species is represented by several specimens (no singletons), most with wide CCZ-distribution. More importantly molecular data confirmed a wide abyssal distribution for one species identified as *Bathychloeia* cf. *sibogae*. This species has been found in CCZ (Central Pacific) and off Australia (South Pacific) with the sampling sites separated by the distance of ca. 7500 km. However, both sampling areas were at similar depths of ca. 4000 m, providing further evidence that genetic connectivity over large geographic areas is more likely to be maintained at similar depths (Taylor and Roterman 2017). Traditionally annelids have been assumed to have wide geographical ranges due to their potential for wide larval dispersal. However, this paradigm has been challenged by molecular studies, which have often revealed the presence of several, sometimes cryptic, species for annelids in general (see Nygren 2014 for details), including families targeted in this study (e.g., Barroso et al. 2010; Borda et al. 2013). Thus, findings of wide geographical ranges for annelids with support of molecular data remain rare (e.g., Ahrens et al. 2013; Georgieva et al. 2015; Eilertsen et al. 2018; Kobayashi et al. 2018; Neal et al. 2018), likely as a result of undersampling within the vast abyssal realm, as well as the reflection of dispersal abilities of different species and presence or absence of barriers to dispersal.

Molecular phylogeny of the family Euphrosinidae has not been undertaken hitherto, as the number of taxa available on GenBank is very low. The difficulties of getting COI from members of Euphrosinidae further complicates the analyses, and more data (both in terms of number of genetic markers and taxa,) is needed to resolve the relationships within this family. Our phylogenetic results (Fig. 5B) suggest a sister taxon relationship between *Euphrosinella georgievae* sp. nov. and Antarctic specimens identified as *Euphrosinella* cf. *cirratiformis* (see also Brasier et al. 2016). Prior to this study, the genus *Euphrosinopsis* had a distribution restricted to the Antarctic waters (Kudenov 1993; Borda and Kudenov 2014), but CCZ has been found to harbour two *Euphrosinopsis* species, both new to science. A relationship between the deep-sea and Antarctic shelf fauna has been long been suggested and a continuity of the benthic fauna by means of the abyss has been proposed by some authors (e.g., Held 2000; Briggs 2003; Gage 2004; Clarke et al. 2005; Brandt et al. 2007; Strugnell et al. 2008). Due to the deeper than usual continental shelf, cold temperatures and at least seasonal darkness, the Antarctic shelf itself could be seen as an analogue to deep-sea environment. Other exclusively deep-sea annelid taxa have been previously found on the Antarctic shelf, e.g., the polynoid subfamily Macellicephalinae (Neal et al. 2012, 2017).

The phylogenetic analyses of the family Amphinomidae resulted in a tree similar to that of Borda et al. (2015), with the genera *Archinome*, *Chloeia*, and *Notopygos* falling into one strongly supported Archinominae clade (Fig. 5A). In this study, we have added the genus *Bathychloeia*, which formed a well-supported clade with the previously analysed Archinominae genera (Fig. 5A).

To summarise, the number of DNA sequences for benthic faunal groups from the CCZ available on GenBank are growing, representing echinoderms (e.g. Glover et al. 2016a; Christodoulou et al. 2020), cnidarians (Dahlgren et al. 2016), molluscs (Wiklund et al. 2017), annelids (Janssen et al. 2015; Bonifácio and Menot 2019; Wiklund et al. 2019; Guggolz et al. 2020; Drennan et al. 2021; Neal et al. 2022), poriferans (Lim et al. 2017) and crustaceans (e.g. Janssen et al. 2015; Kaiser et al. 2018; Bribiesca-Contreras et al. 2021; Mohrbeck et al. 2021). The information presented here therefore represents a further step in improving our understanding of the benthic fauna from the CCZ area, which in turn is essential for informing conservation efforts, as well as eventually providing practical identification guides to the fauna of this region facilitating any future assessments of biodiversity change as part of environmental monitoring programs.

Acknowledgements

We thank the masters, crew, and technical staff on the RV ‘Melville’, RV ‘Thomas G Thompson’, M/V #Pacific Constructor’, and Maersk Launcher for their outstanding support. We acknowledge the expert leadership of the research cruises and ABYSSLINE project by Prof Craig R Smith, University of Hawaii. We received help sorting and sieving samples at sea from science teams in successful deep-sea coring operations on all cruises. Joke Bleeker communicated information about type material held at Naturalis Biodiversity Centre, Leiden. We would also like thank Eva Stewart for providing the map in Fig. 1. This research was supported by funding from UK Seabed Resources Ltd, The Metals Company and Natural Environment Research Council grant ‘SMARTeX – Seabed Mining and Resilience to Experimental Impact’ grant NE/T002913/1. Adrian G. Glover and Thomas D. Dahlgren have received support from TMC the metals company Inc. (The Metals Company) through its subsidiary Nauru Ocean Resources Inc. (NORI). NORI holds exploration rights to the NORI-D contract area in the CCZ regulated by the International Seabed Authority and sponsored by the government of Nauru. This is contribution TMC/NORI/D/[002]. We also acknowledge the continued support of UK Seabed Resources over the last eight years for funding the fundamental taxonomic studies necessary to inform the regulation of potential industrial activity. Furthermore, we acknowledge the continued support from the NHMUK Consultancy team (Harry Rousham, Robyn Fryer, Kate Rowland).

References

- Ahrens JB, Borda E, Barroso R, Paiva PC, Campbell AM, Wolf A, Nugues MM, Rouse GW, Schulze A (2013) The curious case of *Hermodice carunculata* (Annelida: Amphinomidae): evidence for genetic homogeneity throughout the Atlantic Ocean and adjacent basins. *Molecular Ecology* 22(8): 2280–2291. <https://doi.org/10.1111/mec.12263>

- Averincev VG (1972) Benthic polychaetes Errantia from the Antarctic and Subantarctic collected by the Soviet Antarctic Expedition]. *Issledovaniya fauny morei. Zoologicheskii Institut Akademii Nauk USSR* 11(19): 88–292. [Biological Results of the Soviet Antarctic Expeditions, 5]
- Barroso R, Paiva PC (2008) A new deep-sea species of *Paramphinome* (Polychaeta: Amphinomidae) from southern Brazil. *Journal of the Marine Biological Association of the United Kingdom* 88(4): 743–746. <https://doi.org/10.1017/S0025315408001549>
- Barroso R, Paiva PC (2011) A new deep-sea species of *Chloeia* (Polychaeta: Amphinomidae) from southern Brazil. *Journal of the Marine Biological Association of the United Kingdom* 91(2): 419–423. <https://doi.org/10.1017/S0025315410001499>
- Barroso R, Klautau M, Solé-Cava AM, Paiva PC (2010) *Eurythoe complanata* (Polychaeta: Amphinomidae), thecosmopolitan fireworm, consists of at least three cryptic species. *Marine Biology* 157(1): 69–80. <https://doi.org/10.1007/s00227-009-1296-9>
- Barroso R, Kudenov JD, Halanych KM, Saeedi H, Sumida PY, Bernardino AF (2018) A new species of xylophilic fireworm (Annelida: Amphinomidae: Cryptonome) from deep-sea wood falls in the SW Atlantic. *Deep-sea Research. Part I, Oceanographic Research Papers* 137: 66–75. <https://doi.org/10.1016/j.dsr.2018.05.005>
- Barroso R, Kudenov JD, Shimabukuro M, Carrerette O, Sumida PY, Paiva PC, Seixas VC (2021) Morphological, molecular and phylogenetic characterization of a new *Chloeia* (Annelida: Amphinomidae) from a pockmark field. *Deep-sea Research. Part I, Oceanographic Research Papers* 171: 103499. <https://doi.org/10.1016/j.dsr.2021.103499>
- Beckers P, Tilic E (2021) Fine structure of the brain in Amphinomida (Annelida). *Acta Zoologica* 102(4): 483–495. <https://doi.org/10.1111/azo.12383>
- Bely AE, Wray GA (2004) Molecular phylogeny of naidid worms (Annelida: Clitellata) based on cytochrome oxidase I. *Molecular Phylogenetics and Evolution* 30(1): 50–63. [https://doi.org/10.1016/S1055-7903\(03\)00180-5](https://doi.org/10.1016/S1055-7903(03)00180-5)
- Blake JA (2016) *Kirkegaardia* (Polychaeta, Cirratulidae), new name for *Monticellina* Laubier, preoccupied in the Rhabdozoela, together with new records and descriptions of eight previously known and sixteen new species from the Atlantic, Pacific, and Southern Oceans. *Zootaxa* 4166(1): 1–93. <https://doi.org/10.11646/zootaxa.4166.1.1>
- Blake JA (2017) Polychaeta Orbiniidae from Antarctica, the Southern Ocean, the abyssal Pacific Ocean, and off South America. *Zootaxa* 4218(1): 1–45. <https://doi.org/10.11646/zootaxa.4218.1.1>
- Blake JA (2019) New species of Cirratulidae (Annelida, Polychaeta) from abyssal depths of the Clarion–Clipperton Fracture Zone, North Equatorial Pacific Ocean. *Zootaxa* 4629(2): 151–187. <https://doi.org/10.11646/zootaxa.4629.2.1>
- Blake JA (2020) New species and records of deep-water Orbiniidae (Annelida, Polychaeta) from the Eastern Pacific continental slope, abyssal Pacific Ocean, and the South China Sea. *Zootaxa* 4730(1): 1–61. <https://doi.org/10.11646/zootaxa.4730.1.1>
- Böttgermann M (2009) Polychaetes (Annelida) of the abyssal SE Atlantic. *Organisms, Diversity & Evolution* 9(4–5): 251–428.
- Bonifácio P, Menot L (2019) New genera and species from the Equatorial Pacific provide phylogenetic insights into deep-sea Polynoidae (Annelida). *Zoological Journal of the Linnean Society* 185(3): 555–635. <https://doi.org/10.1093/zoolinnean/zly063>

- Borda E, Kudenov JD (2014) Euphrosinidae (Annelida: Amphinomida) collected from Antarctica (R/V Polarstern, 1984, 1986) with comments on the generic placement of *Euphrosine magellanica* Ehlers, 1900. Proceedings of the Biological Society of Washington 126(4): 299–311. <https://doi.org/10.2988/0006-324X-126.4.299>
- Borda E, Kudenov JD, Chevaldonné P, Blake JA, Desbruyères D, Fabri MC, Hourdez S, Pleijel F, Shank TM, Wilson NG, Schulze A (2013) Cryptic species of *Archinome* (Annelida: Amphinomida) from vents and seeps. Proceedings of the Royal Society B: Biological Sciences 280(1770): 20131876. <https://doi.org/10.1098/rspb.2013.1876>
- Borda E, Yáñez-Rivera B, Ochoa GM, Kudenov JD, Sanchez-Ortiz C, Schulze A, Rouse GW (2015) Revamping Amphinomidae (Annelida: Amphinomida), with the inclusion of *Notopygos*. Zoologica Scripta 44(3): 324–333. <https://doi.org/10.1111/zsc.12099>
- Brandt A, Gooday AJ, Brandao SN, Brix S, Brökeland W, Cedhagen T, Choudhury M, Cornelius N, Danis B, De Mesel I, Diaz RJ, Gillan DC, Ebbe B, Howe JA, Janussen D, Kaiser S, Linse K, Maljutina M, Pawlowski J, Raupach M, Vanreusel A (2007) First insights into the biodiversity and biogeography of the Southern Ocean deep-sea. Nature 447(7142): 307–311. <https://doi.org/10.1038/nature05827>
- Brasier MJ, Wiklund H, Neal L, Jeffreys R, Linse K, Ruhl H, Glover AG (2016) DNA barcoding uncovers cryptic diversity in 50% of deep-sea Antarctic polychaetes. Royal Society Open Science 3(11): 160432. <https://doi.org/10.1098/rsos.160432>
- Brenke N (2005) An epibenthic sledger for operations on marine soft bottom and bedrock. Marine Technology Society Journal 39(2): 10–21. <https://doi.org/10.4031/002533205787444015>
- Bribiesca-Contreras G, Dahlgren TG, Drazen JC, Drennan R, Horton T, Jones DO, Leitner AB, McQuaid K, Smith CR, Taboada S, Wiklund H (2021) Biogeography and connectivity across habitat types and geographical scales in Pacific abyssal scavenging amphipods. Frontiers in Marine Science 8: 1028. <https://doi.org/10.3389/fmars.2021.705237>
- Briggs JC (2003) Marine centres of origin as evolutionary engines. Journal of Biogeography 30(1): 1–18. <https://doi.org/10.1046/j.1365-2699.2003.00810.x>
- Christodoulou M, O'Hara T, Hugall AF, Khodami S, Rodrigues CF, Hilario A, Vink A, Martinez Arbizu P (2020) Unexpected high abyssal ophiuroid diversity in polymetallic nodule fields of the northeast Pacific Ocean and implications for conservation. Biogeosciences 17(7): 1845–1876. <https://doi.org/10.5194/bg-17-1845-2020>
- Clarke A, Barnes DK, Hodgson DA (2005) How isolated is Antarctica? Trends in Ecology & Evolution 1(1): 1–3. <https://doi.org/10.1016/j.tree.2004.10.004>
- Cohen BL, Gawthrop A, Cavalier-Smith T (1998) Molecular phylogeny of brachiopods and phoronids based on nuclear-encoded small subunit ribosomal RNA gene sequences. Philosophical Transactions of the Royal Society of London: Series B, Biological Sciences 353(1378): 2039–2061. <https://doi.org/10.1098/rstb.1998.0351>
- Dahlgren TG, Wiklund H, Rabone M, Amon DJ, Ikebe C, Watling L, Smith CR, Glover AG (2016) Abyssal fauna of the UK-1 polymetallic nodule exploration area, Clarion-Clipperton Zone, central Pacific Ocean: Cnidaria. Biodiversity Data Journal 9277: e9277. <https://doi.org/10.3897/BDJ.4.e9277>
- Dean HK (2008) The use of polychaetes (Annelida) as indicator species of marine pollution: A review. Revista de Biología Tropical 56(4): 11–38.

- Detinova NN (1985) Polychaetous worms from the Reykjanes Ridge (the North Atlantic). Bottom Fauna from Mid-Ocean Rises in the North Atlantic. *Trudy Instituta okeanologii im. P.P. Shirshova* 120: 96–136.
- Donoghue MJ (1985) A critique of the biological species concept and recommendations for a phylogenetic alternative. *The Bryologist* 88(3): 172–181. <https://doi.org/10.2307/3243026>
- Drennan R, Wiklund H, Rabone M, Georgieva MN, Dahlgren TG, Glover AG (2021) *Neanthes goodayi* sp. nov. (Annelida, Nereididae), a remarkable new annelid species living inside deep-sea polymetallic nodules. *European Journal of Taxonomy* 760: 160–185. <https://doi.org/10.5852/ejt.2021.760.1447>
- Edgar RC (2004) MUSCLE: Multiple sequence alignment with high accuracy and high throughput. *Nucleic Acids Research* 32(5): 1792–1797. <https://doi.org/10.1093/nar/gkh340>
- Eilertsen MH, Georgieva MN, Kongsrud JA, Linse K, Wiklund H, Glover AG, Rapp HT (2018) Genetic connectivity from the Arctic to the Antarctic: *Sclerolinum contortum* and *Nicomache lokii* (Annelida) are both widespread in reducing environments. *Scientific Reports* 8(4810): 4810. <https://doi.org/10.1038/s41598-018-23076-0>
- Emson RH, Young CM, Paterson GLJ (1993) A fire worm with a sheltered life: Studies of *Benthoscolex cubanus* Hartman (Amphinomidae), an internal associate of the bathyal sea urchin *Archeopneustes hystrix* (A. Agassiz, 1880). *Journal of Natural History* 27(5): 1013–1028. <https://doi.org/10.1080/00222939300770641>
- Fauchald K (1977) The polychaete worms, definitions and keys to the orders, families and genera. Natural History Museum of Los Angeles County: Los Angeles, CA (USA), Science Series 28: 1–188
- Fauchald K, Jumars PA (1979) The diet of worms: A study of polychaete feeding guilds. *Oceanography and Marine Biology – an Annual Review* 17: 193–284.
- Fiege D, Bock G (2009) A new species of *Archinome* (Polychaeta: Archinomidae) from hydrothermal vents on the Pacific-Antarctic Ridge 37 S. Marine Biological Association of the United Kingdom. *Journal of the Marine Biological Association of the United Kingdom* 89(4): 689–696. <https://doi.org/10.1017/S0025315409000174>
- Folmer O, Black M, Hoeh W, Lutz R, Vrijenhoek R (1994) DNA primers for amplification of mitochondrial cytochrome c oxidase subunit I from diverse metazoan invertebrates 3: 294–299.
- Gage JD (2004) Diversity in deep-sea benthic macrofauna: The importance of local ecology, the larger scale, history and the Antarctic. Deep-sea Research. Part II, Topical Studies in Oceanography 51(14–16): 1689–1708. <https://doi.org/10.1016/j.dsr2.2004.07.013>
- Georgieva MN, Wiklund H, Bell JB, Eilertsen MH, Mills RA, Little CT, Glover AG (2015) A chemosynthetic weed: The tubeworm *Sclerolinum contortum* is a bipolar, cosmopolitan species. *BMC Evolutionary Biology* 15(1): 1–7. <https://doi.org/10.1186/s12862-015-0559-y>
- Glover AG, Smith CR, Paterson GL, Wilson GD, Hawkins L, Shearer M (2002) Polychaete species diversity in the central Pacific abyss: Local and regional patterns, and relationships with productivity. *Marine Ecology Progress Series* 240: 157–170. <https://doi.org/10.3354/meps240157>
- Glover AG, Wiklund H, Rabone M, Amon DJ, Smith CR, O'Hara T, Mah CL, Dahlgren TG (2016a) Abyssal fauna of the UK-1 polymetallic nodule exploration claim, Clarion-Clipperton Zone, central Pacific Ocean: Echinodermata. *Biodiversity Data Journal* (4).

- Glover AG, Dahlgren TG, Wiklund H, Mohrbeck I, Smith CR (2016b) An end-to-end DNA taxonomy methodology for benthic biodiversity survey in the Clarion-Clipperton Zone, central Pacific abyss. *Journal of Marine Science and Engineering* 4(1): 2. <https://doi.org/10.3390/jmse4010002>
- Glover AG, Wiklund H, Chen C, Dahlgren TG (2018) Point of view: Managing a sustainable deep-sea ‘blue economy’ requires knowledge of what actually lives there. *eLife* 7: e41319. <https://doi.org/10.7554/eLife.41319>
- Gollner S, Kaiser S, Menzel L, Jones DO, Brown A, Mestre NC, Van Oevelen D, Menot L, Colaço A, Canals M, Cuvelier D, Durden JM, Gebruk A, Egho GA, Haeckel M, Marcon Y, Mevenkamp L, Morato T, Pham CK, Purser A, Sanchez-Vidal A, Vanreusel A, Vink A, Martínez Arbizu P (2017) Resilience of benthic deep-sea fauna to mining activities. *Marine Environmental Research* 129: 76–101. <https://doi.org/10.1016/j.marenvres.2017.04.010>
- Guggolz T, Meißner K, Schwentner M, Dahlgren TG, Wiklund H, Bonifácio P, Brandt A (2020) High diversity and pan-oceanic distribution of deep-sea polychaetes: *Prionospio* and *Aurospio* (Annelida: Spionidae) in the Atlantic and Pacific Ocean. *Organisms, Diversity & Evolution* 18(2): 1–7. <https://doi.org/10.1007/s13127-020-00430-7>
- Gunton LM, Neal L, Gooday AJ, Bett BJ, Glover AG (2015) Benthic polychaete diversity patterns and community structure in the Whittard Canyon system and adjacent slope (NE Atlantic). *Deep-sea Research. Part I, Oceanographic Research Papers* 106: 42–54. <https://doi.org/10.1016/j.dsr.2015.07.004>
- Gunton LM, Kupriyova EK, Alvestad T, Avery L, Blake JA, Biriukova O, Böggemann M, Borisova P, Budaeva N, Burghardt I, Capa M, Georgieva MN, Glasby CJ, Hsueh P-W, Hutchings P, Jimi N, Kongsrud JA, Langeneck J, Meißner K, Murray A, Nikolic M, Paxton H, Ramos D, Schulze A, Sobczyk R, Watson C, Wiklund H, Wilson RS, Zhadan A, Zhang J (2021) Annelids of the eastern Australian abyss collected by the 2017 RV ‘Investigator’ voyage. *ZooKeys* 1020: 1–198. <https://doi.org/10.3897/zookeys.1020.57921>
- Hartman O (1959) Catalogue of the polychaetous annelids of the world. Part I. Allan Hancock Foundation Publications. Occasional Paper 23: 1–353.
- Hartman O (1960) Systematic account of some marine invertebrate animals from the deep basins off southern California. *Allan Hancock Pacific Expeditions* 22(2): 69–216. [plates 1–19]
- Hartmann-Schröder G, Rosenfeldt P (1992) Die Polychaeten der “Polarstern”-Reise ANT V/1 in die Antarktis 1986. Teil 1: Euphrosinidae bis Iphitimidae. *Mitteilungen aus dem Hamburgischen Zoologischen Museum und Institut* 89: 85–124. [page(s): 87]
- Held C (2000) Phylogeny and biogeography of Serolid Isopods (Crustacea, Isopoda, Serolidae) and the use of ribosomal expansion segments in molecular systematics. *Molecular Phylogenetics and Evolution* 15(2): 165–178. <https://doi.org/10.1006/mpev.1999.0739>
- Horst R (1910) On the genus *Chloeia* with some new species from the Malay Archipelago, partly collected by the Siboga-Expedition. *Notes from the Leyden Museum* 32: 169–175.
- Horst R (1912) Polychaeta errantia of the Siboga Expedition. Part 1, Amphinomidae. *Siboga-Expeditie Uitkomsten op Zoologisch, Botanisch, Oceanographisch en Geologisch gebied verzameld in Nederlandsch Oost-Indië 1899-1900, 24a: 1–43* [10 plates] <https://biodiversitylibrary.org/page/2187401> [page(s): 25]
- Janssen A, Kaiser S, Meissner K, Brenke N, Menot L, Martínez Arbizu P (2015) A Reverse Taxonomic Approach to Assess Macrofaunal Distribution Patterns in Abyssal Pacific

- Polymetallic Nodule Fields. PLoS ONE 10(2): e0117790. <https://doi.org/10.1371/journal.pone.0117790>
- Jeffreys RM, Levin LA, Lamont PA, Woulds C, Whitcraft CR, Mendoza GF, Wolff GA, Cowie GL (2012) Living on the edge: Single-species dominance at the Pakistan oxygen minimum zone boundary. Marine Ecology Progress Series 470: 79–99. <https://doi.org/10.3354/meps10019>
- Jumars PA, Dorgan KM, Lindsay SM (2015) Diet of worms emended: An update of polychaete feeding guilds. Annual Review of Marine Science 7(1): 497–520. <https://doi.org/10.1146/annurev-marine-010814-020007>
- Kaiser S, Brix S, Kihara TC, Janssen A, Jennings RM (2018) Integrative species delimitation in the deep-sea genus *Thaumastosoma* Hessler, 1970 (Isopoda, Asellota, Nannoniscidae) reveals a new genus and species from the Atlantic and central Pacific abyss. Deep-sea Research. Part II, Topical Studies in Oceanography 148: 151–179. <https://doi.org/10.1016/j.dsr2.2017.05.006>
- Katoh K, Misawa K, Kuma KI, Miyata T (2002) MAFFT: A novel method for rapid multiple sequence alignment based on fast Fourier transform. Nucleic Acids Research 30(14): 3059–3066. <https://doi.org/10.1093/nar/gkf436>
- Kearse M, Moir R, Wilson A, Stones-Havas S, Cheung M, Sturrock S, Buxton S, Cooper A, Markowitz S, Duran C, Thierer T, Ashton B, Meintjes P, Drummond A (2012) Geneious Basic: An integrated and extendable desktop software platform for the organization and analysis of sequence data. Bioinformatics 28(12): 1647–1649. <https://doi.org/10.1093/bioinformatics/bts199>
- Kirkegaard JB (1995) Bathyal and abyssal polychaetes (errant species). Galathea Report 17: 7–56.
- Kobayashi G, Mukai R, Alalykina I, Miura T, Kojima S (2018) Phylogeography of benthic invertebrates in deep waters: a case study of *Sternaspis* cf. *williamsae* (Annelida: Sternaspidae) from the northwestern Pacific Ocean. Deep-sea Research. Part II, Topical Studies in Oceanography 154: 159–166. <https://doi.org/10.1016/j.dsr2.2017.12.016>
- Kudenov JD (1991) A new family and genus of the order Amphinomida (Polychaeta) from the Galapagos Hydrothermal vents. Ophelia, supplement 5 (Systematics, Biology and Morphology of World Polychaeta): 111–120.
- Kudenov JD (1993) Amphinomidae and Euphrosinidae (Annelida: Polychaeta) principally from Antarctica, the Southern Ocean, and Subantarctic regions. Antarctic Research Series, Biology of the Antarctic Seas XXII 58: 93–150. <https://doi.org/10.1029/AR058p0093>
- Lamarck JB (1818) [volume 5 of] Histoire naturelle des Animaux sans Vertèbres, présentant les caractères généraux et particuliers de ces animaux, leur distribution, leurs classes, leurs familles, leurs genres, et la citation des principales espèces qui s’y rapportent; précédées d’une Introduction offrant la détermination des caractères essentiels de l’Animal, sa distinction du végétal et des autres corps naturels, enfin, l’Exposition des Principes fondamentaux de la Zoologie. Paris, Deterville. Vol 5, 612 pp. <http://biodiversitylibrary.org/page/12886879> [page(s): 327 [as ‘Amphinomae’]]
- Lim SC, Wiklund H, Glover AG, Dahlgren TG, Tan KS (2017) A new genus and species of abyssal sponge commonly encrusting polymetallic nodules in the Clarion-Clipperton Zone, East Pacific Ocean. Systematics and Biodiversity 15(6): 507–519. <https://doi.org/10.1080/14772000.2017.1358218>

- Lodge M, Johnson D, Le Gurun G, Wengler M, Weaver P, Gunn V (2014) Seabed mining: International Seabed Authority environmental management plan for the Clarion–Clipperton Zone. A partnership approach. *Marine Policy* 49: 66–72. <https://doi.org/10.1016/j.marpol.2014.04.006>
- Maciolek NJ (2020) *Anguillosyllis* (Annelida: Syllidae) from multiple deep-water locations in the northern and southern hemispheres. *Zootaxa* 4793(1):1–73. <https://doi.org/10.11646/zootaxa.4793.1.1>
- Maddison WP, Maddison DR (2021) Mesquite: a modular system for evolutionary analysis. Version 3.70. <http://www.mesquiteproject.org>
- McIntosh WC (1885) Report on the Annelida Polychaeta collected by H.M.S. Challenger during the years 1873–1876. Report on the Scientific Results of the Voyage of H.M.S. Challenger during the years 1873–76. *Zoology (Jena, Germany)* 12(part 34).
- Medlin L, Elwood H, Stickel S, Sogin M (1988) The characterization of enzymatically amplified eukaryotic 16S-like rRNA-coding regions. *Gene* 71(2): 491–499. [https://doi.org/10.1016/0378-1119\(88\)90066-2](https://doi.org/10.1016/0378-1119(88)90066-2)
- Mohrbeck I, Horton T, Jazdzewska AM, Arbizu PM (2021) DNA barcoding and cryptic diversity of deep-sea scavenging amphipods in the Clarion-Clipperton Zone (Eastern Equatorial Pacific). *Marine Biodiversity* 51(2): 1–5. <https://doi.org/10.1007/s12526-021-01170-3>
- Neal L, Barnich R, Wiklund H, Glover AG (2012) A new genus and species of Polynoidae (Annelida, Polychaeta) from Pine Island Bay, Amundsen Sea, Southern Ocean – a region of high taxonomic novelty. *Zootaxa* 3542(1): 80–88. <https://doi.org/10.11646/zootaxa.3542.1.4>
- Neal L, Linse K, Brasier MJ, Sherlock E, Glover AG (2017) Comparative marine biodiversity and depth zonation in the Southern Ocean: Evidence from a new large polychaete dataset from Scotia and Amundsen seas. *Marine Biodiversity* 48(1): 581–601. <https://doi.org/10.1007/s12526-017-0735-y>
- Neal L, Taboada S, Woodall LC (2018) Slope-shelf faunal link and unreported diversity off Nova Scotia: Evidence from polychaete data. *Deep-sea Research. Part I, Oceanographic Research Papers* 138: 72–84. <https://doi.org/10.1016/j.dsr.2018.07.003>
- Neal L, Wiklund H, Rabone M, Dahlgren T, Glover AG (2022) Abyssal fauna of polymetallic nodule exploration areas, eastern Clarion-Clipperton Zone, central Pacific Ocean: Annelida: Spionidae and Poecilochaetidae. *Marine Biodiversity* 52(51): 51. <https://doi.org/10.1007/s12526-022-01277-1>
- Nygren A (2014) Cryptic polychaete diversity: A review. *Zoologica Scripta* 43(2): 172–183. <https://doi.org/10.1111/zsc.12044>
- Nygren A, Sundberg P (2003) Phylogeny and evolution of reproductive modes in Autolytinae (Syllidae, Annelida). *Molecular Phylogenetics and Evolution* 29(2): 235–249. [https://doi.org/10.1016/S1055-7903\(03\)00095-2](https://doi.org/10.1016/S1055-7903(03)00095-2)
- Palumbi SR (1996) Nucleic acids II: the polymerase chain reaction. *Molecular Systematics*, 205–247.
- Paterson GL, Neal L, Altamira I, Soto EH, Smith CR, Menot L, Billett DS, Cunha MR, Marchais-Laguionie C, Glover AG (2016) New *Prionospio* and *Aurospio* species from the deep sea (Annelida: Polychaeta). *Zootaxa* 4092(1): 1–32. <https://doi.org/10.11646/zootaxa.4092.1.1>
- Posada D (2008) jModelTest: Phylogenetic model averaging. *Molecular Biology and Evolution* 25(7): 1253–1256. <https://doi.org/10.1093/molbev/msn083>

- Read G, Fauchald K [Eds] (2021) World Polychaeta Database. Amphinomida. [Accessed through: World Register of Marine Species at:] <http://www.marinespecies.org/aphia.php?p=taxdetails&cid=893> [2021-05-14]
- Righi S, Savioli M, Prevedelli D, Simonini R, Malferrari D (2021a) Unravelling the ultrastructure and mineralogical composition of fireworm stinging bristles. *Zoology* 144: 125851. <https://doi.org/10.1016/j.zool.2020.125851>
- Righi S, Savioli M, Prevedelli D, Simonini R, Malferrari D (2021b) Response to Tilic and Bartolomaeus's Commentary on the original Research Paper "Unravelling the ultrastructure and mineralogical composition of fireworm stinging bristles" (*Zoology*, 144). *Zoology* 144: 125889. <https://doi.org/10.1016/j.zool.2020.125889>
- Ronquist F, Teslenko M, Van Der Mark P, Ayres DL, Darling A, Höhna S, Larget B, Liu L, Suchard MA, Huelsenbeck JP (2012) MrBayes 3.2: Efficient Bayesian phylogenetic inference and model choice across a large model space. *Systematic Biology* 61(3): 539–542. <https://doi.org/10.1093/sysbio/sys029>
- Rouse GW, Fauchald K (1997) Cladistics and polychaetes. *Zoologica Scripta* 26(2): 139–204. <https://doi.org/10.1111/j.1463-6409.1997.tb00412.x>
- Sars GO (1872) On some remarkable forms of animal life from the great deeps off the Norwegian coast. Part 1, partly from posthumous manuscripts of the late prof. Mich. Sars. University Program for the 1st half-year 1869. Brøgger & Christie, Christiania viii + 82 pp. [pls 1–6] <http://biodiversitylibrary.org/page/11677777> [page(s): 45–49, pl. 4]
- Sjölin E, Erséus C, Källersjö M (2005) Phylogeny of Tubificidae (Annelida, Clitellata) based on mitochondrial and nuclear sequence data. *Molecular Phylogenetics and Evolution* 35(2): 431–441. <https://doi.org/10.1016/j.ympev.2004.12.018>
- Smith CR, De Leo FC, Bernardino AF, Sweetman AK, Arbizu PM (2008) Abyssal food limitation, ecosystem structure and climate change. *Trends in Ecology & Evolution* 23(9): 518–528. <https://doi.org/10.1016/j.tree.2008.05.002>
- Smith CR, Paterson G, Lambshead J, Glover A, Rogers A, Gooday A, Kitazato H, Sibuet M, Galeron J, Menot L (2011) Biodiversity, species ranges, and gene flow in the abyssal Pacific nodule province: predicting and managing the impacts of deep seabed mining. ISA Technical Study No. 3, International Seabed Authority, Kingston, Jamaica. [ISBN: 978-976-95217-2-841]
- Smith CR, Clark MR, Goetze E, Glover AG, Howell KL (2021) Biodiversity, Connectivity and Ecosystem Function Across the Clarion-Clipperton Zone: A Regional Synthesis for an Area Targeted for Nodule Mining. *Frontiers in Marine Science* 8: e797516. <https://doi.org/10.3389/fmars.2021.797516>
- Strugnell JM, Rogers AD, Prodöhl PA, Collins MA, Allcock AL (2008) The thermohaline expressway: The Southern Ocean as a centre of origin for deep-sea octopuses. *Cladistics* 24(6): 1–8. <https://doi.org/10.1111/j.1096-0031.2008.00234.x>
- Taylor ML, Roterman CN (2017) Invertebrate population genetics across Earth's largest habitat: The deep-sea floor. *Molecular Ecology* 26(19): 4872–4896. <https://doi.org/10.1111/mec.14237>
- Tilic E, Bartolomaeus T (2021) Commentary on: "Unravelling the ultrastructure and mineralogical composition of fireworm stinging bristles" by Righi et al. 2020. *Zoology* 144: 125890. <https://doi.org/10.1016/j.zool.2020.125890>

- Verdes A, Simpson D, Holford M (2018) Are fireworms venomous? Evidence for the convergent evolution of toxin homologs in three species of fireworms (Annelida, Amphinomidae). *Genome Biology and Evolution* 10(1): 249–268. <https://doi.org/10.1093/gbe/evx279>
- Washburn TW, Jones DO, Wei CL, Smith CR (2021) Environmental heterogeneity throughout the Clarion-Clipperton zone and the potential representativity of the APEI network. *Frontiers in Marine Science* 8: e319. <https://doi.org/10.3389/fmars.2021.661685>
- Wedding LM, Friedlander AM, Kittinger JN, Watling L, Gaines SD, Bennett M, Hardy SM, Smith CR (2013) From principles to practice: a spatial approach to systematic conservation planning in the deep sea. *Proceedings of the Royal Society B: Biological Sciences* 280(1773): 20131684. <https://doi.org/10.1098/rspb.2013.1684>
- Weigert A, Helm C, Meyer M, Nickel B, Arendt D, Hausdorf B, Santos SR, Halanych KM, Purschke G, Bleidorn C, Struck TH (2014) Illuminating the base of the annelid tree using transcriptomics. *Molecular Biology and Evolution* 31(6): 1391–1401. <https://doi.org/10.1093/molbev/msu080>
- Wiklund H, Nygren A, Pleijel F, Sundberg P (2008) The phylogenetic relationships between Amphinomidae, Archinomidae and Euphrosinidae (Amphinomida: Aciculata: Polychaeta), inferred from molecular data. *Marine Biological Association of the United Kingdom. Journal of the Marine Biological Association of the United Kingdom* 88(3): 509–513. <https://doi.org/10.1017/S0025315408000982>
- Wiklund H, Taylor JD, Dahlgren TG, Todt C, Ikebe C, Rabone M, Glover AG (2017) Abyssal fauna of the UK-1 polymetallic nodule exploration area, Clarion-Clipperton Zone, central Pacific Ocean: Mollusca. *ZooKeys* 1(707): 1–46. <https://doi.org/10.3897/zookeys.707.13042>
- Wiklund H, Neal L, Glover AG, Drennan R, Rabone M, Dahlgren TG (2019) Abyssal fauna of polymetallic nodule exploration areas, eastern Clarion-Clipperton Zone, central Pacific Ocean: Annelida: Capitellidae, Opheliidae, Scalibregmatidae, and Traviisiidae. *ZooKeys* 883: 1–82. <https://doi.org/10.3897/zookeys.883.36193>

Supplementary material I

DarwinCore database of CCZ Amphinomida

Authors: Muriel Rabone

Data type: excel file

Explanation note: DarwinCore database.

Copyright notice: This dataset is made available under the Open Database License (<http://opendatacommons.org/licenses/odbl/1.0/>). The Open Database License (ODbL) is a license agreement intended to allow users to freely share, modify, and use this Dataset while maintaining this same freedom for others, provided that the original source and author(s) are credited.

Link: <https://doi.org/10.3897/zookeys.1137.86150.suppl1>

On eleven new species of the orb-weaver spider genus *Araneus* Clerck, 1757 (Araneae, Araneidae) from Xishuangbanna, Yunnan, China

Xiaoqi Mi¹, Shuqiang Li²

1 College of Agriculture and Forestry Engineering and Planning, Guizhou Provincial Key Laboratory of Biodiversity Conservation and Utilization in the Fanjing Mountain Region, Tongren University, Tongren 554300, Guizhou, China **2** Institute of Zoology, Chinese Academy of Sciences, Beijing 100101, China

Corresponding author: Shuqiang Li (lisq@ioz.ac.cn)

Academic editor: Zhiyuan Yao | Received 14 October 2022 | Accepted 29 November 2022 | Published 22 December 2022

<https://zoobank.org/CF82430B-B010-4FD4-8A44-8356992F0629>

Citation: Mi X, Li S (2022) On eleven new species of the orb-weaver spider genus *Araneus* Clerck, 1757 (Araneae, Araneidae) from Xishuangbanna, Yunnan, China. ZooKeys 1137: 75–108. <https://doi.org/10.3897/zookeys.1137.96306>

Abstract

Eleven new species of *Araneus* Clerck, 1757 from Xishuangbanna, Yunnan, China are described: *Araneus arcuatus* sp. nov. (♂♀), *A. bidentatus* sp. nov. (♂♀), *A. bidentatoides* sp. nov. (♂♀), *A. complanatus* sp. nov. (♂♀), *A. corrugis* sp. nov. (♀), *A. cucullatus* sp. nov. (♀), *A. minisculus* sp. nov. (♂), *A. ovoideus* sp. nov. (♀), *A. pseudodigitatus* sp. nov. (♂♀), *A. semiorbiculatus* sp. nov. (♀), and *A. tetracanthus* sp. nov. (♂♀). Diagnostic photographs of the habitus and copulatory organs are provided.

Keywords

Arachnida, morphology, species, taxonomy, type

Introduction

A large number of spider species live in the 1125 ha Xishuangbanna Tropical Botanical Garden (XTBG), including 782 spider species recorded through an “All Species Inventory” (Wang et al. 2020; Li et al. 2021; Yao et al. 2021; Liu et al. 2022; Lu et al. 2022; Zhao et al. 2022). The number of known species of the orb-weaver spider family Araneidae Clerck, 1757 in this region continues to increase with ongoing research (Mi and Li 2021a, b).

A total of 3092 species in 183 genera of Araneidae are known worldwide (WSC 2022), of which 402 species in 50 genera have been recorded from China (Li 2020). As the largest genus of the family, *Araneus* Clerck, 1757 includes 552 species worldwide, 342 of them are known only from a single sex or juveniles (WSC 2022). There are great differences in the habitus and copulatory organs among species, which suggests that *Araneus* may be polyphyletic. Scharff et al. (2020) found that 11 purported *Araneus* species from the Austral region belong instead to seven new genera.

In this study, 15 *Araneus* species from XTBG and the surrounding areas were identified, including *A. viridisomus* Gravely, 1921, *A. noegetus* (Thorell, 1895), *A. nidus* Yin & Gong, 1996, *A. fengshanensis* Zhu & Song, 1994, and 11 new species. Even though the 11 species described here significantly differ, they are placed in *Araneus* provisionally until a phylogenetic analysis is conducted.

Materials and methods

All of the specimens were collected by fogging, beating shrubs, or hand collecting and are preserved in 75% ethanol. Type specimens of the new species are deposited in the Institute of Zoology, Chinese Academy of Sciences (IZCAS) in Beijing. The specimens were examined with an Olympus SZ51 stereomicroscope. The epigynes were cleared in lactic acid for examination and imaging. The left male palps were dissected in ethanol for examination, description, and imaging. Photographs of the habitus and copulatory organs were taken with a Kuy Nice CCD mounted on an Olympus BX43 compound microscope. Compound focus images were generated using Helicon Focus v. 6.7.1.

All measurements are given in millimeters. Leg measurements are given as total length (femur, patella + tibia, metatarsus, tarsus). References to figures in the cited papers are listed in lowercase (fig. or figs); figures in this paper are noted with an initial capital (Fig. or Figs). Abbreviations used in the text and figures are as follows: ALE anterior lateral eye; AME anterior median eye; BE broken embolus; C conductor; CD copulatory duct; CO copulatory opening; E embolus; FD fertilization duct; H hood; MA median apophysis; MOA median ocular area; PLE posterior lateral eye; PME posterior median eye; Sc scape; Sp spermatheca; TA terminal apophysis; TE tegular extension.

Taxonomy

Family Araneidae Clerck, 1757

Genus *Araneus* Clerck, 1757

Araneus Clerck, 1757: 22.

Type species. *Araneus angulatus* Clerck, 1757.

***Araneus arcuatus* sp. nov.**

<https://zoobank.org/9ABF17D1-1973-4170-BF40-694237E504CE>

Figs 1, 2, 18A–D

Type material. *Holotype* ♂ (IZCAS-Ar43081), CHINA: Yunnan, Xishuangbanna, Mengla County, Menglun Township, Menglun Nature Reserve, XTBG (21°54.18'N, 101°16.90'E, ca 610 m), 5.V.2019, Y.F. Tong leg. *Paratypes*: 1♂ (IZCAS-Ar43082), same data as holotype; 1♀ (IZCAS-Ar43083), secondary tropical forest, bamboo plantation along G213 roadside (21°53.82'N, 101°16.99'E, ca 610 m), 3.VIII.2018, Z.L. Bai leg.; 1♂ (IZCAS-Ar43084), G213 roadside near Lüshilin (21°53.91'N, 101°17.01'E, ca 620 m), 12.VIII.2018, C. Wang leg.; 2♂2♀ (IZCAS-Ar43085–43088), Masuoxing Village (21°54.02'N, 101°16.90'E, ca 560 m), 27.IV.2019, Y.F. Tong leg.; 1♂ (IZCAS-Ar43089), #3 site around the dump (21°54.34'N, 101°16.79'E, ca 620 m), 2.V.2019, Y.F. Tong leg.; 1♀ (IZCAS-Ar43090), #6 site around the dump (21°54.33'N, 101°16.79'E, ca 620 m), 7.V.2019, Y.F. Tong leg. Other material examined: 1♂ (IZCAS-Ar43091), 55 km from Xishuangbanna National Nature Reserve, artificial *Ficus microcarpa* forest (21°54.97'N, 100°16.05'E, ca 610 m), 21.VIII.2011, Q.Y. Zhao leg.; 1♂ (IZCAS-Ar43092), Mohan Township, Shanggang Village, Xiaolongha, seasonal rainforest (21°24.19'N, 101°37.03'E, ca 660 m), 29.VI.2012, Q.Y. Zhao & Z.G. Chen leg.; 1♀ (IZCAS-Ar43093), same locality (21°24.33'N, 101°37.02'E, ca 800 m), 30.VI.2012, Q.Y. Zhao & Z.G. Chen leg.; 1♀ (IZCAS-Ar43094), Mengla Township, Bubang Village (21°36.64'N, 101°34.91'E, ca 820 m), 10.VII.2012, Q.Y. Zhao & Z.G. Chen leg.; 1♂ (IZCAS-Ar43095), #3 site in Mafengzhai Village (21°53.68'N, 101°17.33'E, ca 540 m), 8.V.2019, Y.F. Tong leg.; 1♀1♂ (IZCAS-Ar43096), Lüshilin Forest Park (21°53.84'N, 101°16.84'E, ca 550 m), 10.V.2019, Z.L. Bai leg.

Etymology. The specific name is derived from the Latin word “arcuatus”, meaning arcuate (curved), referring to the shape of the median apophysis in prolateral view.

Diagnosis. The female of the new species resembles that of *A. cucullatus* sp. nov. in appearance but can be distinguished from it as follows: 1) epigyne about 1.65 times wider than long vs about 2 times wider than long (Fig. 10A); 2) copulatory openings situated on the ventral surface vs the posterior surface (Fig. 10B); 3) spermathecae touching each other vs separated (Fig. 10C); and 4) abdomen lacking sparse, long setae vs having sparse, long setae (Fig. 10D). The male of the new species resembles that of *A. tetracanthus* sp. nov. in appearance but differs as follows: 1) median apophysis has 2 tapered tips vs 4 tapered tips (Fig. 17); 2) tegulum lacks an extension vs with a tegular extension (Fig. 17); and 3) embolus shorter than half of the bulb diameter vs longer than half of the bulb diameter (Fig. 17D).

Description. Male (holotype, Figs 1C, D, 2, 18A–D). Total length 2.45. Carapace 1.20 long, 1.00 wide. Abdomen 1.35 long, 0.95 wide. Clypeus 0.10 high. Eye sizes and interdistances: AME 0.10, ALE 0.08, PME 0.10, PLE 0.08, AME–AME 0.13, AME–ALE 0.08, PME–PME 0.13, PME–PLE 0.10, MOA length 0.30, anterior width 0.28, posterior width 0.28. Leg measurements: I 3.85 (1.10, 1.35, 1.00, 0.40), II 3.70 (1.10, 1.30, 0.90, 0.40), III 2.45 (0.80, 0.75, 0.60, 0.30), IV 3.35 (1.05, 1.10,

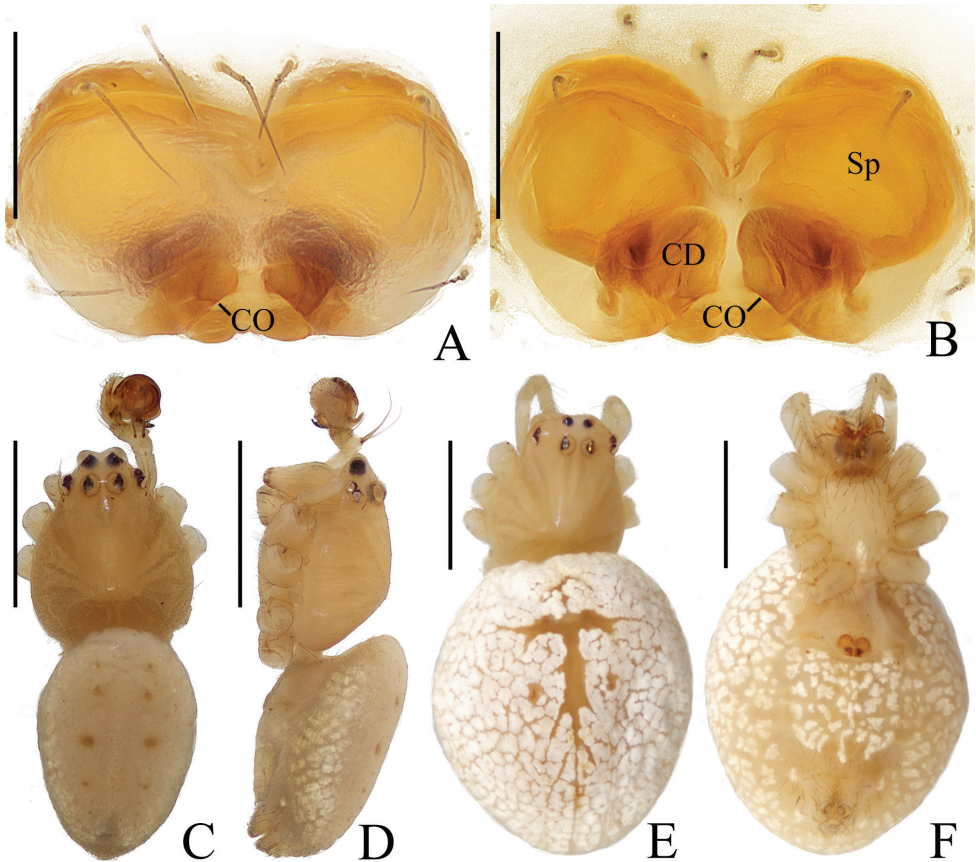


Figure 1. *Araneus arcuatus* sp. nov. **A, B, E, F** female paratype IZCAS-Ar43085 **C, D** male holotype **A** epigyne, ventral view **B** vulva, ventral view **C** habitus, dorsal view **D** *ibid.*, lateral view **E** *ibid.*, dorsal view **F** *ibid.*, ventral view. Scale bars: 0.1 mm (**A, B**); 1 mm (**C–F**).

0.85, 0.35). Carapace pear-shaped, yellow, cervical groove slightly distinct, fovea transverse, inner base of PME's elevated. Chelicerae yellow, 3 promarginal and 3 retromarginal teeth. Endites almost square, yellow with very narrow, dark anterior edge, labium triangular, yellowish brown with yellow edge. Sternum cordiform, yellow with dark setae. Legs yellow without annulus, tibia I with 13 macrosetae, tibia II with 8 macrosetae. Abdomen elliptical, about 1.4 times longer than wide, in life, light yellowish green or grayish yellow when preserved with inconspicuous, white scaly spots; venter grayish yellow with inconspicuous, white scaly spots. Spinnerets yellow.

Palp (Fig. 2): 2 patellar bristles; median apophysis large, arcuate in prolateral view, with two-pointed tips on opposite sides; embolus wide at base, slender and slightly curved distally; conductor triangular, concave at middle part; terminal apophysis about half the length of the bulb diameter, bifurcated distally.

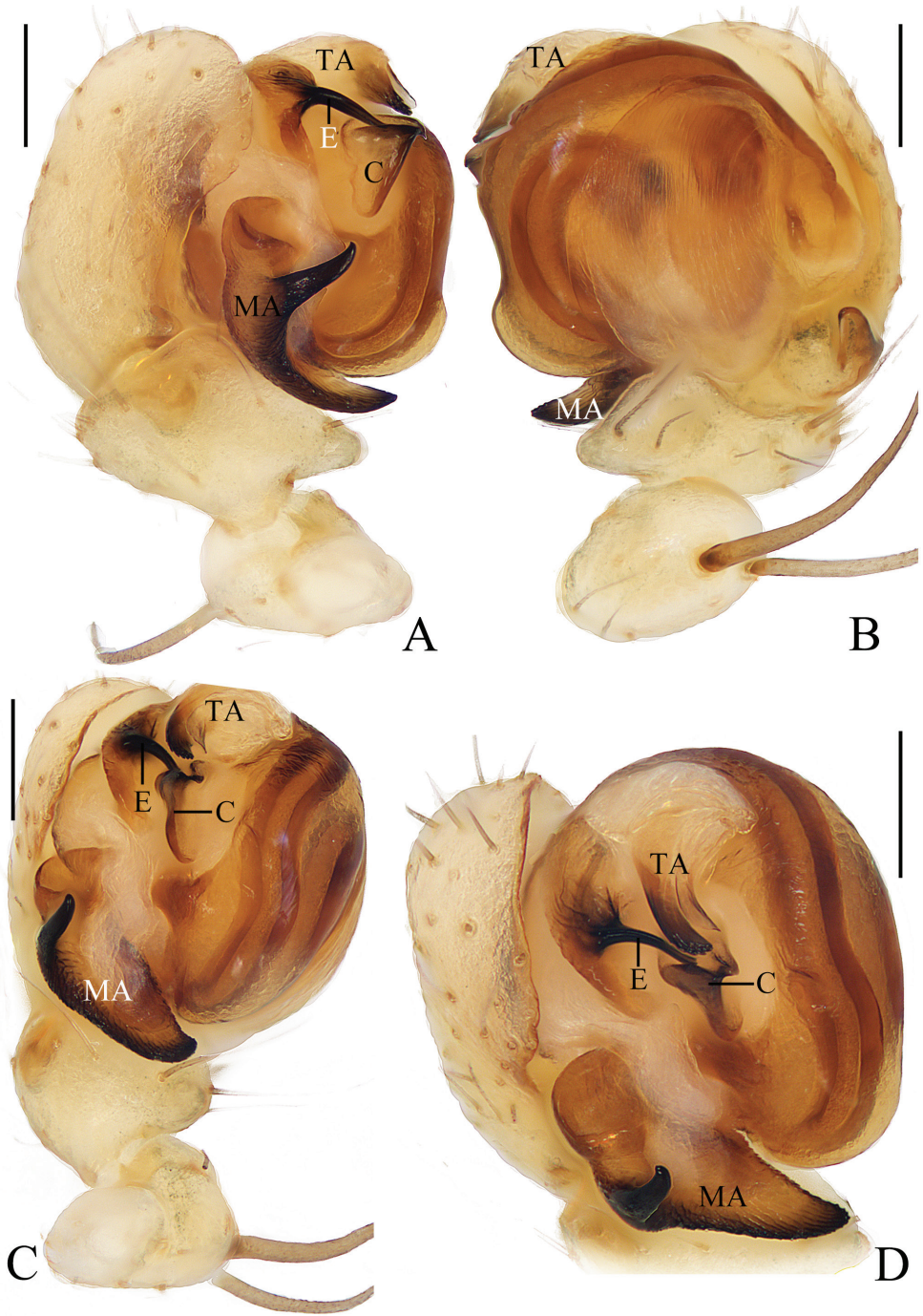


Figure 2. *Araneus arcuatus* sp. nov. male holotype **A** male palp, prolateral view **B** ibid., retrolateral view **C** ibid., ventral view **D** ibid., apical view. Scale bars: 0.1 mm.

Female (paratype IZCAS-Ar43085, Fig. 1A, B, E, F). Total length 3.40. Carapace 1.30 long, 1.15 wide. Abdomen 2.35 long, 2.05 wide. Clypeus 0.08 high. Eye sizes and interdistances: AME 0.10, ALE 0.08, PME 0.13, PLE 0.08, AME–AME 0.13, AME–ALE 0.15, PME–PME 0.15, PME–PLE 0.15, MOA length 0.33, anterior width 0.28, posterior width 0.30. Leg measurements: I 4.50 (1.30, 1.55, 1.20, 0.45), II 4.25 (1.25, 1.55, 1.05, 0.40), III 3.00 (0.95, 0.95, 0.75, 0.35), IV 4.15 (1.30, 1.40, 1.05, 0.40). Habitus similar to that of male, but white scaly spots more distinct.

Epigyne (Fig. 1A, B): about 1.65 times wider than long, lacking scape; copulatory openings slit-like, close to posterior margin; copulatory ducts almost as long as the spermathecae diameter, coiled about 360°; spermathecae spherical, touching each other.

Variation. Total length: ♂♂ 2.35–2.60; ♀♀ 3.15–3.40.

Distribution. Known only from type localities (Yunnan, China).

Araneus bidentatus sp. nov.

<https://zoobank.org/516C5C7D-2580-4672-BF6C-A8B9F58F8674>

Figs 3, 4, 18E–H

Type material. *Holotype* ♂ (IZCAS-Ar43097), CHINA: Yunnan, Xishuangbanna, Menghai County, Menghai Township, Mengweng Village, Wengnan, secondary forest (22°4.94'N, 100°22.03'E, ca 1150 m), 2.VII.2013, Q.Y. Zhao & Z.G. Chen leg.

Paratypes: 1♂1♀ (IZCAS-Ar43098–43099), same data as holotype; 1♂ (IZCAS-Ar43100), Mengla County, Mohan Township, Shanggang Village, Xiaolongha, valley rainforest (21°24.25'N, 101°36.32'E, ca 760 m), 15.VI.2013, Q.Y. Zhao & Z.G. Chen leg.

Etymology. The specific name is a combination of the Latin prefix “bi-” and “dentatus” (two toothed), referring to the two heavily sclerotized denticulate protuberances on the tibia of the male palp.

Diagnosis. The new species resembles *A. bidentatoides* sp. nov. in appearance, but differs in the following: 1) copulatory openings located at lateral ends of the scape groove vs at anterolateral base of the scape (Fig. 5A); 2) copulatory ducts not expanded vs expanded at their origin (Fig. 5C); 3) embolus slender, a bit more slender than the patellar bristle vs embolus stout, several times bigger than the patellar bristle (Fig. 6A, C, D); 4) distal end of the terminal apophysis not tapered to a long tip vs tapered (Fig. 6); 5) median apophysis slightly curved vs curved about 90° (Fig. 6A); 6) tibia with 2 heavily sclerotized denticulate protuberances vs protuberances absent (Fig. 6A, B); and 7) fovea region and sides of thoracic region paler than thoracic region vs unicolor (Fig. 5D–G).

Description. Male (holotype, Figs 3E, F, 4, 18E–H). Total length 2.70. Carapace 1.60 long, 1.20 wide. Abdomen 1.50 long, 0.95 wide. Clypeus 0.13 high. Eye sizes and interdistances: AME 0.13, ALE 0.10, PME 0.13, PLE 0.13, AME–AME 0.13, AME–ALE 0.10, PME–PME 0.13, PME–PLE 0.20, MOA length 0.23, anterior width 0.35, posterior width 0.35. Leg measurements: I 5.45 (1.65, 2.00, 1.15, 0.65), II 4.50 (1.45, 1.55, 0.95, 0.55), III 3.05 (1.00, 1.05, 0.55, 0.45), IV 4.15 (1.40, 1.40,

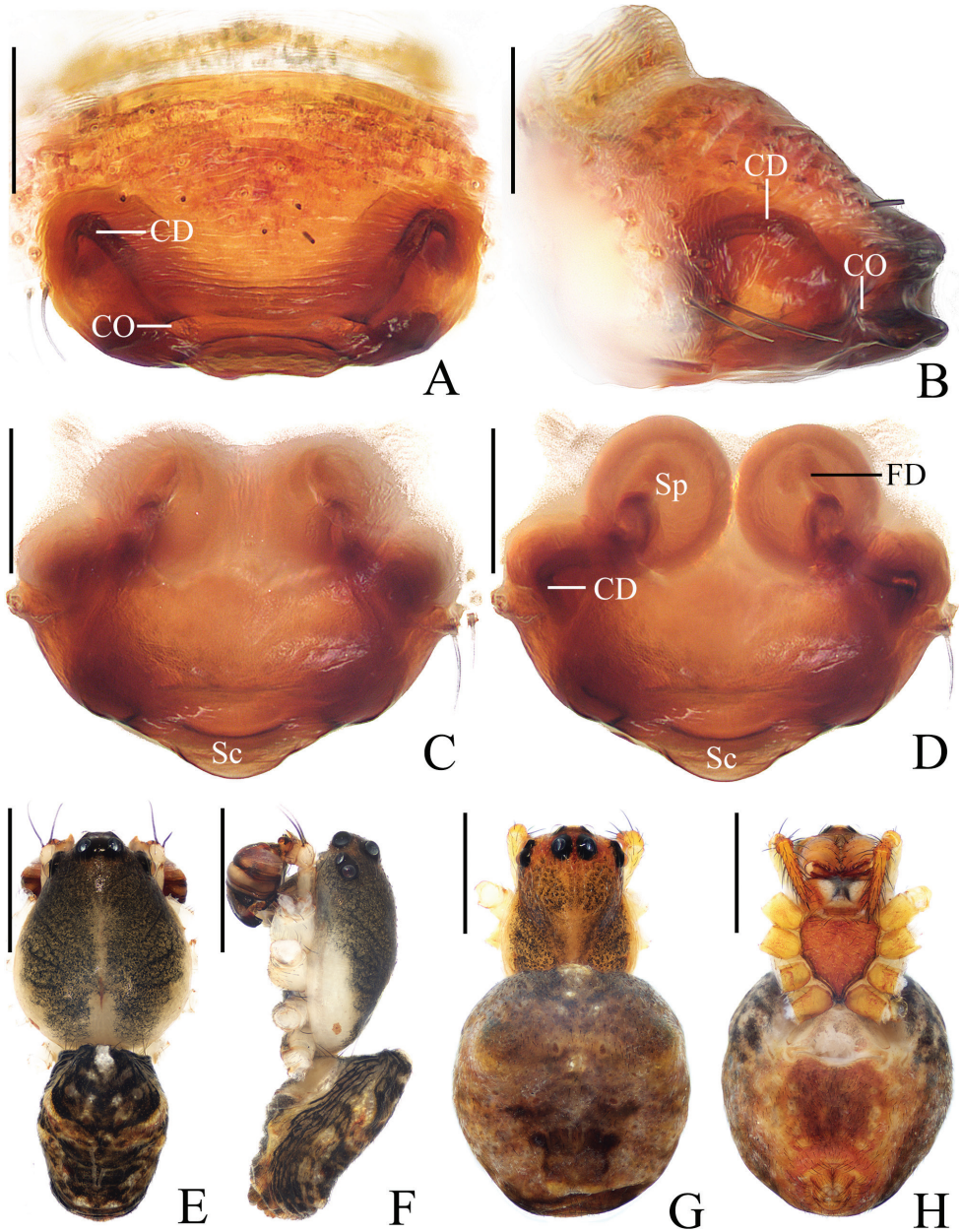


Figure 3. *Araneus bidentatus* sp. nov. **A–D, G, H** female paratype IZCAS-Ar43098 **E, F** male holotype **A** epigyne, ventral view **B** *ibid.*, lateral view **C** *ibid.*, posterior view **D** vulva, posterior view **E** habitus, dorsal view **F** *ibid.*, lateral view **G** *ibid.*, dorsal view **H** *ibid.*, ventral view. Scale bars: 0.1 mm (**A–D**); 1 mm (**E–H**).

0.85, 0.50). Carapace pear-shaped, grayish black with yellow patches around fovea and on lateral edges of thoracic region, ALEs, PME and PLEs with black base, with pale setae, cervical groove inconspicuous. Chelicerae yellowish brown, 5 promarginal

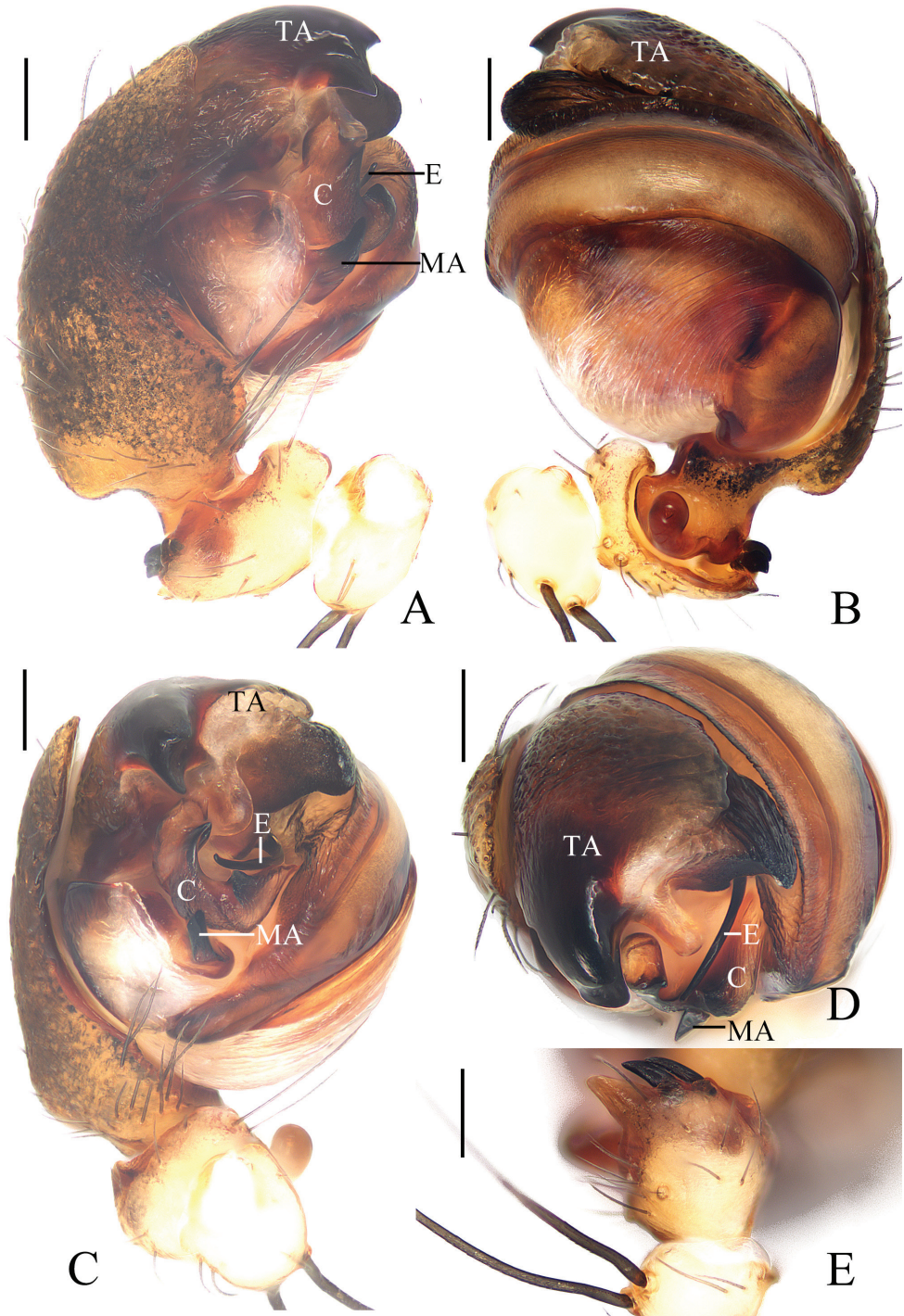


Figure 4. *Araneus bidentatus* sp. nov. male holotype **A** male palp, proteral view **B** *ibid.*, retrolateral view **C** *ibid.*, ventral view **D** *ibid.*, apical view **E** tibia of left male palp, retrolateral view. Scale bars: 0.1 mm.

teeth, 3 retromarginal teeth. Endites and labium dark brown at base, paler distally, endites square, labium triangular. Sternum cordiform, dark brown with dark setae. Legs yellow with grayish brown annuli, tibia I with 9 macrosetae, tibia II with 11 macrosetae, tibia III with 7 macrosetae, tibia IV with 8 macrosetae. Abdomen elliptical, about 1.25 times longer than wide, covered with gray setae, dorsum yellow with white spot anteriorly and irregular black markings; venter yellow with dark brown patches. Spinnerets yellowish brown.

Palp (Fig. 4): patella with 2 bristles; tibia with 2 heavily sclerotized denticulate protuberances (fig. 4B, E); paracymbium widened at base, with a finger-like tip; median apophysis shorter than the conductor, tapered to a pointed tip; embolus slender, slightly curved; conductor very wide, semicircular in prolateral view; terminal apophysis extremely large, heavily sclerotized, with 2 widely separated protuberances in apical view.

Female (paratype IZCAS-Ar43098, Fig. 3A–D, G, H). Total length 3.25. Carapace 1.55 long, 1.15 wide. Abdomen 2.35 long, 1.90 wide. Clypeus 0.08 high. Eye sizes and interdistances: AME 0.13, ALE 0.08, PME 0.13, PLE 0.10, AME–AME 0.13, AME–ALE 0.18, PME–PME 0.15, PME–PLE 0.25, MOA length 0.33, anterior width 0.35, posterior width 0.33. Habitus similar to that of male but with a pair of low anterolateral humps and a little paler.

Epigyne (Fig. 3A–D): about 1.5 times wider than long; scape triangular, very short, about 5 times wider than long, distally with transverse groove; copulatory openings on the ends of the groove; copulatory ducts longer than the spermatheca diameter, curved; spermathecae globular, touching each other.

Variation. Total length: ♂♂ 2.70–3.25.

Distribution. Known only from type localities (Yunnan, China).

Araneus bidentatoides sp. nov.

<https://zoobank.org/BA43FA37-7907-40AF-AE3D-864928F7F4D3>

Figs 5, 6

Type material. Holotype ♂ (IZCAS-Ar43101), CHINA: Yunnan, Xishuangbanna, Jinghong City, Mengyang Township, around Baihuashan tunnel, seasonal rainforest (22°9.51'N, 100°53.22'E, ca 890 m), 25.VI.2013, Q.Y. Zhao & Z.G. Chen leg.

Paratype: 1♀ (IZCAS-Ar43102), Mengla County, Menglun Township, Menglun Nature Reserve, rubber plantation (21°54.73'N, 101°16.72'E, ca 590 m), 27.V.2013, Q.Y. Zhao & Z.G. Chen leg.

Etymology. The specific name is a compound of “bidentatus” and the suffix “-oides”, referring to the resemblance of this species to *A. bidentatus* sp. nov.

Diagnosis. See diagnosis above for the species *A. bidentatus* sp. nov.

Description. Male (holotype, Figs 5D, E, 6). Total length 2.75. Carapace 1.50 long, 1.15 wide. Abdomen 1.75 long, 1.25 wide. Clypeus 0.10 high. Eye sizes and interdistances: AME 0.13, ALE 0.08, PME 0.10, PLE 0.10, AME–AME 0.15, AME–

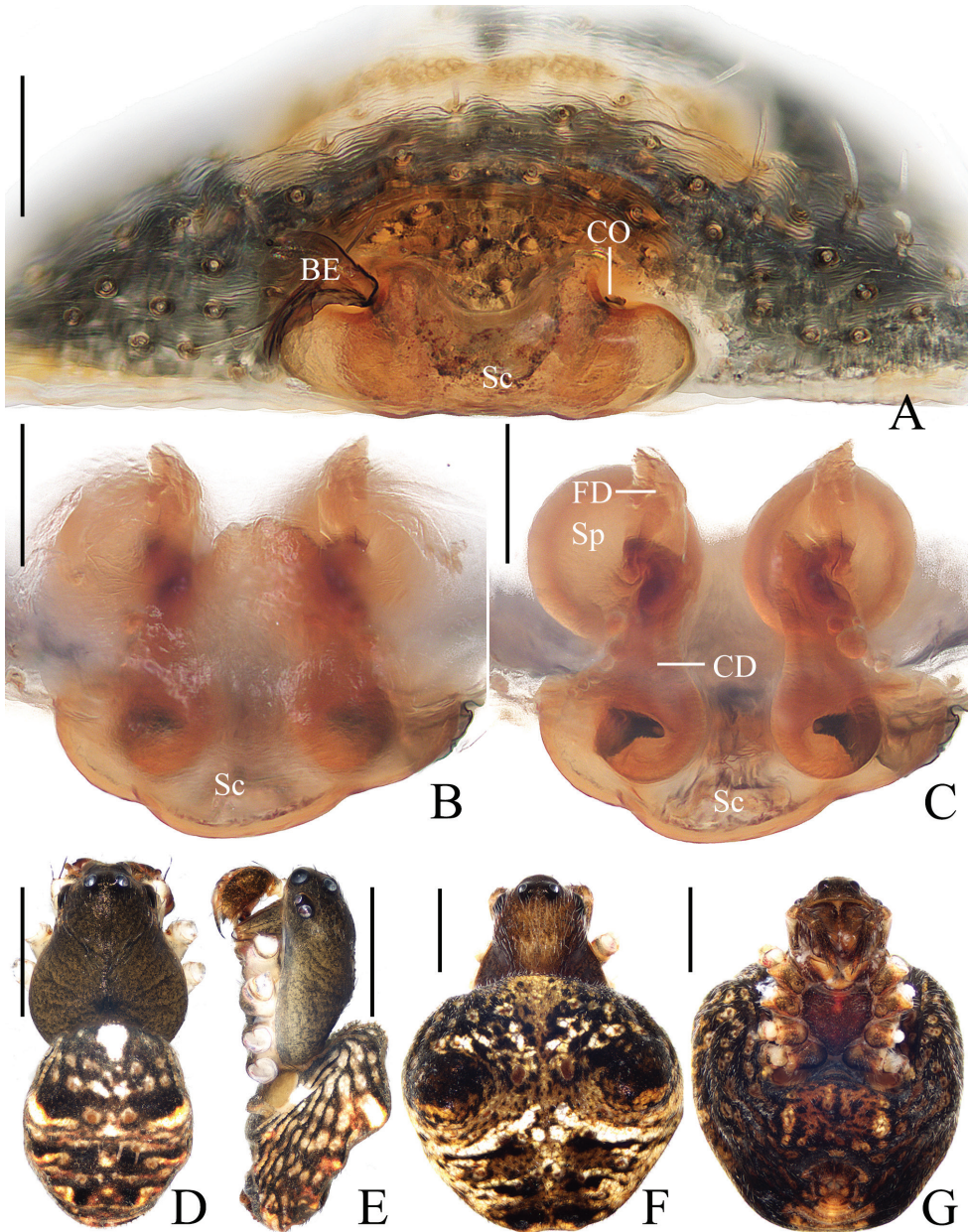


Figure 5. *Araneus bidentatoides* sp. nov. **A–C, F, G** female paratype IZCAS-Ar43102 **D, E** male holotype **A** epigyne, ventral view **B** ibid., posterior view **C** vulva, posterior view **D** habitus, dorsal view **E** ibid., lateral view **F** ibid., dorsal view **G** ibid., ventral view. Scale bars: 0.1 mm (**A–C**); 1 mm (**D–G**).

ALE 0.13, PME–PME 0.23, PME–PLE 0.15, MOA length 0.35, anterior width 0.35, posterior width 0.33. Leg measurements: I 4.35 (1.35, 1.55, 0.95, 0.50), II 3.70 (1.20, 1.25, 0.75, 0.50), III 2.70 (0.90, 0.90, 0.50, 0.40), IV 3.55 (1.15, 1.20, 0.75, 0.45).

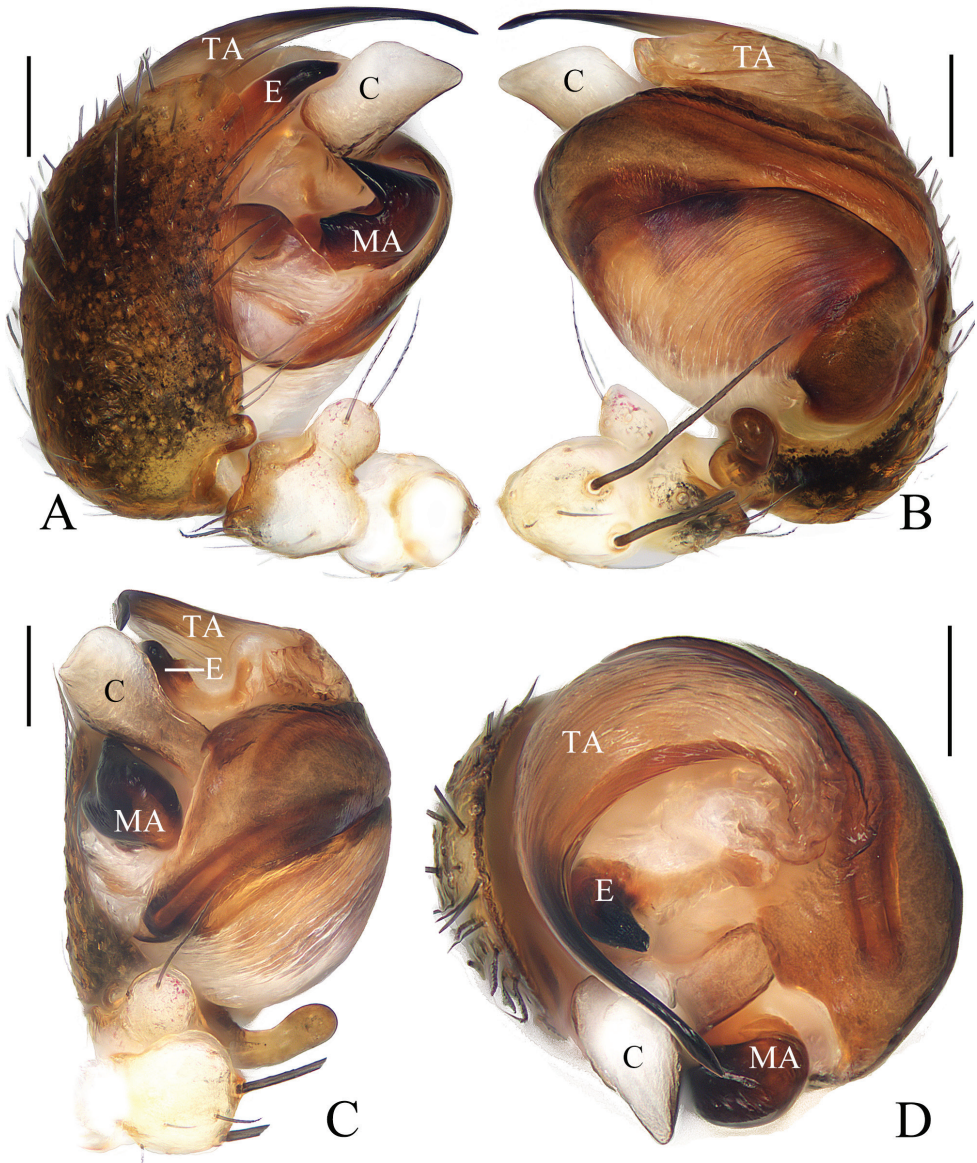


Figure 6. *Araneus bidentatoides* sp. nov. male holotype **A** male palp, prolateral view **B** *ibid.*, retrolateral view **C** *ibid.*, ventral view **D** *ibid.*, apical view. Scale bars: 0.1 mm.

Carapace pear-shaped, dark brown, with pale setae, cervical groove slightly distinct. Chelicerae dark brown, 4 promarginal teeth, 3 retromarginal teeth. Endites wider than long, reddish brown, paler distally, labium triangular, dark brown, paler distally. Sternum cordiform, dark brown with a longitudinal reddish-yellow patch, with pale setae. Legs brown with yellow annuli, tibia I with 9 macrosetae, tibia II with 10 macrosetae, tibia III with 5 macrosetae, and tibia IV with 8 macrosetae. Abdomen elliptical,

about 1.4 times longer than wide, with pair of very low humps anterolaterally, covered with pale setae, dorsum yellow with large white spot anteriorly, anterior half of humps black, posterior half whitish yellow, posterior abdomen with irregular dark markings; venter yellowish brown with irregular dark markings. Spinnerets yellowish brown.

Palp (Fig. 6): with 2 patellar bristles; median apophysis prominent, curved about 90° anticlockwise, distal end pointed toward tip of cymbium; embolus finger-like, tip slightly curved; conductor large, almost square in prolateral view; terminal apophysis with stout base, distally curved about 180° and tapered into tiny tip.

Female (paratype IZCAS-Ar43102, Fig. 5A–C, F, G). Total length 4.20. Carapace 2.20 long, 1.45 wide. Abdomen 3.40 long, 3.20 wide. Clypeus 0.13 high. Eye sizes and interdistances: AME 0.15, ALE 0.08, PME 0.13, PLE 0.10, AME–AME 0.23, AME–ALE 0.23, PME–PME 0.25, PME–PLE 0.38, MOA length 0.43, anterior width 0.45, posterior width 0.45. Leg measurements: I 5.25 (1.65, 1.90, 1.10, 0.60), II 4.65 (1.50, 1.65, 0.95, 0.55), III 3.35 (1.10, 1.15, 0.65, 0.45), IV 4.90 (1.70, 1.75, 0.95, 0.50). Habitus similar to that of male but abdomen slightly longer than wide.

Epigyne (Fig. 5A–C): about 3 times wider than long; scape short, about 5 times wider than long, directed ventrally; copulatory openings concave, located at anterolateral base of scape; copulatory ducts longer than the spermatheca diameter, expanded at origin; spermathecae globular, less than half the spermatheca diameter apart.

Distribution. Known only from type localities (Yunnan, China).

Araneus complanatus sp. nov.

<https://zoobank.org/E78494DB-9CD7-41EA-980B-3B6E55064015>

Figs 7, 8, 18I, J

Type material. *Holotype* ♂ (IZCAS-Ar43105), CHINA: Yunnan, Xishuangbanna, Mengla County, Menglun Township, 48 km from Xishuangbanna National Nature Reserve (21°58.70'N, 101°19.75'E, ca 1090 m), 12.VIII.2011, G. Zheng leg. *Paratype*: 1♀ (IZCAS-Ar43106), Mohan Township, Shanggang Village, Xiaolongha, secondary tropical forest (21°24.33'N, 101°37.02'E, ca 800 m), 30.VI.2012, Q.Y. Zhao & Z.G. Chen leg.

Etymology. The specific name comes from the Latin word “complanatus”, meaning “flattened”, referring to the shape of the abdomen.

Diagnosis. The new species resembles *A. arcuatus* sp. nov. in appearance, but can be distinguished from the latter in the following: 1) epigyne with a triangular scape vs scape absent (Fig. 1A, B); 2) copulatory openings located at the posterior surface vs ventral surface (Fig. 1A, B); 3) median apophysis with 1 tapered tip vs 2 tapered tips (Fig. 2A, C, D); and 4) 1 patellar bristle vs 2 patellar bristles (Fig. 2A–C).

Description. Male (holotype, Figs 7D, E, 8). Total length 2.75. Carapace 1.40 long, 1.25 wide. Abdomen 1.60 long, 1.45 wide. Clypeus 0.13 high. Eye sizes and interdistances: AME 0.13, ALE 0.10, PME 0.13, PLE 0.08, AME–AME 0.13, AME–ALE 0.13,

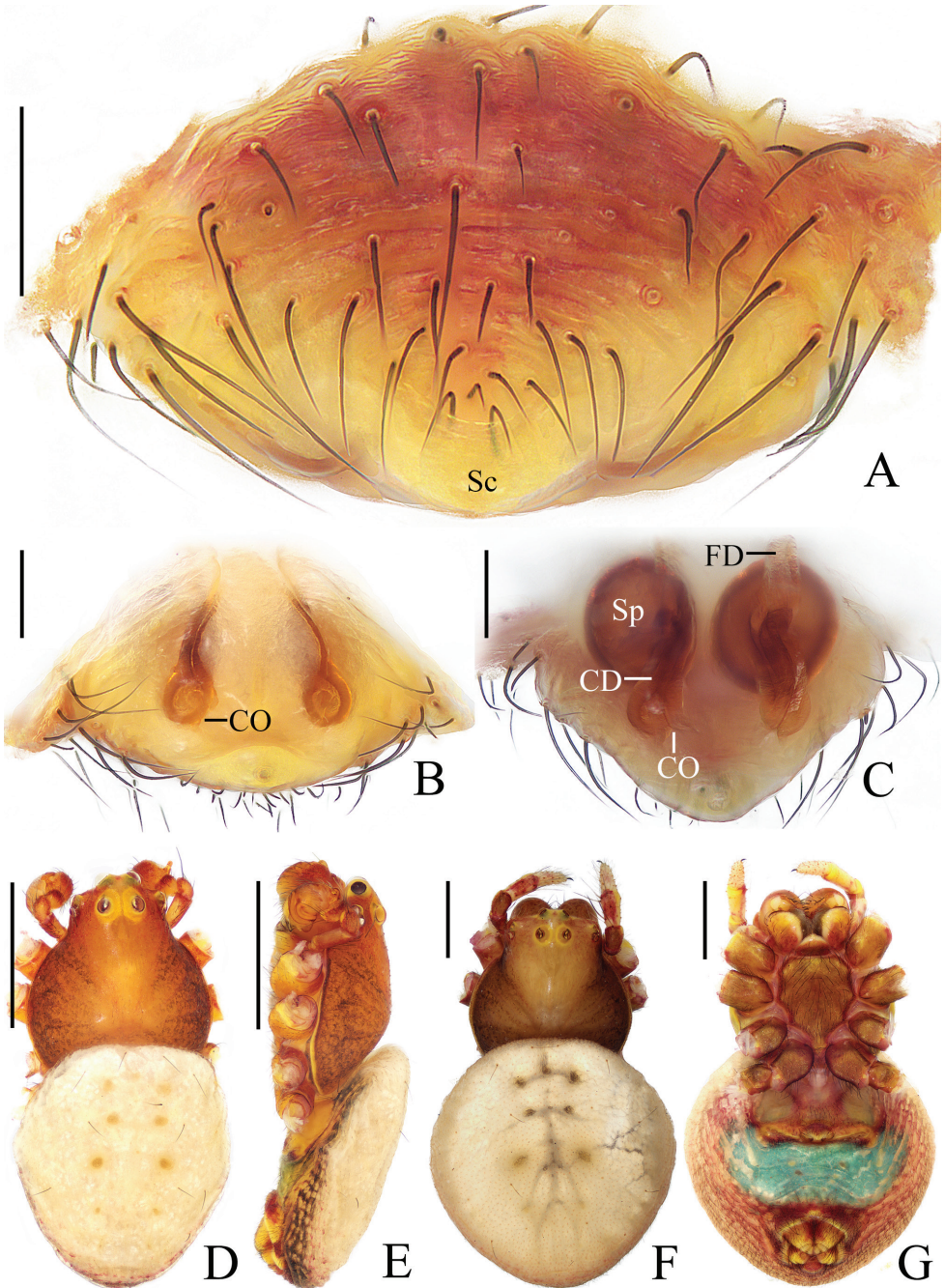


Figure 7. *Araneus complanatus* sp. nov. **A–C, F, G** female paratype IZCAS-Ar43106 **D, E** male holotype **A** epigyne, ventral view **B** ibid., posterior view **C** vulva, posterior view **D** habitus, dorsal view **E** ibid., lateral view **F** ibid., dorsal view **G** ibid., ventral view. Scale bars: 0.1 mm (**A–C**); 1 mm (**D–G**).

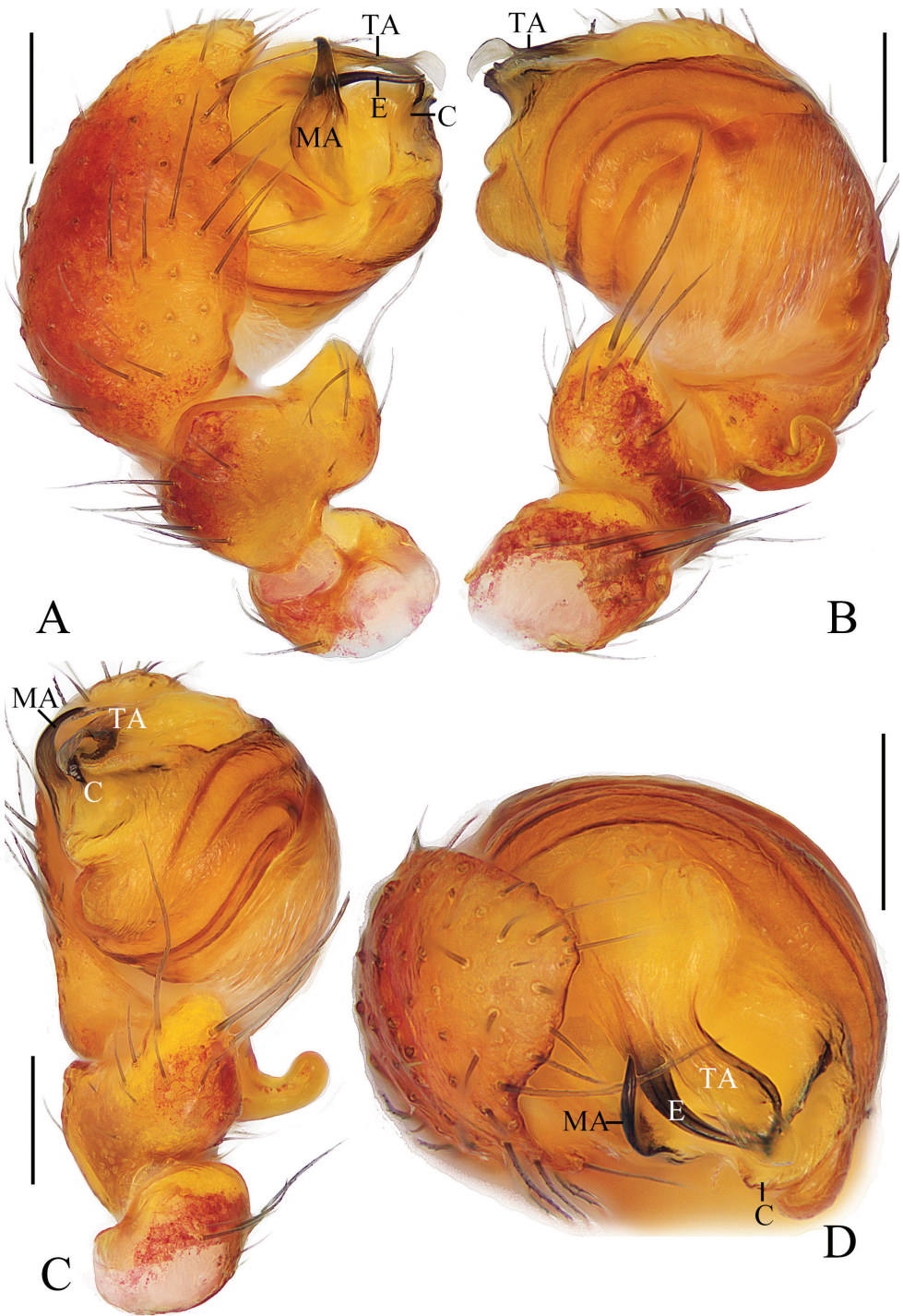


Figure 8. *Araneus complanatus* sp. nov. male holotype **A** male palp, prolateral view **B** ibid., retrolateral view **C** ibid., ventral view **D** ibid., apical view. Scale bars: 0.1 mm.

PME–PME 0.15, PME–PLE 0.13, MOA length 0.33, anterior width 0.30, posterior width 0.30. Leg measurements: I 3.95 (1.15, 1.35, 0.95, 0.50), II 3.65 (1.10, 1.20, 0.90, 0.45), III 2.60 (0.80, 0.85, 0.60, 0.35), IV 3.50 (1.10, 1.15, 0.85, 0.40). Carapace pear-shaped, brown with pale patches around PMEs and dark brown patches on thoracic edges, with gray setae, cervical groove slightly distinct. Chelicerae brown, 4 promarginal and 3 retromarginal teeth. Endites and labium brown at base, paler distally, endites square, labium triangular. Sternum cordiform, yellowish brown with brown setae. Legs reddish brown, with yellowish green patches, tibia, metatarsus, and tarsus of legs I and II with a cluster of dense macrosetae. Abdomen oval, about 1.1 times longer than wide, covered with sparse, dark setae, dorsum yellow with 4 pairs of sigillae, flattened in lateral view; venter yellowish brown with light yellowish-green patch medially. Spinnerets yellow.

Palp (Fig. 8): with 1 patellar bristle; median apophysis stout at base, claw like at tip; embolus slender, slightly curved; conductor broad at base, tapering to narrow tip; terminal apophysis long, membranous distally.

Female (paratype IZCAS-Ar43106, Figs 7A–C, E, G, 18I, J). Total length 4.95. Carapace 2.35 long, 2.15 wide. Abdomen 3.30 long, 3.30 wide. Clypeus 0.13 high. Eye sizes and interdistances: AME 0.13, ALE 0.13, PME 0.13, PLE 0.10, AME–AME 0.20, AME–ALE 0.30, PME–PME 0.23, PME–PLE 0.28, MOA length 0.45, anterior width 0.40, posterior width 0.43. Leg measurements: I 6.20 (1.85, 2.20, 1.45, 0.70), II 6.00 (1.85, 2.10, 1.40, 0.65), III 4.20 (1.40, 1.35, 0.95, 0.50), IV 6.25 (2.05, 2.10, 1.50, 0.60). Habitus similar to that of male but green patch on ventral abdomen more distinct.

Epigyne (Fig. 7A–C): about 1.5 times wider than long; scape triangular, about 2.3 times wider than long; copulatory openings narrow, at posterior surface; copulatory ducts shorter than the spermatheca diameter; spermathecae globular, touching each other.

Distribution. Known only from type localities (Yunnan, China).

***Araneus corrugis* sp. nov.**

<https://zoobank.org/F66E9921-63C5-4F23-81B9-692C261258CC>

Fig. 9

Type material. **Holotype** ♀ (IZCAS-Ar43107), CHINA: Yunnan, Xishuangbanna, Mengla County, Menglun Township, Menglun Nature Reserve, Lüshilin Forest Park, limestone tropical seasonal rainforest (21°54.68'N, 101°16.95'E, ca 640 m), 10.VIII.2018 night, C. Wang leg. **Paratype:** 1♀ (IZCAS-Ar43108), XTBG, eastern part (21°54.07'N, 101°16.36'E, ca 540 m), 22.VII.2018, X.Q. Mi leg.

Etymology. The specific name comes from the Latin word “corrugis”, meaning “wrinkled”, referring to the texture of the epigyne basally; adjective.

Diagnosis. The new species resembles *A. gratiolus* Yin, Wang, Xie & Peng, 1990 in appearance, but it can be distinguished from the latter by the following: 1) distal part of the scape finger-like vs triangular (Yin et al. 1990: figs 79, 80); 2) distal part of the scape not grooved vs grooved (Yin et al. 1990: figs 79, 80); and 3) inner edge of the lateral plate straight in ventral view (arrows in Fig. 9A) vs arcuate (Yin et al. 1990: fig. 79).

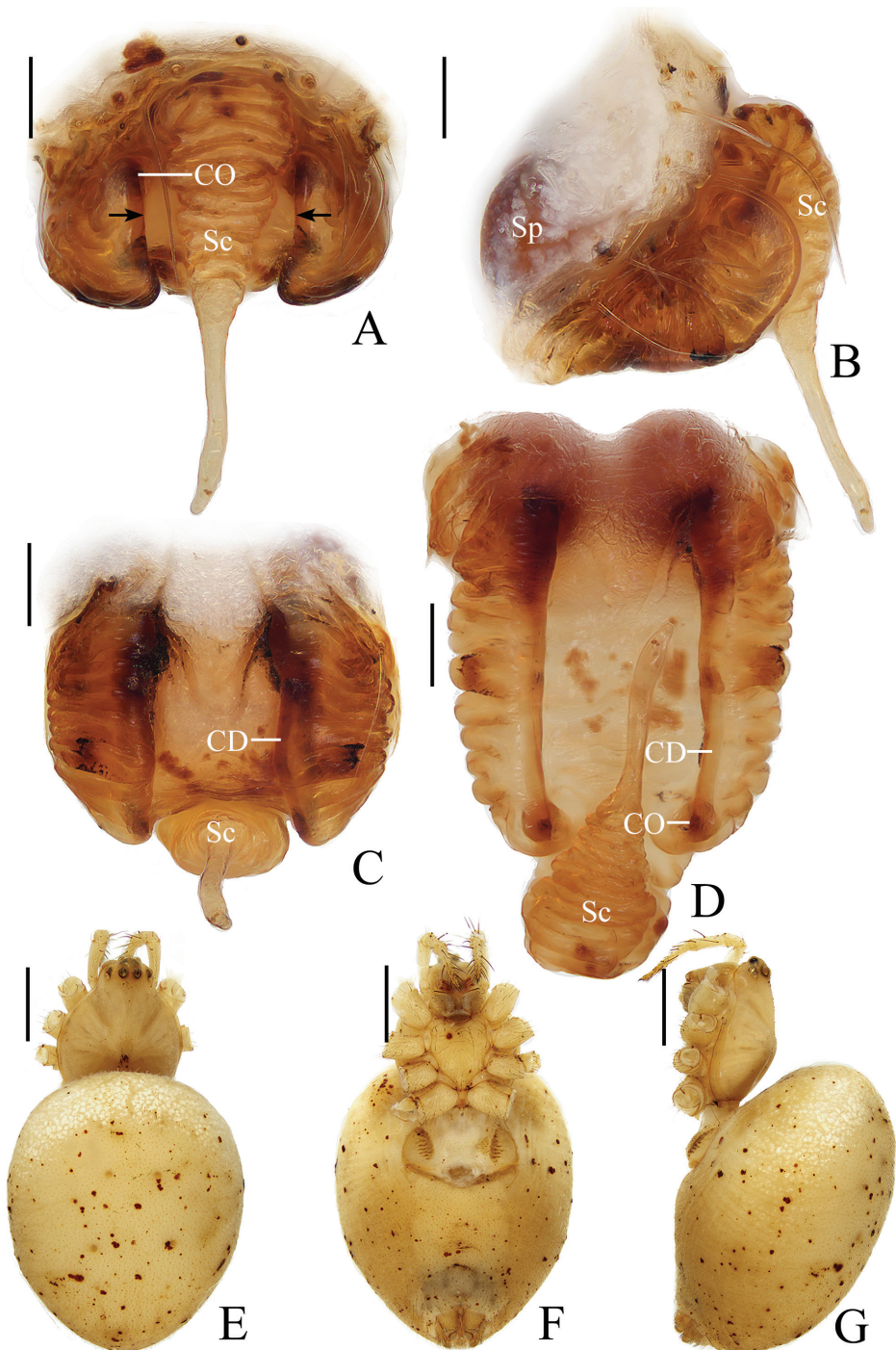


Figure 9. *Araneus corrugis* sp. nov. female holotype **A** epigyne, ventral view **B** *ibid.*, lateral view **C** *ibid.*, posterior view **D** vulva, posterior view **E** habitus, dorsal view **F** *ibid.*, ventral view **G** *ibid.*, lateral view. Scale bars: 0.1 mm (**A–D**); 1 mm (**E–G**).

Description. Female (holotype, Fig. 9). Total length 5.20. Carapace 2.00 long, 1.70 wide. Abdomen 3.80 long, 3.20 wide. Clypeus 0.13 high. Eye sizes and interdistances: AME 0.18, ALE 0.13, PME 0.15, PLE 0.13, AME–AME 0.13, AME–ALE 0.13, PME–PME 0.10, PME–PLE 0.18, MOA length 0.38, anterior width 0.38, posterior width 0.35. Leg measurements: I 11.20 (3.00, 3.50, 3.60, 1.10), II 9.30 (2.70, 3.00, 2.70, 0.90), III 5.40 (1.70, 1.80, 1.30, 0.60), IV 9.10 (2.90, 3.00, 2.40, 0.80). Carapace pear-shaped, yellow, with pale setae, cervical groove distinct. Chelicerae yellowish brown, 4 promarginal and 3 retromarginal teeth. Endites almost rectangular, yellowish brown at base and paler distally, labium triangular, grayish brown, paler distally. Sternum cordiform, yellow, with dark setae. Legs yellow without annulus. Abdomen oval, rounded anteriorly, slightly pointed posteriorly, with 4 pairs of sigillae, yellow with white scaly spots anteriorly; venter yellow. Spinnerets yellow.

Epigyne (Fig. 9A–D): scape exceeding beyond the epigastric furrow, broad and wrinkled at base, distal half finger-like; copulatory openings narrow, near lateral edges of scape base; copulatory ducts 2 times longer than the spermatheca diameter; spermathecae globular, touching each other.

Variation. Total length: ♀♀ 5.20–6.70.

Distribution. Known only from type localities (Yunnan, China).

***Araneus cucullatus* sp. nov.**

<https://zoobank.org/0B06353E-D025-4742-BA39-D1CAAD167DFB>

Figs 10, 18K, L

Type material. Holotype ♀ (IZCAS-Ar43109), CHINA: Yunnan, Xishuangbanna, Mengla County, Menglun Township, Menglun Nature Reserve, Lüshilin Forest Park, limestone seasonal rainforest (21°54.56'N, 101°16.86'E, ca 610 m), 29.XI.2009, G. Tang leg. **Paratype:** 1♀ (IZCAS-Ar43110), Lüshilin Forest Park (21°54.71'N, 101°16.90'E, ca 660 m), 13.XI.2009, G. Tang leg.

Etymology. The specific name comes from the Latin word “cucullatus”, meaning “hooded”, referring to the hood on the ventral surface of the epigyne.

Diagnosis. The new species resembles *A. arcuatus* sp. nov. in appearance, but it can be distinguished from the latter by the following: 1) epigyne about 2 times wider than long vs about 1.65 times wider than long (Fig. 1A, B); 2) copulatory openings situated on posterior surface vs ventral surface (Fig. 1A, B); 3) spermathecae separated vs touching each other (Fig. 1B); and 4) abdomen with sparse, long setae vs lacking sparse, long setae (Fig. 1E).

Description. Female (holotype, Fig. 10, paratype Ar43110, Fig. 18K, L). Total length 4.80. Carapace 1.90 long, 1.50 wide. Abdomen 3.30 long, 2.90 wide. Clypeus 0.13 high. Eye sizes and interdistances: AME 0.13, ALE 0.10, PME 0.13, PLE 0.10, AME–AME 0.15, AME–ALE 0.23, PME–PME 0.15, PME–PLE 0.20, MOA length 0.38, anterior width 0.33, posterior width 0.38. Leg measurements: I 5.10 (1.40, 1.80, 1.30, 0.60), II 4.90 (1.40, 1.70, 1.20, 0.60), III 3.60 (1.10, 1.10, 0.90, 0.50),

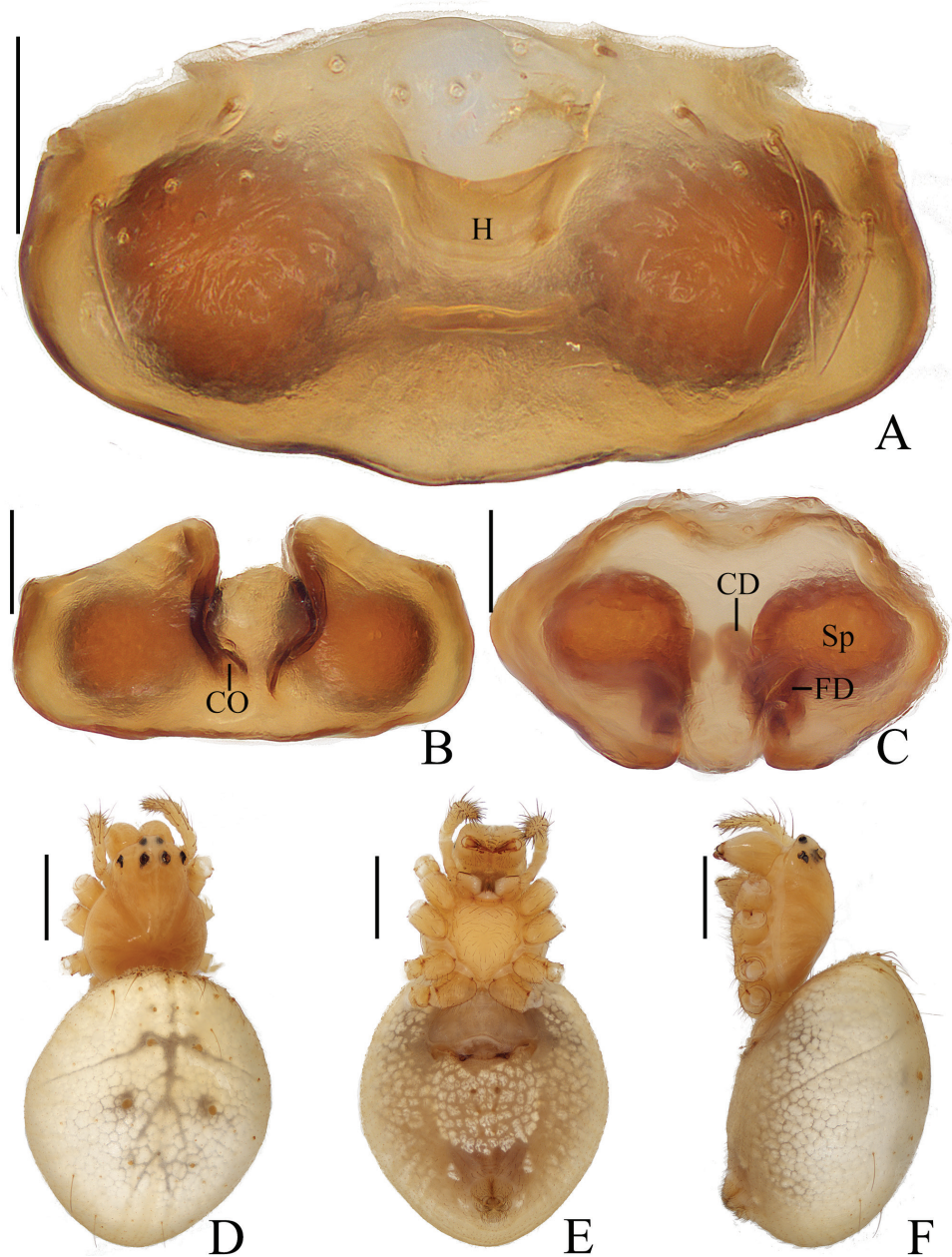


Figure 10. *Araneus cucullatus* sp. nov. female holotype **A** epigyne, ventral view **B** *ibid.*, posterior view **C** vulva, dorsal view **D** habitus, dorsal view **E** *ibid.*, ventral view **F** *ibid.*, lateral view. Scale bars: 0.1 mm (**A–C**); 1 mm (**D–F**).

IV 4.80 (1.40, 1.70, 1.20, 0.50). Carapace pear-shaped, yellow, cervical groove distinct. Chelicerae yellow, 4 promarginal teeth, 3 retromarginal teeth. Endites almost rectangular, yellow with dark anterior edge, labium triangular, yellow. Sternum cor-

diform, yellow, with dark setae. Legs yellow without annulus, distal tibia, metatarsus, and tarsus of legs I and II with a cluster of dense macrosetae. Abdomen elliptical, whitish yellow, with sparse dark setae; venter grayish yellow with white scaly spots. Spinnerets grayish yellow.

Epigyne (Fig. 10A–C): about 2 times wider than long, with a hood; copulatory openings concave, at middle part of posterior surface; copulatory ducts slender, twisted at origin; spermathecae nearly globular, half the diameter apart.

Variation. Total length: ♀♀ 4.30–4.80.

Distribution. Known only from the type locality (Yunnan, China).

***Araneus minisculus* sp. nov.**

<https://zoobank.org/3D55612E-E294-42A2-80F0-8CA8110CA840>

Figs 11, 19A, B

Type material. **Holotype** ♂ (IZCAS-Ar43112), CHINA: Yunnan, Xishuangbanna, Mengla County, Mohan Township, Shanggang Village, Xiaolongha, seasonal rain-forest (21°24.19'N, 101°36.26'E, ca 720 m), 4.VII.2012, Q.Y. Zhao & Z.G. Chen leg. **Paratypes:** 1♂ (IZCAS-Ar43113), Menghai County, Menghai Township, Manzhen Village, Mandazhai, secondary forest (22°1.70'N, 100°23.70'E, ca 1190 m), 28.VII.2012, Q.Y. Zhao & Z.G. Chen leg.; 1♂ (IZCAS-Ar43114), Mengla County, Menglun Township, Menglun Nature Reserve, secondary tropical forest, *Anogeissus acuminata* plantation (about 20 years old), G213 roadside (21°54.03'N, 101°16.89'E, ca 610 m), 2.VIII.2018, Z.L. Bai leg.

Etymology. The specific name is from the Latin word “minisculus”, meaning “small”, referring to the relatively small total length of the habitus.

Diagnosis. The new species can be distinguished from any other congeners by the following combination of characters: 1) male palp with a cluster of tibial bristles; 2) dorsal abdomen with 2 pairs of longitudinal, narrow, pale patches; and 3) small total body length.

Description. Male (holotype, Figs 11, 19A, B). Total length 1.90. Carapace 1.05 long, 0.85 wide. Abdomen 1.05 long, 0.90 wide. Clypeus 0.05 high. Eye sizes and interdistances: AME 0.10, ALE 0.05, PME 0.08, PLE 0.05, AME–AME 0.10, AME–ALE 0.13, PME–PME 0.05, PME–PLE 0.05, MOA length 0.25, anterior width 0.23, posterior width 0.20. Leg measurements: I 3.50 (1.05, 1.20, 0.80, 0.45), II 2.90 (0.85, 1.00, 0.65, 0.40), III 1.70 (0.55, 0.55, 0.30, 0.30), IV 2.35 (0.75, 0.75, 0.50, 0.35). Carapace pear-shaped, dark brown, with pale setae, cervical groove inconspicuous. Chelicerae grayish brown, 4 promarginal teeth, 3 retromarginal teeth. Endites and labium grayish brown at base, paler distally, endites square, labium triangular. Sternum cordiform, dark brown with yellow patch anteriorly, with pale setae. Legs yellow to yellowish brown, without annulus. Abdomen broadly oval, covered with pale setae, dorsum grayish brown with two pairs of longitudinal, narrow, pale patches; venter grayish brown with a pair of yellow patches. Spinnerets grayish brown.

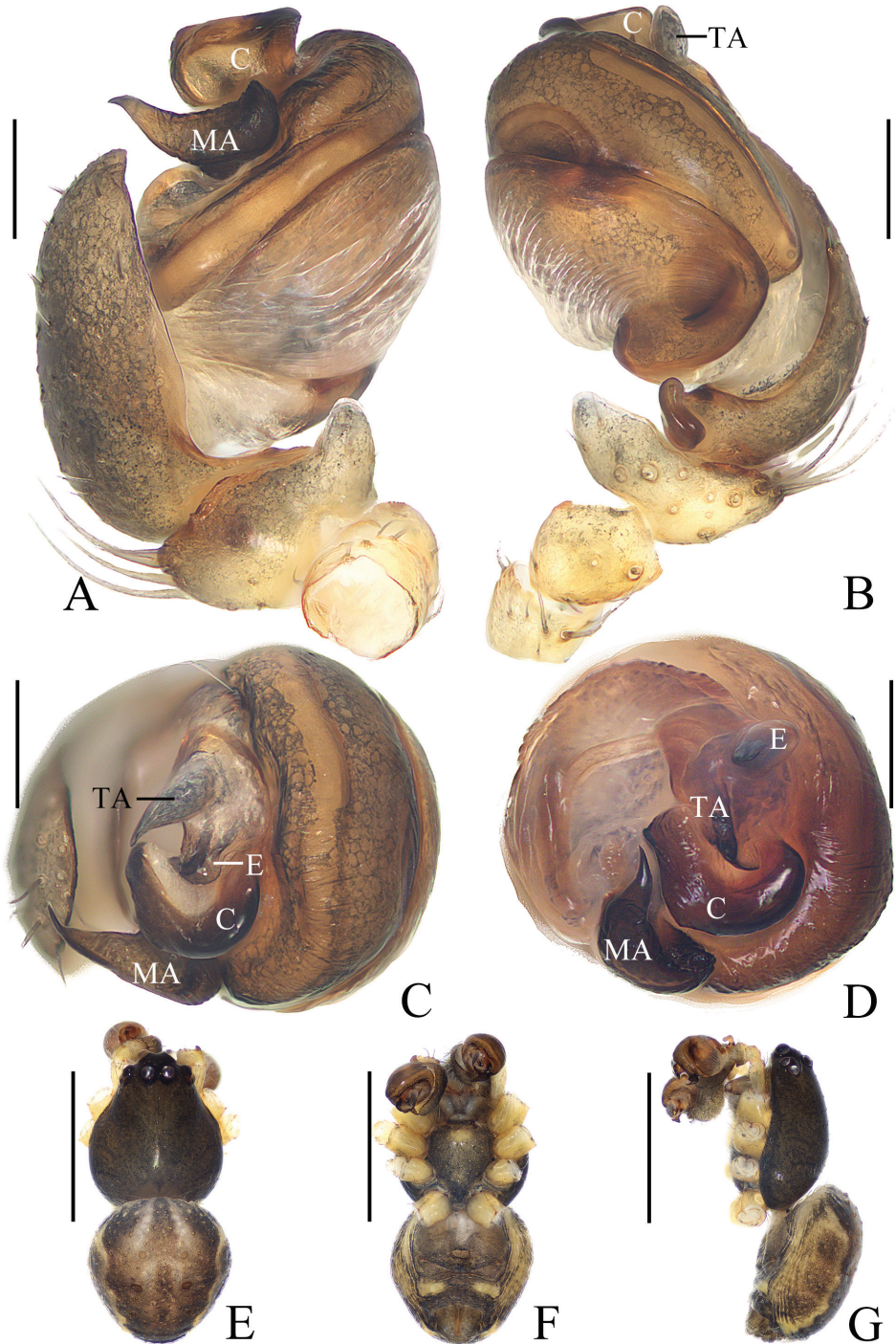


Figure 11. *Araneus minisculus* sp. nov. holotype **A** male palp, prolateral view **B** *ibid.*, retrolateral view **C** *ibid.*, apical view **D** *ibid.*, expanded, apical view **E** habitus, dorsal view **F** *ibid.*, ventral view **G** *ibid.*, lateral view. Scale bars: 0.1 mm (**A–D**); 1 mm (**E–G**).

Palp (Fig. 11A–D): with 1 patellar bristle and a cluster of tibial bristles; median apophysis transverse, with long, tapered spur; embolus short, broad at base; conductor large, heavily sclerotized, curved; terminal apophysis small, about equal length to embolus.

Variation. Total length: ♂♂ 1.80–1.90.

Distribution. Known only from type localities (Yunnan, China).

***Araneus ovoideus* sp. nov.**

<https://zoobank.org/DB876BBB-1F7B-4467-9CAB-FCA7ED57318B>

Figs 12, 19C, D

Type material. **Holotype** ♀ (IZCAS-Ar43115), CHINA: Yunnan, Xishuangbanna, Mengla County, Menglun Township, Menglun Nature Reserve, low evergreen forest along G213 roadside (21°53.79'N, 101°17.15'E, ca 590 m), 27.XI.2009, G. Tang leg. **Paratypes:** 1♀ (IZCAS-Ar43116), Lüshilin, secondary tropical seasonal moist forest (21°54.39'N, 101°16.72'E, ca 690 m), 6.VIII.2011, G. Zheng leg.; 1♀ (IZCAS-Ar43117), secondary tropical forest around garbage dump (21°54.17'N, 101°16.87'E, ca 610 m), 31.VII.2018, Z.L. Bai leg.; 1♀ (IZCAS-Ar43118), XTBG, near the benchland (21°54.24'N, 101°15.99'E, ca 540 m), 13.V.2019, Z.L. Bai leg.

Etymology. The specific name is derived from the Latin word “*ovoides*”, meaning “*oval*”, referring to the shape of the spermathecae.

Diagnosis. The new species can be distinguished from its congeners by the following combination of characters: 1) epigyne triangular; 2) a very large pair of spermathecae; 3) posterior abdomen with 1 yellow transverse patch and 2 yellow longitudinal patches; and 4) ventral abdomen with a square white patch.

Description. **Female** (holotype, Figs 12, 19C, D). Total length 6.80. Carapace 3.10 long, 2.70 wide. Abdomen 4.00 long, 4.10 wide. Clypeus 0.10 high. Eye sizes and interdistances: AME 0.20, ALE 0.15, PME 0.18, PLE 0.15, AME–AME 0.18, AME–ALE 0.20, PME–PME 0.08, PME–PLE 0.35, MOA length 0.53, anterior width 0.53, posterior width 0.40. Leg measurements: I 10.60 (3.10, 3.90, 2.60, 1.00), II 9.90 (3.00, 3.50, 2.50, 0.90), III 6.10 (2.00, 2.10, 1.30, 0.70), IV 9.10 (3.00, 3.10, 2.20, 0.80). Carapace pear-shaped, dark brown, with dense, pale setae. Chelicerae dark brown, 4 promarginal teeth, 3 retromarginal teeth. Endites and labium dark brown basally, yellow distally, endites almost square, labium triangular. Sternum cordiform, yellow with yellowish-brown margins. Legs yellow with wide, brown annuli. Abdomen broadly oval, with dark setae, dorsum whitish yellow, with 2 pairs of grayish-brown patches anteriorly and medially, posteriorly with three grayish-brown patches; venter grayish brown, square white patch medially. Spinnerets brown.

Epigyne (Fig. 12A–D): triangular, about 1.5 times wider than long, with very short, rimmed scape; copulatory openings concave, at posterior surface; copulatory ducts twisted at origin; spermathecae oval, touching each other.

Variation. Total length: ♀♀ 6.80–7.70.

Distribution. Known only from type localities (Yunnan, China).

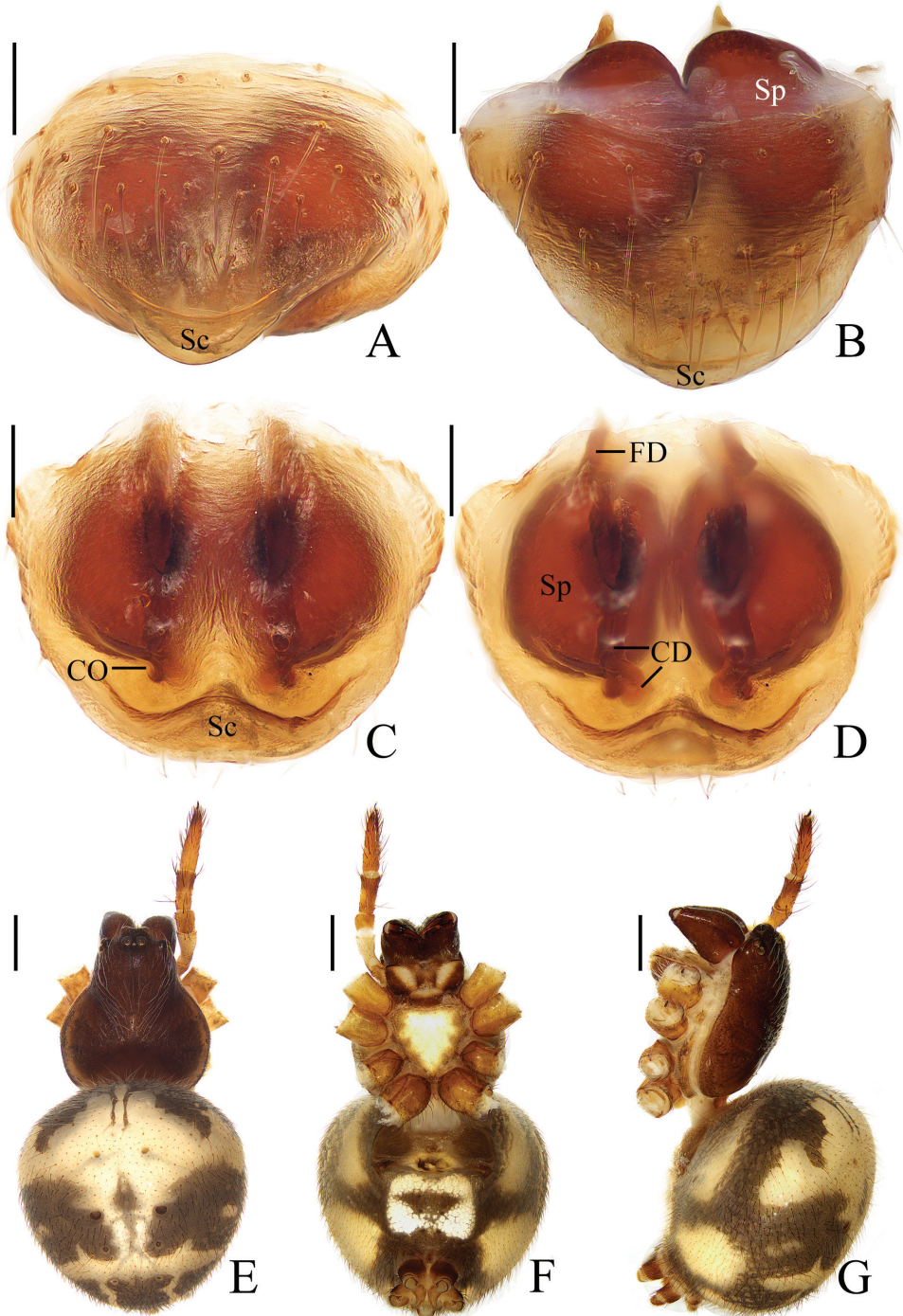


Figure 12. *Araneus ovoideus* sp. nov. female holotype **A** epigyne, ventral view **B** ibid., anterior view **C** ibid., posterior view **D** vulva, posterior view **E** habitus, dorsal view **F** ibid., ventral view **G** ibid., lateral view. Scale bars: 0.1 mm (**A–D**); 1 mm (**E–G**).

***Araneus pseudodigitatus* sp. nov.**

<https://zoobank.org/65E73381-15A3-4C6B-AE4F-CDF75A6B01D0>

Figs 13, 14, 19E–H

Type material. *Holotype* ♂ (IZCAS-Ar43119), CHINA: Yunnan, Xishuangbanna, Mengla County, Menglun Township, Menglun Nature Reserve, XTBG, #6 site around the dump (21°54.33'N, 101°16.79'E, ca 620 m), 7.V.2019, Y.F. Tong leg. *Paratypes*: 1♂1♀ (IZCAS-Ar43120-Ar43121), Masuoxing Village (21°54.02'N, 101°16.90'E, ca 560 m), 27.IV.2019, Y.F. Tong leg.; 1♀ (IZCAS-Ar43122), #4 site around the dump (21°54.34'N, 101°16.79'E, ca 620 m), 2.V.2019, Y.F. Tong leg.; 1♂1♀ (IZCAS-Ar43123-Ar43124), #2 site in Mafengzhai Village (21°55.83'N, 101°14.93'E, ca 540 m), 4.V.2019, Y.F. Tong leg.; 2♀ (IZCAS-Ar43125-Ar43126) Lüshilin Forest Park (21°53.84'N, 101°16.84'E, ca 550 m), 10.V.2019, Z.L. Bai leg.

Etymology. The specific name is a combination of the Latin words “pseudo” and “digitatus”, referring to the resemblance of this species with *A. digitatus* Liu, Irfan, Yang & Peng, 2019; adjective.

Diagnosis. The new species resembles *A. digitatus* in appearance, but it differs by the following: 1) copulatory openings on the posterior surface vs on the ventral surface (Liu et al. 2019: fig. 8A, B); 2) embolus curved clockwise about 135° in prolateral view vs curved <90° (Liu et al. 2019: fig. 7A, C); and 3) abdomen posteriorly pointed in both sexes vs blunt (Liu et al. 2019: fig. 6A, C).

Description. Male (holotype, Figs 13A–F, 19E–H). Total length 3.15. Carapace 1.70 long, 1.40 wide. Abdomen 1.75 long, 1.40 wide. Clypeus 0.13 high. Eye sizes and interdistances: AME 0.13, ALE 0.10, PME 0.13, PLE 0.10, AME–AME 0.13, AME–ALE 0.13, PME–PME 0.10, PME–PLE 0.18, MOA length 0.33, anterior width 0.35, posterior width 0.28. Leg measurements: I 5.50 (1.75, 2.05, 1.15, 0.55), II 5.10 (1.60, 1.85, 1.10, 0.55), III 3.05 (1.05, 1.00, 0.60, 0.40), IV 4.35 (1.45, 1.45, 1.00, 0.45). Carapace pear-shaped, yellow with brown eye bases, with pale setae, cervical groove slightly distinct, fovea longitudinal. Chelicerae yellow, 4 promarginal teeth, 3 retromarginal teeth. Endites yellow, labium yellowish brown, paler distally. Sternum cordiform, yellow. Legs yellow to brown without annulus, tibia I with 10 macrosetae, tibia II with 8 macrosetae, tibia III with 8 macrosetae, tibia IV with 9 macrosetae. Abdomen somewhat long, triangular, about 1.25 times longer than wide, with pale setae, dorsum with a longitudinal grayish-yellow patch anteriorly, and a triangular grayish-brown patch posteriorly; venter grayish brown, with a pair of whitish-yellow longitudinal patches, laterally yellow with irregular gray patches. Spinnerets grayish brown.

Palp (Fig. 13A–D): with 2 patellar bristles; median apophysis large, bifurcated, 1 long, 1 short with serrated tip; embolus large, curved about 135° at middle, tapered distally; conductor somewhat rectangular, with a spur at base; terminal apophysis extremely large, about as long as the bulb diameter.

Female (paratype IZCAS-Ar43125, Figs 13G, H, 14A, C–F, paratype IZCAS-Ar43125, Fig. 14B). Total length 5.10. Carapace 2.00 long, 1.50 wide. Abdomen 3.60 long, 2.70 wide. Clypeus 0.13 high. Eye sizes and interdistances: AME 0.13, ALE

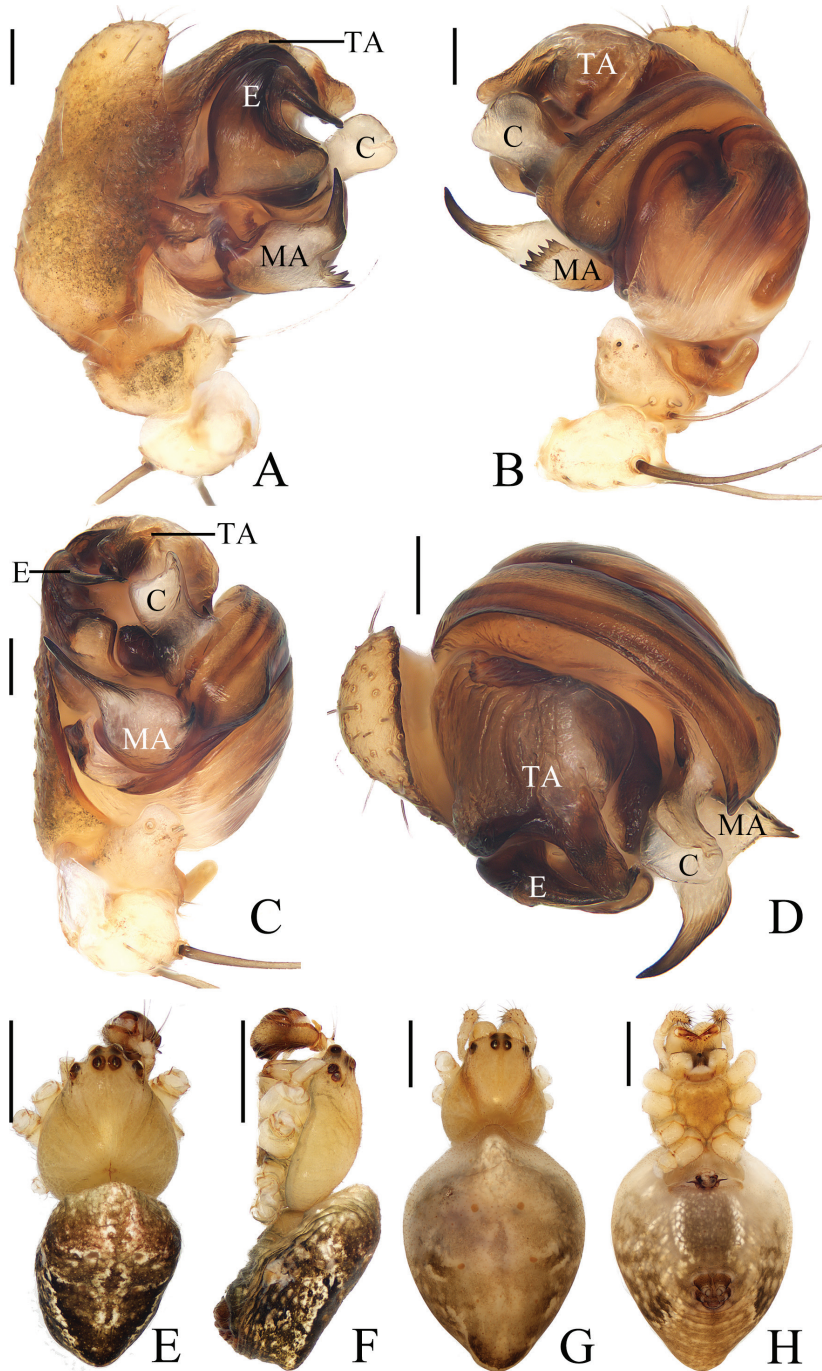


Figure 13. *Araneus pseudodigitatus* sp. nov. **A–F** male holotype **G, H** female paratype IZCAS-Ar43125 **A** male palp, prolateral view **B** *ibid.*, retrolateral view **C** *ibid.*, ventral view **D** *ibid.*, apical view **E** habitus, dorsal view **F** *ibid.*, lateral view **G** *ibid.*, dorsal view **H** *ibid.*, ventral view. Scale bars: 0.1 mm (**A–D**); 1 mm (**E–H**).

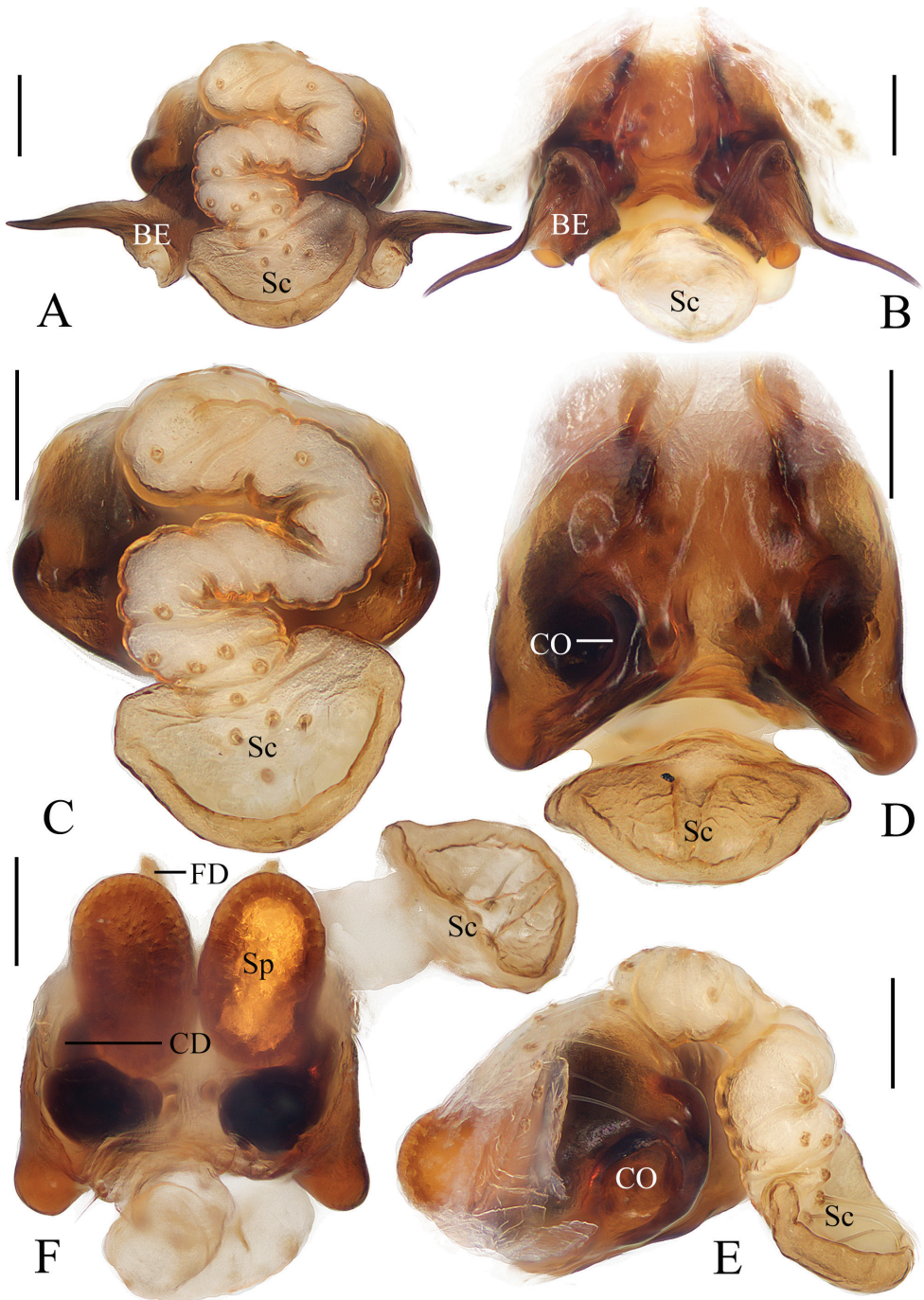


Figure 14. *Araneus pseudodigitatus* sp. nov. **A, C-F** female paratype IZCAS-Ar43125 **B** female paratype IZCAS-Ar43126 **A** epigyne, ventral view **B** ibid., posterior view **C** ibid., ventral view **D** ibid., posterior view **E** ibid., lateral view **F** vulva, anterior view. Scale bars: 0.1 mm.

0.10, PME 0.13, PLE 0.10, AME–AME 0.13, AME–ALE 0.25, PME–PME 0.10, PME–PLE 0.30, MOA length 0.33, anterior width 0.33, posterior width 0.30. Leg measurements: I 5.50 (1.70, 2.00, 1.20, 0.60), II 5.10 (1.60, 1.90, 1.00, 0.60), III 3.30 (1.10, 1.10, 0.70, 0.40), IV 4.90 (1.50, 1.80, 1.10, 0.50). Habitus similar to that of male but a little pale.

Epigyne (Fig. 14): with long, tortuous scape, spoon-shaped, rimmed at tip; copulatory openings deeply concave, at posterior surface; copulatory ducts curved, extremely expanded at origin; spermathecae kidney-shaped, touching each other.

Variation. Total length: ♂♂ 3.10–3.40; ♀♀ 3.90–6.10.

Distribution. known only from type localities (Yunnan, China).

***Araneus semiorbiculatus* sp. nov.**

<https://zoobank.org/AF3DF4B2-B1E8-4451-90D6-EC3F8044B4FB>

Figs 15, 19I, J

Type material. **Holotype** ♀ (IZCAS-Ar43127), CHINA: Yunnan, Xishuangbanna, Mengla County, Menglun Township, Menglun Nature Reserve, XTBG, 26.XII.2006, S.Q. Li leg. **Paratypes:** 1♀ (IZCAS-Ar43128), same data as holotype; 1♀ (IZCAS-Ar43129), Menglun Township, 55 km from Xishuangbanna National Nature Reserve, valley rainforest (21°57.68'N, 101°12.03'E, ca 720 m), 12.VI.2013, Q.Y. Zhao & Z.G. Chen leg.

Etymology. The specific name is from the Latin word “semiorbiculatus”, meaning “semicircle”, referring to the shape of the scape.

Diagnosis. The new species resembles *A. bidentatus* sp. nov., but it can be distinguished from the latter by the following: 1) copulatory openings situated lateral to posterior surface vs at lateral end of the scape groove (Fig. 3A, B); 2) distal end of the scape not grooved vs grooved (Fig. 3A, B); and 3) scape width equal to 2 diameters of a spermatheca vs width about 1.3 times of a spermatheca diameter (Fig. 3D).

Description. Female (holotype, Figs 15, 19I, J). Total length 3.25. Carapace 1.75 long, 1.30 wide. Abdomen 2.40 long, 1.90 wide. Clypeus 0.05 high. Eye sizes and interdistances: AME 0.13, ALE 0.10, PME 0.13, PLE 0.13, AME–AME 0.13, AME–ALE 0.18, PME–PME 0.13, PME–PLE 0.25, MOA length 0.33, anterior width 0.35, posterior width 0.35. Leg measurements: I 4.80 (1.45, 1.70, 1.00, 0.65), II 4.15 (1.25, 1.45, 0.85, 0.60), III 3.00 (0.95, 1.00, 0.55, 0.50), IV 4.20 (1.40, 1.40, 0.85, 0.55). Carapace pear-shaped, brown with yellow patches around the fovea and laterally on thoracic region, ALEs, PMEs, and PLEs with black base, with pale setae, cervical groove distinct. Chelicerae yellowish brown, 5 promarginal teeth, 3 retromarginal teeth. Endites and labium brown at base, paler distally, endites square, labium triangular. Sternum cordiform, yellow with dark brown edges, with dark setae. Legs yellow with inconspicuous grayish-brown annuli. Abdomen elliptical, about 1.25 times longer than wide, covered with gray setae, dorsum grayish yellow with large white spot anteriorly and irregular black markings; venter yellow with dark brown patches. Spinnerets yellow.

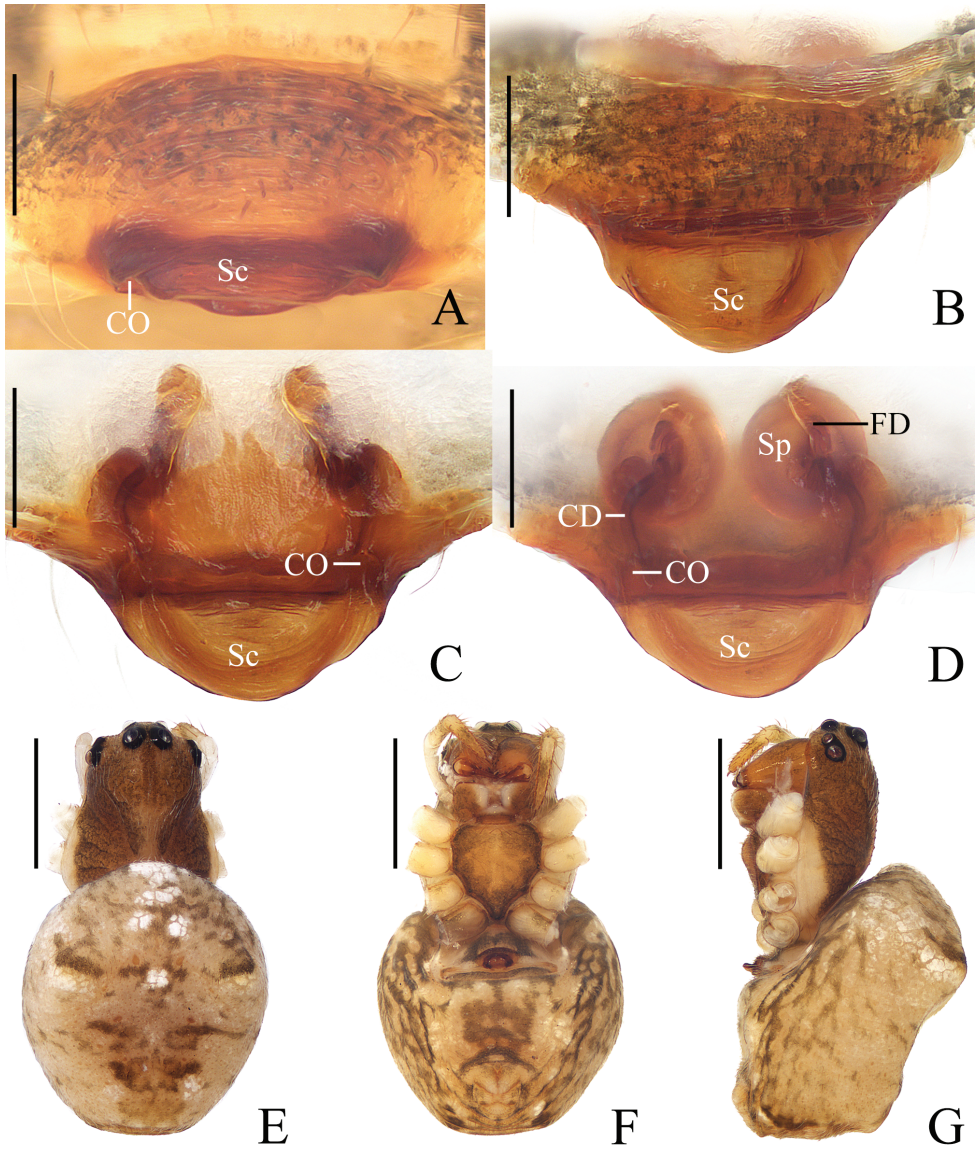


Figure 15. *Araneus semiorbiculatus* sp. nov. female holotype **A** epigyne, ventral view **B** *ibid.*, anterior view **C** *ibid.*, posterior view **D** vulva, posterior view **E** habitus, dorsal view **F** *ibid.*, ventral view **G** *ibid.*, lateral view. Scale bars: 0.1 mm (**A–D**); 1 mm (**E–G**).

Epigyne (Fig. 15A–D): about 1.8 times wider than long, with a semicircular scape, round copulatory openings at lateral to posterior surface; copulatory duct length about equal to the spermatheca diameter, slightly curved; spermathecae globular, less than half the spermathecae diameter apart.

Variation. Total length: ♀♀ 3.20–3.25.

Distribution. Known only from type localities (Yunnan, China).

***Araneus tetracanthus* sp. nov.**

<https://zoobank.org/71CE9BA2-64AC-48B3-892D-C70A9DEF0590>

Figs 16, 17, 19K–N

Type material. *Holotype* ♂ (IZCAS-Ar43130), CHINA: Yunnan, Xishuangbanna, Mengla County, Menglun Township, Menglun Nature Reserve, Lüshilin Forest Park (21°53.84'N, 101°16.84'E, ca 550 m), 10.V.2019, Z.L. Bai leg. *Paratypes*: 1♂ (IZCAS-Ar43131), G213 roadside (21°54.39'N, 101°16.80'E, ca 630 m), 22.XI.2009, G. Tang leg.; 1♂ (IZCAS-Ar43131), G213 roadside (21°53.67'N, 101°16.98'E, ca 590 m), 26.XI.2009, G. Tang leg.; 1♂ (IZCAS-Ar43133), G213 roadside (21°54.09'N, 101°17.02'E, ca 570 m), 28.XI.2009, G. Tang leg.; 1♂ (IZCAS-Ar43134), G213 roadside, bamboo plantation (21°53.64'N, 101°16.94'E, ca 580 m), 3.XII.2009, G. Tang leg.; 1♂1♀ (IZCAS-Ar43135–43136), Masuoxing Village (21°54.02'N, 101°16.90'E, ca 560 m), 27.IV.2019, Y.F. Tong leg.; 1♂ (IZCAS-Ar43137), #1 site in Mafengzhai Village (21°53.44'N, 101°17.40'E, ca 540 m), 29.IV.2019, Y.F. Tong leg.; 1♂ (IZCAS-Ar43138), Lüshilin, secondary tropical seasonal moist forest (21°54.39'N, 101°16.72'E, ca 690 m), 6.VIII.2011, G. Zheng leg.; 1♂ (IZCAS-Ar43139), Mohan Township, Shanggang Village, Xiaolongha, seasonal rainforest (21°24.19'N, 101°37.03'E, ca 660 m), 29.VI.2012, Q.Y. Zhao & Z.G. Chen leg.

Etymology. The specific name comes from the Latin word “tetracanthus”, meaning “four spines”, referring to the four protuberances on the median apophysis.

Diagnosis. The new species resembles *A. arcuatus* sp. nov., but it can be distinguished by the following: 1) epigyne with a scape vs scape lacking (Fig. 1A, B); 2) copulatory openings on the posterior surface vs on the ventral surface (Fig. 1A, B); 3) median apophysis with 4 tapered tips vs 2 tapered tips (Fig. 2A, C, D); 4) tegular extension present vs lacking (Fig. 2); and 5) embolus longer than half the bulb diameter vs shorter than half the bulb diameter (Fig. 2D).

Description. Male (holotype, Figs 16E, F, 17, 19K–N). Total length 2.40. Carapace 1.50 long, 1.25 wide. Abdomen 1.70 long, 1.30 wide. Clypeus 0.15 high. Eye sizes and interdistances: AME 0.10, ALE 0.08, PME 0.10, PLE 0.08, AME–AME 0.10, AME–ALE 0.13, PME–PME 0.10, PME–PLE 0.18, MOA length 0.30, anterior width 0.30, posterior width 0.28. Leg measurements: I 5.40 (1.70, 2.00, 1.25, 0.45), II 4.90 (1.50, 1.75, 1.20, 0.45), III 2.60 (0.85, 0.90, 0.50, 0.35), IV 3.85 (1.20, 1.30, 0.95, 0.40). Carapace pear-shaped, yellow, with sparse setae, cervical groove slightly distinct, inner base of PMEs brown. Chelicerae yellow, with 3 teeth on both margins. Endites yellow, tooth on anterior lateral edge, labium yellow. Sternum yellow, with sparse, dark setae. Legs yellow without annulus, tibia I with 9 macrosetae, tibia II with 10 macrosetae, tibia III with 6 macrosetae, tibia IV with 8 macrosetae. Abdomen slightly pointed anteriorly, blunt posteriorly, about 1.3 times longer than wide, dorsum whitish yellow with irregular grayish-yellow patch; venter grayish yellow, with sparse, dark setae. Spinnerets yellow.

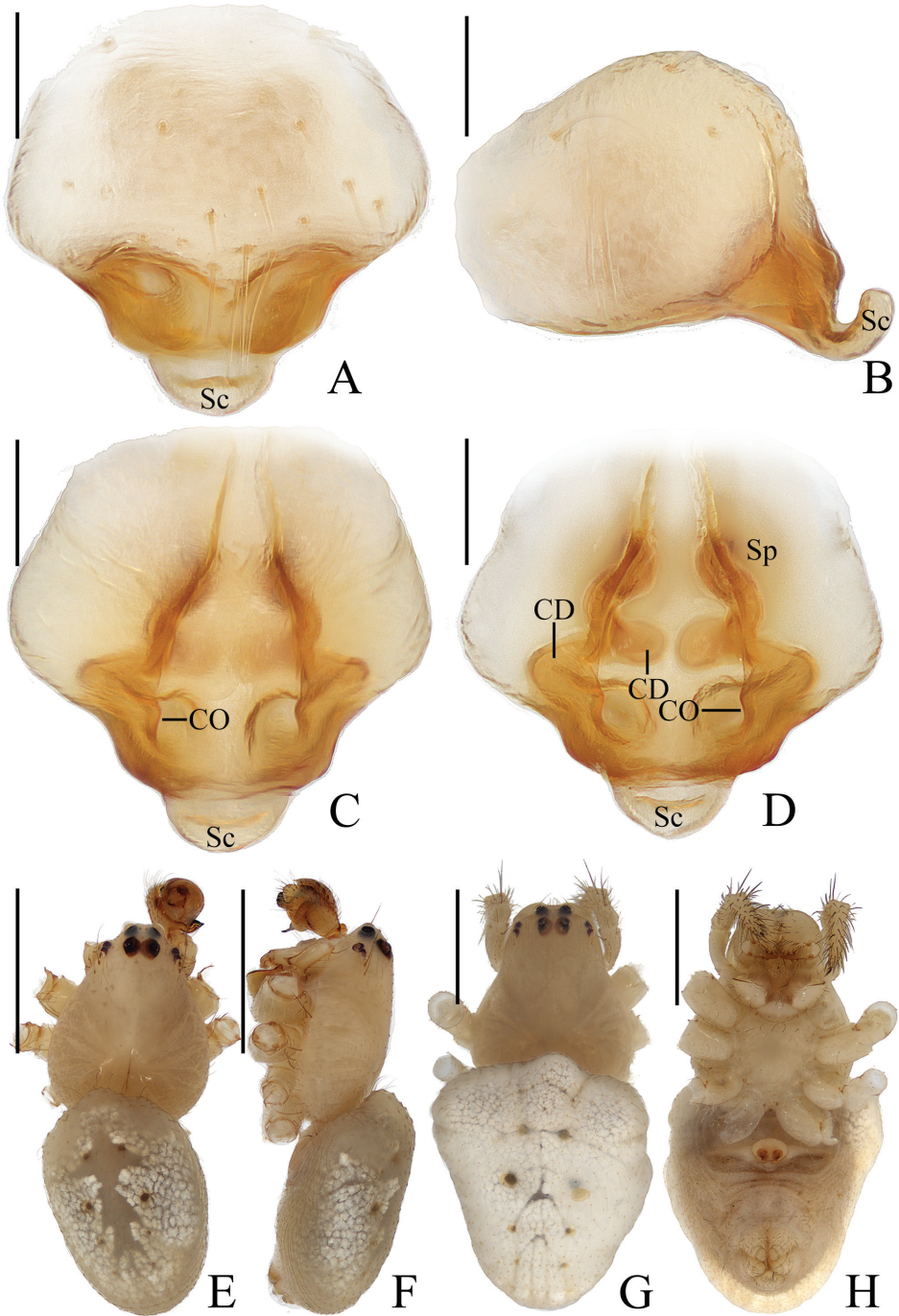


Figure 16. *Araneus tetraacanthus* sp. nov. **A-D, G, H** female paratype IZCAS-Ar43135 **E, F** male holotype **A** epigyne, ventral view **B** *ibid.*, lateral view **C** *ibid.*, posterior view **D** vulva, posterior view **E** habitus, dorsal view **F** *ibid.*, lateral view **G** *ibid.*, dorsal view **H** *ibid.*, ventral view. Scale bars: 0.1 mm (**A-D**); 1 mm (**E-H**).

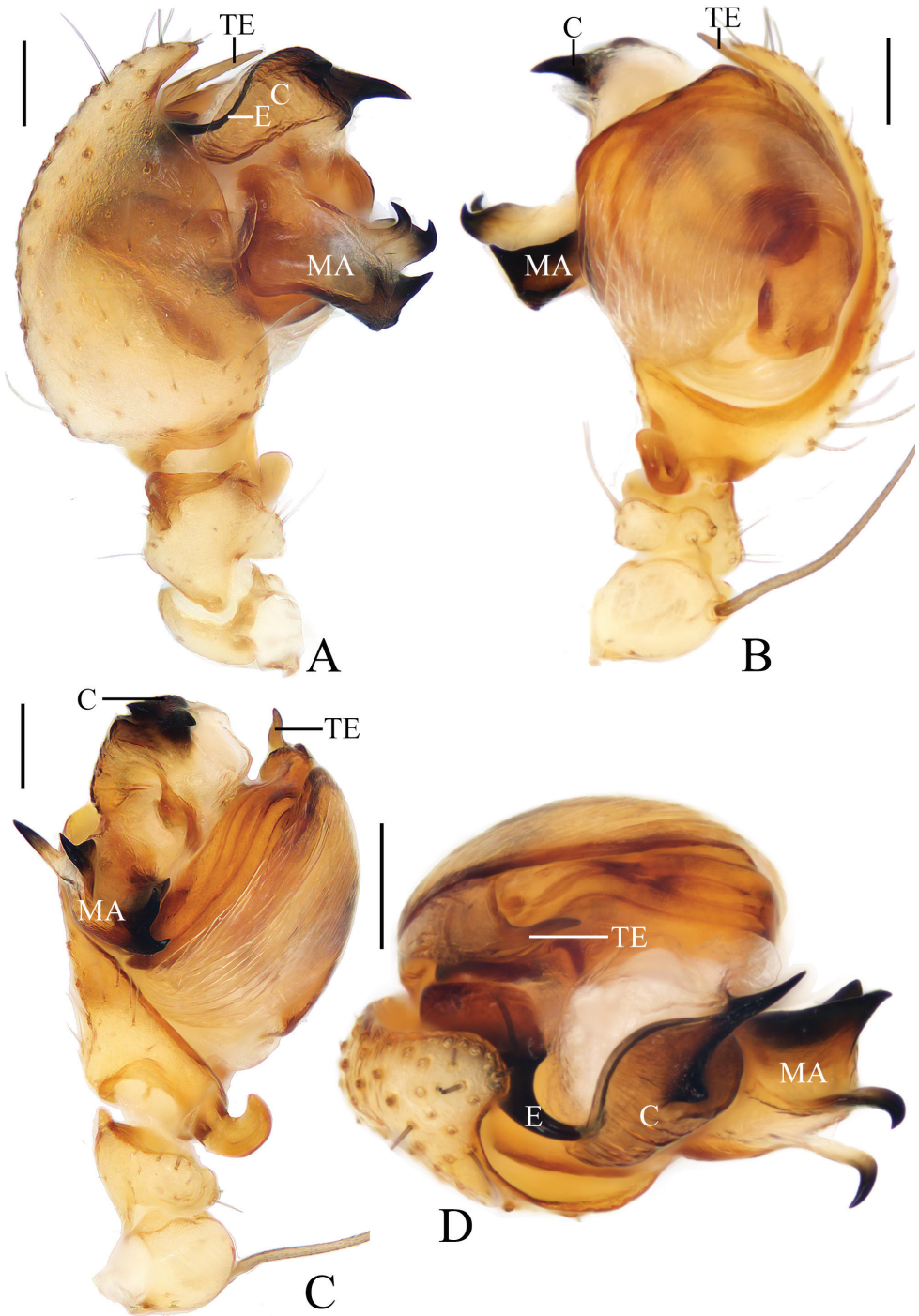


Figure 17. *Araneus tetracanthus* sp. nov. male holotype **A** male palp, prolateral view **B** ibid., retrolateral view **C** ibid., ventral view **D** ibid., apical view. Scale bars: 0.1 mm.



Figure 18. Legs of *Araneus* spp. **A–D** *A. arcuatus* sp. nov., male holotype **A** leg I **B** leg II **C** leg III **D** leg IV **E–H** *A. bidentatus* sp. nov., male holotype **E** leg I **F** leg II **G** leg III **H** leg IV **I, J** *A. complanatus* sp. nov., female paratype Ar43106 **I** leg I **J** leg II **K, L** *A. cucullatus* sp. nov., female paratype Ar43110 **K** leg I **L** leg II. Scale bars: 1 mm.



Figure 19. Legs of *Araneus* spp. **A, B** *A. minisculus* sp. nov., male holotype **A** leg I **B** leg II **C, D** *A. ovoideus* sp. nov., female holotype **C** leg I **D** leg II **E–H** *A. pseudodigitatus* sp. nov., male holotype **E** leg I **F** leg II **G** leg III **H** leg IV **I, J** *Araneus semiorbiculatus* sp. nov., female holotype **I** leg I **J** leg II **K–N** *A. tetracanthus* sp. nov., male holotype **K** leg I **L** leg II **M** leg III **N** leg IV. Scale bars: 1 mm.

Palp (Fig. 17): with 1 patellar bristle; tegulum with tapered, apically pointed extension anterior to embolus; median apophysis prominent, with 4 protuberances; embolus thick at base, distal half slender and covered by edge of conductor; conductor longer than half of the bulb diameter, distally tapered into pointed tip.

Female (paratype IZCAS-Ar43135, Fig. 16A–D, G–H). Total length 3.50. Carapace 1.95 long, 1.35 wide. Abdomen 2.45 long, 1.95 wide. Clypeus 0.08 high. Eye sizes and interdistances: AME 0.10, ALE 0.08, PME 0.10, PLE 0.08, AME–AME 0.18, AME–ALE 0.18, PME–PME 0.13, PME–PLE 0.25, MOA length 0.30, anterior width 0.33, posterior width 0.30. Leg measurements: I 6.50 (2.00, 2.40, 1.55, 0.55), II 5.00 (1.80, 1.90, 0.85, 0.45), III 3.25 (1.20, 1.10, 0.60, 0.35), IV 4.40 (1.40, 1.50, 1.05, 0.45). Habitus similar to that of male except anterior abdomen much wider.

Epigyne (Fig. 16A–D): slightly wider than long, with distally rimmed scape; copulatory openings depressed, posteriorly located; copulatory ducts slender, long, revolved about 360°; spermathecae spherical, touching each other.

Variation. Total length: ♂♂ 2.15–3.00; ♀♀ 3.15–4.00.

Distribution. Known only from type localities (Yunnan, China).

Acknowledgements

The manuscript benefitted greatly from comments by Yuri Marusik, Zhiyuan Yao, Mikhail Omelko, and two anonymous referees. Sarah Crews and Robert Forsyth checked the English. Theo Blick checked etymology. Guo Tang, Guo Zheng, Yanfeng Tong, Zhiyuan Yao, Qingyuan Zhao, Hao Yu, Cheng Wang, Jiahui Gan, Zhigang Chen, Zilong Bai, Yejie Lin, Yuanfa Yang, and Hong Liu helped with fieldwork. This research was supported by the Science and Technology Project Foundation of Guizhou Province ([2020]1Z014), the National Natural Science Foundation of China (NSFC-31660609), and the Key Laboratory Project of Guizhou Province ([2020]2003).

References

- Clerck C (1757) Aranei Svecici. Svenska spindlar, uti sina hufvud-slägter indelte samt under några och sextio särskildte arter beskrefne och med illuminerade figurer uplyste. Laurentius Salvius, Stockholmiae, 154 pp. <https://doi.org/10.5962/bhl.title.119890>
- Li S (2020) Spider taxonomy for an advanced China. *Zoological Systematics* 45(2): 73–77. <https://doi.org/10.11865/zs.202011>
- Li J, Yan X, Lin Y, Li S, Chen H (2021) Challenging Wallacean and Linnean shortfalls: *Ectatosticta* spiders (Araneae, Hypochilidae) from China. *Zoological Research* 42(6): 791–794. <https://doi.org/10.24272/j.issn.2095-8137.2021.212>
- Liu P, Irfan M, Yang S, Peng X (2019) Two new species of *Araneus* Clerck, 1757 (Araneae, Araneidae) and first description of *A. wulongensis* male from China. *ZooKeys* 886: 61–77. <https://doi.org/10.3897/zookeys.886.31163>
- Liu K, Li S, Zhang X, Ying Y, Meng Z, Fei M, Li W, Xiao Y, Xu X (2022) Unknown species from China: The case of phrurolithid spiders (Araneae, Phrurolithidae). *Zoological Research* 43(3): 352–355. <https://doi.org/10.24272/j.issn.2095-8137.2022.055>

- Lu Y, Chu C, Zhang X, Li S, Yao Z (2022) Europe vs China: *Pholcus* (Araneae, Pholcidae) from Yanshan-Taihang Mountains confirms uneven distribution of spiders in Eurasia. *Zoological Research* 43(4): 532–534. <https://doi.org/10.24272/j.issn.2095-8137.2022.103>
- Mi X, Li S (2021a) On nine species of the spider genus *Eriovixia* (Araneae, Araneidae) from Xishuangbanna, China. *ZooKeys* 1034: 199–236. <https://doi.org/10.3897/zookeys.1034.60411>
- Mi X, Li S (2021b) Nine new species of the spider family Araneidae (Arachnida, Araneae) from Xishuangbanna, Yunnan, China. *ZooKeys* 1072: 49–81. <https://doi.org/10.3897/zookeys.1072.73345>
- Scharff N, Coddington J, Blackledge T, Agnarsson I, Framenau V, Szűts T, Hayashi C, Dimitrov D (2020) Phylogeny of the orb-weaving spider family Araneidae (Araneae: Araneoidea). *Cladistics* 36(1): 1–21. <https://doi.org/10.1111/cl.12382>
- Wang C, Li S, Zhu W (2020) Taxonomic notes on Leptonetidae (Arachnida, Araneae) from China, with descriptions of one new genus and eight new species. *Zoological Research* 41(6): 684–704. <https://doi.org/10.24272/j.issn.2095-8137.2020.214>
- WSC (2022) World Spider Catalog, version 23.0. Natural History Museum Bern. <https://doi.org/10.24436/2>
- Yao Z, Wang X, Li S (2021) Tip of the iceberg: Species diversity of *Pholcus* spiders (Araneae, Pholcidae) in Changbai Mountains, Northeast China. *Zoological Research* 42(3): 267–271. <https://doi.org/10.24272/j.issn.2095-8137.2021.037>
- Yin C, Wang J, Xie L, Peng X (1990) New and newly recorded species of the spiders of family Araneidae from China (Arachnida, Araneae). In: *Spiders in China: One Hundred New and Newly Recorded Species of the Families Araneidae and Agelenidae*. Hunan Normal University Press, Changsha, 171 pp.
- Zhao Z, Hou Z, Li S (2022) Cenozoic Tethyan changes dominated Eurasian animal evolution and diversity patterns. *Zoological Research* 43(1): 3–13. <https://doi.org/10.24272/j.issn.2095-8137.2021.322>

Ilyocypris leptolinea Wang & Zhai, sp. nov., an ostracod (Ostracoda, Crustacea) from the late Quaternary of Inner Mongolia, northern China

Qianwei Wang^{1,2}, David J. Horne³, Jiawei Fan⁴, Ruilin Wen^{5,6},
Robin J. Smith⁷, Min Wang⁸, Dayou Zhai^{1,2}

1 Yunnan Key Laboratory for Palaeobiology, Institute of Palaeontology, Yunnan University, Kunming 650500, China **2** MEC International Joint Laboratory for Palaeobiology and Palaeoenvironment, Yunnan University, Kunming 650500, China **3** School of Geography, Queen Mary University of London, Mile End Road, London E1 4NS, UK **4** Institute of Geology, China Earthquake Administration, Beijing 100029, China **5** Key Laboratory of Cenozoic Geology and Environment, Institute of Geology and Geophysics, Chinese Academy of Sciences, 19 Beitucheng West Road, Chaoyang District, Beijing 100029, China **6** CAS Center for Excellence in Life and Paleoenvironment, Beijing, 100044, China **7** Lake Biwa Museum, 1091 Oroshimo, Kusatsu, Shiga 525-0001, Japan **8** Yunnan Key Laboratory of Plateau Geographical Processes and Environmental Changes, Faculty of Geography, Yunnan Normal University, Kunming 650500, China

Corresponding author: Dayou Zhai (dyzhai@ynu.edu.cn)

Academic editor: Ivana Karanovic | Received 30 August 2022 | Accepted 26 November 2022 | Published 22 December 2022

<https://zoobank.org/0FB502BD-2CD1-442A-BAFE-8C5A93D3CB4B>

Citation: Wang Q, Horne DJ, Fan J, Wen R, Smith RJ, Wang M, Zhai D (2022) *Ilyocypris leptolinea* Wang & Zhai, sp. nov., an ostracod (Ostracoda, Crustacea) from the late Quaternary of Inner Mongolia, northern China. ZooKeys 1137: 109–132. <https://doi.org/10.3897/zookeys.1137.94224>

Abstract

Ilyocypris leptolinea Wang & Zhai, **sp. nov.** is described from late Quaternary sediments in central-eastern Inner Mongolia, northern China. The new species, which has a carapace shape and pitted surface typical of the genus, is characterised by double rows of fine, densely arranged marginal ripples, separated by an inner list, along both anterior and posterior calcified inner lamellae in the left valve. Outline analysis and Principal Component Analysis indicate that its morpho-space overlaps with *I. bradyi* Sars, 1890, *I. japonica* Okubo, 1990, and *I. mongolica* Martens, 1991, which have living or fossil representatives in Inner Mongolia, but it is clearly discriminated from *I. innermongolica* Zhai & Xiao, 2013. Judging from the relatively coarse lithology dominated by silt and sand, and the lack of accompanying brackish-water ostracods, *I. leptolinea* Wang & Zhai, **sp. nov.** may have lived in a relatively shallow freshwater lake. It perhaps can be added to the list of species that went extinct during the Quaternary, but the timing and process of extinction await further investigation.

Keywords

Fossil, lacustrine sediment, marginal ripple, new species, outline analysis, Xiaojingou Basin

Introduction

The Ostracoda genus *Ilyocypris* Brady & Norman, 1889, dating back to the Late Cretaceous (Yang 1981; Hou et al. 2002), has a rich, worldwide fossil record. There are at least 40 known extant species: 38 species included in the checklist of Meisch et al. (2019), plus two more erected since by Smith et al. (2019) and Peng et al. (2021). *Ilyocypris* species thrive in various non-marine aquatic habitats, including lakes (e.g., *Ilyocypris salebroso* Stepanaitys, 1960, cf. Smith et al. 2011), ponds (e.g., *Ilyocypris tibeta* Peng et al., 2021), swamps (e.g., *Ilyocypris bradyi* Sars, 1890, cf. Meisch 2000), and running waters (e.g., *Ilyocypris dentifera* Sars, 1903, cf. Smith et al. 2019). Some members of this genus are adapted to artificial environments, such as lotus fields (e.g., *Ilyocypris japonica* Okubo, 1990, cf. Smith et al. 2019) and rice fields (several species, see Smith et al. 2018), and the eggs and/or living individuals of some species are desiccation-resistant (e.g., *Ilyocypris angulata* Sars, 1903 and *I. dentifera*).

Despite the above-mentioned ecological disparity and taxonomic diversity within *Ilyocypris*, the morphological differences between many of its species are so subtle that reliable species identification can be difficult without information of the male reproductive organs (Smith et al. 2019). For palaeontologists who work on valve material, the general similarity of valve morphology within the genus on one hand, and the intra-species variability of the nodes on the other hand, have further complicated the taxonomy (Meisch 2000; Smith et al. 2019).

With the help of Scanning Electron Microscopy (SEM), van Harten (1979) observed the ‘marginal ripples’ on the postero-ventral region of the calcified inner lamella of the left valve of *Ilyocypris*, and Janz (1994) proposed that this character could be useful for species identification. Some later works (Mischke et al. 2003, 2013; Yang et al. 2004; Fuhrmann 2012; Li et al. 2021a) successfully used marginal ripples of *Ilyocypris* as an important taxonomic feature. Meanwhile, Mazzini et al. (2014) demonstrated that outline analysis is also useful for discriminating different species of this genus. We concur with Mazzini et al. (2014), in that outline analyses can quantify shape variation that would be difficult to characterise by observation alone.

In this study we describe a new fossil species of the genus *Ilyocypris*, based on well-preserved material from late Quaternary sediments in Inner Mongolia of China. A variety of morphological features, such as the marginal ripples on the anterior and posterior valve margins, inner lists, valve shape, and ornamentation on the valve surface, are described and compared with those of congeners. A discussion is given about the overlap of morpho-space of the new species with some of its congeners as visualised by outline analysis, Principal Component Analysis (PCA), and cluster analysis.

Materials and methods

Study area and field work

The XJG2 section (43°51'41.9"N, 116°24'57.1"E, Fig. 1) is located c. 30 km southeast of Xilinhot City in central-eastern Inner Mongolia, China (Fig. 1). In this area, summer rainfall generates several intermittent rivers that cut into the underlying lacustrine strata. One of these rivers is named "Xiaojingou" by local people. In May 2015, two sections were sampled on the bank of this river, XJG1 and XJG2. The section XJG2 is presented in this study.

In the field, the XJG2 section was excavated (Fig. 1C) by removing the sediment on the surface of the profile (0–120 cm) and by digging a hole in the river bed (120–240 cm), and in total, 240 samples were taken at 1-cm resolution. The emergence of interstitial water at a depth of 240 cm obstructed digging and sampling beneath this depth. The overlying soil, which is c. 50 cm thick and extensively interrupted with grass roots, was not sampled (Fig. 1C).

Ostracod extraction

In the laboratory, the extraction of ostracod valves generally followed the method described by Zhai et al. (2010). Air-dried sediments were soaked overnight in 0.1% Na₂CO₃-buffered 10% H₂O₂ solution, washed through a 63- μ m mesh, spread onto glass plates with a pipette and dried at room temperature. Subsequently, the ostracods were picked with a fine brush under a SZ6000 stereomicroscope. For illustration, cleaned valves were coated with gold and were imaged with a FEI Quanta 200 (Advanced Analysis and Measurement Center of Yunnan University) or a FEI Quanta 650 (Yunnan Key Laboratory for Palaeobiology, Institute of Palaeontology, Yunnan University) Scanning Electron Microscopes (SEM). All specimens from the section (Table 1) are deposited at the Yunnan Key Laboratory for Palaeobiology, Institute of Palaeontology, Yunnan University (Kunming, China).

Sample dating

In the sample XJG2-140 (depth 139–140 cm), a small number of well-preserved gastropods were found, which were used for ¹⁴C dating.

Pre-treatment of the dating material was done in the Laboratory Test Center, Institute of Geology, China Earthquake Administration (Beijing, China). Brush-cleaned gastropod shells were soaked in 0.1N HCl in an ultra-sonic bath until the surface layer (c. 1/3 in thickness) was eroded away. The residual was rinsed with deionised water and was then oven-dried. Approximately 20 mg of such cleaned, dried shell was dissolved with 1 ml of H₃PO₄ at 70 °C in an airtight reacting system with a pressure of $\sim 10^{-2}$ Pa. The released CO₂ was purified and was deoxidised by H₂, with Fe powder as the catalyst, yielding ~ 1 mg of graphite, which was dated in a NEC 1.5SDH-1 Compact PKUAMS facility at the Institute of Heavy Ion Physics, Peking University (Beijing, China). The ¹⁴C age of the sample was calibrated using the OxCal v. 4.2 program (Bronk Ramsey 2009).

Table 1. Examined valves of *Ilyocypris* from XJG2 section. All the adult left valves are identified as *Ilyocypris leptolinea* Wang & Zhai, sp. nov. based on marginal ripples. Others are tentatively assigned to this species. Note that all the valves of this species used for outline analysis in this study are adult left valves imaged for exterior view. Abbreviations: A, adult; A-1, last juvenile stage before adult; H, height; L, length; LV, left valve; MR, marginal ripples; OL, outline; RV, right valve.

Specimen	Stage	RV/LV	L×H (mm)	Type designation	MR preservation	OL analysis
XJG2-021-1	A	LV	0.94×0.48	paratype	yes	yes
XJG2-136-2	A	LV	0.83×0.45	/	yes	yes
XJG2-138-2	A	LV	0.96×0.52	/	yes	/
XJG2-139-1	A	LV	0.82×0.42	/	yes	/
XJG2-153-1	A	LV	0.90×0.47	/	yes	yes
XJG2-153-2	A	LV	0.87×0.47	/	yes	yes
XJG2-153-3	A	LV	0.92×0.50	/	yes	yes
XJG2-160-1	A	LV	0.91×0.49	/	yes	/
XJG2-174-1	A	LV	0.98×0.53	/	yes	yes
XJG2-177-1	A	LV	0.90×0.47	paratype	yes	yes
XJG2-188-1	A	LV	1.01×0.53	/	yes	/
XJG2-189-1	A	LV	0.81×0.43	/	yes	yes
XJG2-190-1	A	LV	1.05×0.56	paratype	yes	yes
XJG2-192-1	A	LV	0.94×0.51	/	yes	yes
XJG2-192-2	A	LV	0.91×0.50	/	yes	yes
XJG2-192-3	A	LV	0.87×0.48	/	yes	/
XJG2-192-5	A	LV	0.78×0.43	/	yes	/
XJG2-193-1	A	LV	0.91×0.48	paratype	yes	yes
XJG2-196-4	A	LV	0.84×0.46	/	yes	/
XJG2-197-2	A	LV	0.90×0.48	paratype	yes	/
XJG2-199-2	A	LV	0.86×0.46	paratype	yes	/
XJG2-210-1	A	LV	0.94×0.48	holotype	yes	yes
XJG2-212-2	A	LV	0.94×0.52	/	yes	yes
XJG2-218-1	A	LV	0.78×0.42	/	yes	/
XJG2-228-2	A	LV	0.88×0.46	paratype	yes	yes
XJG2-192-4	A-1	LV	0.70×0.39	/	not observed due to aggregation	/
XJG2-196-1	A-1	LV	0.74×0.42	/	yes	/
XJG2-197-1	A-1	LV	0.70×0.39	/	yes	/
XJG2-199-1	A-1	LV	0.74×0.41	/	yes	/
XJG2-202-3	A-1	LV	0.80×0.44	/	yes	/
XJG2-222-1	A-1	LV	0.72×0.39	/	yes	/
XJG2-129-1	A	RV	0.91×0.47	/	/	/
XJG2-136-1	A	RV	0.93×0.50	/	/	/
XJG2-169-1	A	RV	0.87×0.48	/	/	/
XJG2-190-2	A	RV	0.90×0.49	/	/	/
XJG2-191-1	A	RV	0.83×0.45	/	/	/
XJG2-193-2	A	RV	0.90×0.47	/	/	/
XJG2-196-2	A	RV	0.88×0.47	/	/	/
XJG2-196-3	A	RV	0.95×0.50	/	/	/
XJG2-197-5	A	RV	0.83×0.46	/	/	/
XJG2-197-6	A	RV	0.90×0.49	/	/	/
XJG2-202-1	A	RV	0.86×0.46	/	/	/
XJG2-202-4	A	RV	0.85×0.45	/	/	/
XJG2-203-1	A	RV	0.85×0.45	/	/	/
XJG2-203-2	A	RV	0.86×0.45	/	/	/
XJG2-205-2	A	RV	0.85×0.45	/	/	/
XJG2-212-3	A	RV	0.82×0.44	/	/	/
XJG2-216-1	A	RV	0.99×0.53	/	/	/

Specimen	Stage	RV/LV	L×H (mm)	Type designation	MR preservation	OL analysis
XJG2-217-1	A	RV	0.86×0.47	/	/	/
XJG2-218-2	A	RV	0.87×0.47	/	/	/
XJG2-221-1	A	RV	0.81×0.45	/	/	/
XJG2-226-1	A	RV	0.88×0.47	/	/	/
XJG2-228-3	A	RV	0.79×0.43	/	/	/
XJG2-192-6	A-1	RV	0.77×0.42	/	/	/

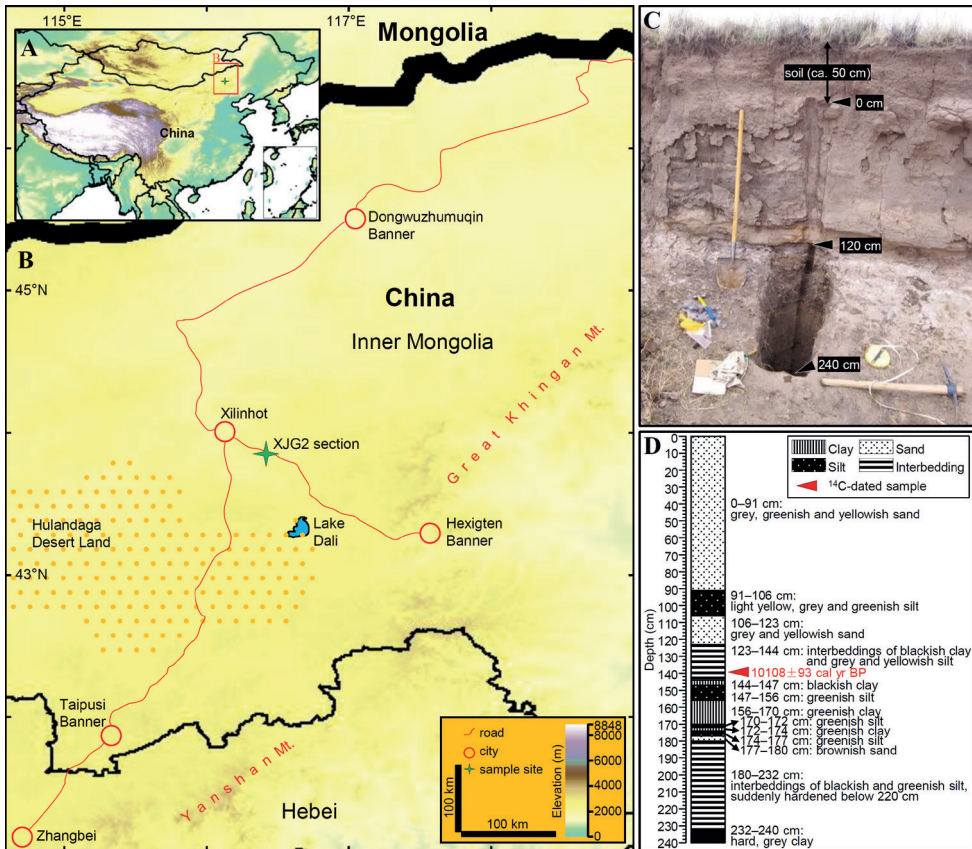


Figure 1. **A** digital Elevation Model showing the position of the study area (red rectangle) in central-eastern Inner Mongolia, China **B** digital Elevation Model showing the location of the XJG2 section **C** field photo of the section **D** lithology of the section. Red triangle indicates the result of ^{14}C dating of gastropods from depth 139–140 cm. See text for details.

Numerical analyses

In order to characterise and then to compare the shapes of different valves, outline analysis was performed, with general principles following those provided by Baltanás and Danielopol (2011). First, each SEM image of the valve was digitised with the

software tpsDig2 (v. 2.31) (Rohlf 2017) to obtain coordinates of the outline. Subsequently, the outline was located (with the geometric centre set at (0, 0)), rotated and flipped if necessary (to obtain the same orientations for exterior and interior views and for left and right valves), and scaled (standardised for the equal surface area of 5000). Afterwards, two different approaches were used to calculate the dissimilarity between the outlines to produce dissimilarity matrices. In the first approach, all the outlines were fixed, i.e., with the antero-ventral and the postero-ventral parts rested on a horizontal axis (cf. Meisch 2000: fig. 3D), and the dissimilarity (Fixed Outline Canberra Dissimilarity, FOCD) was calculated. The second approach allows rotation of one of the two outlines under comparison by ± 20 degrees, and the smallest dissimilarity value, which is called the Minimal Running Canberra Dissimilarity (MRCD) index herein, was used. This approach was to avoid unreasonable superimposing of the length axis that may have been altered by subtle variations of the shapes of the anterior and the posterior ends of the valve. The dissimilarity matrices, resulted from the two different approaches, were used respectively for cluster analysis, which employed a group-average strategy (Sokal and Michener 1958). All the computation and illustration of the outline coordinates were made with the software Microsoft Office Excel 2019 and Microsoft Office PowerPoint 2019.

Principal Component Analysis (PCA) was performed on the polar-coordinate data of the fixed outlines (see above) using the software CANOCO v. 4.5 (Ter Braak and Šmilauer 2002), and biplots of the first two axes of PCA were used to compare the morpho-spaces of different species.

A total of 42 outlines of the valves of *Ilyocypris* were analysed (Tables 1, 2). Apart from the *Ilyocypris* material from the XJG2 section, four other congeneric species with Holocene representatives in eastern Inner Mongolia were included: *I. bradyi*, *Ilyocypris innermongolica* Zhai & Xiao, 2013, *Ilyocypris mongolica* Martens, 1991, and *I. japonica*. The first three species have been found living in eastern Inner Mongolia (Zhai and Xiao 2013; Zhai and Zhao 2014; Zhai et al. 2022). A marginal-ripplelet pattern coinciding with that of *I. japonica* was found by DZ in the *Ilyocypris* material from Holocene sediments of Lake Hulun in northeastern Inner Mongolia, which had been left in open nomenclature in Zhai et al. (2011). In view of the paucity of intact valves from Inner Mongolia, however, images of Quaternary material of *I. bradyi* from UK (including six specimens from DJH's collection and two from the Natural History Museum (London, UK) collection, the latter published in Whittaker and Parfitt 2017) and images of extant material of *I. japonica* from Japan were utilised (Table 2). The exterior views of left valves provided by the Scanning Electron Microscope (SEM) were used, with the following exceptions. First, for *I. innermongolica*, only exterior views of left valves and exterior and interior views of right valves of the type specimens were available due to past experimental design. The single specimen of *I. bradyi* from the study area was used with only the exterior view of the right valve because the left valve had been damaged during dissection.

Table 2. Examined valves of other species of *Ilyocypris*. All the specimens are adults, which can be judged from their larger sizes, wider calcified inner lamellae, and patterns of inner marginal ripplelets (only applied to left valves). Additional abbreviations to those in Table 1: ext, exterior view; int, interior view; MIS, marine isotopic stage.

Species	Specimen number	RV/LV, int/ext	L×H (mm)	Locality	Horizon	OL analysis
<i>I. bradyi</i>	CC22	LV, ext	0.85×0.44	Greenlands Pit, Purfleet, UK	MIS 9 (Pleistocene)	yes
<i>I. bradyi</i>	CC23	LV, ext	0.86×0.44	Greenlands Pit, Purfleet, UK	MIS 9 (Pleistocene)	yes
<i>I. bradyi</i>	CC26	LV, ext	0.85×0.43	Greenlands Pit, Purfleet, UK.	MIS 9 (Pleistocene)	yes
<i>I. bradyi</i>	MTDB-3	LV, ext	1.06×0.55	Marks Tey, UK	MIS 11 (Pleistocene)	yes
<i>I. bradyi</i>	MTDB-5	LV, ext	0.98×0.51	Marks Tey, UK	MIS 11 (Pleistocene)	yes
<i>I. bradyi</i>	MTDB-13	LV, ext	1.04×0.55	Marks Tey, UK	MIS 11 (Pleistocene)	yes
<i>I. bradyi</i>	NHM UK PM OS 19853	LV, ext	no data	Boxgrove, UK (cf. Whittaker and Parfit 2017)	MIS 13 (Pleistocene)	yes
<i>I. bradyi</i>	NHM UK PM OS 19854	LV, ext	no data	Boxgrove, UK (cf. Whittaker and Parfit 2017)	MIS 13 (Pleistocene)	yes
<i>I. bradyi</i>	dyzoc810	RV, ext	0.83×0.43	Creek Y16, Inner Mongolia, China (cf. Zhai et al. 2022)	extant	yes
<i>I. mongolica</i>	dyzoc515	LV, ext	0.80×0.43	Lake X26, Inner Mongolia, China (cf. Zhai et al. 2022)	extant	yes
<i>I. mongolica</i>	dyzoc518	LV, ext	0.89×0.48	Lake X26, Inner Mongolia, China (cf. Zhai et al. 2022)	extant	yes
<i>I. mongolica</i>	LBM 1430009163	LV, ext	0.83×0.46	Pond X36, Inner Mongolia, China (cf. Zhai and Zhao 2014)	extant	yes
<i>I. innermongolica</i>	dyzoc5	LV, int	0.73×0.37	Lake Hulun, China (cf. Zhai and Xiao 2013)	extant	yes
<i>I. innermongolica</i>	dyzoc5	RV, ext	0.71×0.36	Lake Hulun, China (cf. Zhai and Xiao 2013)	extant	yes
<i>I. innermongolica</i>	dyzoc7	LV, int	0.76×0.42	Lake Hulun, China (cf. Zhai and Xiao 2013)	extant	yes
<i>I. innermongolica</i>	dyzoc7	RV, ext	0.74×0.39	Lake Hulun, China (cf. Zhai and Xiao 2013)	extant	yes
<i>I. innermongolica</i>	dyzoc8	LV, int	0.69×0.37	Lake Hulun, China (cf. Zhai and Xiao 2013)	extant	yes
<i>I. innermongolica</i>	dyzoc8	RV, ext	0.69×0.36	Lake Hulun, China (cf. Zhai and Xiao 2013)	extant	yes
<i>I. innermongolica</i>	dyzoc93	LV, int	0.70×0.36	Lake Hulun, China (cf. Zhai and Xiao 2013)	extant	yes
<i>I. innermongolica</i>	dyzoc93	RV, int	0.67×0.35	Lake Hulun, China (cf. Zhai and Xiao 2013)	extant	yes
<i>I. innermongolica</i>	dyzoc100	LV, int	0.74×0.37	Lake Hulun, China (cf. Zhai and Xiao 2013)	extant	yes
<i>I. innermongolica</i>	dyzoc100	RV, ext	0.73×0.36	Lake Hulun, China (cf. Zhai and Xiao 2013)	extant	yes
<i>I. innermongolica</i>	dyzoc114	LV, int	0.73×0.37	Lake Hulun, China (cf. Zhai and Xiao 2013)	extant	yes
<i>I. innermongolica</i>	dyzoc114	RV, ext	0.71×0.36	Lake Hulun, China (cf. Zhai and Xiao 2013)	extant	yes
<i>I. japonica</i>	LBM 1430009143	LV, ext	0.91×0.50	Shiga Prefecture, Japan (cf. Smith et al. 2019)	extant	yes
<i>I. japonica</i>	LBM 1430009146	LV, ext	0.76×0.40	Gyeongsangnam-do, South Korea (cf. Smith et al. 2019)	extant	yes
<i>I. japonica</i>	LBM 1430009147	LV, ext	0.86×0.46	Gyeongsangnam-do, South Korea (cf. Smith et al. 2019)	extant	yes

Results

Lithology and chronology

The 240-cm thick lacustrine XJG2 section consists of clay, silt, and fine-sand fractions and contains no gravels (Fig. 1D). No obvious sedimentary hiatus is detected within the section. Its upper 123 cm is dominated by fine to medium sand but is interrupted by silt at 91–106 cm. The interval of 123–144 cm contains interbeds of clay and silt. The depths from 144 to 180 cm are represented by frequent alternations of clay, silt, and sand layers. Interbeds of silt bands with different colours occur in 180–232 cm. The bottom part of the section, 232–240 cm, consists of hard grey clay.

The gastropod shells (laboratory dating code: CG-2021-1566) from the sample XJG2-140 in the middle part of the XJG2 section (Fig. 1D) yielded a ^{14}C age of 8960 ± 30 yr that is calibrated to 10108 ± 93 cal yr BP (calendar years before the present; present = 1950 AD). This is close to the beginning of the Holocene Epoch, 11700 cal yr BP, based on the International Chronostratigraphic Chart v. 2022/10 (Cohen et al. 2013, updated). Considering the reported sedimentation rates of lakes in eastern Inner Mongolia, which varied from 0.15 m/kyr (Lake Hulun, Zhai et al. 2011) to 1.1 m/kyr (Lake Daihai, Xiao et al. 2004), the age of the bottom part of the XJG2 section probably extends into the late Pleistocene. Therefore, the age of this section should belong to the late Quaternary.

Systematics

In addition to *Ilyocypris*, the fossil ostracods recovered from the XJG2 section include members of the genera *Candona* Baird, 1845, *Cypridopsis* Brady, 1867, *Fabaeformiscandona* Krstić, 1972 and *Pseudocandona* Kaufmann, 1900 (work in progress, to be published elsewhere). Valves of *Ilyocypris* were found between the depths of 240 cm and 20 cm. Examination of the morphologies of the left valves, including shape, ornamentation, and marginal ripplelets, suggests that they belong to a new species, which is described below.

Class Ostracoda Latreille, 1802

Order Podocopida Sars, 1866

Superfamily Cypridoidea Baird, 1845

Family Ilyocyprididae Kaufmann, 1900

Subfamily Ilyocypridinae Kaufmann, 1900

Genus *Ilyocypris* Brady & Norman, 1889

***Ilyocypris leptolinea* Wang & Zhai, sp. nov.**

<https://zoobank.org/A551E7F9-DD93-4A16-9557-2ED465EA4221>

Figs 2–4

Type locality. XJG2 section ($43^{\circ}51'41.9''\text{N}$, $116^{\circ}24'57.1''\text{E}$, Fig. 1), lacustrine outcrop cut by intermittent river in central-eastern Inner Mongolia, China.

Type horizon. Late Pleistocene to Holocene; holotype from 209–210 cm depth in section, c. 70 cm below level of gastropod shells that yielded a calibrated radiocarbon date of $10,108 \pm 93$ calendar years before present (cal yr BP).

Type material. *Holotype*: adult left valve, XJG2-210-1 (XJG2, section code; 210, sample code, corresponding to 209–210 cm depth in section; 1, registration number), length 0.94 mm, height 0.48 mm. *Paratypes*: seven adult left valves, XJG2-021-1, XJG2-177-1, XJG2-190-1, XJG2-193-1, XJG2-197-2, XJG2-199-2, XJG2-228-2. All type specimens with marginal ripples on anterior and posterior calcified inner lamellae well-preserved (Figs 2, 3).

Other material examined. 17 adult left valves, 22 adult right valves, six A-1 juvenile left valves, and one A-1 juvenile right valve (Table 1; Figs 2–5). Adult right valves and juvenile valves provisionally identified as this species in view of monospecific adult left valves in section.

Etymology. From the Greek *leptos* for fine, small, or subtle, and Latin *linea* for line or thread, referring to fine marginal ripples on calcified inner lamellae of LV.

Dimensions. Adult left valves ($n = 25$, Fig. 5A) with length 0.78–1.05 mm, height 0.42–0.56 mm, H/L ratio 0.51–0.55. Adult right valves ($n = 22$, Fig. 5B) with length 0.79–0.99 mm, height 0.43–0.53 mm, H/L ratio 0.52–0.56. Juvenile valves slightly smaller but with size ranges overlapping with those of adult valves (Fig. 5).

Diagnosis. Intermediate-sized *Ilyocypris* (length ranging from 0.78 to 1.05 mm, Table 1) with shape, sulci, and pits typical of genus. Valve surface without nodes, occasionally with tiny spines along anterior and/or posterior margins. Calcified inner lamellae wide, bearing (in left valve only) two rows of densely arranged, fine marginal ripples along entire anterior and posterior valve margins; distal row near valve margin, usually well expressed; proximal row in intermediate area less pronounced, absent in poorly preserved specimens. One inner list present between two rows of marginal ripples in well-preserved specimens.

Description. *Left valves.* Intermediate-sized *Ilyocypris*. Valve sub-reniform in lateral view, with greatest height (antero-dorsal corner) at anterior third. Dorsal margin, i.e., section between antero-dorsal and postero-dorsal corners, nearly straight but with blunt turn immediately behind posterior sulcus due to inflation of postero-dorsal part. Anterior margin broadly rounded, with dorsal part nearly straight and more ventral parts evenly rounded. Posterior margin evenly rounded and less obtrusive. Ventral margin concave. Valve surface carrying two transverse sulci, with anterior sulcus originating from antero-dorsal corner, tapering ventrally, and terminating slightly above mid-height. Posterior sulcus wider and shorter. Adductor muscle scars situated in ovate depression immediately below posterior sulcus. Mandibular scars situated in two small depressions to antero-ventral position of adductor muscle scars. Shell surface densely covered with small pits, with those in front of anterior sulcus, between two sulci and behind posterior sulcus, smaller. Small number of tiny spines present along anterior and posterior margins in some specimens.

Interior view, anterior and posterior calcified inner lamellae comparatively wide but with anterior one slightly wider. Three inner lists present on anterior calcified inner lamella (Figs 2D, J, 3E). First one running in intermediate zone, usually weakly expressed,

sometimes not preserved. Second and third ones running close to inner margin. Inner lists also present on posterior calcified inner lamella but with first one usually very faint or absent (Figs 2C, I, 3B, G). Two rows of fine, densely arranged marginal ripples present on both anterior and posterior calcified inner lamellae (Figs 2, 3): distal row (Figs 2C, D, I, J, 3B, E, G) with each ripple extending from exterior margin of selvage near valve margin to almost first inner list, distributed throughout entire anterior and posterior calcified inner lamellae, usually well expressed; proximal zone (Figs 2C, D, J, 3B, E, G) present between first and second inner lists, better observed at antero-ventral and postero-ventral areas, sometimes not preserved (Fig. 2I). Adductor muscle scars (Fig. 3F), consisting of six scars of different sizes and shapes, arranged in two rows (four anterior scars and two posterior ones). Mandibular scars (Fig. 3F) consisting of two sub-oval elements.

Dorsal view (Fig. 2E) semi-elliptical, with part behind posterior sulcus wider than anterior part. Anterior end pointed. Posterior end bluntly pointed. Antero-dorsal corner with one small blunt expansion representing tooth-structure of hinge. Middle part of ventral calcified inner lamella (corresponding to highest part of ventral margin in lateral view; observed from oblique-dorsal view) with gentle, inward, i.e., adaxial, expansion. Two proximal inner lists, i.e., second and third ones, showing complex crossing patterns on this part (Fig. 2F, G).

Right valves. Shape similar to that of left valve, but dorsal margin straighter (Fig. 4A, B) with posterior section not inflated dorsally (Fig. 4A, B). Valve margin also with three inner lists but first one very faint on anterior calcified inner lamella (Fig. 4C) and almost absent on posterior calcified inner lamella (Fig. 4D).

Valves of A-1 juveniles. Shape similar to that of adults but with dorsal margin more inclined (Fig. 4E, F). Pits on valve surface smaller and shallower. Calcified inner lamellae of left valve narrow, with only one row of densely arranged marginal ripples distally: extending to median area in anterior calcified inner lamella (Fig. 4H), almost to proximal area in postero-ventral area (Fig. 4G). Only one inner list present, running close to inner margin (Fig. 4G, H).

Differential diagnosis. The new species can be easily distinguished from congeners by the fineness, number, and distribution of the two rows of marginal ripples as well as the presence of the outer-most (first) inner list in the intermediate zone that separates the two rows of marginal ripples. *Ilyocypris bradyi*, for example, has fewer, thicker, and more widely spaced ripples confined to the postero-ventral area, typically four or five in the outer row (see e.g., Mazzini et al. 2014: fig. 11). Considering potential taphonomic loss of finer morphologies in fossil material (e.g., the abrasion of the proximal row of marginal ripples and the inner lists), several species with morphologies that may be confused with the poorly preserved specimens of the new species are compared here. *Ilyocypris lacustris* Kaufmann, 1900 seems to have two rows of fine marginal ripples separated by one inner list on the anterior valve margin, which resembles the new species (Fuhrmann 2012: Tafel (= pl.) 76 1b), but the ripples on the posterior part are confined to the postero-ventral margin and consist of only one row (Fuhrmann 2012: Tafel (= pl.) 76 1f and 2d). The highest point of the carapace of *I. lacustris* is situated at approximately the anterior quarter, more anterior than that of the new species. The marginal ripples on the posterior part of *I. salebrosa* are also fine and consist of two

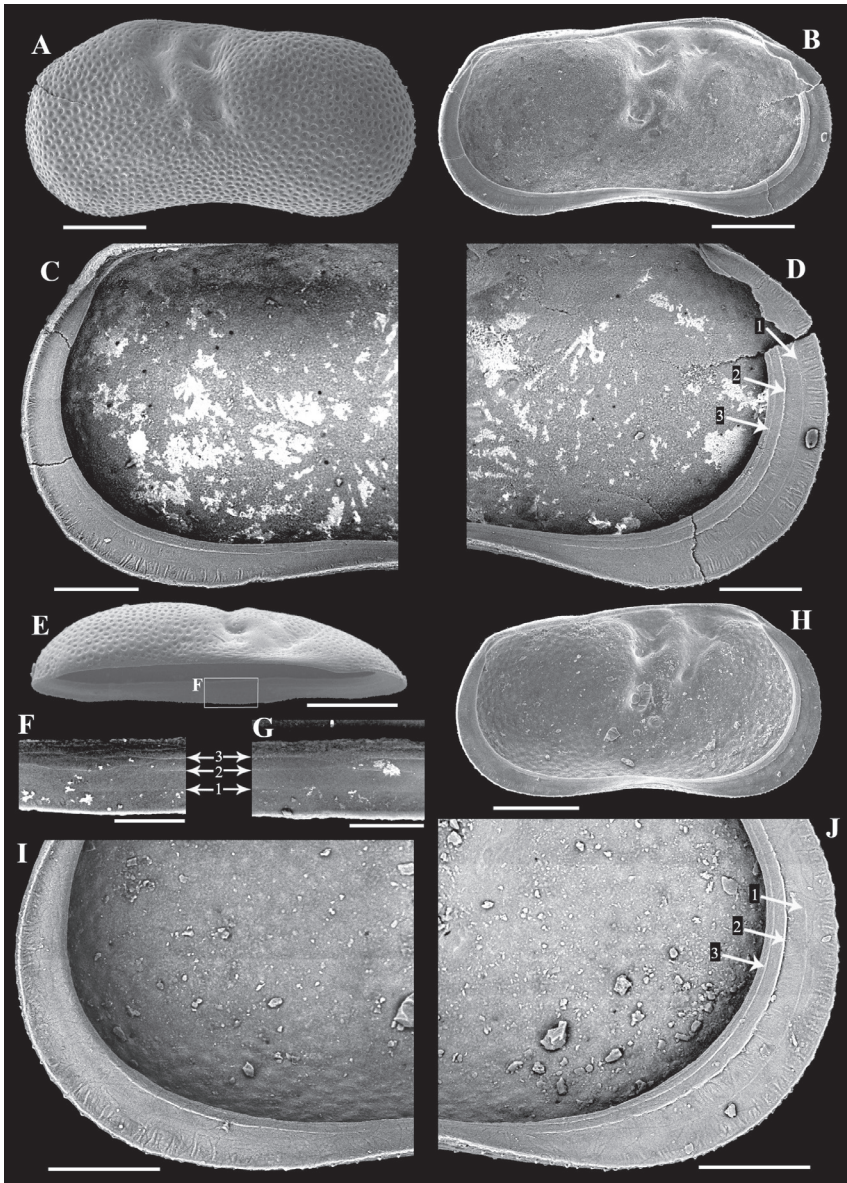


Figure 2. Adult left valves of the ostracod *Ilyocypris leptolinea* Wang & Zhai, sp. nov. from the late Quaternary Xiaojinggou section of Inner Mongolia, China **A–D** XJG2-210-1 (holotype, 0.94 × 0.48 mm) **A** exterior view **B** interior view **C** interior view of the posterior part, showing the marginal ripples **D** interior view of the anterior part, showing the marginal ripples. Arrows and numerals indicate three inner lists on the calcified inner lamella **E, F** XJG2-206-4 **E** oblique-dorsal view **F** enlarged view of the rectangle in (E), showing the crossing pattern of the inner lists at the median part of ventral margin. Arrows and numerals indicate the three inner lists **G** XJG2-206-1, enlarged oblique-dorsal view of the median part of calcified inner lamella, showing the crossing pattern of inner lists **H–J** XJG2-199-2 (paratype) **H** interior view **I** interior view of the postero-ventral part, showing the marginal ripples **J** Interior view of the antero-ventral part, showing the marginal ripples. Arrows and numerals indicate the three inner lists. Scale bars: 200 μm (**A, B, E, H**); 100 μm (**C, D, I, J**); 50 μm (**F, G**).



Figure 3. Adult left valves of the ostracod *Ilyocypris leptolinea* Wang & Zhai, sp. nov. from the late Quaternary Xiaojinggou section of Inner Mongolia, China **A–C** XJG2-21-1 (paratype) **A** exterior view **B** interior view of the postero-ventral part, showing the marginal ripples **C** interior view **D–G** XJG2-197-2 (paratype) **D** interior view **E** interior view of the antero-ventral part, showing the marginal ripples and three inner lists (arrowed) **F** adductor muscle scars (AMS) and mandibular scars (MS) **G** interior view of the posterior part, showing the marginal ripples. Scale bars: 200 μm (**A**, **C**, **D**); 100 μm (**B**, **E**, **G**); 50 μm (**F**).

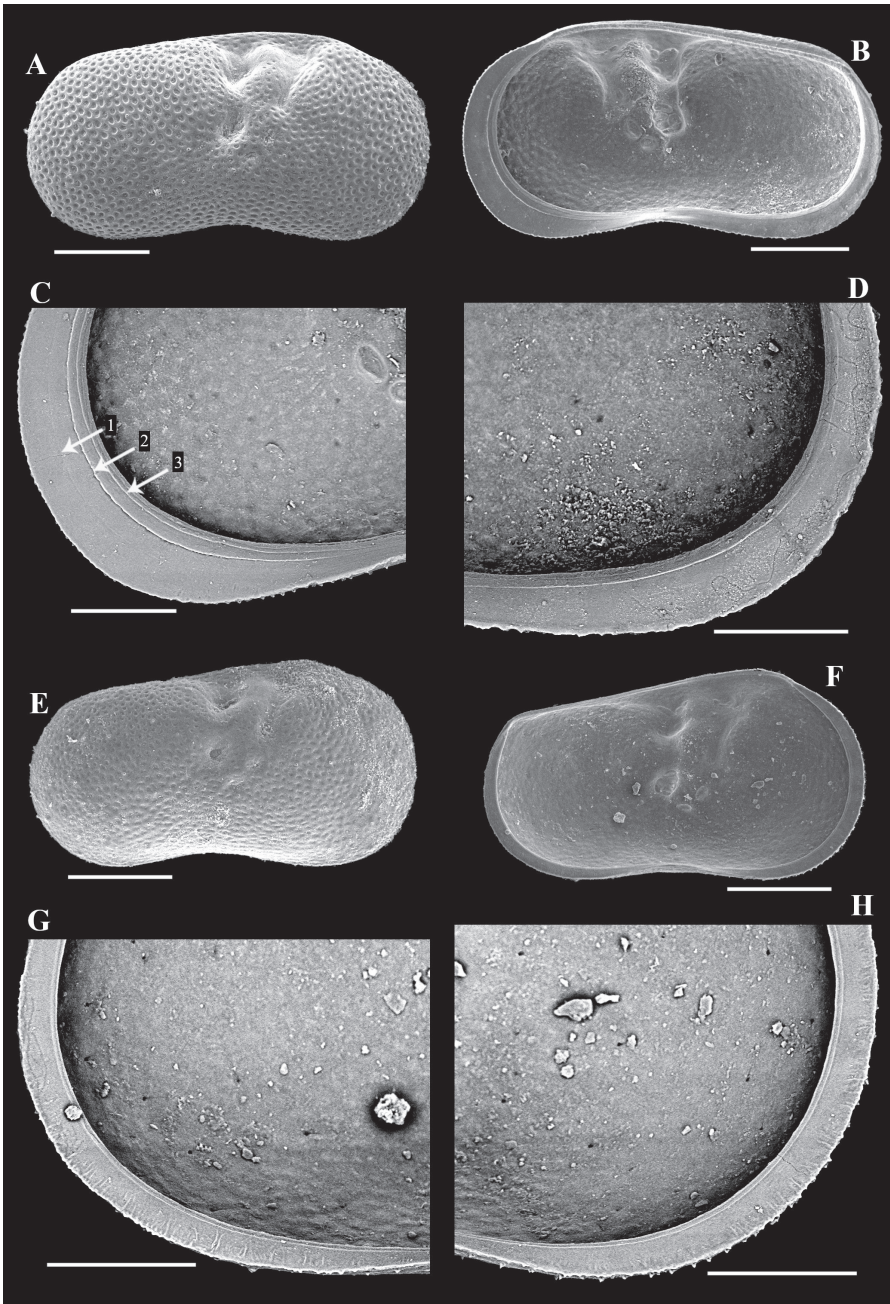


Figure 4. Ostracod valves tentatively identified as *Ilyocypris leptolinea* Wang & Zhai, sp. nov. from the late Quaternary Xiaojinggou section of Inner Mongolia, China **A–D** XJG2-203-1, adult right valve **A** exterior view **B** interior view **C** interior view of the antero-ventral part, showing three inner lists (arrowed) **D** interior view of the postero-ventral part **E** XJG2-193-4, right valve of A-1 juvenile, exterior view **F–H** XJG2-199-1, left valve of A-1 juvenile **F** interior view **G** interior view of the postero-ventral part, showing the marginal ripples **H** interior view of the antero-ventral part, showing the marginal ripples. Scale bars: 200 μm (**A, B, E, F**); 100 μm (**C, D, G, H**).

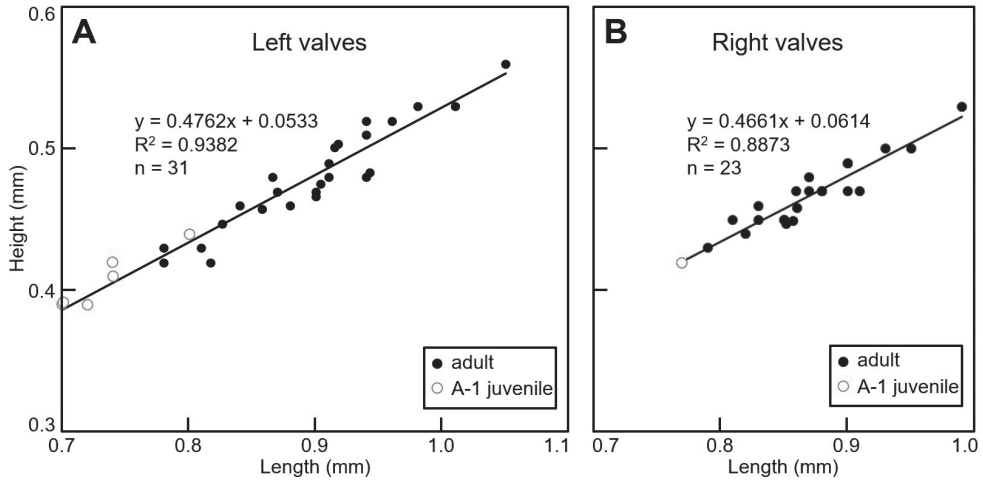


Figure 5. Height–length biplots of the left valves of *Ilyocypris leptolinea* Wang & Zhai, sp. nov. (A) and the right valves tentatively identified as this species (B) from the late Quaternary Xiaojinggou section of Inner Mongolia, China.

rows (Mazzini et al. 2014: fig. 11, panel 8), but are confined to the postero-ventral part too. And the prominent postero-dorsal node on the exterior valve surface offers easy distinction from the new species. *Ilyocypris hanguk* Karanovic & Lee, 2013 described from South Korea, has a valve shape somewhat similar to the new species, and its H/L ratio (0.55 for LV and 0.54 for RV as measured from the holotype in Karanovic and Lee 2013: fig. 6A, B) comes close to that of the new species. However, no marginal ripples were observed on the left valve of *I. hanguk* (Karanovic and Lee 2013: fig. 6A, D). Furthermore, small lateral projections are present on the postero-central part of the valve of *I. hanguk* (Karanovic and Lee 2013: fig. 6B), which are not observed in *I. leptolinea* Wang & Zhai, sp. nov. (Figs 2–4). *Ilyocypris glabella* Fuhrmann & Goth, 2011, *Ilyocypris sebeiensis* Yang & Sun, 2004 (in Yang et al. 2004), *I. tibeta* (Peng et al. 2021), and *Qinghaicypris crassa* Huang, 1979 (Yang et al. 2004) possess marginal ripples distributed along most parts of the anterior and posterior calcified inner lamellae. However, in all these species, there is only one row of ripples distributed near the valve margins, which are thicker and more sparsely arranged compared with the new species. As a result, even if the proximal row of marginal ripples is taphonomically lost in the new species, it would not be confused with these species. Besides, the valves of *I. glabella*, *I. sebeiensis*, and *Q. crassa* are significantly stouter than those of the new species. (Note that Shen et al. (1993) and Hou et al. (2002) considered *Qinghaicypris* a junior synonym of *Ilyocypris* and moved all the species in this genus to *Ilyocypris*).

Valve outlines of different species of *Ilyocypris*

The dissimilarity matrices of the specimens (Tables 3, 4) summarise the intra- and inter-species variabilities of the outlines of different *Ilyocypris* species. Although the

Table 3. Average intra- (**bold**) and inter-species outline dissimilarity of the five species of *Ilyocypris* analysed in this study, based on a Fixed Outline Canberra Dissimilarity (FOCD, %) index between the specimens analysed in this study. Small numerals in parentheses indicate the number of dissimilarity values used for averaging. Species abbreviations: *Ibr*, *I. bradyi*; *Iep*, *I. leptolinea* Wang & Zhai, sp. nov.; *Iin*, *I. innermongolica*; *Ija*, *I. japonica*; *Imo*, *I. mongolica*.

Species	<i>Iep</i>	<i>Ibr</i>	<i>Imo</i>	<i>Iin</i>	<i>Ija</i>
<i>Iep</i>	1.00 ₍₁₀₅₎				
<i>Ibr</i>	1.18 ₍₁₃₅₎	0.84 ₍₃₆₎			
<i>Imo</i>	1.01 ₍₄₅₎	1.21 ₍₂₇₎	0.81 ₍₃₎		
<i>Iin</i>	1.49 ₍₁₈₀₎	1.14 ₍₁₀₈₎	1.58 ₍₃₆₎	0.83 ₍₆₆₎	
<i>Ija</i>	1.00 ₍₄₅₎	0.92 ₍₂₇₎	0.80 ₍₉₎	1.17 ₍₃₆₎	0.61 ₍₃₎

Table 4. Average intra- (**bold**) and inter-species outline dissimilarity of the five species of *Ilyocypris* analysed in this study, based on a Minimal Running Canberra Dissimilarity (MRCD, %) index. Small numerals in parentheses indicate the number of dissimilarity values used for averaging. Species abbreviations: *Ibr*, *I. bradyi*; *Iep*, *I. leptolinea* Wang & Zhai, sp. nov.; *Iin*, *I. innermongolica*; *Ija*, *I. japonica*; *Imo*, *I. mongolica*.

Species	<i>Iep</i>	<i>Ibr</i>	<i>Imo</i>	<i>Iin</i>	<i>Ija</i>
<i>Iep</i>	0.96 ₍₁₀₅₎				
<i>Ibr</i>	1.10 ₍₁₃₅₎	0.76 ₍₃₆₎			
<i>Imo</i>	0.95 ₍₄₅₎	1.10 ₍₂₇₎	0.70 ₍₃₎		
<i>Iin</i>	1.38 ₍₁₈₀₎	1.07 ₍₁₀₈₎	1.42 ₍₃₆₎	0.71 ₍₆₆₎	
<i>Ija</i>	0.93 ₍₄₅₎	0.87 ₍₂₇₎	0.72 ₍₉₎	1.12 ₍₃₆₎	0.61 ₍₃₎

intra-species dissimilarity values are generally small (FOCD of 0.61–1.00 and MRCD of 0.61–0.96, respectively), they show considerable overlap with the range of the inter-species dissimilarity values among the species analysed (FOCD of 0.80–1.58 and MRCD of 0.72–1.42, respectively) (Tables 3, 4). In particular, *I. leptolinea* Wang & Zhai, sp. nov. exhibits considerable intra-species shape variation (e.g., FOCD of 1.00, Table 3) that is comparable to its inter-species difference with *I. bradyi*, *I. japonica*, and *I. mongolica* (Table 3). Correspondingly, the superimposition of the outlines of different specimens reveals considerable within-species variation (Fig. 6A) while comparatively small between-species difference (Fig. 6B). Although these species show some shape difference on the postero-dorsal, posterior, and postero-ventral valve areas (Fig. 6B), such disparities are small. In fact, the morpho-space of *I. leptolinea* Wang & Zhai, sp. nov. comes very close to, or even overlaps with those of *I. bradyi*, *I. japonica*, and *I. mongolica*, although separated from that of *I. innermongolica* (Fig. 6C).

In the cluster analyses based on the two dissimilarity indices (Fig. 7A, B), *I. leptolinea* Wang & Zhai, sp. nov. exhibits a ‘mixed’ pattern with *I. bradyi*, *I. japonica*, and *I. mongolica*, albeit separated from *I. innermongolica*. In both cluster dendrograms, most of the specimens of *I. leptolinea* Wang & Zhai, sp. nov. are distributed in small clusters encompassed by the big cluster (a4 or b4 in Fig. 7) that also contains *I. bradyi*, *I. japonica*, and *I. mongolica*. Among all the species, *I. innermongolica* is the only one that can be readily distinguished from others by valve outline alone (clusters a1 and a3; b2 and b5 in Fig. 7), although its various specimens do not form a single clade

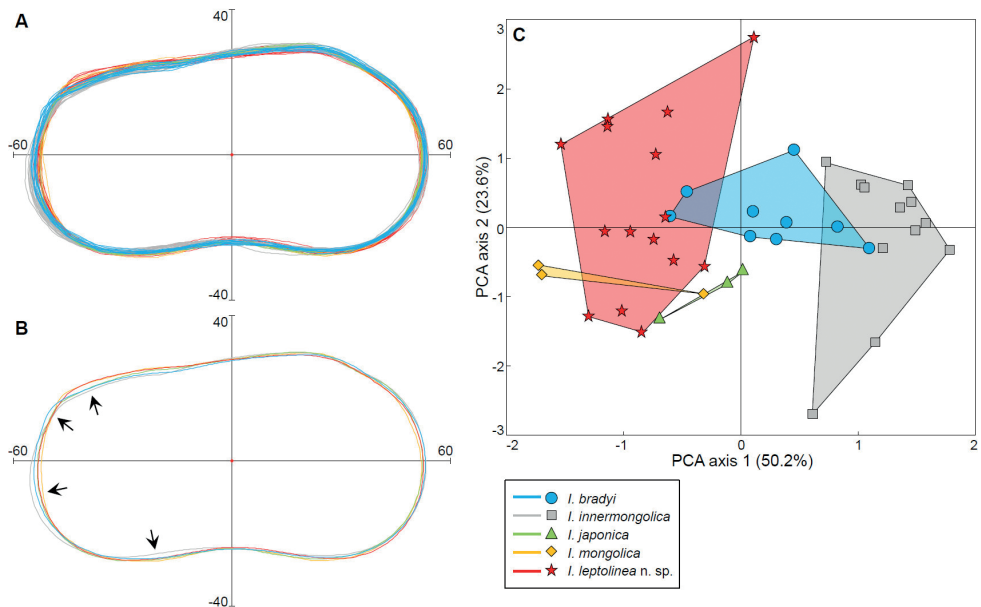


Figure 6. Illustrations showing the overlap of the outline morpho-spaces of five species of *Ilyocypris* that have living or Quaternary representatives in eastern Inner Mongolia. All outlines have been standardised for equal surface area, rotated with the antero-ventral and the postero-ventral parts resting horizontally, and with the geometric centres set at (0, 0) **A** outlines of 42 valves **B** mean outlines of the five species. Arrows indicate areas showing relatively large inter-species variability, i.e., the postero-dorsal–posterior and the postero-ventral areas **C** principal Component Analysis (PCA) biplot of 42 valves based on their outline data. Coloured shaded areas indicate the morpho-spaces of the five species, cast on the two-dimensional space defined by PCA axis 1 and 2.

(Fig. 7A, B). Most of the specimens of *I. bradyi* may also be recognised by valve outline (clusters a2, a5 and a6; b1 and b3 in Fig. 7), but these small clusters are embedded in the same cluster with either *I. leptolinea* Wang & Zhai, sp. nov., *I. japonica*, and *I. mongolica* (clusters a5 and a6 in Fig. 7A) or with *I. innermongolica* (cluster a2 in Fig. 7A and clusters b1 and b3 in Fig. 7B).

The above-mentioned partial-separation pattern of *Ilyocypris* species in the cluster dendrograms (Fig. 7) is in correspondence with the similar valve shapes of these species (Fig. 6B), as well as the intra-species shape plasticity (Fig. 6C).

Discussion

Taxonomy of the valve material of *Ilyocypris*

Based on the morphologies of valve material, we have herein erected *Ilyocypris leptolinea* Wang & Zhai, sp. nov. from late Quaternary lacustrine strata of Inner Mongolia. This

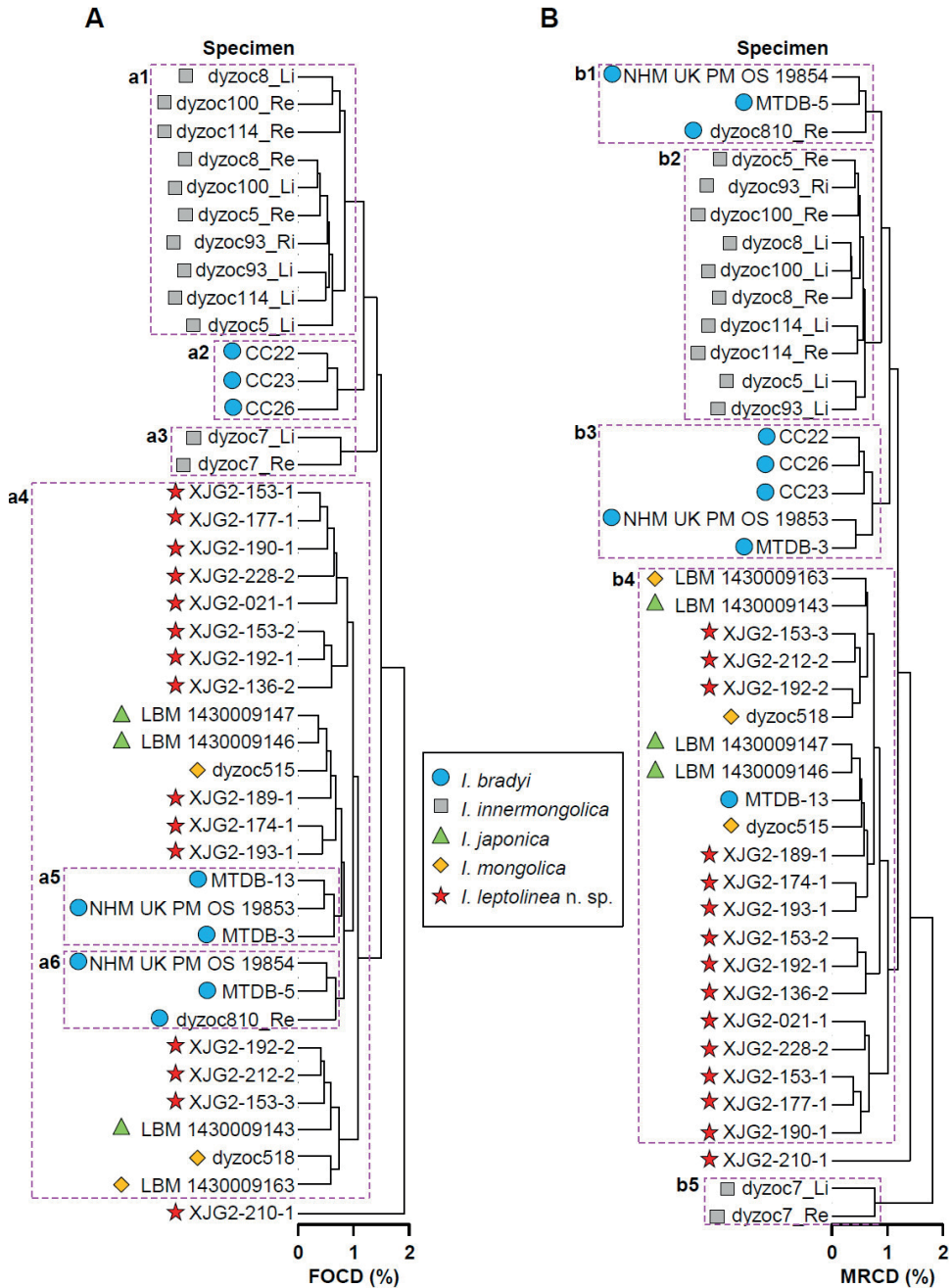


Figure 7. Cluster dendrograms of the valve outlines of *Ilyocypris* species based on the matrices of ‘Fixed Outline Canberra Dissimilarity’ (FOCD, with antero-ventral and postero-ventral parts of valves placed horizontally) (A) and ‘Minimal Running Canberra Dissimilarity’ (MRCD) (B) showing overlap of the morpho-spaces between congeners. The analysed *Ilyocypris* species are those with living or Quaternary representatives in eastern Inner Mongolia. Pink dashed rectangles indicate groups of specimens mentioned in the text. See text for details.

species is best recognised by its two rows of densely arranged fine inner marginal ripples on both the anterior and the posterior calcified inner lamellae of the left valve. Other features, such as the three inner lists, the relatively great width of the calcified inner lamella, and the node-free valve surface may also help diagnose the new species (Figs 2, 3).

Mazzini et al. (2014) made detailed observations on the morphologies of nine *Ilyocypris* species from Italy and concluded that, although the marginal ripples are constant within populations of each species, the pattern reported by different authors can be different. Apart from intra-species variability, we think that at least three possible reasons may be responsible for such inconsistencies. Firstly, as fine structures, the marginal ripples can be concealed by organic material that has not been removed in extant specimens. Secondly, they can be lost or hidden in fossil material due to various reasons including post-mortem abrasion, partial dissolution, chemical precipitation during diagenesis, and/or the tight closure of the carapace. Thirdly, the morphology of the marginal ripples may sometimes be inaccurately presented in the interpretive drawings. In regard of the above, we propose that the marginal ripples can still be useful for species identification of *Ilyocypris*, provided that specimens are properly prepared and possible taphonomic artefacts are considered.

Outline analyses indicate that although *I. leptolinea* Wang & Zhai, sp. nov. can be distinguished from *I. innermongolica* by valve shape, its morpho-space exhibits considerable overlap with other *Ilyocypris* species that have living/fossil representatives in Inner Mongolia, namely *I. bradyi*, *I. japonica*, and *I. mongolica* (Figs 6, 7). This indicates that outline analyses are useful but would not be able to distinguish all the *Ilyocypris* species. Therefore, we suggest that a combination of the valve shape (e.g., Mazzini et al. 2014) and the marginal ripples (e.g., Janz 1994; Mischke et al. 2003), among other morphological features, should be utilised in the species identification of this genus.

The drawback of valve outline is that it is usually a continuous or semi-continuous feature that generates overlapping patterns between species (Figs 6C, 7). Because of the general similarity of the valve shapes of the species in the genus *Ilyocypris* (Meisch 2000; Smith et al. 2019), with the inclusion of more species and more morpho-types into the outline analysis, we would expect that the subtle differences between some of the species may be filled by ‘marginal’ morpho-types of each species, obscuring the inter-species boundary. Nevertheless, outline analysis should still be useful in recognising some of the species, like *I. innermongolica* in our study (Figs 6, 7). We may also be optimistic that, in the future, with the increased feasibility of three-dimensional observation techniques, like 3D scanning and micro-CT, the present-day 2D outline analysis can potentially evolve into 3D-shape analysis, which would capture more shape information for species discrimination.

Most of the valve-shape difference among different *Ilyocypris* species is present in the posterior part of the valves while the shapes of the anterior parts are almost identical (Fig. 6B). This possibly implies that the areas holding the soft parts responsible for walking (the sixth limbs and the uropods), digestion and reproduction exhibit more inter-species variation. Measurement data of the various limb podomeres, chaetotaxy

structures, and other soft parts of *Ilyocypris* would be helpful for testing this assumption. However, the hitherto published work of such kind, Zhai et al. (2017: fig. 14), measured only 23 body structures of only two *Ilyocypris* species covered in our study, namely *I. innermongolica* and *I. mongolica*, and this is inadequate for explaining the inter-species shape difference that is accentuated in the posterior part of the valves (Fig. 6B).

Palaeoenvironmental implications

The prevalence of lacustrine sediments in the Xiaojinggou Basin indicates the existence of a lake in this area during the late Quaternary. From the lithology of the section XJG2, which is dominated by silt and sand fractions and shows a trend of becoming coarser towards the upper part (Fig. 1D), we suggest that the corresponding environment at the sampling site represented a shallow lake, or littoral to intermediate zone of a large lake, with the water becoming shallower across the studied time span. The ostracod composition of the section lacks the species *Limnocythere inopinata* (Baird, 1843), which dominates the small and large brackish waterbodies in the area nowadays (Zhai et al. 2010, 2013, 2015, 2022). This species was also abundant in the large brackish lakes in eastern Inner Mongolia during the late Quaternary (Shen et al. 2001; Zhai et al. 2011; Yue et al. 2022). This may indicate that the palaeo-lake in Xiaojinggou Basin was freshwater, although *L. inopinata* is known from freshwater environments elsewhere (Meisch 2000). Alternatively, as *L. inopinata* is typical of permanent waterbodies, its absence could be because the lake periodically dried up. Given the close position of the XJG2 section to one of the three largest brackish lakes, Dali, in eastern Inner Mongolia (Fig. 1B), the presence of an ephemeral and/or freshwater lake would be significant for palaeoenvironmental reconstruction of the area. However, before quantitative assemblage data of the ostracods from different intervals of the section are available, it would be difficult to draw more specific inferences on the palaeoenvironmental conditions in this area. Although van Harten (1979) speculated that frequent marginal ripples on the left valves of *Ilyocypris* (as also occurs in *I. leptolinea* Wang & Zhai, sp. nov.) could denote environmental instability, this assumption has not been tested with modern datasets and is therefore not applied in the present study.

The disappearance of *I. leptolinea* Wang & Zhai, sp. nov. above the depth of 20 cm in the XJG2 section may be significant, perhaps even indicative of its extinction. This species has not been reported from Quaternary sediments elsewhere or from modern habitats, and it may have been endemic to the Xiaojinggou area during the late Quaternary, with a comparatively narrow ecological niche. It would not only add to our knowledge of the animals that went extinct during the Quaternary (Deng et al. 2013; Zhang et al. 2019; Li et al. 2021b), but should also imply certain underlying mechanisms. Whether and how natural or artificial environmental changes have resulted in its extinction, however, will remain unknown before the exact timing of its disappearance and the accompanying changes in fauna, flora, and human activities in the study area can be reconstructed. These issues should be left to future studies.

Conclusions

This work is the first investigation of the lacustrine sediments and the ostracod fossils in the Xiaojinggou Basin, and future works will endeavour to reconstruct the palaeoenvironments of this area based on more analyses of the ostracods and other proxies. With previous palaeoenvironmental investigations in eastern Inner Mongolia focused on the three large brackish-water lakes (Xiao et al. 2004, 2008, 2009; Zhai et al. 2011), the discovery of a palaeo-lake in the Xiaojinggou Basin with freshwater conditions would be unique.

Although *Ilyocypris leptolinea* Wang & Zhai, sp. nov. is ‘ordinary’ among the species of the genus as judged from its carapace size, shape, and not noded, pitted valve surface, the patterns of marginal ripplelets and the inner lists on its left valves are unique. The erection of this species based on the observations of various features, especially the marginal ripplelets and the outline analyses, could become a case study for describing new species of the genus *Ilyocypris* based on valve material. Judged from the lithology and accompanying ostracods in the section, *I. leptolinea* Wang & Zhai, sp. nov. may have lived in intermediate depth to shallow freshwater, although as an extinct species it could hardly provide independent environmental indications. The new species may add to the knowledge of extinct animals in the late Quaternary and provides basic data for studying environmental changes during this period.

Acknowledgements

This study is supported by NSFC grants 32160116 and 41902011, the Key Research Program of the Institute of Geology & Geophysics, Chinese Academy of Sciences (IGGCAS-201905), and Yunnan Provincial Grants 202101AT070158 and YNWR-QN-BJ-2019-295. We thank Fangzhi Peng (Advanced Analysis and Measurement Center of Yunnan University) and Xiangtong Lei (Institute of Palaeontology, Yunnan University) for imaging the ostracod specimens. The comments from Peter Frenzel (Friedrich Schiller University Jena) and an anonymous reviewer are much appreciated.

References

- Baird W (1843) Notes on British Entomostraca. The Zoologist - A Popular Miscellany of Natural History 1: 193–197.
- Baird W (1845) Arrangement of the British Entomostraca, with a list of species, particularly noticing those which have as yet been discovered within the bounds of the club. Transactions of the Berwickshire Naturalists’ Club 2: 145–416.
- Baltanás A, Danielopol DL (2011) Geometric Morphometrics and its use in ostracod research: a short guide. Joannea—Geologie und Palaontologie 11: 235–272.
- Brady GS (1867) A synopsis of the recent British Ostracoda. The Intellectual Observer 12: 110–130.

- Brady GS, Norman AM (1889) A monograph of the marine and freshwater Ostracoda of the North Atlantic and of Northwestern Europe. Section I: Podocopa. Scientific Transactions of the Royal Dublin Society, Series 2 4: 63–270.
- Bronk Ramsey C (2009) Bayesian analysis of radiocarbon dates. *Radiocarbon* 51(1): 337–360. <https://doi.org/10.1017/S0033822200033865>
- Cohen KM, Finney SC, Gibbard PL, Fan JX (2013, updated) The ICS International Chronostratigraphic Chart. *Episodes* 36(3): 199–204. <https://doi.org/10.18814/epiiugs/2013/v36i3/002>
- Deng T, Qiu Z, Wang B, Wang X, Hou S (2013) Late Cenozoic biostratigraphy of the Linxia Basin, northwestern China. In: Wang X, Flynn LJ, Fortelius M (Eds) *Neogene Terrestrial Mammalian Biostratigraphy and Chronology of Asia*. Columbia University Press, New York, 243–273. <https://doi.org/10.7312/columbia/9780231150125.003.0009>
- Fuhrmann R (2012) Atlas quartärer und rezenter Ostrakoden Mitteleuropas. *Altenburger Naturwissenschaftliche Forschungen* 15: 1–320.
- Fuhrmann R, Goth K (2011) Neue und weitere bemerkenswerte Ostrakoden aus dem Quartär Mitteldeutschlands. *Palaeontographica, Abt. A: Paläozoologie - Stratigraphie* 294: 91–201. <https://doi.org/10.1127/pala/294/2011/95>
- Hou Y, Gou Y, Chen D (2002) *Fossil Ostracoda of China*. Science Press, Beijing, 1090 pp. [In Chinese]
- Huang B (1979) Plates 95–96 and their text explanations. In: Academia Sinica's Lanzhou Geological Institute, Institute of Hydrobiology, Institute of Microbiology & Nanjing Institute of Geology and Palaeontology. Report of combined investigation into Lake Qinghai. Science Press, Beijing, 270 pp. [In Chinese]
- Janz H (1994) Zur Bedeutung des Schalenmerkmals 'Marginalrippen' der Gattung *Ilyocypris* (Ostracoda, Crustacea). *Stuttgarter Beiträge zur Naturkunde. Serie B, Geologie und Palaontologie* 206: 1–19.
- Karanovic I, Lee W (2013) On the ostracod genus *Ilyocypris*, with description of one new species from Korea and the first report of males of *I. bradyi* (Crustacea: Ostracoda: Podocopida). *Proceedings of the Biological Society of Washington* 126(1): 39–71. <https://doi.org/10.2988/0006-324X-126.1.39>
- Kaufmann A (1900) Cypriden und Darwinuliden der Schweiz. *Revue Suisse de Zoologie* 8(3): 209–423. <https://doi.org/10.5962/bhl.part.10584>
- Krstić N (1972) Rod *Candona* (Ostracoda) iz Kongerijiskikh Slojeva Juzhnog dela Panonskog Basena. *Monographs of the Serbian Academy of Sciences and Arts, section of Natural and Mathematical Sciences* 39: 1–145.
- Latreille PA (1802) *Histoire naturelle, générale et particulière des crustacés et des insectes*. Ouvrage faisant suite à l'Histoire Naturelle générale et particulière, composée par Leclerc de Buffon, et rédigée par C. S. Sonnini, membre de plusieurs Sociétés savantes. Tome 3. F. Dufart, Paris, 467 pp.
- Li X, Zhai D, Wang Q, Wen R, Ji M (2021a) Depth distribution of ostracods in a large freshwater lake on the Qinghai–Tibet Plateau and its ecological and palaeolimnological significance. *Ecological Indicators* 129: 108019. <https://doi.org/10.1016/j.ecolind.2021.108019>
- Li Y, Xiong W, Wang L, He W, Sun B (2021b) First record of *Machairodus aphanistus* Kaup, 1833 (Carnivora, Felidae, Machairodontinae) in East Asia from a late Miocene deposit of

- the Linxia Basin, Gansu Province, China. *Historical Biology* 34(5): 930–939. <https://doi.org/10.1080/08912963.2021.1952574>
- Martens K (1991) On a small collection of non-marine ostracods from Mongolia, with the description of a new species (Crustacea, Ostracoda). *Miscellanea Zoologica Hungarica* 6: 53–60.
- Mazzini I, Gliozzi E, Rossetti G, Pieri V (2014) The *Ilyocypris* puzzle: A multidisciplinary approach to the study of phenotypic variability. *International Review of Hydrobiology* 99(6): 395–408. <https://doi.org/10.1002/iroh.201301729>
- Meisch C (2000) Freshwater Ostracoda of Western and Central Europe. In: Schwoerbel J, Zwick P (Eds) *Süßwasserfauna von Mitteleuropa* 8(3). Spektrum Akademischer Verlag, Heidelberg, Berlin, 522 pp.
- Meisch C, Smith RJ, Martens K (2019) A subjective global checklist of the extant non-marine Ostracoda (Crustacea). *European Journal of Taxonomy* 492: 1–135. <https://doi.org/10.5852/ejt.2019.492>
- Mischke S, Herzsich U, Kürschner H, Fuchs D, Zhang J, Meng F, Sun Z (2003) Sub-Recent Ostracoda from Qilian Mountains (NW China) and their ecological significance. *Limnologia* 33(4): 280–292. [https://doi.org/10.1016/S0075-9511\(03\)80023-3](https://doi.org/10.1016/S0075-9511(03)80023-3)
- Mischke S, Lai Z, Zhang C (2013) Re-assessment of the paleoclimate implications of the Shell Bar in the Qaidam Basin, China. *Journal of Paleolimnology* 51(2): 179–195. <https://doi.org/10.1007/s10933-012-9674-6>
- Okubo I (1990) Sixteen species of freshwater Ostracoda from Japan. *Bulletin of the Biogeographical Society of Japan* 45: 9–50.
- Peng P, Zhai D, Smith R, Wang Q, Guo Y, Zhu L (2021) On some modern Ostracoda (Crustacea) from the Tibetan Plateau in SW China, with descriptions of three new species. *Zootaxa* 4942(4): 501–542. <https://doi.org/10.11646/zootaxa.4942.4.2>
- Rohlf FJ (2017) tpsDig, digitize landmarks and outlines, version 2.31. Department of Ecology and Evolution, State University of New York at Stony Brook. <http://life.bio.sunysb.edu/morph>
- Sars GO (1866) Oversigt af Norges marine ostracoder. *Forhandlinger I Videnskabs-Selskabet I Christiania* 1865: 1–130.
- Sars GO (1890) Oversigt af Norges Crustaceer med forelobige bemærkninger over de nye eller mindre bejkendte arter: 2 (Branchiopoda, Ostracoda, Cirripedia). *Forhandlinger I Christiania Videnskabs-Selskabet* 1: 1–80.
- Sars GO (1903) Freshwater Entomostraca from China and Sumatra. *Archiv for Mathematik og Naturvidenskab* 25: 1–44.
- Shen Z, Cheng G, Le C, Liu S (1993) The Quaternary saliferous strata and sedimentary environments of Qaidam Basin. *Geology Publishing House, Beijing*, 1–162. [in Chinese]
- Shen J, Matsumoto R, Wang S, Zhu Y (2001) Quantitative reconstruction of the paleosalinity in the Daihai Lake, Inner Mongolia, China. *Chinese Science Bulletin* 46(1): 73–76. <https://doi.org/10.1007/BF03183214>
- Smith RJ, Janz H, Okubo I (2011) Recent Cyprididae and Ilyocyprididae (Crustacea: Ostracoda) from Lake Biwa, Japan, including a summary of the lake's ostracod fauna. *Zootaxa* 2874(1): 1–37. <https://doi.org/10.11646/zootaxa.2874.1.1>

- Smith RJ, Zhai D, Savatnalinton S, Kamiya T, Yu N (2018) A review of rice field ostracods (Crustacea) with a checklist of species. *Journal of Limnology* 77: 1–16. <https://doi.org/10.4081/jlimnol.2017.1648>
- Smith RJ, Zhai D, Chang CY (2019) *Ilyocypris* (Crustacea: Ostracoda) species in North East Asian rice fields; description of one new species, and redescription of *Ilyocypris dentifera* Sars, 1903 and *Ilyocypris japonica* Okubo, 1990. *Zootaxa* 4652(1): 56–92. <https://doi.org/10.11646/zootaxa.4652.1.2>
- Sokal RR, Michener CD (1958) A statistical method for evaluating systematic relationships. *The University of Kansas Science Bulletin* 38: 1409–1438.
- Stepanaitys NE (1960) New species of ostracods from the Neogene-Quaternary deposits of SW Turkmenia. *Trudy Instituta Geologii Akademii Nauk Turkmenskoi SSR* 2: 298–315. [In Russian]
- Ter Braak CJF, Šmilauer P (2002) CANOCO 4.5: Biometrics. Wageningen University and Research Center, Wageningen, 500 pp.
- van Harten D (1979) Some new shell characters to diagnose the species of the *Ilyocypris gibba-biplicata-bradyi* group and their ecological significance. *Proceedings of the 7th International Symposium on Ostracods, Belgrade*, 71–76.
- Whittaker JE, Parfitt SA (2017) The palaeoenvironment of the important Middle Pleistocene hominin site at Boxgrove (West Sussex, UK) as delineated by the foraminifera and ostracods. In: Williams M, Hill T, Boomer I, Wilkinson IP (Eds) *The archaeological and forensic applications of microfossils. The Micropalaeontological Society, Special Publications*, Geological Society, London, 9–34. <https://doi.org/10.1144/TMS7.2>
- Xiao J, Xu Q, Nakamura T, Yang X, Liang W, Inouchi Y (2004) Holocene vegetation variation in the Daihai Lake region of north-central China: a direct indication of the Asian monsoon climatic history. *Quaternary Science Reviews* 23(14–15): 1669–1679. <https://doi.org/10.1016/j.quascirev.2004.01.005>
- Xiao J, Si B, Zhai D, Itoh S, Lomtadze Z (2008) Hydrology of Dali Lake in central-eastern Inner Mongolia and Holocene East Asian monsoon variability. *Journal of Paleolimnology* 40(1): 519–528. <https://doi.org/10.1007/s10933-007-9179-x>
- Xiao J, Chang Z, Wen R, Zhai D, Itoh S, Lomtadze Z (2009) Holocene weak monsoon intervals indicated by low lake levels at Hulun Lake in the monsoonal margin region of northeastern Inner Mongolia, China. *The Holocene* 19(6): 899–908. <https://doi.org/10.1177/0959683609336574>
- Yang R (1981) Ostracods assemblage and its geological significance from Dabeigou Formation, Luanping Group, in northern Hebei. *Symposium of the first meeting of China Society of Micropalaeontology*. Science Publishing House, Beijing, 76–84. [in Chinese]
- Yang F, Sun Z, Qiao Z, Zhang Y (2004) Revision of the diagnosis of the genus *Qinghaicypris* Huang, 1979 (Ostracoda) and the environmental significance of its type species. *Acta Micropalaeontologica Sinica* 21: 367–381. [In Chinese with English Summary]
- Yue J, Xiao J, Wang X, Meckler AN, Modestou SE, Fan J (2022) “Cold and wet” and “warm and dry” climate transitions at the East Asian summer monsoon boundary during the last deglaciation. *Quaternary Science Reviews* 295: 107767. <https://doi.org/10.1016/j.quascirev.2022.107767>

- Zhai D, Xiao J (2013) On a new species of the genus *Ilyocypris* Brady & Norman, 1889 from Hulun Lake, China. *Naturalista Siciliano, Series IV* 37: 465–469.
- Zhai D, Zhao W (2014) On some Recent non-marine ostracods from northern China, with description of a new species. *Crustaceana* 87(8–9): 985–1026. <https://doi.org/10.1163/15685403-00003339>
- Zhai D, Xiao J, Zhou L, Wen R, Pang Q (2010) Similar distribution pattern of different phenotypes of *Limnocythere inopinata* (Baird) in a brackish-water lake in Inner Mongolia. *Hydrobiologia* 651(1): 185–197. <https://doi.org/10.1007/s10750-010-0295-7>
- Zhai D, Xiao J, Zhou L, Wen R, Chang Z, Wang X, Jin X, Pang Q, Itoh S (2011) Holocene East Asian monsoon variation inferred from species assemblage and shell chemistry of the ostracodes from Hulun Lake, Inner Mongolia. *Quaternary Research* 75(3): 512–522. <https://doi.org/10.1016/j.yqres.2011.02.008>
- Zhai D, Xiao J, Fan J, Zhou L, Wen R, Pang Q (2013) Spatial heterogeneity of the population age structure of the ostracode *Limnocythere inopinata* in Hulun Lake, Inner Mongolia and its implications. *Hydrobiologia* 716(1): 29–46. <https://doi.org/10.1007/s10750-013-1541-6>
- Zhai D, Xiao J, Fan J, Wen R, Pang Q (2015) Differential transport and preservation of the instars of *Limnocythere inopinata* (Crustacea, Ostracoda) in three large brackish lakes in northern China. *Hydrobiologia* 747(1): 1–18. <https://doi.org/10.1007/s10750-014-2118-8>
- Zhai D, Smith R, Peng P, Yu N, Ma S, Li X (2017) Cluster analyses of Ostracoda based on dimensions of body structures: Implications for taxonomic classification. *Crustaceana* 90(4): 471–502. <https://doi.org/10.1163/15685403-00003667>
- Zhai D, Yu N, Ma S, Wen R, Wang M, Wang Q (2022) Disturbed aquatic habitats in central-eastern Inner Mongolia revealed by the prevalence of widespread ostracod species. *Ecological Indicators* 143: 109301. <https://doi.org/10.1016/j.ecolind.2022.109301>
- Zhang W, Appel E, Wang J, Fang X, Zan J, Yang Y, Miao Y, Yan X (2019) New paleomagnetic constraints for *Platybelodon* and *Hipparion* faunas in the Linxia Basin and their ecological environmental implications. *Global and Planetary Change* 176: 71–83. <https://doi.org/10.1016/j.gloplacha.2019.03.002>

First report of the *Euconnus* Thomson subgenus *Cladoconnus* Reitter in the New World, represented by thirteen new Appalachian species (Coleoptera, Staphylinidae, Scydmaeninae)

Michael S. Caterino¹

¹ Dept of Plant & Environmental Sciences, Clemson University, Clemson, SC 29634, USA

Corresponding author: Michael S. Caterino (mcateri@clemson.edu)

Academic editor: Jan Klimaszewski | Received 3 November 2022 | Accepted 27 November 2022 | Published 22 December 2022

<https://zoobank.org/DFA4D0BD-CBA6-49D4-87AC-C741E6C216E9>

Citation: Caterino MS (2022) First report of the *Euconnus* Thomson subgenus *Cladoconnus* Reitter in the New World, represented by thirteen new Appalachian species (Coleoptera, Staphylinidae, Scydmaeninae). ZooKeys 1137: 133–175. <https://doi.org/10.3897/zookeys.1137.97068>

Abstract

Thirteen new species of *Euconnus* Thomson (Staphylinidae: Scydmaeninae: Glandulariini) are described from the southern Appalachian Mts, USA: *Euconnus megalops* **sp. nov.**, *E. vexillus* **sp. nov.**, *E. cumberlandus* **sp. nov.**, *E. vetustus* **sp. nov.**, *E. adversus* **sp. nov.**, *E. astrus* **sp. nov.**, *E. cultellus* **sp. nov.**, *E. falcatus* **sp. nov.**, *E. cataloochee* **sp. nov.**, *E. kilmeri* **sp. nov.**, *E. draco* **sp. nov.**, *E. tusquitee* **sp. nov.**, and *E. attritus* **sp. nov.** These share a number of morphological characters with the Old World subgenus *Cladoconnus* Reitter, representing a diversification of species distinct from anything previously known from the western hemisphere. Most of the species occur at higher elevations, some at the tops of the region's highest mountains, and a few are single-peak endemics. No females of these species are winged, and in several species neither sex is winged. A preliminary phylogeny suggests the wingless species represent a clade within a clade of wing-dimorphic species.

Keywords

Biodiversity, dark taxa, leaf litter, metabarcoding

Introduction

Following a century of near neglect, the hyperdiverse scydmaenine (Staphylinidae) genus *Euconnus* Thomson has seen something of a resurgence of interest. With over 2500 described species, the genus ranks as one of the most species-rich genera of organisms on the planet. Paweł Jałoszyński (2012 and others) has recently attempted to bring some order to the classification of these species on a global scale, revising the types of most of the 30+ subgenera, elevating, synonymizing, or validating the species of most, motivated by and also acknowledging the fact that many hundreds of undescribed species exist, many of uncertain placement in the cumbersome and inconsistent intra-generic taxonomy.

On the North American front, Stephan et al. (2021) recently revised the ‘then’-valid subgenus *Napochus*, describing and redescribing more than 100 species in the group. Jałoszyński’s (2021) subgeneric revision subsequently demoted *Napochus* to synonymy with the nominate *Euconnus* s. str., finding no consistent characters to distinguish them. Synonymizing the monotypic *Pycnophus* in the same paper, following several other changes (e.g. Jałoszyński 2017) leaves *Euconnus* with only three valid subgenera in the Nearctic, *Psomophus* Casey, *Tetramelus* Motschulsky, and *Euconnus* s. str., compared with 10 subgenera recognized in American Beetles (O’Keefe 2001). Apart from those formerly contained in *Napochus*, none of these has been revised since the foundational treatment of Casey (1897), with few species even having been described in the interim.

Recent work in the higher parts of the southern Appalachian mountains of the southeastern USA revealed numerous new *Euconnus* species. This on its own was not particularly surprising, but the difficulty of assigning all of them to subgenus was. Several of these species exhibit a sexual dimorphism that turns out to be known from only a single subgenus, *Cladoconnus* Reitter, hitherto known only from the Palaearctic region (Hlaváč and Stevanović 2013; Jałoszyński 2018), the males having longitudinal carinae on the inner edges of the 8th and 9th antennomeres. Careful comparison of these species with the other defining characters of the group in Jałoszyński (2018, 2019) suggest that this subgenus is, in fact a member of the North American fauna.

The subgenus *Cladoconnus* comprises thirty-seven extant species distributed predominantly in the Western Palaearctic region (although recent discoveries by Hoshina and colleagues (Hoshina 2004; Hoshina et al. 2018; Hoshina and Park 2020) suggest that the east Asian diversity is considerable as well) and one fossil species from ~ 40 MY Baltic amber (Jałoszyński and Perkovsky 2021). Here I report this subgenus for the first time from the western hemisphere, represented by 13 previously undescribed species. At the same time, these species require a redefinition of the subgenus, because they exhibit considerable variability in morphology, notably not all having the most conspicuous defining character of the subgenus, the carinae of the male 8th and 9th antennomeres.

This group also has significance from a regional, faunistic perspective, as it seems to represent a wholly undocumented high Appalachian radiation. Such endemic radiations are known in numerous other taxa, both arthropods (Barr 1979; Gusarov 2002;

Miller and Wheeler 2005; Wheeler and Miller 2005) and other organisms. *Cladoconnus* are somewhat unusual among even these, however, in having no other close relatives (at least as far as currently documented) elsewhere in North America. Other regional species of *Euconnus sensu stricto* (where these species might otherwise have keyed out, in e.g., O’Keefe 2001) do not appear to be closely related, most in the southeastern US exhibiting a distinct suite of sexual dimorphisms, particularly on the male abdominal ventrites. On a regional scale, these separate lineages show no geographical overlap, with *Euconnus s. str.* records coming mainly from low-lying areas in the coastal plain. Most records of the species assigned to *Cladoconnus* are from ~ 1000 m or above, and some subgroups primarily above 1500 m in the highly restricted spruce-fir habitats of the highest peaks.

In addition to describing these species, I report COI barcode sequences for most of them, several being represented by sequences from multiple localities, allowing a preliminary assessment of their internal phylogenetic relationships, as well as an even more preliminary exploration of their possible relationships among *Euconnus* species on a broader scale.

Materials and methods

Specimens used in this paper originated in or are deposited in the following collections:

- AMNH** The American Museum of Natural History, New York;
- FMNH** The Field Museum, Chicago;
- CNCI** The Canadian National Collection of Insects, Ottawa;
- CUAC** The Clemson University Arthropod Collection, Clemson;
- UNHC** The University of New Hampshire Collection, Durham.

Most of the 679 specimens used in this study were collected as part of a larger inventory of leaf litter inhabiting arthropods. Litter samples were obtained from numerous high elevation localities (> 3300 ft or 1000 m) across five states (Virginia, North Carolina, Tennessee, South Carolina, Georgia) during the years 2015–2021, visiting most sites on two different dates, roughly in spring and fall timeframes, and collecting at least three separate litter samples on each visit. Many of the highest elevation samples come from spruce-fir forest, where litter consists of deep decomposing needles, with minor components of deciduous leaves and fine woody debris. But at lower sites, deciduous leaf litter or *Rhododendron* litters were often sampled. Litter was sifted down to the soil surface (or to a depth where litter was so decayed as to be indistinguishable from soil, where the interface was not a hard boundary), over an area of ca. 1 m², through an 8-mm mesh, until a bag of ~ 6 L was filled. Samples were processed in the lab using Berlese-Tullgren funnels, running subsamples until thoroughly dry, ~ 12 hours per batch. Specimens were collected directly into 100% ethanol, and moved to -20 °C storage after each subsample was complete.

Conventions

Despite availability of many more specimens of most species, type series are generally restricted to single localities, acknowledging the possibility of cryptic diversity within some of these species. Type specimens are all dissected males or specimens that we've been able to associate with dissected males through DNA sequences. Label data for primary and secondary types are quoted; data for non-type specimens are summarized. Full specimen-level data for all material examined, along with voucher codes, extraction codes, and GenBank accession numbers are detailed in an Excel supplement.

Following Hlaváč and Stevanović (2013), measurements conform with the following conventions:

- **BL** – total body length is a sum of the lengths of head (anterior labral margin to summit of vertex), pronotum and elytra measured separately;
- **HW** – width of head is measured across eyes;
- **PW & PL** – pronotal width and length are the maximum widths and lengths;
- **EW** – elytral width is the maximum width;
- **EL** – length of elytra along suture.

Sequencing

Many specimens reported here were processed through a voucher-based high-throughput sequencing protocol in an attempt to generate a barcode database for the high Appalachian litter arthropod fauna. Subsequently, I also selected additional specimens, many dry, from older collections to complement these, representing additional localities and potential species. Most barcoded specimens were imaged prior to extraction, with images archived on a Flickr page: https://www.flickr.com/search/?user_id=183480085%40N02&text=Cladoconnus. The supplementary specimens were not imaged, but other sequencing procedures were similar. Dry specimens were removed from points by soaking in 100% ethanol. Every specimen was subdivided or punctured to permit tissue digestion, and placed in a separate well in a 96-well plate. Tissues were digested with lysis buffer and proteinase K (Omega BioTek, Norcross, GA). The liquid fraction was removed to a new plate, leaving behind the voucher remains for further dissection and archiving. Following digestion, remains of extracted specimens were recombined with any non-extracted body parts, labelled, assigned unique CUAC (Clemson University Arthropod Collection) identifiers, and curated into the CUAC. The digested tissue mixture was purified using Omega BioTek's MagBind HDQ Blood and Tissue kit on a Hamilton Microlab Star automated liquid handling system, eluting with 150 µL elution buffer.

Analyses reported here include sequences from two separate sequencing approaches, both based on a 'mini-barcode', a 421 bp fragment of the mitochondrial COI gene amplified using the primers BF2-BR2 (GCHCCHGAYATRGCHTTYCC & TCDGGRTGNCCRAARAAYCA, respectively; Elbrecht and Leese 2017), corresponding to the downstream two-thirds of the standard barcoding region. Primer pairs for each well were tagged with a unique combination of forward and reverse 9 bp indexes

to allow multiplexing, synthesized as part of the primer by Eurofins Genomics (Louisville, KY). These indexes were derived from a list provided by Meier et al. (2016). All PCRs were conducted in 12.5 μ L volumes (5.6 μ L water, 1.25 μ L Taq buffer, 1.25 μ L dNTP mix [2.5 mM each], 0.4 μ L MgCl [50 mM], 1.5 μ L each primer, 0.05–0.09 μ L Platinum Taq polymerase, 1–2 μ L DNA template, with a 95 °C initial denaturation for 5 minutes, followed by 35–45 cycles of 94 °C (30 sec), 50 °C (30 sec), 72 °C (30 sec), and a 5 minute 72 °C final extension on an Eppendorf Gradient Mastercycler.

Earlier barcodes (pre-2022) were generated on an Illumina MiSeq, later ones on an Oxford Nanopore MinION sequencer. For Illumina library preparation, PCR products were combined and purified using Omega Bio-Tek's Mag-Bind Total Pure NGS Kit, in a ratio of 0.7:1 (enriching for fragments >300 bp). Illumina adapters and sequencing primers were ligated to PCR products using New England BioLab's Blunt/TA Ligase Master Mix. The amplicon+adapter library was again purified using Mag-Bind Total Pure NGS, and quantified using a Qubit fluorometer. This library was sequenced on an Illumina MiSeq using a v.3 2x300 paired-end kit. Nanopore libraries were prepared using the ligation sequencing kit LSK-112 (Oxford Nanopore Technologies, Oxford, UK) and sequenced using a v10.4 flowcell.

Illumina reads were processed with bbtools software package (<https://jgi.doe.gov/data-and-tools/bbtools/>; v38.87, Bushnell et al. 2017) to merge paired read ends, remove PhiX reads, trim Illumina adapters, filter reads for the correct size, remove reads with quality score<30, cluster sequences by similarity allowing 5 mismatches (-1%), and generate a final matrix in FASTA format. Nanopore reads were basecalled using the 'super-accurate' algorithm of Guppy (v6.1.2), then demultiplexed using ONTbarcode v0.1.9 (Srivathsan et al. 2021), with minimum coverage set at 5. Final barcode sequences were submitted to GenBank, under accession numbers OP779401–OP779518 (see Suppl. material 1 for details).

Phylogeny

FASTA files from all sequencing methods were combined and aligned with the online version of Mafft v7 (Katoh et al. 2017) using the 'auto' strategy. To attempt to determine the placement of putative Appalachian *Cladoconnus* species among global *Euconnus* diversity, sequences were combined with other barcode-region sequences for *Euconnus* available on BOLD and GenBank, making a combined matrix of 389 sequences. These include 117 American putative *Cladoconnus*, two European *Cladoconnus*, 265 other *Euconnus* sequences (multiple individuals for many species, as well as many unidentified) representing other subgenera (*Neonapochus*, *Tetramelus*, *Napochus*, and *Euconnus* s. str., Old World and New), and five outgroups from the also-Glandulariini genus *Brachyiceps* Brendel. Phylogenetic reconstructions were performed using maximum likelihood (ML) with W-IQ-TREE v. 2.0 (Trifinopoulos et al. 2016), available at <http://iqtree.cibiv.univie.ac.at>. This program was used also to determine the best substitution model for the data. Analyses used a perturbation strength of 0.4. and an IQ-TREE stopping rule value at 200. Branch support is based on an ultrafast bootstrap analysis (Minh et al. 2013), run with 1,000 bootstrap replicates with a minimum correlation coefficient of 0.99.

Results

Taxonomy

Genus *Euconnus* Thomson, 1859

Subgenus *Cladoconnus* Reitter, 1909

Cladoconnus Reitter, 1909: 226, as subgenus of *Euconnus* Thomson. Type species: *Scydmaenus motschulskii* Motschulsky, 1837 (subsequent designation by Newton and Franz 1998: 145).

Euconnus (*Cladoconnus*) Reitter: Hlaváč and Stevanović 2013 (diagnosis); Jałoszyński 2018 (diagnosis).

Diagnosis. Previous diagnoses of Palaearctic *Cladoconnus* have focused primarily on the presence in males of serrulate carinae on the inner margins of antennomeres VIII and IX, a character not known elsewhere in *Euconnus*. Jałoszyński (2018) further noted the unique presence of a bell-shaped, setose pronotum with 3 basal foveae in an inward-pointing triangular arrangement on each side of a short median basal pronotal carina, straddling short sublateral carinae. He also noted a unique mandibular shape in which the outer margin is interrupted where the apical portion narrows abruptly. The species described here do not entirely conform to this diagnosis, showing variability in most of these characters among them. All are small, with total body lengths ranging from 1.3 to 1.7 mm, not differing much between the sexes (Table 1). The highly distinctive male antennal carinae are evident in most of these species (Figs 4E, 6, 9E, 14C, 16C), but are completely absent in a couple that otherwise seem to be related by other morphological characters and by DNA sequences (Figs 1E, 8A, 13E). Most are consistent in having a bell-shaped pronotum, narrowed basally in some, with the triangle pattern of posterior foveae and at least short sublateral carinae (Figs 4F, 9F). A median basal pronotal carina is evident in several (e.g., Fig. 4F), but in others it is so weak as to be essentially absent (e.g., Fig. 9F). Only one species (*E. vetustus*) exhibits the distinctive bi-arcuate mandible, the others appearing to have simply arcuate mandibles. Similar to all Palaearctic species, American *Cladoconnus* have male genitalia with complex, asymmetrical endophallic armature. Metathoracic wings have not been described for European species, but illustrations and descriptions of body and metathoracic shape suggest that most described species are fully winged in both sexes. Hoshina et al. (2018) notes apparent sexual dimorphism in wingedness in three Asian species. Several of the new American species are flightless in both sexes, and some appear to be flightless in females only. Females associated by sequencing show reduced eyes relative to males, and have smaller, unmodified antennomeres, in several species having the club reduced to only three antennomeres (e.g., Fig. 9D). Due to this variability, it is likely that future revision of *Cladoconnus* will be necessary, but for now these new species seem to have clear relationships to those in the Old World, and are relatively easy to recognize among New World *Euconnus*.

Table 1. Measurements of *E. (Cladoconnus)* species, in mm. Each cell has separate averages for males / females, with total number measured in the last column.

	HL	HW	PL	PW	EL	EW	BL	n
<i>E. megalops</i>	0.4/0.4	0.3/0.3	0.4/0.4	0.3/0.4	0.9/0.9	0.6/0.6	1.7/1.7	3 / 3
<i>E. falcatus</i>	0.3/0.3	0.2/0.2	0.3/0.3	0.3/0.3	0.7/0.7	0.5/0.5	1.3/1.3	3 / 3
<i>E. cataloochee</i>	0.3/0.3	0.2/0.2	0.3/0.3	0.3/0.3	0.7/0.7	0.5/0.5	1.4/1.3	3 / 3
<i>E. tusquitee</i>	0.3	0.3	0.3	0.3	0.7	0.4	1.3	1 / 0
<i>E. kilmeri</i>	0.3	0.3	0.3	0.3	0.7	0.4	1.3	1 / 0
<i>E. draco</i>	0.3/0.3	0.2/0.2	0.3/0.3	0.3/0.3	0.7/0.7	0.5/0.5	1.3/1.3	3 / 2
<i>E. vetustus</i>	0.3/0.4	0.3/0.3	0.3/0.4	0.4/0.4	0.9/0.8	0.6/0.6	1.5/1.5	3 / 3
<i>E. attritus</i>	0.3/0.3	0.3/0.3	0.4/0.4	0.3/0.3	0.8/0.8	0.5/0.5	1.5/1.5	3 / 3
<i>E. astrus</i>	0.4/0.4	0.3/0.3	0.3/0.4	0.3/0.3	0.8/0.9	0.6/0.6	1.5/1.6	3 / 3
<i>E. vexillus</i>	0.4/0.4	0.3/0.3	0.4/0.4	0.4/0.4	0.9/0.9	0.7/0.7	1.7/1.7	3 / 3
<i>E. adversus</i>	0.4/0.4	0.3/0.3	0.4/0.4	0.3/0.4	0.9/0.9	0.6/0.6	1.6/1.6	3 / 3
<i>E. cumberlandus</i>	0.4/0.4	0.3/0.3	0.4/0.4	0.4/0.4	0.9/0.9	0.6/0.6	1.7/1.7	3 / 3
<i>E. cultellus</i>	0.3/0.3	0.3/0.2	0.3/0.3	0.3/0.3	0.7/0.7	0.5/0.5	1.3/1.3	3 / 3

There is little point writing a key to these species because most can only definitely be identified by male genitalia, with a few externally similar species even sympatric in a few places. There are three main morphotypes, dark and stout (*Euconnus vexillus* and *E. vetustus*), dark with rufescent highlights, more gracile (*Euconnus megalops*), and small and pale (flightless), with a mix of modified and non-modified male antennomeres (all remaining species). All share a generally similar form of male genitalia: the basal bulb is large and voluminous, narrowing at the shoulders to a variously tapered median lobe (sensu Stephan et al. 2021; equivalent to the dorsal apical projection of Jałoszyński 2012). The opposite side (morphologically ventral) exhibits a thin, weakly sclerotized compressor plate (sensu Stephan et al. 2021; equivalent to the ventral apical projection of Jałoszyński 2012). They all have a crescent-shaped diaphragm plate sclerite, and relatively thin, weakly curving parameres, bearing a small number of apical setae. They vary much more, however, in the sclerites of the endophallus, which are always asymmetrical, including two or more long, curving, often opposing hooks or spikes. These may bear secondary hook-like processes, or other variously acute projections. In descriptions ‘upper’ and ‘lower’ are used to refer to the diaphragm and foramen sides, respectively, and ‘left’ and ‘right’ referring to the structures as drawn (upper side up), not to true morphological position.

***Euconnus (Cladoconnus) megalops* sp. nov.**

<https://zoobank.org/92355F93-458D-455B-B19E-CFE0D3DFE12E>

Figs 1, 2A, 3

Type material. *Holotype* ♂, deposited in FMNH: “USA: NC: Haywood Co., 35.6721°N, 83.1760°W, Smoky Mts NP, 6150’, Big Cataloochee Mt., xi.5.2020, sifted litter, M.Caterino & F.Etzler” / “[QR code] CLEMSON-ENT CUAC000135174”

/ “Caterino DNA Voucher Extraction MSC6486, Morphosp. BCat.B.316”. **Paratypes** (33, CUAC, FMNH, CNCI, UNHC) – 3 ♀, 6 ♂: same data as type; 1 ♀, 3 ♂: “USA: NC: Haywood Co., 35.6686°N, 83.1749°W, Smoky Mts NP, 5725’, Big Cataloochee Mt., vii.14.2020, sifted litter, M.Caterino, F.Etzler”; 3 ♀: “USA: NC: Haywood Co., 35.6722°N, 83.1758°W, Smoky Mts NP, 6155’, Big Cataloochee Mt., vii.14.2020, sifted litter, M.Caterino, F.Etzler”; 2 ♀: “USA: NC: Haywood Co., 35.6414°N, 83.1958°W, SmokyMtsNP, Balsam Mt.Tr., 4752’, xi.5.2020, M.Caterino & F.Etzler, Sifted litter”; 3 ♀: “USA: NC: Haywood Co., 35.6425°N, 83.2007°W, SmokyMtsNP, Balsam Mt.Tr., 5167’, xi.5.2020, M.Caterino & F.Etzler, Sifted litter”; 9 ♀, 3 ♂: “USA: NC: Haywood Co., 35.6453°N, 83.2025°W, SmokyMtsNP, Balsam Mt.Tr., 5086’, xi.5.2020, M.Caterino & F.Etzler, Sifted litter”.

Other material. (229 adults, 7 larvae) **GA:** Rabun Co., Chattahoochee NF, Rabun Cliffs, 4082 ft., 11-May-2021 (7 ♀, 3 ♂); Towns Co., Chattahoochee NF, Brasstown Bald, 4495 ft., 17-Nov-2020 (1 ♀, 1 ♂); **NC:** Buncombe Co. Co., Pisgah National Forest, Big Butt Trail, 5190 ft., 19-Mar-2016 (1 ♀, 2 ♂); Cherokee Co., Nantahala National Forest, Hickory Branch trail, 4156 ft., 26-Jul-2015 (1 ♀); Clay Co., Nantahala National Forest, Riley Knob, 4330 ft., 11-May-2020 (1 ♀); Clay Co., Nantahala National Forest, Shooting Creek Bald, 4809 ft., 11-May-2020 (1 ♀); Clay Co., Nantahala National Forest, Tusquitee Bald, 4656–5015ft, 1-Sep-2020 (4 ♀, 2 ♂); Clay Co., Nantahala National Forest, Chunky Gal Trail, 4014 ft., 1-Sep-2020 (2 ♀, 1 ♂); Graham Co., Nantahala National Forest, Teyahalee Bald, 4060–4663ft., 12-Apr-2022 (2 ♀, 3 ♂); Graham Co., Nantahala National Forest, Cherohala Skyway – Wright Ck., 4702 ft., 4-May-2020 (2 ♀, 3 ♂); Graham Co., Nantahala National Forest, Huckleberry Knob, 5491–5522 ft., 4-May-2020 & 13-Oct-2020 (10 ♀, 5 ♂); Graham Co., Nantahala National Forest, jct. Indian & Santeetlah Cks., 2770–2833 ft., 24-Jun-2015 (11 ♀, 10 ♂); Graham Co., Nantahala National Forest, Joyce Kilmer Forest, 2696–2942 ft., 20-Jul-2015 (2 ♀, 5 ♂); Haywood Co., Blue Ridge Parkway National Park, Mt. Hardy, 6110 ft., 8-Sep-2020 (9 ♀, 6 ♂); Haywood Co., Pisgah National Forest, Mountains to Sea Trail, 5540 ft., 8-Sep-2020 (1 ♀); Haywood Co., Pisgah National Forest, Black Balsam Knob, 6072 ft., 7-May-2018 (1 ♀); Haywood Co., Blue Ridge Parkway National Park, Richland Balsam Mt., 6207 ft., 11-Sep-2019 (1 ♀); Haywood Co., Blue Ridge Parkway National Park, Pisgah Mt., 5245 ft., 10-Aug-2021 (1 ♀, 1 ♂); Jackson Co., Sumter National Forest, Ellicott Rock Wilderness, Bad Creek trail, 2397 ft., 3-Jun-2015 (1 ♀, 2 ♂); Jackson Co., Nantahala National Forest, Whiteside Mt., 4740 ft., 22-Jun-2022 (1 ♀); Jackson Co., Cashiers, Hwy 64, 3700 ft., 1-Feb-2020 & 16-Feb-2020 (6 ♀, 2 ♂); Jackson Co., Nantahala National Forest, Toxaway Mt., 4770 ft., 5-Aug-2020 (2 ♀, 1 ♂); Jackson Co., Blue Ridge Parkway National Park, along Blue Ridge Pkwy, 5572 ft., 11-Sep-2019 (2 ♀); Jackson Co., Balsam Mountain Preserve, Doubletop Mountain, 4839 ft., 17-Jun-2015 (3 ♀, 2 ♂); Jackson Co., Balsam Mountain Preserve, Sugarloaf Mountain, 4484 ft., 15-Jun-2015 (2 ♀); Jackson Co., Balsam Mountain Preserve, Boar ridge, 4040 ft., 16-Jun-2015 (4 ♀, 1 ♂); Jackson Co., Balsam Mountain Preserve, Dark ridge, 3290 ft., 20-Jun-2015 (2 ♀, 7 ♂); Jackson Co., Blue Ridge Parkway National Park, Waterrock Knob, 6281 ft., 29-May-2018 (1 ♀,

1 ♂); Macon Co., E Highlands, Hwy 64, 3880–3990 ft., 1-Mar-2020 (6 ♀, 2 ♂); Macon Co., Nantahala National Forest, Jones Gap, 4447 ft., 16-Jul-2015 (1 ♀); Macon Co., Nantahala National Forest, Jones Knob, 4237 ft., 28-Jul-2015 (1 ♀); Macon Co., nr. Wayah Bald, 5280 ft., 16-Mar-2016 (2 ♀); Macon Co., Nantahala National Forest, Copper Ridge Bald, 5144 ft., 9-Jul-2019 (1 ♀, 1 ♂); Macon Co., Nantahala National Forest, Cowee Bald, 4839–4942ft., 9-Jul-2019 (5 ♀, 5 ♂); Macon Co., Hwy. 64, nr. Dry Falls, 16-May-1986 (1 ♂); Madison Co., Pisgah National Forest, Camp Creek Bald, 4741 ft., 1-Mar-2022 (1 ♂); McDowell, Pisgah National Forest, Snooks Nose Trail, 2219 ft., 25-Aug-2015 (1 ♀, 2 ♂); Polk, Melrose Falls (lower), 1103 ft., 10-Aug-2021 (1 ♀, 3 ♂); Polk, Green River Game Lands, Lower Bradley Falls Tr., 1620 ft., 19-Mar-2018 (3 ♀, 1 ♂); Polk, Green River Game Lands, Green River Cove Tr., 1070 ft., 18-Mar-2018 (1 ♀); Polk, Green River Game Lands, 1740, 18-Mar-2018 Polk, Green River Game Lands, 1740 ft., 18-Mar-2018 (1 ♀, 1 ♂); Buncombe Co. Co., Blue Ridge Parkway National Park, Bull Gap, 3100 ft., 1-May-1990 (1 ♂); Swain Co., Great Smoky Mountains National Park, Clingmans Dome, 6264–6500 ft., 4-Jun-2018 & 14-Sep-2021 (4 ♂); Swain Co., Great Smoky Mountains National Park, Lakeshore Tr., Payne Ck., 1816 ft., 12-Apr-2022 (1 ♀, 2 ♂); Transylvania Co., Pisgah National Forest, Hwy 215, 1 mi. S. Blue Ridge Pkwy, 5122 ft., 7-May-2018 (1 ♀); Yancey Co., Pisgah National Forest, Woody Ridge Tr., 5086–5301ft., 15-Jun-2020 & 19-Oct-2021 (1 ♀, 2 ♂); **SC:** Greenville Co., Chestnut Ridge Heritage Preserve, 1090 ft., 8-Apr-2018 (1 ♀); Pickens Co., Eastatoe Creek Heritage Preserve, 1421 ft., 30-Apr-2015 (1 ♂); Pickens Co., Sassafras Mountain summit, 3347 ft., 10-Jun-2015 (1 ♂); Oconee Co., Sumter National Forest, Ellicott Rock Wilderness, 2113–2679 ft., 3-Jun-2015 & 4-May-2015 (5 ♀, 4 ♂); Oconee Co., Sumter National Forest, Riley Moore Falls, 900 ft., 3-Mar-2018 (2 ♀); Oconee Co., Coon Branch Nat. Area, 1950 ft., 28-Feb-2016 (3 ♀, 1 ♂); **TN:** Unicoi, Cherokee Co. National Forest, Big Bald, 5346–5430 ft., 5-Aug-2020 & 21-May-2021 (5 ♀); Blount Co., Great Smoky Mountains National Park, Whiteoak Sink, 1724 ft., 27-Oct-2021 (1 ♂); Sevier Co., Great Smoky Mountains National Park, Alum Cave Bluff Trail, 5196 ft., 25-Jun-2019 (3 ♀, 1 ♂); Sevier Co., Great Smoky Mountains National Park, Appalachian Trail nr. Newfound Gap, 5456 ft., 4-Jun-2018 (4 ♀, 1 ♂); Sevier Co., Great Smoky Mountains National Park, Off Hwy 441, 4575 ft., 12-Mar-2020 (2 ♀). **LARVAE:** **NC:** Swain Co., Great Smoky Mountains National Park, Clingmans Dome, 14-Sep-2021; Haywood Co., Great Smoky Mountains National Park, Big Cataloochee Mt., 5-Nov-2020; Haywood Co., Great Smoky Mountains National Park, Balsam Mt. Trail, 5-Nov-2020; Jackson Co., Blue Ridge Parkway National Park, Browning Knob, 22-Sep-2020; **TN:** Sevier Co., Great Smoky Mountains National Park, Alum Cave Bluff Tr., 28-Sep-2021; **GA:** Rabun Co., Chattahoochee NF, Rabun Cliffs, 25-Nov-2019.

Description. Males winged, females lacking fully developed flight wings; large, elongate, generally dark but elytra reddish at humeri and often along elytral suture (Fig. 1C), female generally darker (Fig. 1D); male eyes large, protuberant, with ~ 30 large ommatidia (Fig. 1A, E); female eyes smaller, flush with side of head, comprising ~ 12 ommatidia (Fig. 1B, F); scape and pedicel similar in length, ca. as long as width of eye,

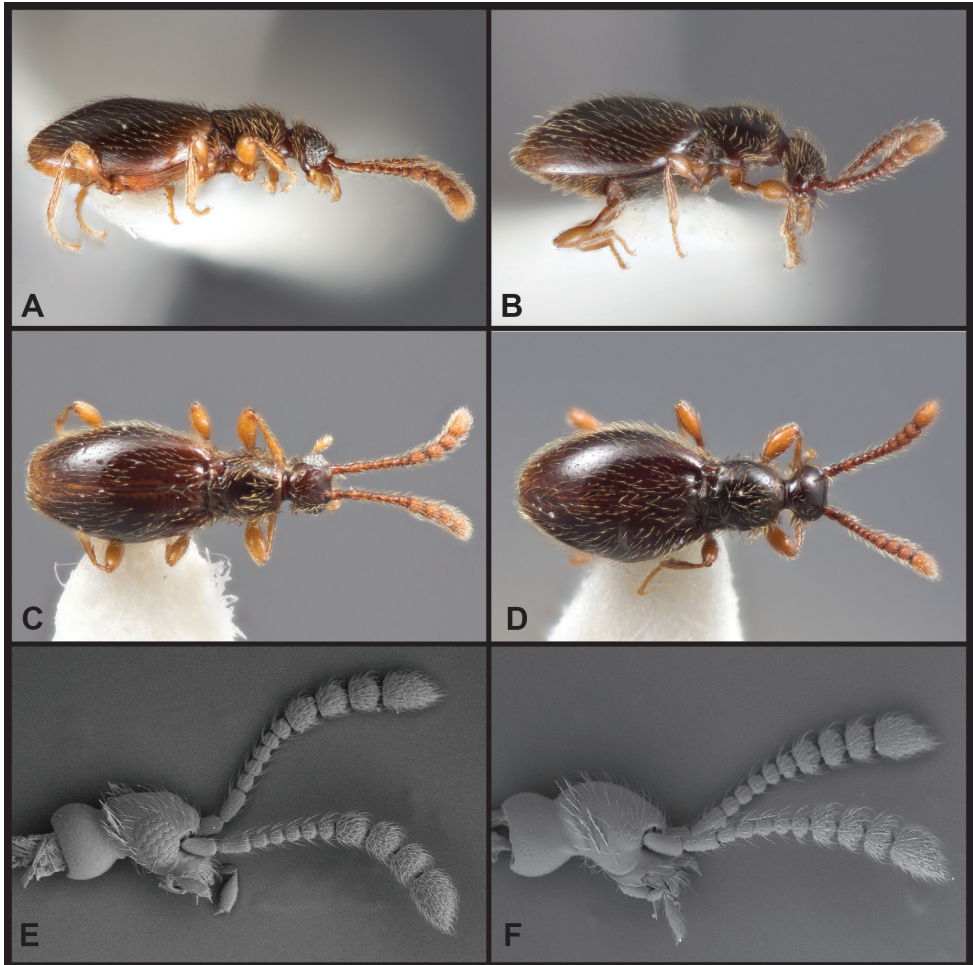


Figure 1. Habitus and character photos of *Euconnus megalops* **A** male, lateral view **B** female, lateral view **C** male, dorsal view **D** female, dorsal view (BgBld.B.349) **E** SEM of male head, lateral **F** SEM of female head, lateral.

antennomeres 3–6 uniformly shorter, ca. as long as wide, male antennomere VII weakly asymmetrical, slightly narrowed anterad, male antennomeres VIII–XI enlarged and elongate (longer than wide) but none carinate on anterior edges (Fig. 1E); female with antennal club tetramerous, antennomeres shorter than width (Fig. 1F). Frons and vertex with long, erect setae, each ca. as long as scape; vertex narrowed to a broadly rounded point; neck ca. one-half maximum head width; frons shallowly depressed between antennal bases; epistoma deeply depressed below antennae; labrum with anterior margin evenly rounded, with comb of short setae at middle. Pronotum densely setose at sides and anteriorly, more sparsely posterad, ‘bell-shaped’, widest just beyond middle, narrowed anterad and posterad, posterior margin slightly widening; pronotum depressed along

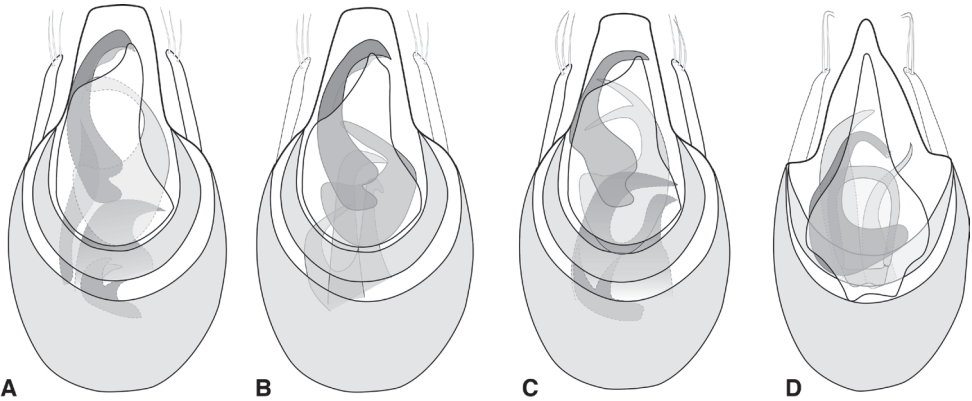


Figure 2. Aedeagus **A** *Euconnus megalops* **B** *Euconnus vexillus* **C** *Euconnus cumberlandus* **D** *Euconnus vetustus*.

posterior margin with very short median longitudinal carina and stronger lateral longitudinal carinae, a distinct fovea on either side between these carinae; a weak sublateral carina merging with lateral one at posterior pronotal corner, a distinct fovea between them (apparently the anterior-most of the two shown for *E. (C.) motschulskii* in Jałoszyński [2018]), and an additional shallow fovea below, on the side; prosternum rather short in front of procoxae, lacking median carina, with dense fringe of setae along anterior margin; elytron sparsely covered with fine setae, with pair of deep foveae at base, longitudinally weakly depressed behind these; elytral apices rounded; mesoscutellar shield hidden; mesoventrite with strong carina, setose along its crest, separating mesocoxae, extending anterad to separate apices of procoxae, posteriorly merging with metaventrite immediately behind mesocoxae; mesepimera densely setose, produced laterad mesocoxa; metacoxae narrowly separated by metaventral process; abdominal ventrites unmodified; legs generally slender, setose; protibia with only weakly expanded adhesive setae along inner margin of apical third. Aedeagus (Fig. 2A) with median lobe broadly truncate, parameres thin, rather short, straight, tapered to apex, each with three or four setae extending to or just beyond apex of median lobe; compressor plate asymmetrical, with apex obliquely truncate to weakly lobed off center; endophallus with asymmetrical armature; upper armature comprising two long curved sclerites, one longer, nearly reaching apex of median lobe at rest, abruptly curved near apex with thin inner blade bridging the apex, its inner edge concave, the other upper sclerite curving opposite, thinner, bluntly rounded at apex; lower armature comprising three separate processes: one basal, short, strongly curved, and with a bifid or trifid apex; one longer, medial, broadly hooked; the third lateral and more slender, elongate, apex acute and variously straight or bending mediad.

Distribution. This species is the most abundant and widespread of the Appalachian *Cladoconnus* species, occurring from Brasstown Bald in the southwest, northeast to Celo Knob in the Black Mts. It also exhibits the widest elevational range of the species, from ca. 900 ft in upstate South Carolina, all the way to the top of Clingmans Dome at 6500 ft.

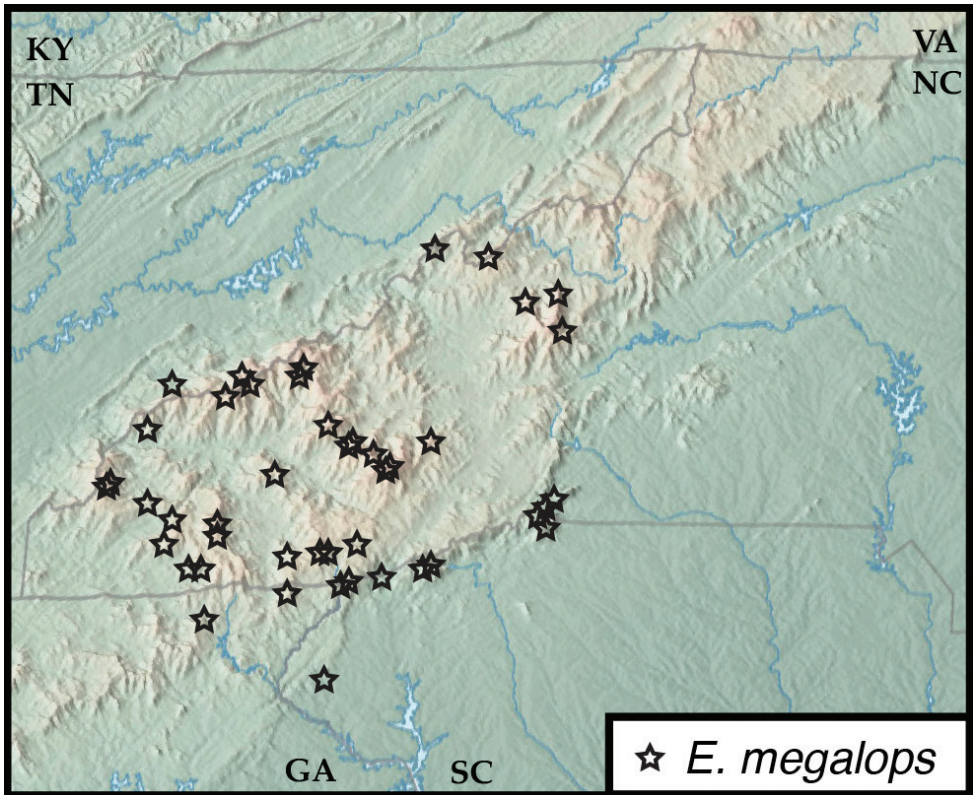


Figure 3. Map of collecting records for *Euconnus (Cladoconnus) megalops*.

Remarks. This species' morphology is relatively invariant across its broad range. The upper sclerites of the endophallic armature vary slightly in apical curvature and shape, but without obvious geographic trends. Similarly, none of these variants correspond to a geographically dispersed, divergent genetic subclade within the broader species, a peculiar result that merits further investigation.

This species name refers to the conspicuously enlarged eyes of the males.

***Euconnus vexillus* sp. nov.**

<https://zoobank.org/47ED180B-4423-46AC-8CA4-3BB1FEDCDB19>

Figs 2B, 4, 5

Type material. *Holotype* ♂, deposited in FMNH: “USA:SC: Greenville Co. 35.1523°N, 82.2814°W, Chestnut Ridge Heritage Preserve, vi.05.2015, S. Myers, Hardwood litter” / “[QR code] CLEMSON ENT CUAC000026944”. *Paratypes* (10, CUAC, FMNH) – 2 ♂, 2 ♀: same data as type; 1 ♂, 1 ♀: “USA:SC: Greenville Co. 35.1518°N, 82.2839°W, Chestnut Ridge Heritage Preserve, vi.05.2015, S. Myers, Hardwood

litter”; 1 ♀: “USA:SC: Greenville Co. 35.1501°N, 82.2820°W, Chestnut Ridge Heritage Preserve, vi.05.2015, S. Myers, Hardwood litter”; 2 ♀: “USA:SC: Greenville Co. 35.1406°N, 82.2790°W, Chestnut Ridge Heritage Preserve, vi.05.2015, S. Myers, Hardwood litter”; 1 ♀: “USA:SC: Greenville Co. 35.1506°N, 82.2799°W Chestnut Ridge Heritage Preserve, iv.08.2018, M. Caterino & L. Vásquez-Vélez, sifted litter”.

Other material. (26) **WV:** Mercer Co., Camp Creek State Forest, 23-Jul-1971, leaf litter (4 ♂, 11 ♀); ‘Black Mts’, x.1901 (3 ♂); **NC:** Caldwell Co., Grandfather Mt. State Park, Nuwati Trail, 4020 ft., 17-May-2021 (1 ♂); McDowell Co., Pisgah National Forest, Mackey Mountain Trail, 3433 ft., 25-Aug-2015 (2 ♂); McDowell Co., Pisgah National Forest, Snooks Nose Trail, 1998 ft., 25-Aug-2015 (3 ♀, 1 ♂); Polk Co., Green River Game Lands, 1740 ft., 18-Mar-2018 (1 ♂).

Diagnostic description. This species is very similar to the preceding species and can best be distinguished by male genitalic and antennal characters. Like the preceding, males are winged, while females appear not to be. A few noteworthy external differences can also be cited: males with distinct carinae on antennomeres VIII and IX (Fig. 4E); female antennae less distinctly tetramerous, with antennomere VIII intermediate in size between antennomeres VII and IX (Fig. 4D); body darker, stout, with only faintly rufescent elytral humeri, most distinctly lighter along posterior half of elytral suture; male eyes smaller, less protuberant, with only ~ 25 ommatidia; median basal carina of pronotum slightly better developed to base (Fig. 4F); aedeagus (Fig. 2B) with median lobe broadly truncate at apex; parameres short, tapered, bearing three apical setae; compressor plate strongly asymmetrical, rather short; endophallic armature with strong pair of upper processes: the left long and strongly hooked apically, with a thin inner laminar blade, its inner edge concave; the right shorter, more strongly curved toward middle of longer process; lower endophallic armature consisting of three hook-like processes of varying lengths, the lateral-most rather short and strongly curved, the medial-most of intermediate length, the one between them the longest, its tip just visible between bases of upper processes (in ‘dorsal’ view).

Distribution. This species has been found at several widely scattered localities east and northeast of the Asheville Depression, from the headwaters of the French Broad near the southern end of its range, at Chestnut Ridge, South Carolina, to southern West Virginia in the northeast. Most of its occurrences are at middle elevations, from 1090 to 4020 ft, most below 2000.

Remarks. This species is similar and, judging by male genitalia, closely related to *E. megalops*. Both have similar opposing hooked upper endophallic sclerites, though the shorter right one (Fig. 2B) of *E. vexillus* is distinctive. Moreover, the lower trio of endophallic sclerites are quite distinct in *E. vexillus*, with three hooks projecting distad to varying lengths. In males, the carinae of antennomeres VII and IX will immediately distinguish this species from *E. megalops*, and the only weakly tetramerous club of females can be used to distinguish most of those, although they are similar to darker females of *E. adversus*.

This species name means ‘standard (or flag)-bearer’, referring to its possession of *Cladoconnus*-typical carinae, borne proudly on its antennae.

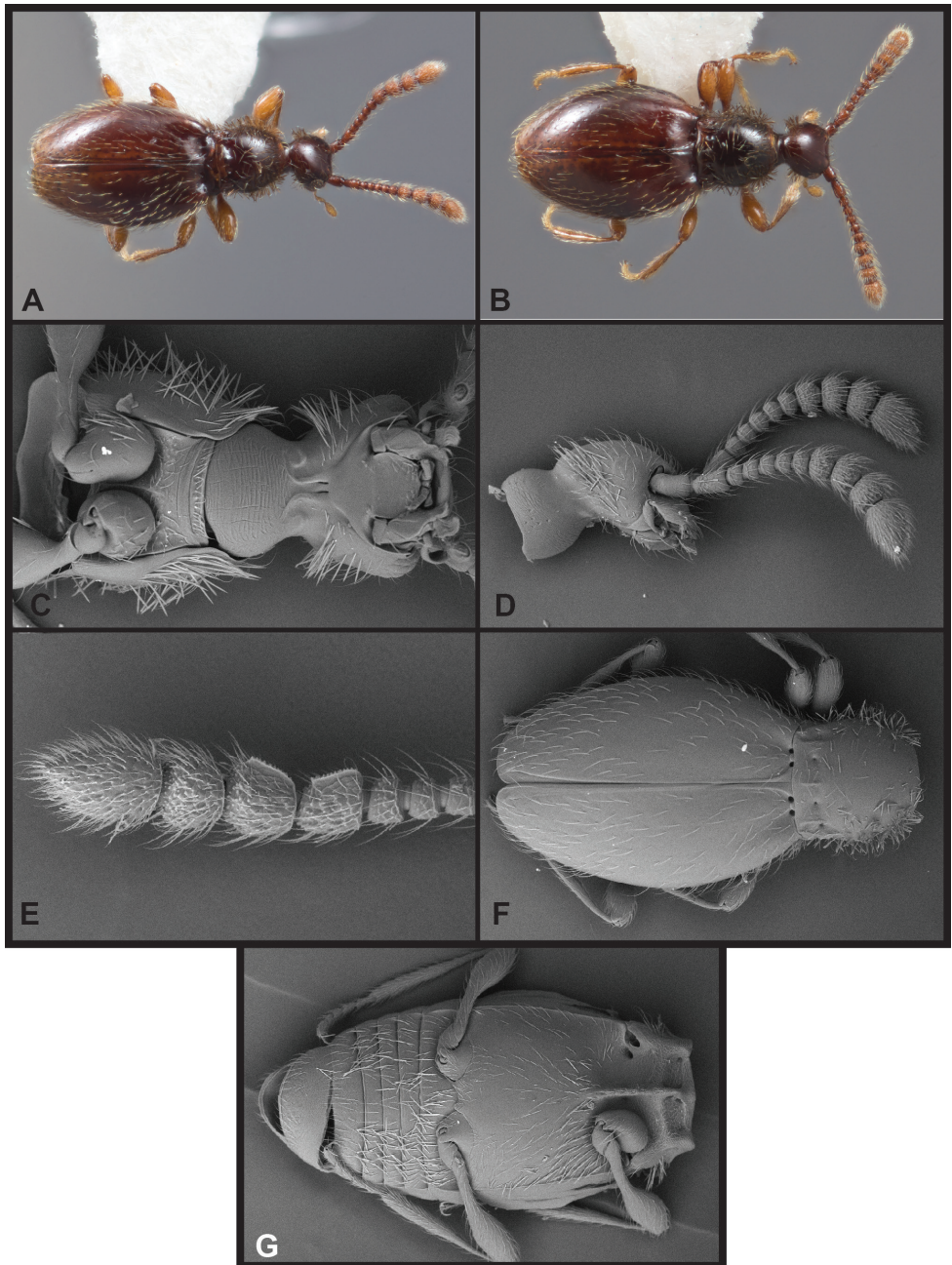


Figure 4. Habitus and character photos of *Euconnus vexillus* **A** male, dorsal view **B** female, dorsal view **C** SEM of mouthparts, ventral view **D** SEM of female head, lateral **E** SEM of male antenna, lateral **F** SEM of elytra and pronotum **G** SEM of meta- and mesoventrites.

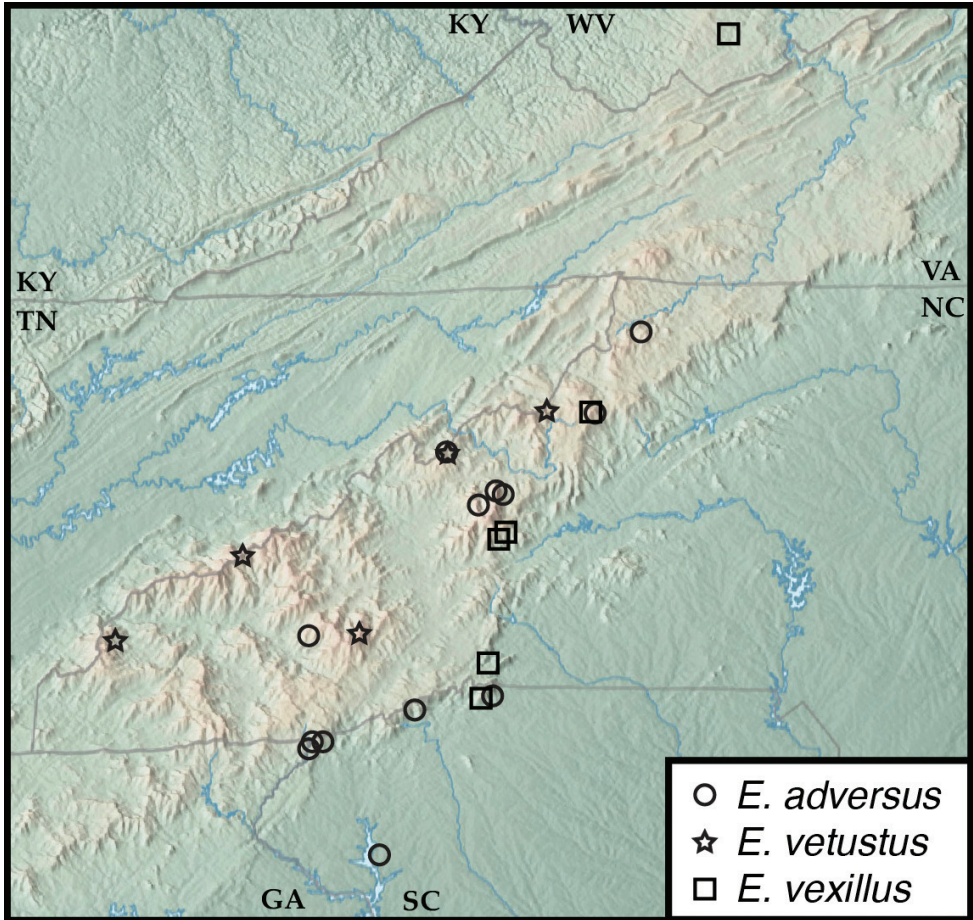


Figure 5. Map of collecting records for *Euconnus* (*Cladoconnus*) *vexillus* (squares), *E. (C.) vetustus* (stars), and *E. (C.) adversus* (circles).

***Euconnus cumberlandus* sp. nov.**

<https://zoobank.org/8E94B9B6-C01A-4460-AC19-4E34FFFE452D>

Figs 2C, 6, 7

Type material. *Holotype* ♂, deposited in FMNH: “Fall Creek Falls S.Pk., Van Buren Co., TENN, 13.X.1962” / “*Rhododendron* duff, H.R.Steeves, leg.” / “Caterino DNA Voucher Extraction MSC12284”. *Paratypes* (9, FMNH, CUAC, CMNC): 2 ♂, 2 ♀: same data as type; 3 ♀, 2 ♂: “Fall Creek Falls S.Pk., Fall Creek Falls Pit, Bledsoe Co., TENN., 14.X.1961” / “*Rhododendron* duff, H.R.Steeves, leg.”.

Other material. (12, CMNC, CUAC, FMNH) **TN:** Grundy Co., Savage Gulf State Natural Area, 1150ft., 4-May-2021, Litter – bottom of canyon (2 ♀); Pickett Co., Jamestown, Jordan Motel, 16-Jun-1962, forest floor near falls (1 ♀); **GA:** Dade

Co., Cloudland Canyon State Park, 16-May-1972, rhododendron litter (2 ♂, 5 ♀); Dade Co., Cloudland Canyon State Park, 7-Aug-1962, forest floor (1 ♂, 1 ♀).

Diagnostic description. This species is very similar to the preceding species and can best be distinguished by male genitalic characters. Like the preceding, males are winged, while females appear not to be. The antennal carinae of male antennomeres VIII and IX are present but rather weakly developed (Fig. 6), with neither quite spanning the entire length of the antennomere itself; female antennae less distinctly tetramerous, with antennomere VIII intermediate in size between antennomeres VII and IX; body darker, stout, with only faintly rufescent elytral humeri, most distinctly lighter along posterior half of elytral suture; male eyes smaller, less protuberant, with only ~ 25 ommatidia; aedeagus (Fig. 2C) with median lobe broad, apex weakly rounded, slightly narrowed subapically; parameres short, tapered, bearing three apical setae; compressor plate asymmetrical, produced to subacute tip on right side; endophallic armature with strong pair of upper processes: the left long and strongly hooked apically; the right shorter, strongly bifid, its apices extending beneath left process; lower endophallic armature consisting of four hook-like processes of varying lengths, two longer and moderately to strongly hooked, two shorter ones borne on a single sclerite, apices directed distad.

Distribution. This species is known from northwestern Georgia to north-central Tennessee. Two of the Tennessee localities, including the northernmost, are represented only by females, and they can be assigned only tentatively to this species.

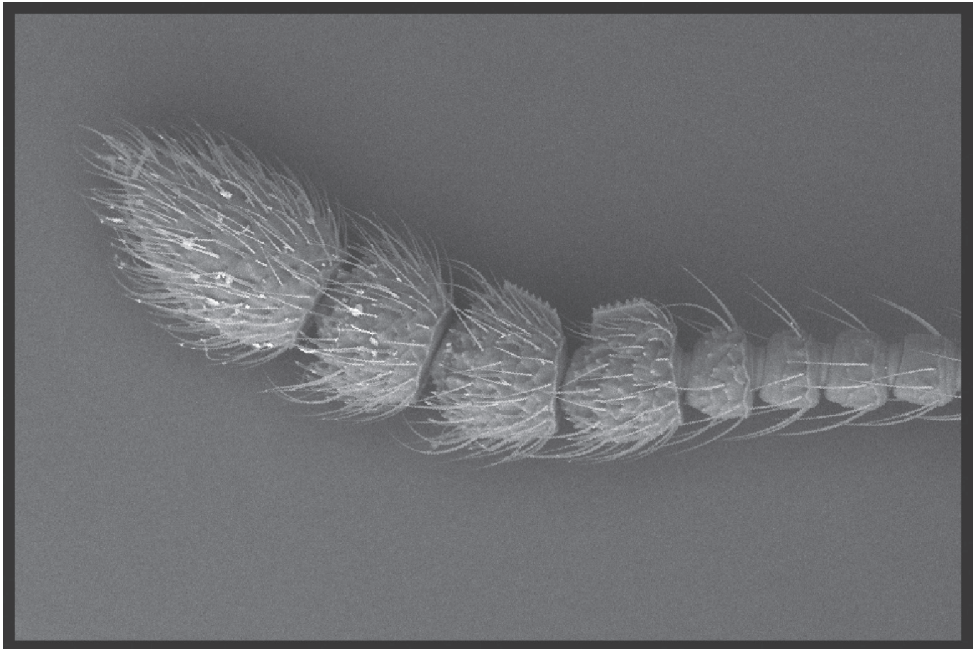


Figure 6. Antennal carina of *E. cumberlandus*.

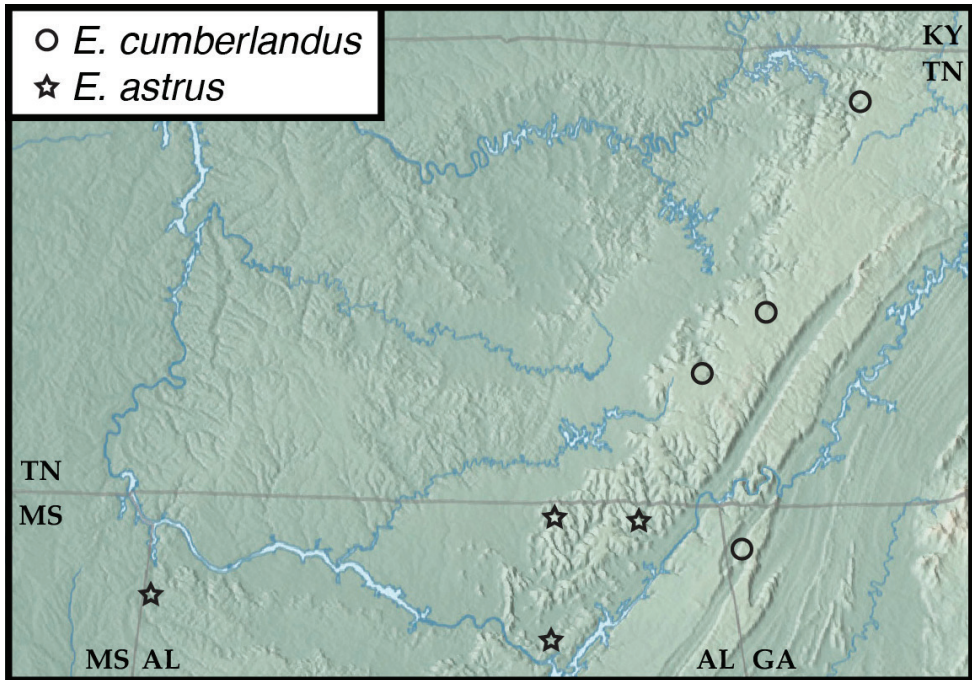


Figure 7. Map of collecting records for *Euconnus* (*Cladoconnus*) *cumberlandus* (circles) and *E. (C.) astrus* (stars).

Remarks. This species is similar to and apparently closely related to *E. megalops* and *E. vexillus*. The only sequenced specimen of this species is a female from Savage Gulf, TN, a locality not yet represented by males. Sequences from other localities, including the type locality would help confirm the species' unity as circumscribed here.

***Euconnus vetustus* sp. nov.**

<https://zoobank.org/417B9BE8-BE69-4792-926B-3B4FA19CD3DD>

Figs 2D, 5, 8

Type material. *Holotype* ♂, deposited in FMNH: “USA: NC: Mitchell Co., 36.1038°N, 82.0809°W, PisgahNF, vi.8.2020 Grassy Ridge Bald, 6083’, M. Caterino, deciduous shrub litter” / “[QR code] CLEMSON-ENT CUAC000004025” / “Caterino DNA Voucher Extraction MSC4491, Morphosp. GrB.A.336”. *Paratypes* (4) – 2 ♀, 2 ♂: same data as type.

Other material. (7) – **NC:** Graham Co., Nantahala National Forest, Huckleberry Knob, 5511 ft., 13-Oct-2020 (1 ♂); Haywood Co., Pisgah National Forest, Black Balsam Knob, 6072 ft., 7-May-2018 (1 ♂); Yancey Co., Pisgah National Forest, Devils Gap, 3813 ft., 24-Aug-2015 (2 ♂); ‘Black Mts’ (1 ♀); **TN:** Unicoi Co., Cherokee

National Forest, Big Bald, 5430–5464 ft., 5-Aug-2020 & 21-May-2021 (1 ♀, 2 ♂); Sevier Co., Great Smoky Mountains National Park, Off Hwy 441, 4575 ft., 12-Mar-2020 (1 ♀).

Diagnostic description. This species is similar to the preceding species being dark in color and wing-dimorphic, and can best be distinguished by male genitalic characters. External differences, however, include smaller body size, entirely dark coloration (Fig. 8A); head, especially crest of vertex, rounder; frons only weakly depressed between antennal bases; male and female eyes do not differ appreciably in size, both having ~ 20 ommatidia; the protibia of both sexes is shorter, widened apically, and bears conspicuously modified setae on the apical half (Fig. 8C); male antennal club tetramerous, with the club segments slightly longer than wide (Fig. 8A), no antennomeres bearing carinae; female antenna shorter, with club 4-segmented, club segments ca. as long as wide (Fig. 8B); aedeagus (Fig. 2D) with median lobe narrowed to narrowly rounded apex; rather straight parameres bear two apical setae extending just to apex of median lobe, these setae finely bent inward at apex; compressor plate symmetrical, narrow, reaching nearly to apex of median lobe; upper endophallic armature with one short curved hook, not extending beyond shoulders of tegmen, its apex blunt and distinctly fringed (at higher magnification); immediately internal to it is a rather broadly rounded thin plate (the apical margin of which is strongly sclerotized, appearing as if maybe a second opposing hook); lower endophallic armature with a long bifid process extending from deep in the basal bulb to beyond its shoulders, the inner blade thin, curving weakly upward, the outer blade longer, reaching to near apex of compressor plate, its apex finely fimbriate.

Distribution. This species occurs over a relatively broad but disparate range, spanning the Asheville Depression, from the Unicois (Huckleberry Knob) in the southwest to the Roan Highlands and Big Bald in the northeast. So far it has not been found in the Black Mts or on Grandfather Mountain. Known occurrences are all at higher elevations, from 4575 to 6100 ft.

Remarks. Individuals from across the broad range of this species show considerable genetic variation, and the male genitalia do show slight variation. Northern examples (Big Bald, Roan Highlands) exhibit a more strongly hooked upper endophallic process. A few specimens, from scattered localities (e.g., Smokies, Balsam Mts., and Roan Highlands), have the bi-arcuate mandibles described for European *Cladoconnus*. But this character varies as well; specimens from Big Bald, NC, have mandibles that are less distinctly arcuate, as well as longer and more slender. Male genitalia have been re-examined with this in mind, but no corresponding differences emerge. Further genetic work and longer series of males may justify separating some of these. Females from Devil's Gap, NC are light in color (perhaps teneral) but match in other characters, including DNA.

The name of this species comes from the Latin for 'old', referring to the possibility the species has inhabited the area for a long time, as judging by its broad distribution, only distant relation to the rest of the species described here, and deep genetic divergences among populations.

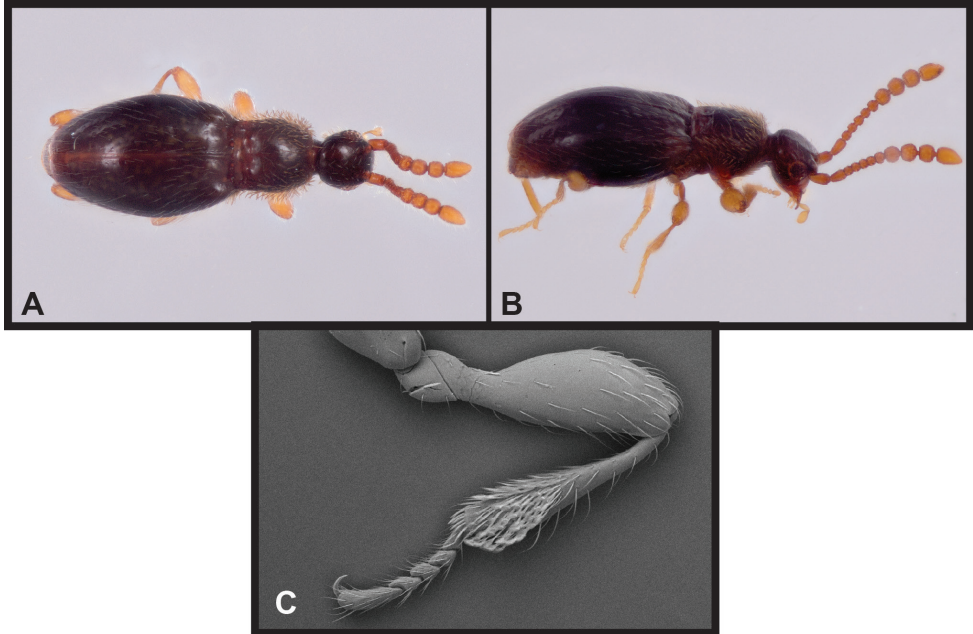


Figure 8. Habitus and character photos of *Euconnus vetustus* **A** male habitus, dorsal (BBK.A.020) **B** male habitus, lateral (GRB.A.336) **C** SEM of protibial setae.

***Euconnus falcatus* sp. nov.**

<https://zoobank.org/868CC7AB-B90A-4337-AE0E-F8329719CAAC>

Figs 9, 10A, B, 11

Type material. *Holotype* ♂, deposited in FMNH: “USA: NC: Swain Co., 35.5566°N, 83.4966°W, SmokyMts NP, 6272’, Clingmans Dome, sifted litter, ix.14.2021, M.Caterino & E.Recuero” / “[QR code] CLEMSON-ENT CUAC000156725” / “Caterino DNA Voucher Extraction MSC7899, Morphosp. CD.B.307”. *Paratypes* (40, CUAC, CNCI, FMNH, UNHC) – 1 ♂: “USA: NC: Swain Co., 35.5613°N, 83.5006°W, SmokyMts NP, 6364’, ClingmansDome, W. slope, sifted litter, vi.5.2018, M.Caterino” / “[QR code] CLEMSON-ENT CUAC000079152” / “Caterino DNA Voucher Extraction MSC2834 Morphosp. CD.A.021”; 1 ♀, 3 ♂: “USA: NC: Swain Co., 35.5824°N, 83.3979°W, SmokyMtsNP,offHwy 441, 4610’, iii.12.2020, M.Caterino & F.Etzler, sifted litter”; 1 ♀: “USA: TN: Swain Co., 35.6237°N, 83.4163°W, SmokyMtsNP,offHwy 441, 4575’, iii.12.2020, M.Caterino & F.Etzler, sifted litter” / “[QR code] CLEMSON-ENT CUAC000110837” / “Caterino DNA Voucher Extraction MSC4193 Morphosp. Hwy.A.006”; 1 ♀, 8 ♂: “USA: TN: Sevier Co., 35.6160°N, 83.4149°W, SmokyMts NP, 5456’, App.Tr. E of Newfound Gap, sifted litter, vi.5.2018, M.Caterino”; 2 ♀, 9 ♂: “USA: TN: Sevier Co., 35.6308°N, 83.3904°W, SmokyMts NP, 6190’, Mt. Kephart, vi.5.2018, M.Caterino”; 1 ♂: “USA: TN: Sevier Co., 35.6311°N, 83.3895°W, SmokyMts NP, 6183’, Mt. Kephart,sifted

litter, vi.5.2018, M.Caterino” / “[QR code] CLEMSON-ENT CUAC000079110” / “Caterino DNA Voucher Extraction MSC2790 Morphosp. MK.A.009”; 1 ♂: “USA: TN: Sevier Co., 35.6311°N, 83. 3893°W, SmokyMts NP, 6187’, Mt. Kephart, sifted litter, ix.14.2021, M.Caterino & E.Recuero” / “[QR code] CLEMSON-ENT CUAC000156767” / “Caterino DNA Voucher Extraction MSC7941 Morphosp. MK.B.482”; 4 ♀, 4 ♂: “USA: TN: Sevier Co., 35.6425°N, 83.4427°W, SmokyMts NP, 5196’, Alum Cave Tr., vi.25.2019, M.Caterino & M.Ferro, sifted mixed litter”; 1 ♂: “USA: TN: Sevier Co., 35.6529°N, 83.4378°W, SmokyMts NP, 6467’, Mt LeConte, vi.25.2019 M.Caterino & M.Ferro, sifted conifer litter” / “[QR code] CLEMSON-ENT CUAC000079302” / “Caterino DNA Voucher Extraction MSC3483 Morphosp. MLc.009”; 1 ♀, 1 ♂: “USA: TN: Sevier Co., 35.6541°N, 83.4364°W, SmokyMts NP, 6588’, Mt LeConte, ix.28.2021, M.Caterino, sifted litter”; 1 ♂: “NC Gr.Sm.Mts.N.P., Clingmans Dome, 1950–2020m 2.VI.86 A.Smetana” (CMNC); 1 ♂: “TENN:Great Smoky Mts.St.Pk.: Newfound Gap” / “X.24.1969 W.Shear + F.Coyle leg.” / “FM(HD) 69–62 Spruce litter” (FMNH).

Other material. (36, CUAC, UNHC, CNCI) – **NC:** Haywood Co., Pisgah National Forest, Black Balsam Knob, 6033–6072ft, 7-May-2018 & 20-Oct-2020 (3 ♂); Haywood Co., Pisgah National Forest, Mountains to Sea Trail, 5540ft., 8-Sep-2020 (1 ♂); Haywood Co., Blue Ridge Parkway National Park, Mt. Pisgah, 5420ft., 13-Sep-2022 (1 ♀, 1 ♂); Jackson Co., Blue Ridge Parkway National Park, Mt. Lyn Lowry, 6097 ft., 15-Jun-2021, sifted litter (1 ♀); Jackson Co., Blue Ridge Parkway National Park, Mt. Lyn Lowry, 6205 ft., 22-Sep-2020, sifted litter (1 ♀); Jackson Co., Blue Ridge Parkway, National Park, along Blue Ridge Pkwy, 5572ft., 11-Sep-2019 (1 ♀, 1 ♂); North Carolina, Jackson Co., Blue Ridge Parkway National Park, Browning Knob, 6140–6221, 22-Sep-2020 & 29-May-2018 (3 ♀, 1 ♂); Jackson Co., Blue Ridge Parkway National Park, Waterrock Knob, 6059, 29-May-2018 (4 ♀, 4 ♂); Jackson Co., Blue Ridge Parkway National Park, Waterrock Knob, 6281, 29-May-2018; Jackson Co., Balsam Mountain Preserve, Doubletop Mountain, 5396–5480, 7-Feb-2015 & 15-Jun-2015 (4 ♂); Jackson Co., Nantahala National Forest, Toxaway Mt., 4750, 5-Aug-2020 (1 ♂); Jackson Co., Wolf Mt. overlook, 26-May-1986 (3 ♂); Jackson Co., Blue Ridge Parkway National Park, 5572, 11-Sep-2019 (1 ♀); Macon Co., Nantahala National Forest, Copper Ridge Bald, 5144, 9-Jul-2019 (1 ♂); Macon Co., Hwy. 64, nr. Dry Falls, 16-May-1986 (2 ♀, 1 ♂); Macon Co., Coweeta Hydrological Lab, Shope Fork, 3200, 28-May-1983 (1 ♂).

Description. Body rufescent (Fig. 9A–D), weakly translucent; head and elytra sparsely setose, pronotum densely setose, especially at sides; head with frons weakly depressed between antennal bases (Fig. 9H), vertex convex, neck just over one-half maximum head width; eyes of male moderately large, protuberant, comprising ca. 15 distinct ommatidia (Fig. 9H), situated immediately behind antennal insertions, width slightly more than that of tempora behind; eyes of female smaller (Fig. 9G), less prominent, comprising < 8 ommatidia, width only one-third that of tempora; antennae inserted under blunt frontal shelf; antennae of male with scape and pedicel

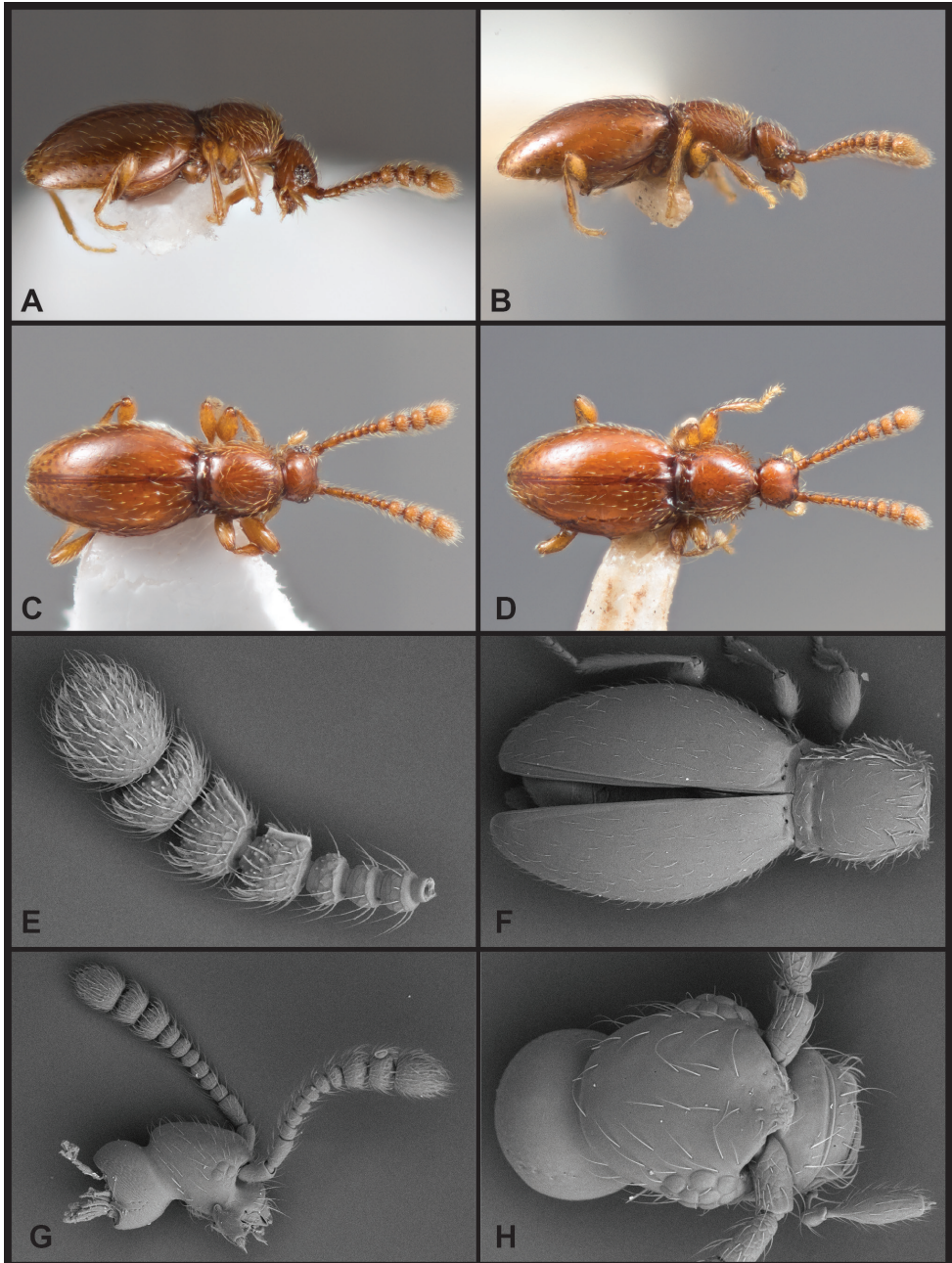


Figure 9. Habitus and character photos of *Euconnus falcatus* **A** male, lateral view **B** female, lateral view **C** male, dorsal view **D** female, dorsal view **E** SEM, male antenna **F** SEM, pronotum and elytra **G** SEM, female head, lateral view **H** SEM, male head, anterior view.

similar in length, ca. twice length of antennomeres III–VI, antennomere VII slightly larger, asymmetrical, slightly produced on anterior margin, antennomeres VIII–XI distinctly larger, antennomeres VIII and IX with longitudinal carinae on anterior margin (Fig. 9E), that of VIII more or less parallel to antennal axis, that of IX more strongly produced at apex, antennomeres VIII–X similar in length, terminal antennomere ca. twice as long; female antennae shorter, club composed of only three short, wide antennomeres (Fig. 9D, G); pronotum weakly bell-shaped, with sides arcuate (Fig. 9F), widest ca. one-fourth behind straight anterior margin, narrowed posteriorly, similar in width to anterior, with short longitudinal carinae on either side, transversely depressed between, with small submedian foveae on either side of low median ridge (median basal carina absent), and two small foveae outside lateral carina, pronotal sides very densely bristled; mesoscutellar shield hidden; elytra broadly rounded, widest just anterad middle, each with two small basal foveae, sparse setae randomly arranged; flight wings poorly developed or absent in both sexes; abdominal ventrites without secondary sexual differences; aedeagus (Fig. 10A) broadly rounded basally, apex of median lobe narrowed, pinched before apex, subtruncate; parameres thin, close to median lobe, with two long apical setae extending beyond median lobe apex; dorsal diaphragm crescent-shaped; compressor plate thin, narrowly rounded at apex, slightly asymmetrical; endophallus with two asymmetrical primary sclerites, an upper one almost linear, weakly sinuous to acute apex, the lower one strongly sickle-shaped, bearing a single conspicuous and sometimes an additional small secondary processes on its inner surface.

Distribution. *Euconnus falcatus* exhibits a wide distribution, especially considering its flightlessness, including the Great Smoky Mountains, continuing along the high Blue Ridge Parkway corridor into the Plott Balsams and Great Balsams, as well as slightly lower parts of the Nantahala and Cowee Mountains. In elevational range it occurs from 3200 ft at Coweeta to its highest occurrences on Clingmans Dome and Mt. LeConte above 6500 ft.

Remarks. A more complete description of this species is provided to serve as a general description for several subsequent species that differ in few or no obvious external characters, including *E. cataloochee*, *E. kilmeri*, *E. draco*, *E. tusquitee*, *E. attritus*, *E. cultellus*, *E. adversus*, and *E. astrus*. The modified male antennomeres differ significantly in a couple of these (*E. adversus* and *E. astrus*), but only slightly or not at all in the others. *Euconnus falcatus* can only be unambiguously distinguished from the others by male genitalic characters. Specifically, the lower endophallic sclerite is long, sickle-shaped, and bears a small secondary hook near its midpoint. The apex of the median lobe is more narrowly knobbed than most others, and the apex of the compressor plate is only subtly asymmetrical. There appear to be some differences in exact shapes of endophallic sclerites among localities (e.g., Fig. 10B). Some of this variation may be real, but some also appears to result from varying degree of extroversion of the lower hooked sclerite relative to the upper one.

This species name refers to the distinctively ‘sickle-shaped’ hook of the endophallic armature.

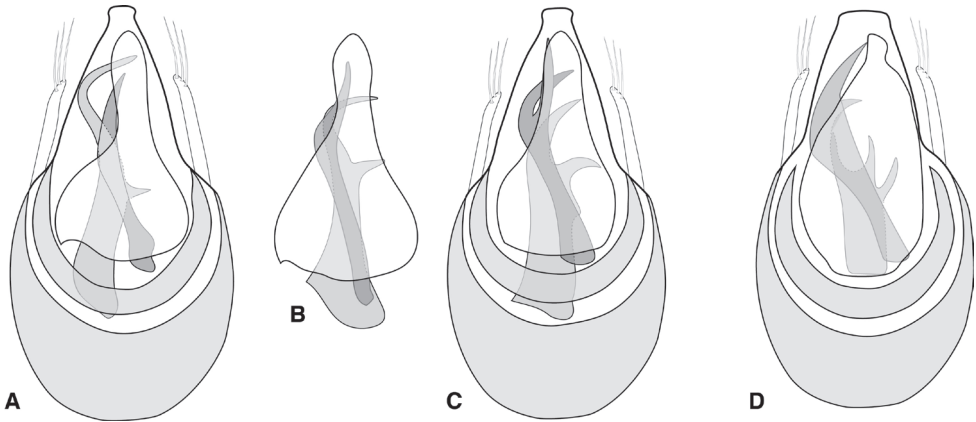


Figure 10. Aedeagus. **A** *Euconnus falcatus* **B** compressor plate and upper endophallic armature of *Euconnus falcatus* (Plott Balsams variant) **C** *Euconnus cataloochee* **D** *Euconnus kilmeri*.

***Euconnus cataloochee* sp. nov.**

<https://zoobank.org/FD84FEAD-72A4-4FBD-B0D6-B3A76AA6B697>

Figs 10C, 11

Type material. *Holotype* ♂, deposited in FMNH: “USA: NC: Haywood Co., 35.6721°N, 83.1760°W, Smoky Mts NP, 6150’, Big Cataloochee Mt., xi.5.2020, sifted litter, M.Caterino & F.Etzler” / “[QR code] CLEMSON-ENT CUAC000135173” / “Caterino DNA Voucher Extraction MSC6485 Morphosp. BCat.B.315”. *Paratypes* (32 – CUAC, FMNH, CNCI, UNHC): 7 ♀, 7 ♂: same data as type; 5 ♀, 5 ♂: “USA: NC: Haywood Co., 35.6453°N, 83.2025°W, SmokyMtsNP, Balsam Mt.Tr., 5086’, xi.5.2020, M.Caterino & F.Etzler, Sifted litter”; 1 ♀, 1 ♂: USA: NC: Haywood Co., 35.6686°N, 83.1749°W, Smoky Mts NP, 5725’, Big Cataloochee Mt., vii.14.2020, sifted litter, M.Caterino, F.Etzler”; 1 ♂: “USA: NC: Haywood Co., 35.6724°N, 83.1761°W, Smoky Mts NP, 6130’, Big Cataloochee Mt., vii.14.2020, sifted litter, M.Caterino, F.Etzler”; 3 ♀, 2 ♂: “USA: NC: Haywood Co., 35.6675°N, 83.1805°W, Smoky Mts NP, 5586’, MtSterlingTr@Lost BottomCk, vii.14.2020 M.Caterino& F.Etzler, sifted litter”.

Diagnostic description. This species exhibits no obvious external differences from the preceding species and can only be distinguished by male genitalic characters. Antennomere VIII of male slightly more strongly produced at inner basal corner, slightly oblique to antennal axis; aedeagus (Fig. 10C) with median lobe slightly narrowed, pinched near apex, bluntly rounded; parameres curving slightly inward at tips, each with three apical setae; compressor plate weakly asymmetrical and narrowly rounded; endophallus with two asymmetrical primary sclerites, one long, sinuate, apically bifid, with lateral hook curving beneath a median apically directed spear; lower endophallic sclerite originating nearer base, broad at base, subdivided into two widely spaced apical hooks, curving the same direction as inner hook of upper sclerite.

Distribution. This is a very restricted species, only known from a couple localities on or very near Big Cataloochee Mountain in the Smokies, and is only known above 5100 ft.

Remarks. The bifid apex of the upper endophallic sclerite is similar to that of *E. cultellus*, but the subapical (lower) tip is more strongly developed, almost appearing as a separate sclerite. The two well-developed hooks on a shorter overall lower endophallic sclerite distinguish it from *E. falcatus*. Sequence differences from the latter are minimal to non-existent, suggesting either very recent ancestry or introgression, as they do seem to be sympatric in the central Great Smoky Mountains, the only locality known for *E. cataloochee*.

This species is named for its type locality, Big Cataloochee Mt., as it is known from only a small area near its summit. The name apparently comes from a Cherokee word referring to the prominent wooded ridges in this region of the Great Smoky Mountains.

***Euconnus kilmeri* sp. nov.**

<https://zoobank.org/435F225A-A9C8-4F63-AEE1-262A9852E969>

Figs 10D, 11

Type material. *Holotype* ♂, deposited in FMNH: “USA:NC: Graham Co., 35.3433°N, 83.96207°W, Joyce Kilmer, VII.20.2015 S. Myers, Sifted litter” / “[QR code] CLEMSON-ENT CUAC000011399” / “Caterino DNA Voucher Extraction MSC11827”; *Paratypes* (0).

Diagnostic description. This species exhibits no obvious external differences from the preceding two species, and can best be distinguished by male genitalic characters; antennal carinae slightly weaker than preceding; aedeagus (Fig. 10D) with median lobe rather short, narrowed to bluntly rounded apex, only very weakly knobbed; parameres with apices obliquely truncate, bearing three long, curved setae; compressor plate strongly asymmetrical, apex narrowly knobbed and displaced to one side; endophallus with dominant upper sclerite sickle-shaped, with long straight inner edge, outer edge strongly curved, broadest just beyond middle, bearing a secondary inner tooth directed mediad and inward; lower endophallic sclerite shorter, bearing two widely separated distally pointing spikes, and an obliquely directed subapical spike on one side.

Distribution. *Euconnus kilmeri* is only known from a single locality within the Joyce Kilmer Memorial Forest in far western North Carolina. This site sits at an elevation of 2800ft.

Remarks. The aedeagus of *E. kilmeri* is quite distinct in the shape of the strongly asymmetrical compressor plate, the long, straight inner edge of the upper endophallic sclerite, and in the trifid lower sclerite, with two apically pointing spines similar in length.

This species is named to honor the American poet Joyce Kilmer “I think that I shall never see, a poem as lovely as a tree...” for whom the type locality stands as a proper monument to his appreciation for nature.

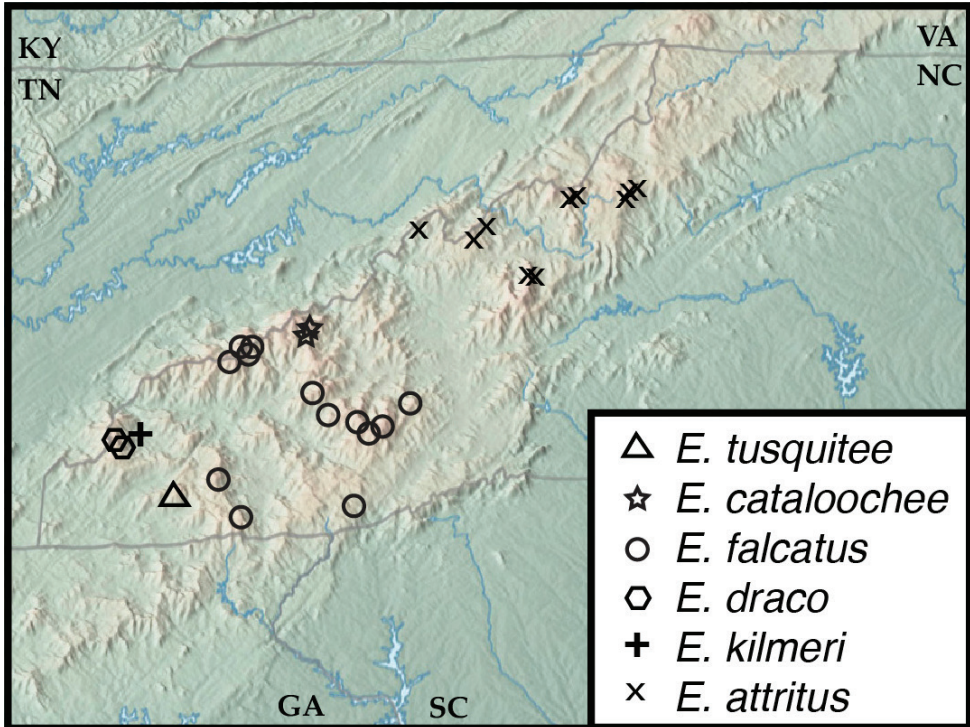


Figure 11. Map of collecting records for *Euconnus* (*Cladoconnus*) *falcatus* complex. *E. (C.) falcatus* (circles), *E. (C.) cataloochee* (stars), *E. (C.) tusquitee* (triangles), *E. (C.) draco* (hexagons), *E. (C.) kilmeri* (plus sign), and *E. (C.) attritus* (x).

***Euconnus draco* sp. nov.**

<https://zoobank.org/4C7107D3-59AB-4C24-BBFF-A56EDD2568AB>

Figs 11, 12A

Type material. *Holotype* ♂, deposited in FMNH: “USA:NC: Graham Co., 35.3216°N, 83.9929°W, NantahalaNF, v.4.2020 5522’, Huckleberry Knob, M.Caterino & F.Etzler, sifted spruce litter” / “[QR code] CLEMSON-ENT CUAC000135352” / “Caterino DNA Voucher Extraction MSC6877 Morphosp.HKnb.B.329”. *Paratypes* (6, CUAC, FMNH) – 3 ♂: same data as type; 1 ♀: “USA:NC: Graham Co., 35.3210°N, 83.9934°W, NantahalaNF, v.4.2020, 5491’, Huckleberry Knob, M.Caterino&F.Etzler, sifted deciduous litter” / “[QR code] CLEMSON-ENT CUAC000003924” / “Caterino DNA Voucher Extraction MSC4308 Morphosp.HKnb.A.048”; 1 ♀, 1 ♂: “USA:NC: Graham Co., 35.3171°N, 83.9833°W, NantahalaNF, v.4.2020, 4702’, Cherohala Skyway, M.Caterino & F.Etzler, sifted deciduous litter”

Diagnostic description. This species exhibits no obvious external differences from the preceding three, and can best be distinguished by male genitalic characters; its male antennomere IX has the apical corner quite dentate; aedeagus (Fig. 12A) with apex

of median lobe narrowly knobbed and bluntly rounded; parameres weakly curving inward to apices, each bearing three long apical setae; compressor plate weakly asymmetrical, broadly rounded, nearly reaching to apex of median lobe; endophallus with two asymmetrical primary sclerites, upper sclerite long and narrowly sickle-shaped, its apex straight and acute; lower sclerite with three inwardly directed hooks, the apical-most long, thin, curved, median hook thicker, more strongly bent inward, basal-most thick, short, close to median.

Distribution. *Euconnus draco* is also basically a single site endemic, known only from the vicinity of Huckleberry Knob, at 5500ft in the Unicoi Mts. The second, Cherochala Skyway locality is only 1km away, and just slightly lower at 4700ft.

Remarks. The long, trifid lower endophallic sclerite of *E. draco*, with the apical hook long and thin, best distinguishes this species. The shape of the median lobe, compressor plate, and upper endophallic sclerite are otherwise quite similar to *E. falcatus*.

This name of this species derives from the Latin ‘dragon’, as its type locality is near the popular motoring route ‘Tail of the Dragon’.

***Euconnus tusquitee* sp. nov.**

<https://zoobank.org/7F5099B6-92EE-4C41-B3FE-7C6203F5554D>

Figs 11, 12B

Type material. *Holotype* ♂, deposited in FMNH: “USA:NC: Clay Co., 35.1419°N, 83.7269°W, NantahalaNF, Tusquitee Bald, vii.6.2021, 5270’, *Quercus/Tsuga* litter M.Caterino & E.Recuero” / “[QR code] CLEMSON-ENT CUAC000171987” / “Caterino DNA Voucher Extraction MSC11727 Morphosp.TsqBld_171987”.

Paratypes (1) – DNA only, voucher lost in extraction: same data as type, DNA Extract 7816, MorphospeciesTsqB.A.223.

Diagnostic description. This species exhibits no obvious external differences from the preceding species, and can best be distinguished by male genitalic characters; carina of male antennomere VIII slightly oblique, ~ 20 degrees off the long axis of the antenna; aedeagus (Fig. 12B) with apex of median lobe narrowed to near truncate apex, not knobbed; parameres weakly curved, bearing three apical setae; compressor plate short, strongly asymmetrical, sinuate with blunt median and acute lateral lobes; endophallus with dominant upper asymmetrical sclerite long, broad to middle, with narrow, curving apical portion nearly reaching apex of median lobe, bearing an inner, medially directed secondary tooth just beyond middle; lower endophallic sclerite shorter, reaching just to middle of upper, curving strongly opposite.

Distribution. Another single-site endemic, *Euconnus tusquitee* is only known from Tusquitee Bald in the western Nantahala Mts, at an elevation of 5270 ft.

Remarks. The strongly asymmetrical and unevenly bilobed apex of the compressor plate is the best character for recognizing *E. tusquitee*. The strongly opposing hook on the lower endophallic sclerite is also distinctive. Its sickle-shaped upper endophallic sclerite is longer than, but otherwise similar to that of *E. kilmeri*.

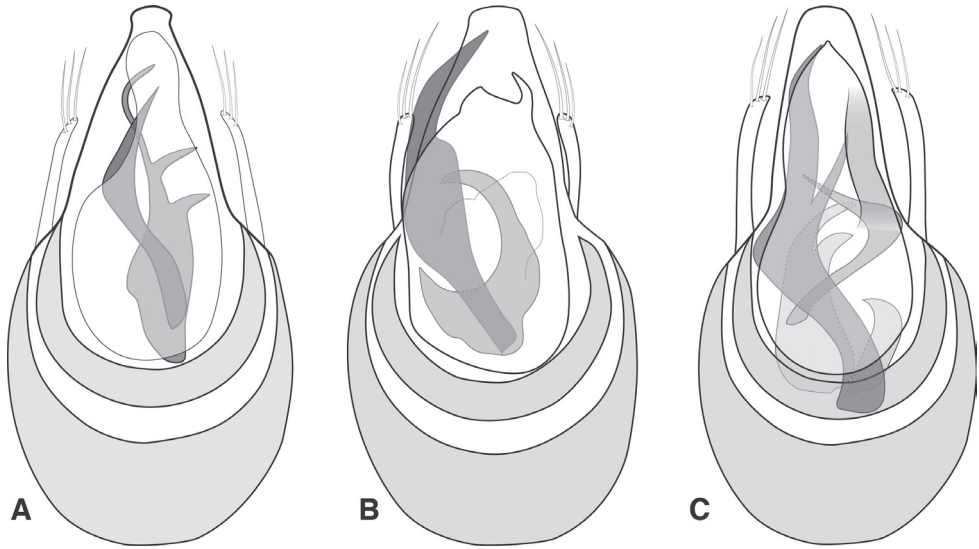


Figure 12. Aedeagus. **A** *Euconnus draco* **B** *Euconnus tusquitee* **C** *Euconnus attritus*.

DNA of two specimens of this species was extracted. The first one was lost in the extraction process, though its DNA and images on the Flickr site (morphospecies code TsqB.A.223) remain. Unfortunately, neither extract sequenced well, so the placement of this species among the others of the *E. falcatus* complex remains uncertain.

This species name refers to its type and only known locality, Tusquitee Bald.

***Euconnus attritus* sp. nov.**

<https://zoobank.org/37927727-6073-4A5B-8B1C-9281D47B3699>

Figs 11, 12C, 13

Type material. *Holotype* ♂, deposited in FMNH: “USA:NC: Mitchell Co., 36.0931°N, 82.1453°W, Roan High Bluff, 6225’ viii.15.2018, M.Caterino, sifted *Abies* litter” / “[QR code] CLEMSON-ENT CUAC000003146” / “Caterino DNA Voucher Extraction MSC3360 Morphosp.RHB.A.012”; *Paratypes* (62, CUAC, FMNH, CNCI, UNHC) – 3 ♀, same data as type; 18 ♀, 16 ♂: “USA:NC: Mitchell Co., 36.0933°N, 82.1447°W, Roan High Bluff, 6251’ viii.15.2018, M.Caterino, sifted *Abies* litter”; 1 ♀, 1 ♂: “USA:NC: Mitchell Co., 36.0999°N, 82.1345°W, Roan High Bluff, 6146’, viii.15.2018, M.Caterino, *Rhododendron* litter”; 2 ♀, 12 ♂: “USA: NC: Mitchell Co., 36.1041°N, 82.1223°W, PisgahNF, vi.8.2020, Roan High Knob, 6276’, M. Caterino, conifer litter”; 5 ♀, 4 ♂: “USA: NC: Mitchell Co., 36.1045°N, 82.1224°W, PisgahNF, vi.8.2020, Roan High Knob, 6286’, M. Caterino, conifer litter”.

Other material. (52) – **TN:** Unicoi Co., Cherokee National Forest, Big Bald, 5237–5346ft, 5-Aug-2020 (1 ♀, 5 ♂); **NC:** Avery Co., Grandfather Mt., 5240–5370ft.,

21-Apr-2022 (4 ♀, 5 ♂); Caldwell Co. Grandfather Mt. State Park, Calloway Peak, 6-Oct-2020 & 17-May-2021, 5775–5915ft. (12 ♀, 13 ♂); Caldwell Co. Grandfather Mt. State Park, Nuwati Tr., 4190ft. (1 ♂); Yancey Co., Pisgah National Forest, Woody Ridge Tr., 5086–5387ft., 15-Jun-2020 (5 ♀, 4 ♂); Yancey Co., Pisgah National Forest, Celo Knob, 6300ft., 19-Oct-2021 (1 ♂); Madison Co., Pisgah National Forest, Camp Creek Bald, 4741ft., 1-Mar-2022 (1 ♂).

Diagnostic description. This species is extremely similar in external morphology to many of the preceding, and is also best distinguished by male genitalic characters. However, it does exhibit a few unusual characters. The male antennomeres VIII-IX are slightly enlarged, but lack carinae on their inner/anterior edges (Figs. 13A, E); the female's antennal club is shorter, and essentially trimerous (Fig. 13D), though antennomere VIII is slightly enlarged relative to VII; males and females flightless; median

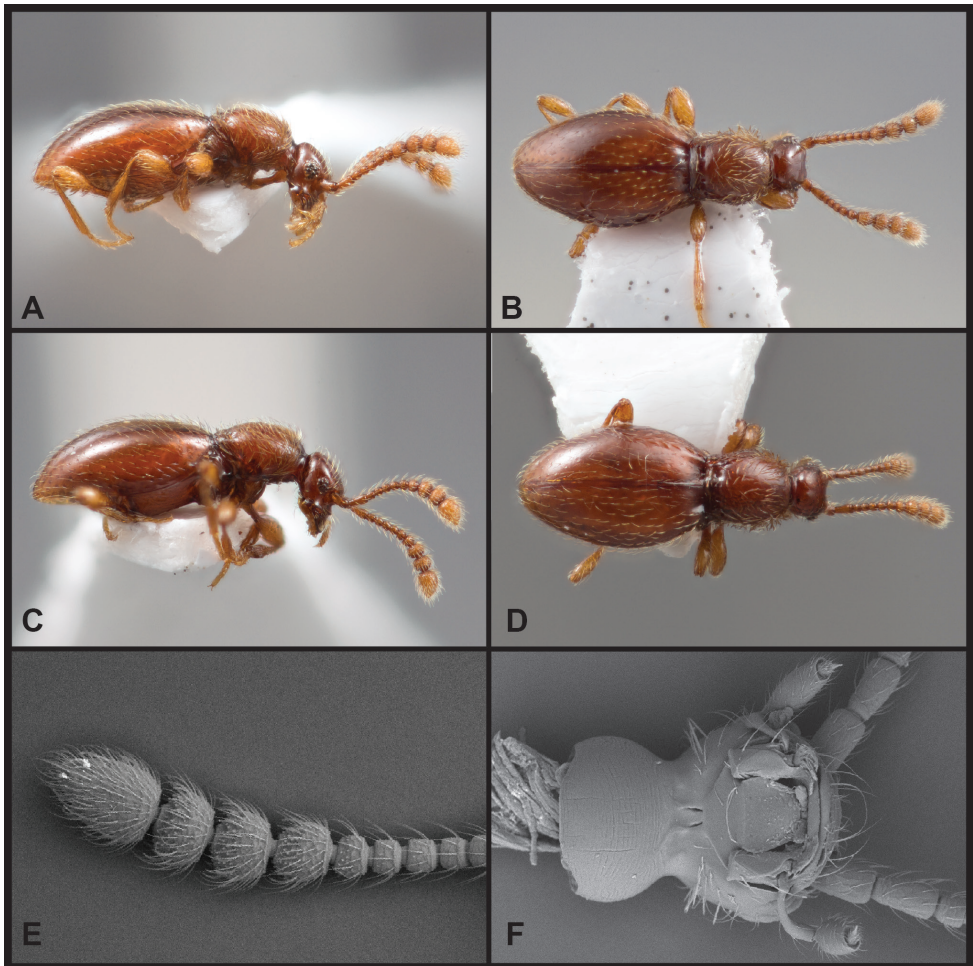


Figure 13. Habitus and character photos of *Euconnus attritus* **A** male, lateral view **B** male, dorsal view **C** female, lateral view **D** female, dorsal view **E** SEM of male antenna **F** SEM of venter of head.

lobe of aedeagus (Fig. 12C) relatively long, nearly as long as basal bulb, narrowed to bluntly rounded, but not knobbed apex; shoulders of aedeagus sloped; parameres weakly curved, apices tapered, bearing three (rarely two) long straight setae; compressor plate symmetrical, parallel-sided to near apex, then narrowed to subacute apex, nearly as long as median lobe; endophallus with single long, upper sclerite, strongly sinuate, apically acute, bearing a sharp secondary process near its midpoint; the right side of the compressor plate sclerotized in a linear band, appearing as a second similar linear sclerite; actual second upper sclerite is much shorter, bent strongly at thickened midpoint, tapering to a thin, acute tip; lower endophallic sclerite a similar-length, trifid claw-like process on a sinuate stem originating near basal orifice.

Distribution. This species is known only from northeast of the Asheville depression, although there it is moderately widespread, occurring in all the major ranges: the Black Mts, Roan Highlands, Grandfather Mountain, Big Bald, and Camp Creek Bald. Its known localities span an elevation range of 3800–6300 ft. There is a CUAC specimen labelled ‘Toxaway Mountain’ (in the more southerly Nantahala Mts.) that is almost certainly mislabeled, as that site was visited the same day as the Big Bald locality.

Remarks. Of the pale species of *Cladoconnus*, this species is only sympatric with *E. adversus* (it is also sympatric with the larger and darker *E. vetustus* and *E. vexillus*). Males of *E. adversus* have very conspicuous antennal carinae, which are completely lacking in *E. attritus*. Females, however, will be indistinguishable. Males of *E. attritus* have very distinctive endophallic sclerites, particularly the long, sinuate left upper sclerite, with its secondary median spike.

The name of this species suggests that the subgenus-typical male antennal carinae are ‘worn away’.

***Euconnus adversus* sp. nov.**

<https://zoobank.org/E8D7FF15-E9B6-48EE-9191-E1C4E7ABE41B>

Figs 11, 14, 15A, B

Type material. *Holotype* ♂, deposited in FMNH: “USA: NC: Yancey Co., 35.8524°N, 82.2485°W, PisgahNF, CeloKnob, x.19.2021, 6300’, M.Caterino, E.Recuero, & A.Haberski, sifted litter” / “[QR code] CLEMSON-ENT CUAC000157519” / “Caterino DNA Voucher Extraction MSC9225 Morphosp.CK.B.370”. *Paratypes* (4, CUAC) – 1 ♂: “USA: NC: Yancey Co., 35.8447°N, 82.2369°W, PisgahNF, Woody Ridge Tr., vi.15.2020, 5244’, M.Caterino, F.Etzler, sifted litter” / “[QR code] CLEMSON-ENT CUAC000137633” / “Caterino DNA Voucher Extraction MSC5528 Morphosp.WR.A.046”; 1 ♂: “USA: NC: Caldwell Co., 36.1184°N, 81.7909°W, Grandfather Mt.SP, 4020’, Nuwati Tr., v.17.2021, A.Haberski, P. Wooden, sifted litter” / “[QR code] CLEMSON-ENT CUAC000135057” / “Caterino DNA Voucher Extraction MSC6364 Morphosp.NT.A.009”; 1 ♂: “USA: NC: Buncombe Co.Co. 35.7955°N, 82.3392°W, Big Butt Tr.,iii.19.2016, S.Myers, L.Vasquez-Velez, sifted litter” / “[QR code] CLEMSON-ENT CUAC00026846”; 1 ♂: “USA: TN: Unicoi Co., 35.9950°N,

82.48972°W, Cherokee NF, Big Bald, v.21.2021, CW. Harden, A.Haberski, P.Wooden, sifted litter” / “[QR code] CLEMSON-ENT CUAC000135395” / “Caterino DNA Voucher Extraction MSC6920 Morphosp.BgBld.A.026”.

Other material. (19): **NC:** Jackson Co., Balsam Mountain Preserve, Sugarloaf Mountain 4491ft, 7-Feb-2015, Sifting litter, oak litter in old stump depression; Ashe Co., Mt. Jefferson State Park, SE Reservoir, 4-Jul-1960; **SC:** Greenville Co., Chestnut Ridge Heritage Preserve, 1140 & 1220 ft., 5-June-2015; Pickens Co., Clemson Experimental Forest, Seed Orchard Rd., 700ft, 12-Jul-2016; Oconee Co., Ellicott Rock Wilderness, East Fork Chattooga River, 2110ft, 4-May-2015; Oconee Co., Ellicott Rock Wilderness, Indian Camp Creek, 2822ft, 4-May-2015; Greenville Co., Mtn. Bridges Wilderness, 2230ft., 10-Mar-2018; **GA:** Rabun Co., NE Pine Mt., Chattooga R., 1800ft, 5-Jun-1981 (CUAC, CNCI, FMNH).

Diagnostic description. This species is generally very similar to the preceding, and can best be distinguished by male genitalic characters; it and the following, however, exhibit the most prominent antennal carinae among American *Cladoconnus*, those on antennomeres VIII and IX both being strong and oblique (Fig. 14C), that of VIII most produced at base and that of IX most produced at apex; antennomere VII also exhibits some expansion along its inner margin; males may be wing-poly-morphic, winged individuals appearing larger and darker in body color; female wings not observed; aedeagus (Figs. 15A, B) with median lobe evenly tapered and narrowly rounded at apex; parameres thin, each bearing three short terminal setae, the setae not reaching apex of median lobe; compressor plate short, asymmetrical, truncate on one side ('left' as drawn), produced on other; upper endophallic armature comprising two dominant curved sclerites, one tapered to narrowly subacute apex, the shorter one much broader, more weakly curved inward to a bluntly truncate apex that meets the apex of the other; the lower endophallic armature consisting of a shorter, deeply bifurcate (or trifurcate) process, the apices slightly varied in curvature, generally directed distad.

Distribution. This species is widespread but rare, found at scattered lower elevation sites across northwestern South Carolina, to higher elevations in the Nantahalas, Blacks, Grandfather Mountain, and Mount Jefferson in northernmost North Carolina. It has a broad elevational range as well, from just 700 ft up to the highest peaks in the region at 6500 ft. A single male labelled as from the Florida panhandle is almost certainly mislabeled. Collected by Stewart Peck on 8 June 1981, it was collected just 3 days after he collected another specimen of this species in Rabun County, Georgia. The 'Florida' specimen probably belongs to the Georgia series.

Remarks. The strongly modified antennomeres of male *E. adversus* will distinguish them immediately from anything sympatric (though not the more western *E. astrus*, below). There is considerable variation site-to-site in the detailed shapes of the upper and lower endophallic armature. In males from the Balsam Mt. Preserve (NC), the innermost endophallic sclerite is deeply trifurcate, whereas in those from the Chestnut Ridge Heritage Preserve (SC) the right tip of the lower endophallic sclerite is curved inward (compare Fig. 15B and Fig. 15A, respectively). None of these southern

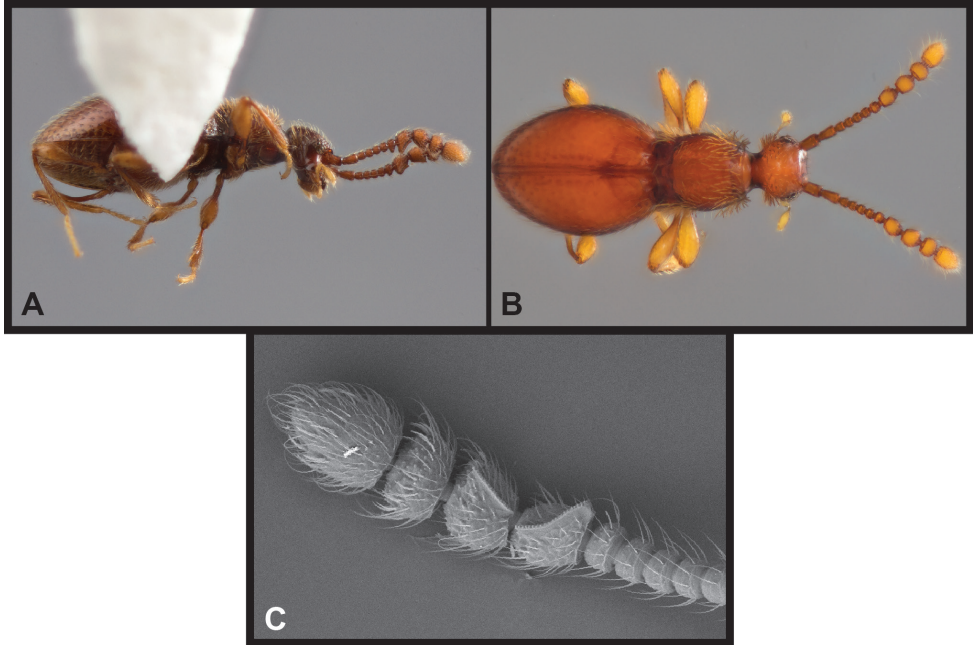


Figure 14. Habitus and character photos of *Euconnus adversus* **A** male, lateral view **B** male, dorsal view (NTA.009) **C** SEM of male antenna.

localities, however, are represented by sequence data, so before recognizing these variants taxonomically, better representation for molecular data would be advisable.

The name of this species refers to the seemingly ‘opposable’ carinae of male antennomeres VIII and IX.

***Euconnus astrus* sp. nov.**

<https://zoobank.org/D02BE2CE-A8EE-44C8-995F-5C69F95FB117>

Figs 7, 15C

Type material. *Holotype* ♂, deposited in CMNC: “ALA., Jackson Co., 5mi.N.W.Princeton, 19.V.1972, S.Peck. Ber.240” / “Caterino DNA Voucher Extraction MSC12286 Cladoconnus(AL)”; *Paratypes* (3): 1 ♂, same data as type; (FMNH); 1 ♂, 1 ♀: “nr. Jess Elliot Cave, Jackson Co., ALA. 8.IV.1961” / “Hollow Tree, V.D.Patrick, H.R.Steeves, leg.”

Other material. (4) – **AL:** Marshall Co., Grant, 25-May-1958 (1 ♂); Colbert Co., Maud, nr. McCluskey Cave, 26-Mar-1962 (3 ♀, 1 ♂).

Diagnostic description. This species is externally identical to *E. adversus*, above, and can only be distinguished by male genitalic characters. Both species share very prominent antennal carinae (e.g., Fig. 14C), those on antennomeres VIII and IX both strong and

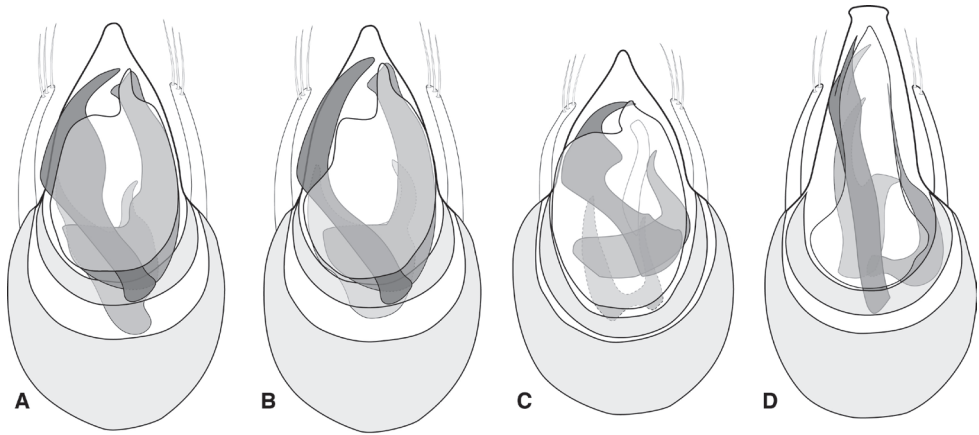


Figure 15. Aedeagus **A** *Euconnus adversus* (type locality – Celo Knob, NC) **B** *Euconnus adversus* (non-type locality – Chestnut Ridge, SC) **C** *Euconnus astrus* **D** *Euconnus cultellus*.

oblique, that of VIII most produced at base and that of IX most produced at apex. They similarly appear to be wing-dimorphic, with winged males and wingless females; aedeagus (Fig. 15C) with median lobe evenly tapered and narrowly rounded at apex; parameres thin, each bearing three short terminal setae, the setae not reaching apex of median lobe; compressor plate short, asymmetrical, truncate on one side (left as drawn), narrowly and unevenly produced on other; left upper endophallic sclerite strongly hooked, with prominent, blunt median tooth on inner margin; right upper endophallic sclerite a short curved spine, the tip pointing laterad; lower endophallic armature comprising a deeply bifurcate process, with two long, slightly sinuate spikes pointed distad.

Distribution. This species is only definitely known from northeastern Alabama, where it has been found in a few caves, as well as a few free-living situations. A series from Colbert County, in northwestern Alabama, comprises only females. Males from this locality would be interesting to examine.

Remarks. This species appears closely related to *E. adversus*, but differs substantially in genitalic characters, with the right upper endophallic sclerite quite different, and the lower endophallic sclerites much more elongate. The species name means ‘starry’, referring to the nearby NASA rocket science and spacecamp facilities.

***Euconnus cultellus* sp. nov.**

<https://zoobank.org/796C1879-2BB4-4515-815D-FDBDAF6C43AD>

Figs 15D, 16, 17

Type material. *Holotype* ♂, deposited in FMNH: “USA: GA: Rabun Co., 34.9658°N, 83.2997°W, ChattahoocheeNF, Rabun Bald, 4663’, v.11.2021, sifted litter, M.Caterino & A.Haberski” / “[QR code] CLEMSON-ENT CUAC000146083” / “Caterino DNA Voucher Extraction MSC12039”. *Paratypes* (8) – 5 ♀, 5 ♂: same data as type.

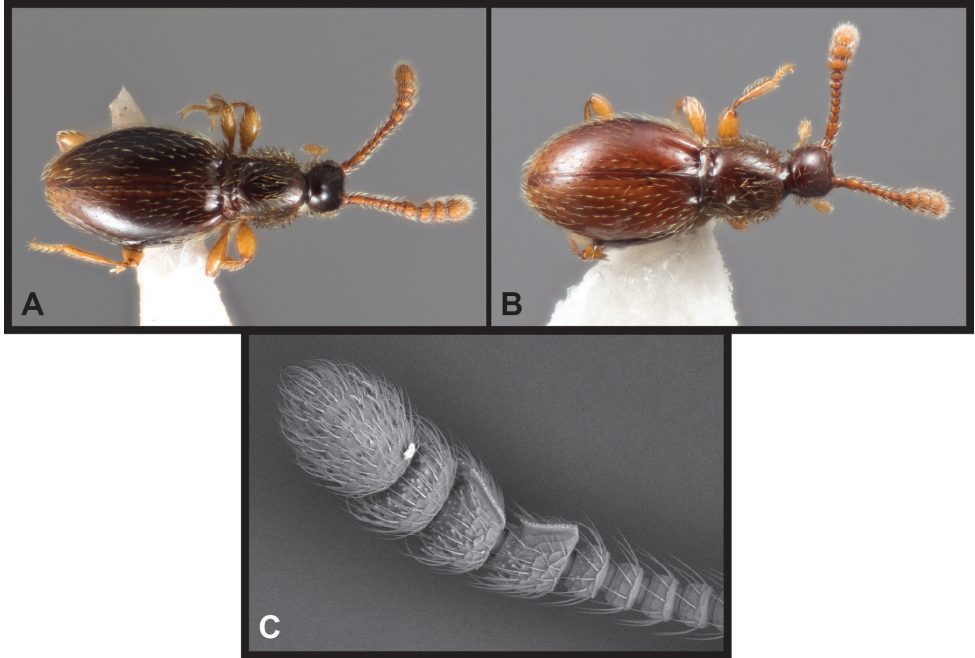


Figure 16. Habitus and character photos of *Euconnus cultellus* **A** male, dorsal view **B** female, dorsal view **C** SEM of male antenna.

Other material. (28) **GA:** Clay Co., Chattahoochee National Forest, Brasstown Bald, 4590ft., 19-Sep-2015 (3 ♂); **NC:** Cherokee Co., Nantahala National Forest, Hickory Branch trail, 3923ft., 26-Jul-2015 (1 ♂); Cherokee Co., London Bald Tr., 4108ft., 26-Jul-2015 (2 ♀); Graham Co., Nantahala National Forest, Teyahalee Bald, 4591ft., 12-Apr-2022 (1 ♂); Macon Co., Nantahala National Forest, Cowee Bald, 4942ft., 9-Jul-2019 (2 ♂); Macon Co., Nantahala National Forest, E. Highlands, Hwy 64, 3880ft., 1-Mar-2020 (1 ♀ 1 ♂); Macon Co., Nantahala National Forest, Copper Ridge Bald, 5032ft., 15-Sep-2020 (1 ♂); Swain Co., Nantahala National Forest, Miller Cove app trail, 2323ft., 20-Jul-2015 (2 ♀, 6 ♂); **SC:** Oconee Co., Buzzards Roost Heritage Preserve, 1250ft., 16-Jan-2015 (1 ♂); Oconee Co., Chau-Ram Country Park, 850ft., 15-Oct-2015 (1 ♀, 1 ♂); Oconee Co., Sumter National Forest, Yellow Branch Falls, 1560ft., 12-Oct-2017 (2 ♀, 1 ♂); Oconee Co., Sumter National Forest, Chattooga river, 1580ft., 2-Apr-2015 (1 ♂); Clay Co., Nantahala National Forest, Tusquitee Bald, 5015ft., 1-Sep-2020 (1 ♂).

Diagnostic description. This species exhibits few obvious external differences from the preceding ‘*falcatus* complex’, and can best be distinguished by male genitalic characters; body color sometimes darker (Fig. 16A); carina of male antennomere VIII (Fig. 16C) more strongly inclined, produced further at the base, than in most of the previous (except *E. adversus* and *E. astrus*), and carina of male antennomere IX slightly oblique, ~ 20 degrees off the long axis of the antenna; males at least sometimes

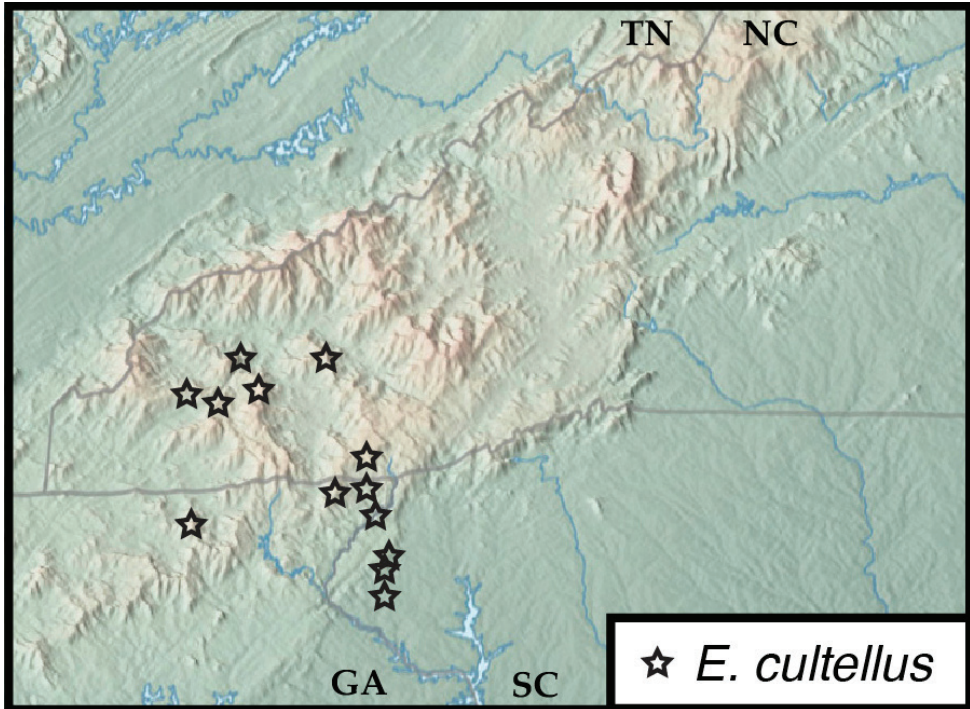


Figure 17. Map of collecting records for *Euconnus (Cladoconnus) cultellus*.

winged, females apparently wingless; aedeagus (Fig. 15D) with apex of median lobe knobbed, bluntly truncate; parameres short, curved, bearing 3 setae at their apices; compressor plate more or less symmetrical, narrow, parallel-sided from near base, sinuately tapering to subacute apex; endophallic armature with upper blade long, nearly straight, widened beyond middle, curving and tapered to bifid, acute apices (a second tooth projecting straight behind the uppermost); a second upper sclerite bends laterad strongly from the base, curving distad and tapering to long thin apex beneath ‘right’ edge of compressor plate; lower sclerite with two strong hooks, the basalmost broad and blunt, the apicalmost sinuately curving behind apex of upper endophallic sclerite.

Distribution. *Euconnus cultellus* occurs across a relatively limited portion of western North Carolina, in the Cowee and Nantahala Mts, northeast Georgia, and upstate South Carolina. Its distribution seems to be limited on the east by the Little Tennessee River system, not (yet) found east of the Tuckasegee tributary, and not having been found in the Great Smoky Mountains, or on any of the spruce-fir peaks sampled. That limit aside, it has a broad elevational range, occurring from 850–5000ft.

Remarks. The bifid apex of the upper endophallic sclerite is distinct from all other *Cladoconnus* species except *E. cataloochee*. The distinctive broad basal hook of the lower endophallic sclerite differentiates *E. cultellus* from all others, as does the deeply curved, apically slender, tapering right arm of the upper armature.

This species is named for the ‘cutting’ edge of the males finely serrate antennal carinae.

Phylogeny

Phylogenetic analysis of available COI sequences does not support monophyly of American *Cladoconnus* relative to all other *Euconnus* (Fig. 18). Most of the new species fall out in one large clade. But *Euconnus vetustus* is resolved as a separate clade outside all the others. This is a dark, flightless species that lacks male antennal modifications. It is also an unusually widespread species, known from several localities on both sides of the Asheville depression. Neither lineage falls out near the two European *Cladoconnus*, *E. (C.) denticornis* Müller & Kunze and *E. (C.) carinthiacus* Ganglbauer for which COI sequences are available, with those forming a sister lineage to most of the rest of *Euconnus* (within which the *Cladoconnus vetustus* lineage falls out). However, it must be acknowledged that all these lineages (the three distinct ‘*Cladoconnus*’ lineages) are highly divergent (> 20% K2P distance), and COI struggles to resolve these deeper relationships. It is worth noting that two American *Euconnus sensu stricto* species fall out near some European members of that subgenus, and far from any of the newly described *Cladoconnus* – these new species had initially been considered as potentially belonging there. Overall, these deeper results are based on a very sparse sampling of global *Euconnus* diversity, and only a small fragment of a single mitochondrial gene, so can only be given so much credence.

Within the main American *Cladoconnus* lineage, the species are divided into two main clades, one containing *Euconnus megalops*, *E. cumberlandus*, *E. vexillus*, *E. adversus*, and *E. kilmeri*. *Euconnus astrus* is not represented by molecular data, but it may be expected to be a member of this group, likely as sister to *E. adversus*. *Euconnus megalops* is probably not yet adequately resolved, as one sample considered to belong there (the Brasstown Bald locality) falls well outside the main group, as sister to a *Euconnus megalops* + *E. vexillus* lineage. But this male’s genitalia do not differ obviously from the rest of *E. megalops*. *Euconnus vexillus*, on the other hand, exhibits distinct male genitalia and male antennal characters, so is clearly a distinct species. More sequences and more genitalia from outlying localities will be necessary to resolving this uncertainty. There is also considerable genetic diversity within the widespread species *E. megalops*. But it shows relatively little geographic structure, with populations from both sides of the Asheville Basin somewhat intermingled. There is one subclade within this that shows a higher degree of genetic variation, from mostly southwestern localities (Huckleberry Knob, Tusquitee Bald, etc.). But these show no obvious morphological coherence.

The other large clade has *Euconnus cultellus* as sister to *Euconnus attritus* and several very closely related species of the *Euconnus falcatus* complex. *Euconnus cultellus* occurs in only the southern part of the region, from scattered localities in the Nantahala Mountains just into far western South Carolina. There is considerable genitalic variation site-to-site, but their sequences, while showing some diversity, don’t suggest significant differentiation. *Euconnus attritus* occurs only in the northeastern part of the region, including the Blacks, Grandfather Mt., and the Roan Highlands, showing potentially meaningful COI differences among the localities. The *Euconnus falcatus* complex, on the other hand, includes three quite distinctive genitalic forms that show surprisingly little COI differentiation. One, *Euconnus cataloochee*, is even scattered

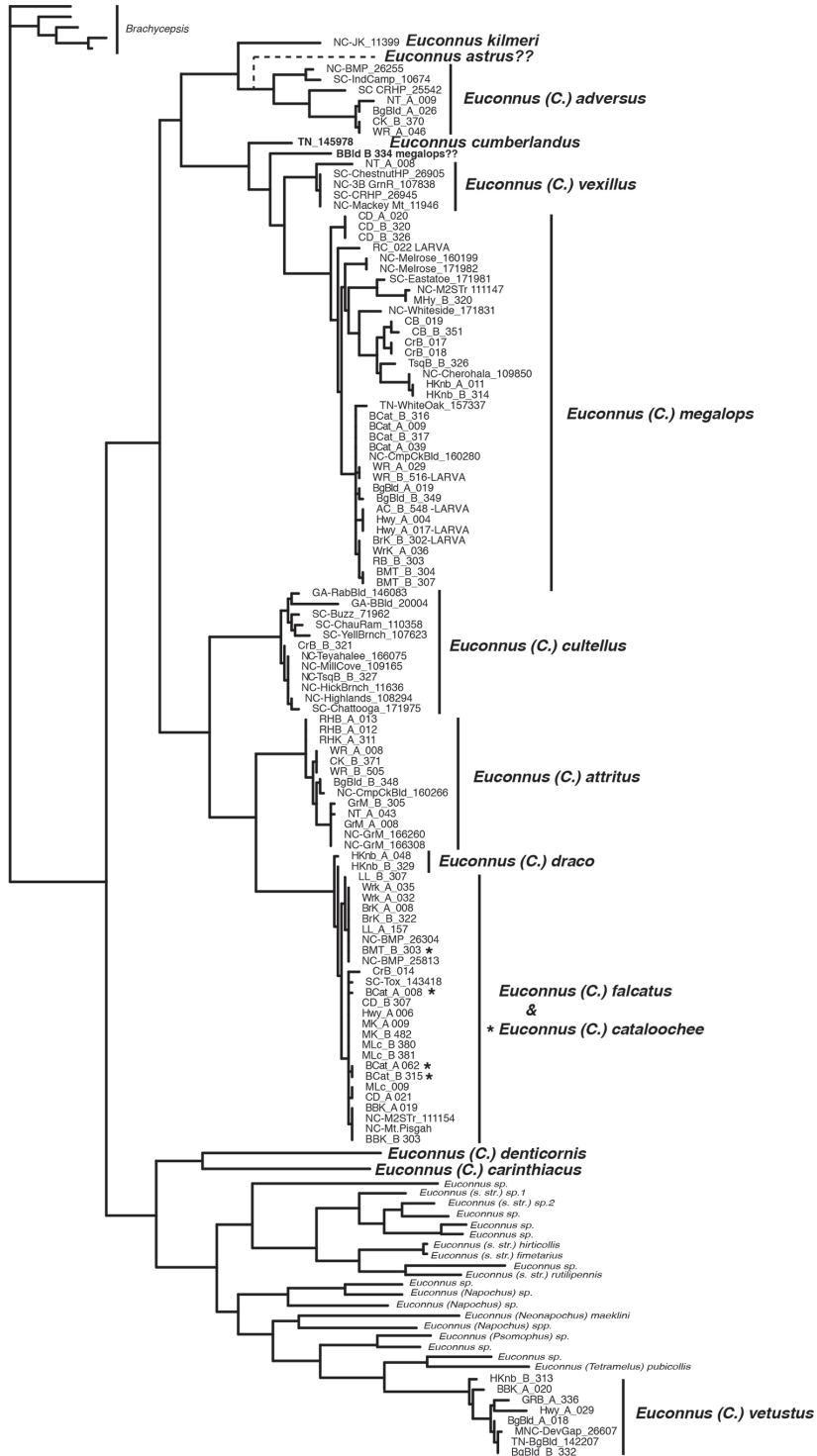


Figure 18. Phylogeny of American species of *Euconnus* (*Cladoconnus*). Hypothesized position of *E. astrus*, for which no sequence data is available, is indicated with a dotted line.

within another both genetically and geographically (they are marked by asterisks in Fig. 18). This non-monophyly is peculiar and requires further genetic data to resolve. The genitalic differences between *E. falcatus* and *E. cataloochee* are marked and consistent. Two individuals representing *E. draco* resolve as sisters to the remainder of this clade, but are not themselves monophyletic (despite coming from the same locality, Huckleberry Knob). *Euconnus tusquitee* would also be expected to be very similar to these, but it has not yet yielded clean sequence data. These results together indicate either rapid speciation, over a time frame insufficient for coalescence of species-specific haplotypes, or a significant slow-down in mitochondrial evolution. Again, additional markers will be necessary to resolve this question.

Discussion

The discovery of a diverse, previously unreported radiation of beetles in the southern Appalachians is surprising, even considering their small size and cryptic habits. The region has been popular with collectors and researchers for many years, and while new species are still encountered commonly, it is rare for major lineages to have escaped detection. Scydmaeninae have perhaps received less attention from taxonomists over the years than more prominent groups, and one could imagine other 'hidden' radiations in other similarly neglected arthropod taxa.

While only European members of *Cladoconnus* have previously been sequenced, it is worth considering whether the relationships of the Appalachian species lie among the Asian species. There aren't any particular morphological characters that suggest such a relationship. But the existence in Japan and Korea of species that are sexually dimorphic in the possession of flight wings, as observed in several Appalachian species, might be informative. Then again, that begs the question of how a lineage with flightless females may have reached the area to begin with. But the deep genetic divergences, and somewhat incongruous distributions of some of the species (in particular, *E. vetustus* ignoring the biogeographically significant Asheville Depression) together suggest that *Cladoconnus* has been resident in the southeastern US for a very long time. Given that, however, it is surprising that their overall distribution is still somewhat limited. The species found to the west, in parts of the Cumberland Plateau, extend somewhat beyond Appalachia proper. But none have yet been found to occur in higher elevations of Virginia. Some older lineages of Appalachian arthropods find relatives in the Ouachita Mts of Arkansas (flightless *Lathrobium*, for example – Watrous and Haberski, pers. comm.; *Arianops* Brendel – Carlton 1990; *Anillinus* Casey – Allen 1990, Carlton and Robison 1998). It might be worth examining such collections more closely for overlooked representatives.

Our 'barcode-everything' approach revealed several larvae of *Cladoconnus*, all, as definitely associated by DNA placement, of *E. (C.) megalops* (Fig. 19). Of the seven extracted and sequenced, vouchers of six survived the process more or less intact. No larvae of the larger genus *Euconnus* have yet been formally described (Newton 1991; Jałoszyński, pers. comm.), and I do not do so here. However, these represent a



Figure 19. Larvae of *Euconnus* (*Cladoconnus*) *megalops* **A** dorsal view (specimen from Rabun Cliffs, GA) **B** lateral view (specimen from Woody Ridge Trail, NC).

potentially valuable source for future character data for reconstructing scydmaenine relationships. Generally, the larvae resemble other described Glandulariini, such as *Stenichnus* Thomson (Wheeler and Pakaluk 1983; Newton 1991; Jałoszyński and Kilian 2012), prognathous, elongate, setose, slightly flattened, with a rather broad abdomen, and a large antennomere II with a simple, domelike apical cap.

While the bulk of our records seem to suggest an exclusively high-elevation restricted group, with more than two-thirds of the available records coming from above 4500 feet (Fig. 20), the ranges of many of the species extend considerably lower, even below 1000 feet. These lower records tend to be from deep riparian canyons, and the higher humidity of such locations is probably part of the explanation. However, there is also a clear sampling bias here, in that recent fieldwork by our lab has targeted high elevation sites. Still, scanning our own older, lower elevation samples, and attempting to borrow specimens from other collections where lower elevation samples were better represented turned up relatively few additional specimens. It may be that many of these beetles have been ignored or overlooked in the abundant morass of litter microcoleoptera. But there have been a number of dedicated devotees over the years, including Sean O’Keefe, Donald Chandler, Christopher Carlton, Walter Suter, Thomas Barr, and others, so the apparent predilection of *Cladoconnus* for higher elevations seems likely to be real.

Activity patterns of the species present similar questions. The majority of records come from late spring and early summer samples (Fig. 21), and such a pattern would conform to many species in the region. Our own sampling has had some of this bias, although for the past several years, during which most of these beetles were collected, similar emphasis was given to fall sampling, in September and October, and there is no indication of a secondary peak of specimen records, so there is probably some meaningful signal there, as well.

The range in genitalic diversity, especially among the apparently closely related species in the *E. falcatus* complex, is remarkable. In those species known from multiple

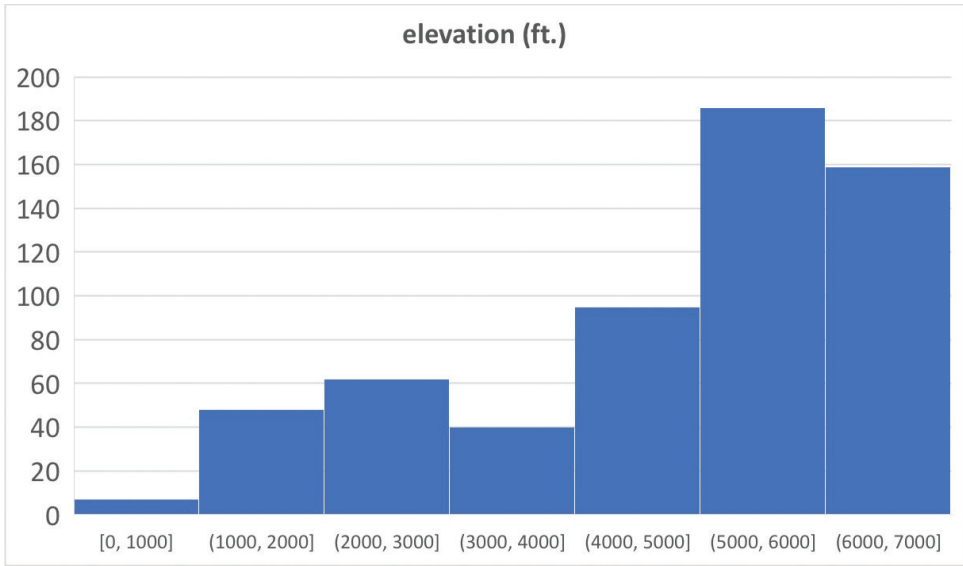


Figure 20. Histogram of record counts (y-axis) by elevation (x-axis, range in feet).

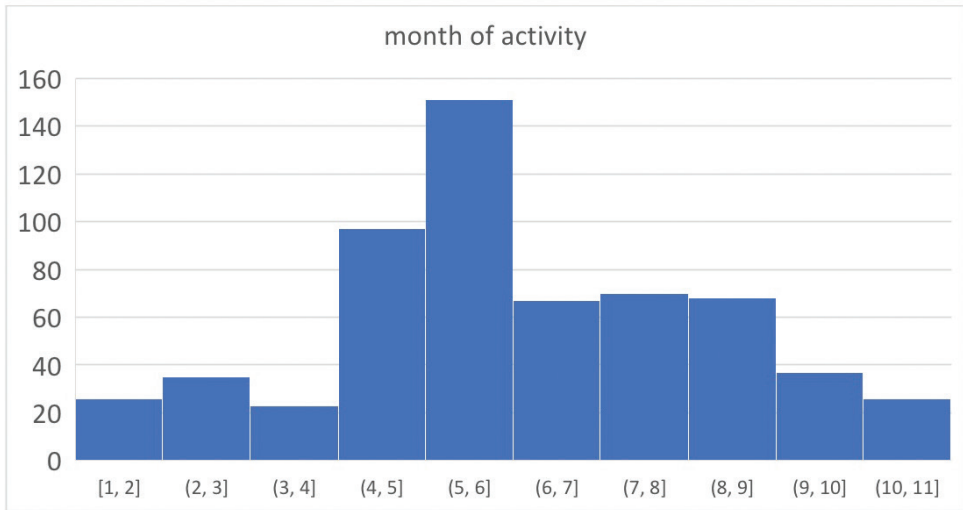


Figure 21. Histogram of record counts (y-axis) by month (x-axis).

localities, it seems to be the rule that variation in specific conformation of endophallic sclerites can be seen. I've taken a generally conservative approach in considering many to be widespread, variable species for now. But closer study could well split some of these more finely.

It would be fascinating to understand the *in situ* mechanisms of these species incredibly complex genitalia. It is tempting to hypothesize explanations of sperm competition and perhaps rival sperm removal, or of active female choice spurring an arms-race of male elaborations for maintaining hold and proper position. The dimorphic antennomeres of at least some of these species might also point to some similar sorts of intersexual dynamics. Unfortunately, for the present such a discussion would be pure speculation. Simply understanding the physical mechanisms that deploy the endophallic sclerites during intromission would constitute a major undertaking. Yet it might repay the effort, as similar dynamics may pertain to the diversification of a wide variety of ‘dark taxa’, within Staphylinoidea at least, where such structures are commonplace. For now, it must suffice to call attention to these remarkable creatures, and hope that future workers with a more applicable skillset take up the challenge.

Acknowledgements

This study was funded by the U.S. National Science Foundation (Award DEB-1916263 to MSC) and the Clemson University Experiment Station (SC-1700596 to MSC). I also acknowledge the support of the John and Suzanne Morse Endowment for Arthropod Biodiversity. For permissions and assistance with field work I am grateful to the North Carolina State Parks, Great Smoky Mountains National Park, Blue Ridge Parkway National Park, Monica Martin, Frank Etzler, Ernesto Recuero, Curt Harden, Anthony Deczynski, Patricia Wooden, Adam Haberski, Roy Kucuk, Laura Vasquez-Velez, Laary Cushman, Paul Marek, Michael Ferro, and Will Kuhn. For other advice and specimens I thank Pawel Jałoszyński, Peter Hlaváč, Donald Chandler, Alfred Newton, Anthony Davies, Zachary Falin, and Christopher Carlton; and for assistance in the lab I thank Mary Atieh, Caroline Dukes, Caroline McCluskey, Grace Holliday, Grace Arnold, Hannah Skinner, and Anthony Villanueva. Finally, thank you to Reginald Webster for comments that helped improve the manuscript. This paper represents Technical Contribution No. 7105 of the Clemson University Experiment Station.

References

- Allen RT (1990) Insect endemism in the interior highlands of North America. *The Florida Entomologist* 73(4): 539–569. <https://doi.org/10.2307/3495270>
- Barr TC (1979) Revision of Appalachian *Trechus* (Coleoptera: Carabidae). *Brimleyana* 2: 29–75.
- Bushnell B, Rood J, Singer E (2017) BBMerge – Accurate paired shotgun read merging via overlap. Biggs PJ (Ed.). *PLoS ONE* 12(10): e0185056. <https://doi.org/10.1371/journal.pone.0185056>
- Carlton CE (1990) A new species of *Arianops* from central Arkansas and biogeographic implications of the interior highlands *Arianops* species (Coleoptera: Pselaphidae). *Coleopterists Bulletin* 44: 365–371.

- Carlton CE, Robison HW (1998) Diversity of litter-dwelling beetles in the Ouachita Highlands of Arkansas, USA (Insecta: Coleoptera). *Biodiversity and Conservation* 7(12): 1589–1605. <https://doi.org/10.1023/A:1008840427909>
- Casey TL (1897) Coleopterological notices. VII. *Annals of the New York Academy of Sciences* 9(1): 285–684. <https://doi.org/10.1111/j.1749-6632.1896.tb55435.x>
- Elbrecht V, Leese F (2017) Validation and development of COI metabarcoding primers for freshwater macroinvertebrate bioassessment. *Frontiers in Environmental Science* 5: 11. <https://doi.org/10.3389/fenvs.2017.00011>
- Gusarov VI (2002) A revision of nearctic species of the genus *Geostiba* Thomson, 1858. *Zootaxa* 81(1): 1–88. <https://doi.org/10.11646/zootaxa.81.1.1>
- Hlaváč P, Stevanović M (2013) A review of the subgenus *Cladoconnus* Reitter of the genus *Euconnus* Thomson (Coleoptera: Staphylinidae: Scydmaeninae) from the Balkan Peninsula, Turkey and Caucasus. *Zootaxa* 3646(4): 401–425. <https://doi.org/10.11646/zootaxa.3646.4.5>
- Hoshina H (2004) First new species of the subgenus *Cladoconnus* of the genus *Euconnus* from Japan (Coleoptera: Scydmaenidae). *Entomological Problems* 34: 119–123.
- Hoshina H, Park S-J (2020) A new species, *Euconnus* (*Cladoconnus*) *odaesanensis* sp. nov. (Coleoptera: Staphylinidae: Scydmaeninae), from Korea. *Japanese Journal of Systematic Entomology* 26: 93–94.
- Hoshina H, Miyata T, Miyata T (2018) Second new species of the subgenus *Cladoconnus* of the genus *Euconnus* from Japan (Coleoptera: Staphylinidae: Scydmaeninae). *Japanese Journal of Systematic Entomology* 24: 296–298.
- Jałoszyński P (2012) Taxonomy of “*Euconnus* complex”. Part I. Morphology of *Euconnus* s. str. and revision of *Euconnomorphus* Franz and *Venezolanoconnus* Franz (Coleoptera: Staphylinidae: Scydmaeninae). *Zootaxa* 3555(1): 55–82. <https://doi.org/10.11646/zootaxa.3555.1.3>
- Jałoszyński P (2017) Taxonomy of “*Euconnus* complex”. Part XVI. *Alloconophron* Franz transferred to *Anhoraemorphus* Franz as subgenus, with notes on systematic position of *Noctophus* Casey (Coleoptera, Staphylinidae, Scydmaeninae). *Zootaxa* 4358(2): 328–338. <https://doi.org/10.11646/zootaxa.4358.2.6>
- Jałoszyński P (2018) Taxonomy of “*Euconnus* complex”. Part XVII. Status of subgenera defined by male antennal characters: *Androconnus* Franz and *Cladoconnus* Reitter (Coleoptera, Staphylinidae, Scydmaeninae). *Zootaxa* 4415(2): 369–380. <https://doi.org/10.11646/zootaxa.4415.2.7>
- Jałoszyński P (2019) The first Korean species of *Euconnus* (*Cladoconnus*), with a synopsis of the *E. ussuriensis* species group (Coleoptera, Staphylinidae, Scydmaeninae). *Zootaxa* 4615(3): 481–488. <https://doi.org/10.11646/zootaxa.4615.3.4>
- Jałoszyński P (2021) Taxonomy of “*Euconnus* complex”. Part XXIII. Status of *Napochus* Thomson, *Pycnophus* Casey, and *Filonapochus* Franz revisited (Coleoptera, Staphylinidae, Scydmaeninae). *Zootaxa* 5026(2): 255–270. <https://doi.org/10.11646/zootaxa.5026.2.6>
- Jałoszyński P, Kilian A (2012) Larval morphology of *Scydmaenus tarsatus* and *S. hellwigii*, with notes on feeding behaviour and a review of the bibliography on the preimaginal stages of ant-like stone beetles (Coleoptera: Staphylinidae: Scydmaeninae). *European Journal of Entomology* 109(4): 587–601. <https://doi.org/10.14411/eje.2012.073>

- Jałoszyński P, Perkovsky E (2021) A new bizarre species of *Euconnus* (*Cladoconnus*) in Upper Eocene Rovno amber (Coleoptera: Staphylinidae: Scydmaeninae). *Zootaxa* 5004(2): 395–400. <https://doi.org/10.11646/zootaxa.5004.2.8>
- Katoh K, Rozewicki J, Yamada KD (2017) MAFFT online service: multiple sequence alignment, interactive sequence choice and visualization. *Briefings in Bioinformatics* bbx108: 1–7. <https://doi.org/10.1093/bib/bbx108>
- Meier R, Wong W, Srivathsan A, Foo M (2016) \$1 DNA barcodes for reconstructing complex phenomes and finding rare species in specimen-rich samples. *Cladistics* 32(1): 100–110. <https://doi.org/10.1111/cla.12115>
- Miller KB, Wheeler QD (2005) Slime-mold beetles of the genus *Agathidium* Panzer in North and Central America: Coleoptera, Leiodidae. Part 2. *Bulletin of the American Museum of Natural History* 291(1): 1–167. [https://doi.org/10.1206/0003-0090\(2005\)291<0001:SBOTGA>2.0.CO;2](https://doi.org/10.1206/0003-0090(2005)291<0001:SBOTGA>2.0.CO;2)
- Minh BQ, Nguyen MAT, Von Haeseler A (2013) Ultrafast approximation for phylogenetic bootstrap. *Molecular Biology and Evolution* 30(5): 1188–1195. <https://doi.org/10.1093/molbev/mst024>
- Newton AF (1991) Scydmaenidae. In: Stehr FW (Ed.) *Immature Insects*, Vol. 2. Kendall/Hunt, Dubuque, IA, 330–334.
- Newton AF, Franz H (1998) World catalog of the genera of Scydmaenidae (Coleoptera). *Koleopterologische Rundschau* 68: 137–165.
- O’Keefe ST (2001) Scydmaenidae. In: Arnett RH, Thomas MC (Eds) *American Beetles*, Vol. 1. Archostemata, Myxophaga, Adephaga, Polyphaga: Staphyliniformia. CRC Press, Boca Raton, FL, 259–271.
- Reitter E (1909) *Fauna Germanica. Die Käfer des Deutschen Reiches*. Vol. 2. K.G. Lutz, Stuttgart, 392 pp.
- Srivathsan A, Lee L, Katoh K, Hartop E, Kutty SN, Wong J, Yeo D, Meier R (2021) ONTbarcoder and MinION barcodes aid biodiversity discovery and identification by everyone, for everyone. *BMC Biology* 19(1): 217. <https://doi.org/10.1186/s12915-021-01141-x>
- Stephan K, Chandler DS, O’Keefe ST, Riley EG (2021) A revision of the North American species of *Euconnus* (*Napochus*) Thomson, north of Mexico (Coleoptera: Staphylinidae: Scydmaeninae). *Memoirs of the American Entomological Society* 51: 1–319. <https://doi.org/10.1649/0010-065X-75.4.868>
- Trifinopoulos J, Nguyen LT, von Haeseler A, Minh BQ (2016) W-IQ-TREE: A fast online phylogenetic tool for maximum likelihood analysis. *Nucleic Acids Research* 44(W1): W232–W235. <https://doi.org/10.1093/nar/gkw256>
- Wheeler QD, Miller KB (2005) Slime-mold beetles of the genus *Agathidium* Panzer in North and Central America: Coleoptera, Leiodidae. Part 1. *Bulletin of the American Museum of Natural History* 290: 1–95. [https://doi.org/10.1206/0003-0090\(2005\)290<0001:SBOTGA>2.0.CO;2](https://doi.org/10.1206/0003-0090(2005)290<0001:SBOTGA>2.0.CO;2)
- Wheeler QD, Pakaluk J (1983) Descriptions of larval *Stenichnus* (*Cyrtoscydmus*): *S. turbatus* and *S. conjux*, with notes on their natural history (Coleoptera: Scydmaenidae). *Proceedings of the Entomological Society of Washington* 85: 86–97.

Supplementary material 1

Specimen data for all material examined

Authors: Michael S. Caterino

Data type: occurrence

Explanation note: Specimen level data for all *Cladoconnus* specimens examined in this paper. Columns include type status, repository, voucher numbers (for Clemson University Arthropod Collection), morphospecies designation (which can be searched on Flickr for additional images), DNA extraction number (extractions in Caterino Lab/CUAC collection), GenBank accession numbers, and collection event and geographical information.

Copyright notice: This dataset is made available under the Open Database License (<http://opendatacommons.org/licenses/odbl/1.0/>). The Open Database License (ODbL) is a license agreement intended to allow users to freely share, modify, and use this Dataset while maintaining this same freedom for others, provided that the original source and author(s) are credited.

Link: <https://doi.org/10.3897/zookeys.1137.97068.suppl1>

Supplementary material 2

Phylogenetic character data (COI barcoding region)

Authors: Michael S. Caterino

Data type: DNA sequence

Explanation note: Nexus file containing all sequences analyzed in this paper, including *Brachycephis* outgroups, new *Cladoconnus* species, new sequences for Nearctic *Euconnus* (*Napochus*) and *Euconnus* s. str. spp., and previously published *Euconnus* sequences from GenBank and BOLD. Line names contain their BOLD and/or GenBank Accession numbers for previously published sequences.

Copyright notice: This dataset is made available under the Open Database License (<http://opendatacommons.org/licenses/odbl/1.0/>). The Open Database License (ODbL) is a license agreement intended to allow users to freely share, modify, and use this Dataset while maintaining this same freedom for others, provided that the original source and author(s) are credited.

Link: <https://doi.org/10.3897/zookeys.1137.97068.suppl2>

Comment and integration to Andreone et al. 2022 “Reconnecting research and natural history museums in Italy and the need of a national collection biorepository”

Marco Benvenuti¹, Fausto Barbagli², Francesca Maggiore³

1 SMA Museum System of the University of Florence, Via G. La Pira 4, 50121 Firenze, Italy **2** ANMS National Association of Scientific Museums, Via G. La Pira 4, 50121 Firenze, Italy **3** CNR -ISMAR National Research Council - Institute of Marine Sciences, Arsenale - Tesa 104, Castello 2737/E, 30122 Venezia, Italy

Corresponding author: Marco Benvenuti (presidente.sma@unifi.it)

Academic editor: Pavel Stoev | Received 17 October 2022 | Accepted 31 October 2022 | Published 22 December 2022

<https://zoobank.org/BDA9E5A2-6C49-40C3-9D18-A888E0318015>

Citation: Benvenuti M, Barbagli F, Maggiore F (2022) Comment and integration to Andreone et al. 2022 “Reconnecting research and natural history museums in Italy and the need of a national collection biorepository”. ZooKeys 1137: 177–179. <https://doi.org/10.3897/zookeys.1137.96414>

Abstract

In Andreone et al. (2022), the authors described a background about the Italian Natural History Museums (NHMs) situation, highlighting difficulties regarding the coordination among institutes due to the fragmented landscape, from the past until today. They suggested how having a national institute, the Future National Biodiversity Centre (FCNB), would represent the best solution to the problem. Our vision regarding the lack of a national natural history museum in Italy does not coincide with that of the authors, but we do not consider clarifying this aspect in the present letter. On the other hand, since the authors reported how “the present fragmentation of museums and associated collections does not allow for an effective participation of Italy to global models of aggregated natural history databases (such as the VertNet, iDigBio, GBIF)”, we believe it is necessary to address the issue linked to the digital sharing of Italian collections. We present more clarifications about Italy’s commitment to the digitisation and sharing of NH collections data through the DiSSCo RI “Distributed System of Scientific Collections Research Infrastructure” of which Italy is one of the 23 European partner countries since 2018.

Keywords

Data digitisation, DiSSCo, FAIR, natural history museum collections

Dear Editor,

In the commentary “Reconnecting research and natural history museums in Italy and the need of a national collection biorepository” (Andreone et al. 2022) the authors described a broad background concerning the Italian Natural History Museums (hereafter NHMs) situation, providing an overview on the several difficulties about coordination among the different institutes. Our vision regarding the lack of a national natural history museum in Italy does not coincide with that of the authors, but we do not consider this the right place to propose an alternative view. On the other hand, we believe it is necessary to address the issue linked to the digital sharing of Italian collections. A proposal to establish a National Biodiversity Centre (Centro Nazionale per la Biodiversità, CNB) as a reference point for all the Italian NHMs has more recently been concretised within the Italian PNRR (National Recovery and Resilience Plan). There is an urgent need to improve digital tools and the interoperability among digital infrastructures and data management systems. This has been further put in evidence after the COVID-19 pandemic and one of the primary purposes of the PNRR is to improve the digitisation in any working field. Thus, it perfectly suits with the digitisation of museum collections, offering an incredible opportunity to finalise what has not been possible to do until now.

It is true that much work still needs to be done in Italy in order to digitise the Natural History Collections (hereafter NHCs) and to share the richness of the information embedded there (in both the biological and geo-mineralogical field) worldwide. Nevertheless, by only focusing on the national level, the authors seem unaware that a strong strategy to facilitate and improve NHCs interoperability already exists at the international (European) level. DiSSCo RI (Distributed System of Scientific Collections Research Infrastructure; <https://www.dissco.eu/>), indeed, aims to digitally unify all European NHCs thanks to shared access and curation policies and practices, ensuring that all the data and metadata are linked to a digital twin of the physical specimens (the so-called “Digital specimens”) and accomplish the FAIR (Findable, Accessible, Interoperable and Reusable) principles. DiSSCo is currently still in the preparatory phase, but some services are already developed and a very large scientific community (including Italian institutions) has been fully involved in this project for several years, tightly connected with a broader international panel of similar initiatives (GBIF, iDigBio, Atlas of Living Australia).

It is essential to underline that Italy is one of the 23 DiSSCo partner countries and has been taking part to this process since 2018 through a DiSSCo’s Italian consortium, led by the Florence NHM as National Node and also including eight other institutions representing the whole Italian NHCs community: CNR (National Research Council), ANMS (National Association of Scientific Museums), National Academy of Sciences, National Academy of Entomology, Italian Society of Biogeography, Italian Paleontological Society, Italian Geological Society, and the Italian Botanical Society (<https://www.dissco.eu/it/>). Moreover, Italy is represented in the CETAF (Consortium of European Taxonomic Facilities) by the Florence and Genoa

NHMs since 2002, recently joined by the Pisa Herbarium and Botanical Garden (Bartolozzi 2013; Innocenti et al. 2017).

This is the first concrete step toward the alignment of Italian NHMs with the FAIR principles, which will make even the natural science data in our country shareable beyond the actual physical position, management, and constraints of the specimens themselves.

In this wider overview, the CNB (National Biodiversity Centre) would represent a node for communication and coordination at national level, connecting the Italian scientific community and the NHMs holding biological collections with DiSSCo, working in synergy to achieve a common final goal.

References

- Andreone F, Boero F, Bologna MA, Carpaneto GM, Castiglia R, Gippoliti S, Massa B, Minelli A (2022) Reconnecting research and natural history museums in Italy and the need of a national collection biorepository. *ZooKeys* 1104: 55–68. <https://doi.org/10.3897/zookeys.1104.79823>
- Bartolozzi L (2013) I musei naturalistici italiani nel contesto delle iniziative internazionali sulla biodiversità. *Museologia Scientifica, Memorie* 9: 17–20.
- Innocenti G, Cianfanelli S, Corti C, Nistri A, Nocita A, Vanni S (2017) Researches on biodiversity at the Natural History Museum, Florence University. *BioSyst.EU 2017, Abstract Vol. 9*, 1–103. https://iapt-taxon.org/files/2017_BioSysteEu_Abstracts.pdf

Italian natural history museums need specimen digitization and much more: a reply to Benvenuti et al.

Franco Andreone¹, Ferdinando Boero², Marco A. Bologna³,
Giuseppe M. Carpaneto³, Riccardo Castiglia⁴, Spartaco Gippoliti⁵,
Bruno Massa⁶, Alessandro Minelli⁷

1 Museo Regionale di Scienze Naturali, Via G. Giolitti, 36, I-10123 Torino, Italy **2** CNR-IAS, Stazione Zoologica Anton Dohrn, Villa Comunale, I-80121 Napoli, Italy **3** Department of Sciences, Università Roma Tre, Viale G. Marconi, 446, I-00146 Roma, Italy **4** Dipartimento di Biologia e Biotecnologie “Charles Darwin”, Università “La Sapienza” di Roma, Via A. Borelli, 50, I-00161 Roma, Italy **5** Società Italiana per la Storia della Fauna “Giuseppe Altobello”, Viale Liegi, 48A, I-00198 Roma, Italy **6** Dipartimento di Scienze agrarie, alimentari e forestali, Università di Palermo, Viale Scienze, 13, I-90128 Palermo, Italy **7** Dipartimento di Biologia, Università di Padova, Via Ugo Bassi, 58B, I 35131 Padova, Italy

Corresponding author: Franco Andreone (franco.andreone@regione.piemonte.it, franco.andreone@gmail.com)

Academic editor: Pavel Stoev | Received 16 November 2022 | Accepted 22 November 2022 | Published 22 December 2022

<https://zoobank.org/394E6E7A-C47D-467B-B637-645361A388CD>

Citation: Andreone F, Boero F, Bologna MA, Carpaneto GM, Castiglia R, Gippoliti S, Massa B, Minelli A (2022) Italian natural history museums need specimen digitization and much more: a reply to Benvenuti et al. ZooKeys 1137: 181–185. <https://doi.org/10.3897/zookeys.1137.97631>

Abstract

We reply to the comments made by Benvenuti et al. (2022) about our paper on the Italian natural history museums and scientific collections and the need of a centralized hub and repository. While agreeing that digitization is a useful tool to valorize each museum and collection, we still believe that the suggestion of a centralized hub is valid and necessary. This would largely help in boosting coordination among museums, sharing personnel and resources, and in providing a place to deposit scientific collections that do not fit the scope of smaller museums.

Keywords

Digitization, repository, scientific collections, specimens

We have read with great interest the letter of our colleagues in Florence Natural History Museum and National Research Council (CNR) (Benvenuti et al. 2022) about our proposal (Andreone et al. 2022) to create a centralized repository within the actions of the National Biodiversity Future Center (NBFC). In responding to the comments by these

authors on our paper, we take the opportunity to provide more details about natural history museums (NHMs) in Italy and their effectiveness as research and conservation centers. NHMs are universally recognized as strongholds for taxonomic and environmental monitoring studies that are key tools for biodiversity inventories and species description and keeping trace of loss of taxa, climate change, and pathogenic information on zoonotic diseases and crop pests (Suarez and Tsutsui 2004; DuBay and Fuldner 2017). In their letter, the authors stressed the utility of DISSCo (Distributed System of Scientific Collections), a collaborative network which deals with the digitization of scientific collections and artifacts stored in museums to facilitate access of the international community to scientific collections, but disagreed with our suggestion of creating a new structure and/or upgrading an existing museum to act as a national repository/center. A more detailed explanation of the reasons that led these authors to dissent with such a proposal would have been helpful to better understand their criticism. We agree that digitization is needed, but we still believe that a centralized hub and repository is necessary.

Andreone et al. (2022) suggested that the past geo-political fragmentation of pre-unitarian Italy in small states led to the birth and persistence of small to medium sized scientific museums that were not capable of coalescing into a single larger museum or into an operational coordinated distributed museum of national importance (Andreone et al. 2014). Other countries (i.e., France, Hungary, UK, etc.) adopted the model of a large centralized museum where major scientific collections are deposited. In Germany, where the fragmentation in “Länder” (federate states) somehow mirrors the historical conditions of Italy, many museums aggregated within a network (i.e., Senckenberg Gesellschaft für Naturforschung) or became autonomous research institutions (typical in this sense is the name of the former Zoologisches Forschungsmuseum Alexander Koenig in Bonn, i.e., “Zoological Research Museum...”). Unfortunately, no step in this direction occurred in Italy, where museums are still mostly managed by local public administrations or universities.

While we are convinced that local museums are extremely helpful to raise awareness of biodiversity, we believe that they cannot serve (or only partly serve) to monitor and check biodiversity at a national level, a necessity that is crucial to safeguard animal and plant populations, species and ecosystems. Already in 1898 William Henry Flower stated that “it is only in national museums that the fulfillment of both functions [research and education] in fairly equal proportions can be expected. In almost all other museums the diffusion of knowledge, or popular education, will be the primary function” (Flower 1898: 38). For this reason, also we reaffirm that a centralized hub and repository is necessary, since it would support not only digitization, but also a wider array of activities that serve the mission of biodiversity research and conservation in Italy, namely the maintenance and increase of natural history collections and their continuative taxonomic revisions. To this aim, the training of technical, curatorial and taxonomic staff to be employed in a national museum is a priority to ensure long-term life to biodiversity research in Italy.

The letter also raised attention to the digitization of collections, stressing the importance of the DISSCo program, as already emphasized by Bartolozzi (2013) and Andreone et al. (2014). We totally agree with this claim, since digitization is an obvious tool to make collections more accessible and usable (Baird 2010). Finally, we also agree with the necessity of networking museum data, beginning with textual data, but also iconographic (i.e., with the use of 3D photographs or CT scans), and favoring the creation of an online catalogue of the primary types preserved in Italy. Eventually, large-scale digitization will become mandatory the path for most museums (Blagoderov et al. 2012), contributing to speed taxonomic research worldwide (Engel et al., 2021). This advantage became particularly tangible during the COVID19 pandemics, when it was difficult to visit collections, and online services were particularly precious. Such a digitization project is given high priority among the activities of the NBFC related to a national museum of biodiversity.

Unfortunately, the small size and generalized lack of personnel and fund shortfalls that affect most Italian NHMs hinders the capacity to advance the digitization of natural history collections and old catalogues. In fact, the number of curatorial personnel working in Italian NHMs is rarely over ten. In many museums, curators are too often considered technicians or polyvalent figures dedicated not only to collection management, but also (and sometimes eminently) to other activities such as exhibit preparation, communication, and administration. To make a comparison, the Natural History Museum in London has more than 80 curators, in addition to technicians, post-docs and other scientific personnel. Furthermore, due to personnel inadequacy, in Italy most museum collections are rarely taxonomically revised, new material is acquired through scientific expeditions only occasionally, and old catalogues are very rarely digitized and updated. Unfortunately, as stressed by several authors (i.e., Boero 2001; Vomero 2014), curators of Italian museums are too infrequently taxonomists and quite often devoted to other disciplines (i.e., ecologists, science historians, faunistics). Further, it should also be taken into account that Italian collections are rarely used as key taxonomic resources in international projects, and Italian museums were absent from the SYNTHESYS+ program (Bartolozzi 2013). Incidentally, the authors of the letter quote, beside Florence NHM, a few other entities adhering to DISSCo, such as the National Research Council (CNR), National Association of Scientific Museums (ANMS), National Academy of Sciences, National Academy of Entomology, Italian Society of Biogeography, Italian Paleontological Society, Italian Geological Society, and Italian Botanical Society (<https://www.dissco.eu/it>). With the exception of the CNR (which is also the coordinator of the constituting NBFC), the others are all scientific societies, with no primary functions in biodiversity collection and cataloguing. Of the more than 160 NHMs adhering to the CollMap initiative - a national census of major collections spread over Italian museums (Vomero 2013; <http://www.anms.it/pagine/istituzioni>) - only the Florence NHM is within the DISSCo network, whereas other large museums (like the ones in Genoa, Milan, Pisa, Turin, Rome, and Verona) are not included.

So far, DISSCo and other systems and networks, such as Global Biodiversity Information Facility (GBIF), VertNet, and Integrated Digitized Biocollections (iDigBio), are powerful tools which foster transnational collaboration and represent operative tools for the future, above all for the online study of specimens whose loans to scientists are increasingly difficult: the development of digital technologies will make it possible to send images online, without moving precious specimens. This is one of the necessary steps to get a better functionality and interconnection among Italian museums, but it should go together with a national coordination hub, so as to hire a critical mass of taxonomists and technicians. The need of a centralized repository for collections that do not fit the scopes of smaller museums, and/or do not have a primary exhibition value is also urgent. All this would also help, as Minelli (2013) already stressed, to share resources and better address research activities at a national and international level.

References

- Andreone F, Bartolozzi L, Boano G, Boero F, Bologna M, Bon M, Bressi N, Capula M, Casale A, Casiraghi M, Chiozzi G, Delfino M, Doria G, Durante A, Ferrari M, Gippoliti S, Lanzinger M, Latella L, Maio N, Marangoni C, Mazzotti S, Minelli A, Muscio G, Nicolosi P, Pievani T, Razzetti E, Sabella G, Valle M, Vomero V, Zilli A (2014) Italian natural history museums on the verge of collapse? *ZooKeys* 456: 139–146. <https://doi.org/10.3897/zookeys.456.8862>
- Andreone F, Boero F, Bologna MA, Carpaneto GM, Castiglia R, Gippoliti S, Massa B, Minelli A (2022) Reconnecting research and natural history museums in Italy and the need of a national collection biorepository. *ZooKeys* 1104: 55–68. <https://doi.org/10.3897/zookeys.456.8862>
- Baird R (2010) Leveraging the fullest potential of scientific collections through digitization. *Biodiversity Informatics* 7(2): 130–136. <https://doi.org/10.17161/bi.v7i2.3987>
- Bartolozzi L (2013) I musei naturalistici italiani nel contesto delle iniziative internazionali sulla biodiversità. *Museologia Scientifica* 9: 17–20.
- Benvenuti M, Barbagli F, Maggiore F (2022) Comment and integration to Andreone et al. 2022 “Reconnecting research and natural history museums in Italy and the need of a national collection biorepository”. *ZooKeys* 1137: 177–179. <https://doi.org/10.3897/zookeys.1137.96414>
- Blagoderov V, Kitching I, Livermore L, Simonsen T, Smith V (2012) No specimen left behind: Industrial scale digitization of natural history collections. *ZooKeys* 209: 133–146. <https://doi.org/10.3897/zookeys.209.3178>
- Boero F (2001) Light after dark: The partnership for enhancing expertise in taxonomy. *Trends in Ecology & Evolution* 16(5): 266–266. [https://doi.org/10.1016/S0169-5347\(01\)02133-4](https://doi.org/10.1016/S0169-5347(01)02133-4)
- DuBay SG, Fuldner CC (2017) Bird specimens track 135 years of atmospheric black carbon and environmental policy. *Proceedings of the National Academy of Sciences of the United States of America* 114(43): 11321–11326. <https://doi.org/10.1073/pnas.1710239114>

- Engel MS, Ceríaco LMP, Daniel GM, Dellapé PM, Löbl I, Marinov M, Reis RE, Young MT, Dubois A, Agarwal I, Lehmann P, Alvarado M, Alvarez N, Andreone F, Araujo-Vieira K, Ascher JS, Baêta D, Baldo D, Bandeira SA, Barden P, Barrasso DA, Bendifallah L, Bockmann FA, Böhme W, Borkent A, Brandão CRF, Busack SD, Bybee SM, Channing A, Chatzimanolis S, Christenhusz MJM, Crisci JV, D'elía G, Da Costa LM, Davis SR, De Lucena CAS, Deuve T, Elizalde FS, Faivovich J, Farooq H, Ferguson AW, Gippoliti S, Gonçalves FMP, Gonzalez VH, Greenbaum E, Hinojosa-Díaz IA, Ineich I, Jiang J, Kahono S, Kury AB, Lucinda PHF, Lynch JD, Malécot V, Marques MP, Marris JWM, Mckellar RC, Mendes LF, Nihei SS, Nishikawa K, Ohler A, Orrico VGD, Ota H, Paiva J, Parrinha D, Pauwels OSG, Pereyra MO, Pestana LB, Pinheiro PDP, Prendini L, Prokop J, Rasmussen C, Rödel M-O, Trefaut Rodrigues M, Rodríguez SM, Salatnaya H, Sampaio I, Sánchez-García A, Shebl MA, Santos BS, Solórzano-Kraemer MM, Sousa ACA, Stoev P, Teta P, Trape J-F, Van-Dúnem Dos Santos C, Vasudevan K, Vink CJ, Vogel G, Wagner P, Wappler T, Ware JL, Wedmann S, Zacharie CK (2021) The taxonomic impediment: A shortage of taxonomists, not the lack of technical approaches. *Zoological Journal of the Linnean Society* 193(2): 381–387. <https://doi.org/10.1093/zoolinlean/zlab072>
- Flower WH (1898) *Essays on museums and other subjects connected with natural history*. Macmillan, New York. <https://doi.org/10.5962/bhl.title.32815>
- Minelli A (2013) Il Museo virtuoso. Proposte per un archivio responsabile della biodiversità globale. In: Mazzotti S, Malerba G (Eds) *I musei delle scienze e la biodiversità*. Atti del XX Congresso ANMS, Ferrara, 17–19 Novembre 2010, *Museologia Scientifica, Memorie* 9: 41–43.
- Suarez AV, Tsutsui ND (2004) The value of museum collections for research and society. *Bioscience* 54(1): 66–74. [https://doi.org/10.1641/0006-3568\(2004\)054\[0066:TVOMC F\]2.0.CO;2](https://doi.org/10.1641/0006-3568(2004)054[0066:TVOMC F]2.0.CO;2)
- Vomero V (2013) Biodiversità, banche dati tassonomiche e musei scientifici. Il progetto nazionale CollMap come premessa per il lancio di un istituto diffuso italiano di tassonomia. *Museologia Scientifica Memorie* 9: 21–27.
- Vomero V (2014) Per non far morire la ricerca nei (ed i) musei scientifici / To keep research in scientific museums (and the museums themselves) alive. *Museologia Scientifica Memorie* 11: 2–5.

